STUDY OF NANO-SIZE PARTICLE DYNAMICS IN URBAN ROAD MICROENVIRONMENT IN DELHI

By

KANAGARAJ RAJAGOPAL

Environmental Engineering Department

Submitted

In fulfilment of the requirements of the degree

of

DOCTOR OF PHILOSOPHY

to

DEPARTMENT OF ENVIRONMENTAL ENGINEERING

DELHI TECHNOLOGICAL UNIVERSITY

DELHI-110042, INDIA

MAY 2025

STUDY OF NANO-SIZE PARTICLE DYNAMICS IN URBAN ROAD MICROENVIRONMENT IN DELHI

A Thesis

Submitted in fulfilment of the requirements for the award of the degree Of

DOCTOR OF PHILOSOPHY
In
Environmental Engineering

By
KANAGARAJ RAJAGOPAL
Roll No. 2K19/PhDEN/504

ENVIRONMENTAL ENGINEERING DEPARTMENT

Under the guidance of
Dr. Rajeev Kumar Mishra
And
Prof. S. Ramachandran
Physical Research Laboratory, Ahmedabad

DEPARTMENT OF ENVIRONMENTAL ENGINEERING
DELHI TECHNOLOGICAL UNIVERSITY
DELHI-110042, INDIA

MAY 2025

DELHI TECHNOLOGICAL UNIVERSITY

(Formerly Delhi College of Engineering)

Department of Environmental Engineering

Shahbad Daulatpur, Bawana road, Delhi- 110042

DECLARATION

I hereby declare that the research work presented in this thesis entitled " **Study of nano-size particle dynamics in urban road microenvironment in Delhi**" is original and carried out by me under the supervision of Dr. Rajeev Kumar Mishra, Associate Professor, Department of Environmental Engineering, Delhi Technological University, Delhi, and co-supervision of Prof. S. Ramachandran, Senior Professor, Space and Atmospheric Sciences Division, Physical Research Laboratory, Ahmedabad being submitted for the award of Ph.D. degree to Delhi Technological University, Delhi, India. The content of this thesis has not been submitted either in part or whole to any other university or institute for the award of any degree or diploma.

Date: / / 2025 (Kanagaraj Rajagopal)

Place: DTU, Delhi. Roll. No. – 2K19/PhDEN/504

DELHI TECHNOLOGICAL UNIVERSITY

(Formerly Delhi College of Engineering)

Department of Environmental Engineering

Shahbad Daulatpur, Bawana road, Delhi- 110042

Date: - / / 2025

CERTIFICATE

This is to certify that the Ph.D. thesis entitled "**Study of nano-size particle dynamics in urban road microenvironment in Delhi**", is being submitted by Mr. Kanagaraj Rajagopal for the fulfilment of the requirements for the award of the degree of Doctor of Philosophy in Environmental Engineering, to the Department of Environmental Engineering, Delhi Technological University, Delhi, India, is a bonafide record of original research work carried out by him under our supervision. The results embodied in this thesis have not been submitted to any other university or institution for the award of any degree or diploma.

Dr. Rajeev Kumar Mishra
Supervisor
Environmental Engineering Dept
Delhi Technological University

Prof. S. Ramachandran
Co - supervisor
Space and Atmospheric
Sciences Division
Physical Research Laboratory

DELHI TECHNOLOGICAL UNIVERSITY

(Formerly Delhi College of Engineering)

Department of Environmental Engineering

Shahbad Daulatpur, Bawana road, Delhi- 110042

PLAGIARISM VERIFICATION

Thesis Entitled" **Study of nano-size particle dynamics in urban road microenvironment in Delhi**" containing 272 Pages of the research scholar "KANAGARAJ RAJAGOPAL" Under the supervision of Supervisor (s)

(1) Dr. Rajeev Kumar Mishra

(2) Prof S. Ramachandran

This is to report that the above thesis was scanned for similarity detection. Process and outcome are given below:

Software used: Turnitin Similarity Index: 2% Total Word Count: 59,799

Date: 23-12-2024

Candidate's Signature **Signature of Supervisor(s)**

Dedicated

To

My Parents

Mr. Rajagopal,

Mrs. Bagavathy

And

My family members & Friends

ACKNOWLEDGEMENT

I would like to express my appreciation to the people who have helped me most during my research work. First and foremost, I am deeply grateful to my research supervisor, Dr. Rajeev Kumar Mishra, and co- supervisor Prof. S. Ramachandran for their nonstop guidance, enduring patience, and nurturing support throughout this research journey. It has been a valuable experience and honour to be associated with such supporting supervisors and learn from their experience.

I accord my heartfelt thanks to Prof. A.K Haritash, Head, Department of Environmental Engineering, DTU and other faculty members of the department, my DRC committee members for their consistent constructive suggestions throughout my Ph.D. journey. I would like to thank all my UG and PG faculty members who inspired me to take up this research work.

I extend my thanks to Dr. Shailendra Kumar Yadav, for his continuous support from my under graduation till date. I am grateful to my seniors, Dr. Amrit Kumar, Dr. Abhinav Pandey, Dr. Amrit Krishnan, and my colleagues Mr. Vignesh Mohan, Ms. Monika Sharma, Mr. Ravi Pratap Singh Jadon, Mr. Anil Mann, and Mr. Abhishek Kumar Yadav for providing me with critical comments and suggestions and all those who directly or indirectly helped, interacted and exchanged ideas with me in completing the research. It would not have been possible without the support of instrumentation facilities, laboratory technicians (Mr. Anil Bharadwaj and Mr. Mahesh); I am thankful to them.

I want to extend special thanks to my family's immense contribution, especially my Sister Loganayaki Rajagopal, Suresh Santhamoorthy (brother in law) and Nethra (Niece) who not only encouraged and supported me but also stood by me like a pillar and gave me constant motivation. All my family members have shown enormous patience during this process and have cheerfully sacrificed the time that rightfully belonged to them. Finally, I extend a profound expression to my school friends showered me with their blessings and made me who I am today.

LIST OF PUBLICATIONS

Published

1.**Rajagopal, K.,** Ramachandran, S., and Mishra, R.K (2025). Traffic-induced nanoparticle emissions and associated respiratory risk analysis using measurements conducted in a roadside environment. *Air quality atmosphere and Health.* https://doi.org/10.1007/s11869-024-01689-x.

2.**Rajagopal, K.,** Ramachandran, S., and Mishra, R.K (2025). Influence of local meteorology and gaseous emission on atmospheric nanoparticle concentrations in the pedestrian way in the urban region. *Atmospheric pollution research***.** 102358. https://doi.org/10.1016/j.apr.2024.102358.

3.**Rajagopal, K.,** Ramachandran, S., and Mishra, R.K (2024). Seasonal variation of particle number concentration in a busy urban street with exposure assessment and deposition in human respiratory tract. *Chemosphere*. 366, 143470. https://doi.org/10.1016/j.chemosphere.2024.143470.

4.**Rajagopal, K.,** Ramachandran, S., and Mishra, R.K (2024). Size resolved particle contribution to vehicle induced ultrafine particle number concentration in a metropolitan curbside region. *Atmospheric Environment*. 337, 120773. https://doi.org/10.1016/j.atmosenv.2024.120773.

5.**Rajagopal, K**., Mohan, V. and Mishra, R.K. (2024). Are Delhi residents exposed to lesser particle number concentration due to the firework ban in the city? *Air Quality, Atmosphere & Health*, 17, 1617-16271. https://doi.org/10.1007/s11869-024-01532-3.

6.**Rajagopal, K.,** Ramachandran, S., and Mishra, R.K. (2023). Roadside measurements of nanoparticles and their dynamics in relation to traffic sources in Delhi: Impact of restrictions and pollution events. *Urban Climate, 51,* 101625. https://doi.org/10.1016/j.uclim.2023.101625.

7. Sharma, k., Goyal, M., Mishra, R.K., Vijayakumar, T., Kumar, P., and **Rajagopal, K.** (2025) Air quality status and estimated health exposure in major metropolitan Indian cities *Aerosol Science and Engineering*, https://doi.org/10.1007/s41810-024-00278-w.

In Revision

8.Saxena. M., **Rajagopal, K.,** and Mishra, R.K., Air Pollution Associated Health Impact Assessment in a Higher Educational Institution of South Asian megacity Delhi. (**Under Review: ASEN- D-24-00119R2).**

9.**Rajagopal, K.,** Gupta, A., Gupta, A., Jha, S., Sharma, M., and Mishra, R.K., Comprehensive measures to mitigate air quality during G20 summit: A practical way for sustainability. (**Under Review: JESS-D-25-00072R1).**

In Review

10.**Rajagopal, K.,** Mohan, V., Sharma, M., Yadav, S.K., Sahu, V., Mishra, R.K., Gautam., S, Gurjar, B. R., and Kumar, P. Impact of the odd even scheme on particulate matter reduction in Delhi traffic intersection (**CJOE-2025-0249).**

11.Yadav, S.K., Sharma, M., **Rajagopal, K.,** Mohan, V., Yadav, S.K., Sahu, V., Mishra, R.K., Gurjar, B. R. Evaluating the impact of Odd-Even transportation scheme on particle number concentration on air quality profiles in megacity Delhi **(CLEAN - Soil, Air, Water).**

12. **Rajagopal, K.,** Shahi, C., Aryan, Sharma, A., Mishra, R.K., and Jena, C. Air quality changes due to the dust storm events in western coast region in Indian subcontinent**.** (**Theoretical and Applied Climatology**)

In Preparation

13. **Rajagopal, K.,** Ramachandran, S., and Mishra, R.K. Urban atmospheric nano particles sources, concentration and health effects in different micro environment – A Global review.

15. **Rajagopal, K.,** Mohmmed R.H.H., Mohan, V., and Mishra, R.K. Policy measure to combat pollution events in urbanizing global south region**.**

16. Sharma, M., Khera1, A., Kaistha, A., Sharma, C., **Rajagopal, K.,** Mishra, R.K. School children exposure to indoor air quality in urban regions**.**

Book chapters (Published)

17. Goyal, M., Sharma, K., Mishra, R.K., Vijayakumar, T., **Rajagopal, K.** (2024) Fuel usage policy implementation towards sustainability and household air pollution reduction in Indian subcontinent: prediction and analysis**.** https://doi.org/10.1007/978-3-031-82559-0_7.

Conference Proceedings (Accepted)

18. **Rajagopal, K**., S. Ramachandran, Mishra, R.K. (Dec 2023). Traffic-Induced ultrafine particle concentration in megacity Delhi. Lecture Notes in Civil Engineering.

19. **Rajagopal**, **K**., S. Ramachandran, Mishra R.K. (Nov 2022). Measurements ofSize Resolved Nanoparticle Concentration and its Distribution in Polluted Urban Environment during Induced Firework Event. Lecture Notes in Civil Engineering 582. https://link.springer.com/book/9789819623587.

ABSTRACT

Due to rapid urbanization, Delhi experiences frequent pollution events, and the particulate matter load exceeds the prescribed limit often. This study analyzes nanoparticle (10 to 1090 nm) during different emission scenarios, seasonal and meteorological conditions in two phases: April to June 2021 (Period I) and October to November 2021 (Period II). Period I experienced around 31% less concentration of particles (~2.4×10^4 cm^{-3}) due to lockdown restrictions and, on the other hand, particle concentration increased by 35% compared to normal conditions due to the sudden rise in firework emissions in Period II. Except for the post-Diwali phase (10^4 cm^{-3} to 10^5 cm^{-3}), the concentrations lie between 10^3 $cm^{-3}$and 10^5 cm^{-3}. The Aitken modes contribute 10 to 30% of total concentration in both periods. Particles in nucleation and accumulation modes contribute 30 to 40%, 20 to 30%, 15 to 25%, and 35 to 50% in Periods I and II, respectively. Concentration and behavior of nano particles in different seasons (winter, spring, summer, monsoon, and autumn) are examined, for the first time. Concentration of particles is classified into four different sizes as N_{nuc} (10 to 30 nm, nucleation), N_{satk} (30 to 50 nm, small Aitken), N_{latk} (50 to 100 nm, large Aitken), and N_{acc} (100 to 1000 nm, accumulation mode), and the total (10 to 1000 nm) particle number concentration (PNC) as N_{total}. PNC ranges between 10^4 cm^{-3} and 10^6 cm^{-3} over Delhi during the year, and the highest concentration occurs in winter. Winter concentration is 2 times higher than monsoon, summer, autumn and spring concentrations, respectively. N_{nuc}, N_{satk}, N_{latk} and N_{acc} and their respective contributions to total PNC exhibit significant seasonal variations. During winter N_{latk} and N_{acc} contribute more to total PNC due to coagulation, with N_{acc} alone contributing >40% to total PNC. N_{nuc}, N_{satk}, and N_{latk} are higher in spring and summer during mid-day due to nucleation and/or ultrafine particle burst events. The direct primary emissions from engine exhaust produce a prominent double hump structure during morning and evening

peak hours in winter and autumn. PNC and their contributions exhibit day-night variations as they are influenced by emission sources and variations in meteorological parameters (wind speed, relative humidity, temperature, solar radiation and boundary layer height) between day and night. Carbon monoxide correlates positively with N_{acc} in all seasons (R^2~0.5) as fossil fuel emission is predominant source for gases and particles in study environment. The concentration of UFP size range particles is dominantly higher (70 to 80%) during peak hours than the non-peak hours. The variations in particle number concentration depend on the intensity and emissions of sources during peak, and non-peak hours. UFP contributes ~60 to 80% to the total particle number concentration in the urban roadside microenvironment, and its contribution increases during peak hours. During the winter season, the average total particle number concentration was observed to be maximum (4.1×10^4 cm^{-3}) with a higher surface area of particles of 3.5×10^{-3} mm^2m^{-3}. Compared to the monsoon season, the concentration of NO_X was 5 times higher in winter. The boundary layer height in the study region ranged from 600 to 2400 m during different seasons, and the maximum ventilation coefficient was observed to be >3000 m2s-1 during summer. Precipitation reduced the concentration of particles by half, from 2.2 x 10^4 to 1.1 x 10^4 cm^{-3}, due to wet scavenging. The study revealed that the concentrations of particles depend not only on primary emissions but also are influenced by local meteorology and other co-emitted pollutants. The Multiple Path Particle Dosimetry (MPPD) model simulated values show that the order of deposition goes as alveoli > bronchiole > bronchus. The deposition in the study area ranges between 10 and 18 million nanoparticles during different hours of the day, whereas the estimated inhalable particles vary between 0.5 to 1 billion. The concentration of total inhalable particles and the actual particles deposited in the lung varies. The seasonal sequence of deposition of nanoparticles is winter > monsoon > summer > autumn > spring. The

deposition of nanoparticle in adults is 30 to 40% higher than in children and infants, and further, the deposition is higher in the alveolar region than in the bronchiole and trachea regions. About 90% of the particles get deposited in the alveolar regions, 6 to 8% in the bronchiole region, and 2% in the trachea region. The estimated deposition of nanoparticles for an individual working 8 hours a day in the near road conditions is 338 µg/year in Delhi. The deposition increases almost linearly as a function of time, and is 3 times higher (1016 µg/year) for a person residing near the road throughout the day (24 h). The deposition fraction of particles ranges between 0.05 and 0.10 µg/day in alveolar region, <0.05 µg/day in the bronchiole region, and lies between 0.02 and 0.04 µg/day in the trachea. The nanoparticles deposited in the respiratory system can lead to the development of various diseases such as asthma, chronic obstructive pulmonary disease, and can lead to carcinogenicity. Number concentration-based studies are essential for estimating the potential impacts on human health due to air pollution. The study provides information regarding vehicle emission-based particle concentration under various emission scenarios in urban cities, which is crucial for estimation of emissions, health impact assessment, future policy formulation and strategy measures. These quantitative results on seasonal variations of air pollutants together with the knowledge on seasonal variations in meteorological parameters and atmospheric dynamics provide a foundation which can positively contribute to the planning and devising mitigation measures aimed at improving air quality and public health. The study provides new insights on inhalable particle concentration during the day that are crucial for strategy development, emission mitigation, and health hazard assessment for the citizens. Understanding the dynamics of atmospheric nanoparticles in urban roadside environments provides on the deposition of nanoparticles in humans residing near roadside conditions are crucial to estimate the

human health risk potential, and to formulate mitigation measures for exposure reduction which can result in a better and sustainable future.

TABLE OF CONTENTS

CHAPTER -3

CHAPTER -4

CHAPTER -5

LIST OF FIGURES

LIST OF TABLETS

LIST OF ABBREVIATIONS

ANOVA	Analysis of Variance
AQI	Air Quality Index
AT	Atmospheric Temperature
BAU	Business as Usual
CCN	Cloud Condensation Nuclei
CFD	Computational Fluid Dynamics
CNG	Compressed Natural Gas
COVID	Coronavirus Disease
CPC	Condensation Particle Counter
CPCB	Centre Pollution Control Board
CPMA	Centrifugal Measurement of Particle Mass
CS	Condensation Sink
DLPI	Dekati Low Pressure Impactor
DMA	Differential Mobility Analyzer
DMPS	Differential Mobility Particle Sizers
DMS	Differential Mobility Spectrometer
DPF	Diesel Particulate Filter
EAA	Electrical Aerosol Analyzer
EC	Elementary Carbon

EDA	Exploratory Data Analysis
ELPI	Electrical Low-Pressure Impactor
EPA	Environmental Protection Agency
FIMS	Fast Integrated Mobility Spectrometer
FMPS	Fast Mobility Particle Sizer
FR	Formation Rate
GAM	Generalized Additive Model
GIS	Geographic Information System
GMD	Geometric Mean Diameter
GR	Growth Rate
HCV	Heavy Commercial Vehicle
HDV	Heavy-Duty Vehicles
HEI	Health Effects Institute
ICP-MS	Inductively Coupled Plasma Mass Spectrometry
IPCC	Intergovernmental Panel on Climate Change
KW-Test	Kruskal-Wallis Test
LCV	Light Commercial Vehicles
LDMA	Long Differential Mobility Analyzer
LDV	Light Duty Vehicles
LII	Laser Induced Incandescence
LPI	Low Pressure Impactor

LUR	Land Use Regression
MPPD	Multiple Path Particle Dosimeter model
NAAQS	National Ambient Air Quality Standards
NCR	National Capital Region
NOAA	National Oceanic and Atmospheric Administration
NPF	New Particle Formation
OPC	Optical Particle Counter
PMC	Particle Mass Concentration
PNC	Particle Number Concentration
PND	Particle Number Distribution
PNSD	Particle Number Size Distribution
PTEF	Polytetrafluoroethylene Membrane Filters
RDD	Respirable Depository Dose
RH	Relative Humidity
ROS	Reactive Oxygen Species
SD	Standard Deviation
SEM	Scanning Electron Microscope
SLPE	State-Level Public Enterprises
SMPS	Scanning Mobility Particle Sizer
SR	Solar Radiation
TEM	Transmission Electron Microscopy

TEOM	Tapered Element Oscillating Microbalances
UFP	Ultra Fine Particulates
URMe	Urban Road Microenvironment
VOC	Volatile Organic Compounds
WHO	World Health Organization
WRF	Weather Research Forecast
WS	Wind Speed

CHAPTER-1

INTRODUCTION

1.1 Background

Environmental pollution is a major concern globally (Rentschler and Leonova, 2023). Pollution not only affects the features of the environment but also poses a serious threat to human health and other living creatures (Jbaily et al., 2022). Air is one of the major components of the environment, and on average, around 12kg of air is consumed by an individual for survival (Kulshreshtha and Khare, 2010). Air intake is 12 to 15 times more than the volume of food consumed (Reggente et al., 2015). The pollutants present in the air are more harmful than the pollutants present in the food (De Nazelle et al., 2017). Clean air is free from any impurities such as solid, liquid, or gaseous substance, which is essential for human beings (Patel et al., 2021). Air pollution is becoming a major issue in all major Indian cities (Kumar et al., 2012). Both natural and anthropogenic sources cause the air pollution (Resmi et al., 2019). The natural sources include volcanic eruption, forest fires, pollen, and occasionally lightning activities. Similarly, anthropogenic activities involve industrial processes, burning fossil fuels, automobiles, etc (Moreno-Ríos et al., 2022). The emissions released from natural activities are occasional (Junkermann and Hacker, 2022). Also, they remain in the atmosphere for a short period, whereas in anthropogenic activities, the emissions are continuous throughout the year, and they are emitted into the atmosphere in regular intervals, which also stays for a long time due to the frequent emissions (Lv et al., 2020).

The issue of air pollution in urban regions began in the 20th century from various sources that use fossil fuels. The various sources include smoke from factories, furnaces, boilers, ovens, steam engines, exhaust fumes from automobiles, powerplant emissions, major industries such as oil and zinc refineries, chemical and meteorological industries, iron and steel plants, food industries contribute to the different types of air pollution (Zhu et al., 2022). Among all these sources, automobile sources contribute to more urban emissions (Al–Dabbous et al., 2017). Air pollution is broadly classified into primary and secondary pollutants (Table 1.1). Primary pollutants are emitted directly into the atmosphere through identifiable sources, either

by natural or anthropogenic activities. The major primary pollutants include suspended particulate matter, oxides of nitrogen (NO, NO_2, NO_x), Sulphur (SO_2), carbon (CO, CO_2), and volatile organic compounds (VOCs) (Yadav et al., 2021.). These primary pollutants react with each other or with other compounds in the atmosphere, such as water vapor, with or without the influence of sunlight, to form different types of pollutants, which are referred to as secondary pollutants (Zhang et al., 2021). The secondary pollutants are chemical substances that are produced from the chemical reactions of natural or anthropogenic sources. Major secondary pollutants are sulphuric acid (H_2SO_4), ozone (O_3), formaldehyde, and Peroxy-acryl-nitrate (PAN) (Nelson et al., 2022.).

The suspended particulate matter in the air is found in solid or liquid form in the atmosphere and is based on the size of the particles. The majorly known particulate matter are Particulate matter with a size lesser than 10µm (PM_{10}) or particles with a size lesser than 2.5 µm ($PM_{2.5}$) (Fatima et al., 2022). The particles larger than a molecule but small enough to remain suspended in the air are called aerosols.

Table 1.1 Classification of particulates in suspended matter (Hinds, et al., 1999)

Type of particles	Terminology	Meaning	Examples
Liquid particles	Mist	Aerosols, which have liquid droplets	Sulphuric acid mist
	Fog	Aerosols, which have water droplets	
Solid particles	Dust	Solid aerosol particles are generated through the grinding down of larger particles.	Dust storm
	Smoke	Solid aerosol particles produced by chemical reactions	Cigarette smoke, smoke from the burning garbage

	Fumes	Similar to smoke but are produced by condensation of hot vapor of metals	Zinc/lead fumes.

The aerosol particle concentration in the ambient atmosphere may range from 10^6 to 10^7 cm^{-3}, irrespective of the urban or remote environment (Baldauf et al., 2013). Highly polluted urban regions can exhibit a higher magnitude of concentration. The diameter of the particles ranges from a few nanometers to 100 µm (Meier et al., 2015). The aerosol particles from combustion processes such as automobiles, power generation, and wood burning can produce particles from 10 nm to 1 µm (Manigrasso et al., 2020). The aerosols generated from windblown dust, pollens, plant fragments, and sea salts are generally larger than 1 µm (Garg, 2018). The particles produced in the atmosphere through the photochemical process are typically found to be smaller than 1 µm(Gerling and Weber, 2022). The particles' properties and size also vary significantly based on the generation size. The classification of particles of different sizes based on the sources is shown in Fig.1.1.

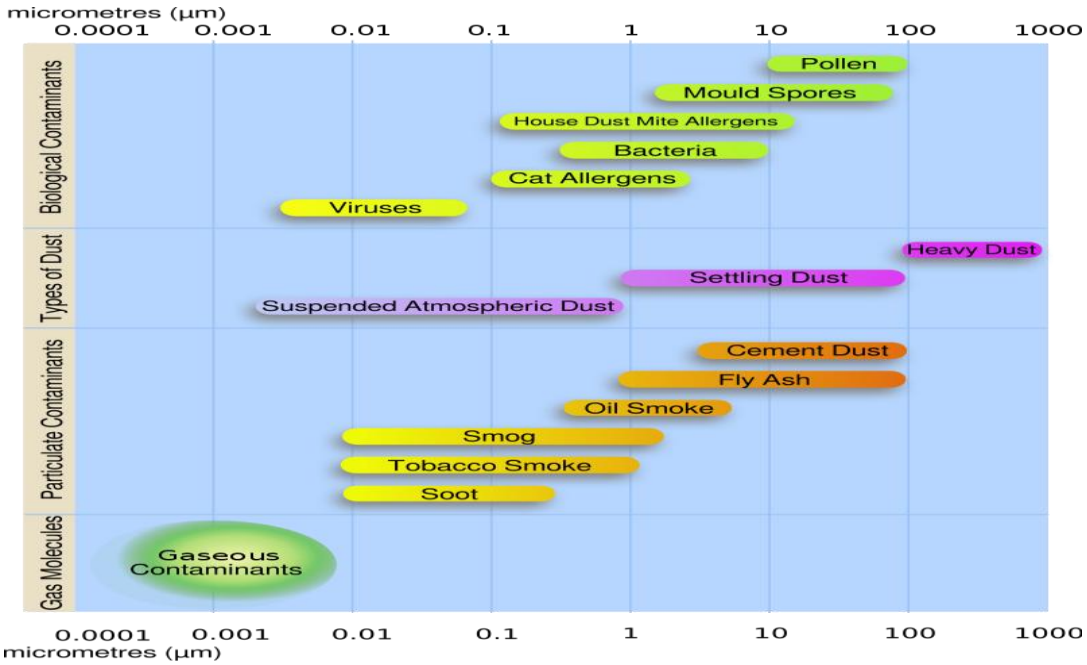

Figure: 1.1 Different types and sizes of major atmospheric particles (Hawk et al., 2020)

Generally, PM_{10}, and $PM_{2.5}$ particulate matter, is measured in mass concentration basic, but ultrafine and nanoparticles (due to negligible mass) are estimated based on the particle number per unit volume as particle number per cm^3 (PNC) (Sarangi et al., 2018). The higher-size particles, calculated in mass concentration, show less numbers than the particles smaller particles, or the aerosols are measured in number concentration, which will be found in more numbers (Gerling et al., 2020). However, their mass will be low (Fig.1.2). The aerosol particles generated through various processes are further classified into nucleation (10 to 30 nm), Aitken (30 to 100nm), and accumulation mode (100 to 1000nm) particles based on their size distribution (Agudelo-Castañeda et al., 2013). The Aitken mode particles can be further classified into small Aitken (30 to 50 nm) and large Aitken mode (50 to 100 nm) particles. The emissions from the transportation sector with size ranges (10 to 100 nm) are often called ultrafine particles (Sabaliauskas et al., 2013). The ultrafine particles are ubiquitous in the environment, and this size range of particles can contribute up to 70 to 80% of the total particle number concentration (Zhu et al., 2002).

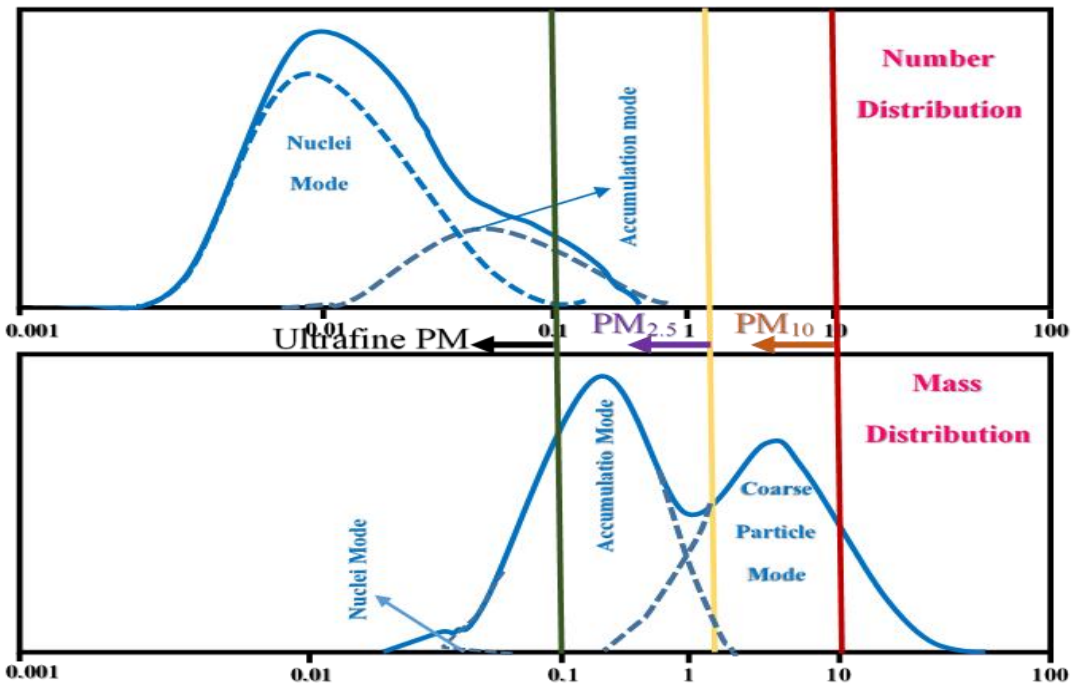

Figure.1.2. UFP size and mass distribution (Adopted from – Hinds 1999)

1.2 Need for the study

Delhi is the national capital of the country and one of the highly urbanized cities where air quality is a major concern. The air quality perspective of India 2023 shows that the daily average concentration of PM_{10} is 205 μg/m^{3,} and for $PM_{2.5}$, it was 100 μg/m^{3,} which is higher than the prescribed standards (Arub et al., 2021). The cumulative analysis for the years 1990 to 2022 in Delhi shows that the contribution of vehicular sources for air pollution is more, i.e., 10 to 35%, followed by constructional activities (10 to 30 %), industrial activities (10 to 30%), cooking activities (< 10 %) in summer and < 30% in winter, open waste burning contributes to around 5 to 15%, dust storm activities up to 5%, agricultural residue burning up to 3% (Jose et al., 2021). Air quality is directly associated with human health, and the recent report by the Indian state-level disease burden initiative estimates that the death rate due to outdoor air quality has increased by 115 percent (Bhandari et al., 2020). The northern and central parts of the country face more economic losses due to air pollution, around 1.4 % of GDP, and increased premature deaths. In 2019, the country attributed to around 67 million deaths, accounting for around 17 % of the total deaths in the country (Manojkumar and Srimuruganandam, 2021). Among them, outdoor air pollution contributed to around 0.98 million, and indoor or household air pollution contributed to around 0.61 million.

On the other hand, the death rate due to outdoor air quality increased to around 115% (Dahari et al., 2022). Delhi records the highest per capita economic losses due to air pollution, followed by Haryana. Out of eight deaths in India, one is attributed to air pollution as per the Global burden of diseases (Machaczka et al., 2021). Air pollution is one of the risk factors for death in India, so it is necessary to do various research activities to estimate, control, and mitigate air quality in this domain (Hussein et al., 2022). Various studies are conducted in the study domain, estimating various concentrations of particulate matter and gaseous pollutants in its sources. Very few studies have been done to estimate the ambient concentration of aerosols/ultrafine particles. The region receives most of the emissions from the transportation sector, so estimating the aerosols concerning the transport sector is necessary to develop strategies for reducing the emissions from the transportation sector. Another major

need for the study is to estimate the potential human health impact assessment due to these emissions. The particles of lesser size will have more penetration into the human respiratory system and will seriously threaten human health, so quantifying the particles is necessary to estimate the residents' exposure.

1.3 Objectives of the study

Considering the impact of the transportation sector and its contribution to air pollution, the research has been undertaken with the following research objectives.

1. To measure and quantify the nano-size particles in urban roadside micro-environment (URME).

2. To study the role of meteorological parameters in particle number size distribution (PNSD).

3. To investigate the nano-size particle dynamics over different seasons at a selected transport corridor.

1.4 Organization of the Thesis

The thesis comprises five major chapters, and the brief outline is provided below chapter-wise.

Chapter 1 deals with the introduction, which consists of different types and sources of air pollution and status of air quality in Delhi (study region) and displays the study's major objectives with a special emphasis on the need for the study. This chapter establishes the platform for writing the subsequent thesis chapters, such as the literature review and result and discussion section.

Chapter 2 includes a comprehensive literature survey which is available related to the study. The literature review is in different sections, such as the scenario of air pollution in Delhi, how the concentration of air pollution and sources changes during different seasons of Delhi, various studies done globally to estimate the particle number concentration, size distribution of the particles in the different environmental conditions and sources. The literature review also includes dynamics of the variation of particle numbers based on the sources. The chapter also includes the various types

of measurement instruments and the concentration status in different countries. The final section of the chapter includes literature related to health impacts, its penetration into the human body, and its deposition in different regions of the respiratory system.

Chapter 3 represents the information regarding the study area where the study is conducted, along with the information regarding the instrument used. The methodology adopted to conduct the study, various instruments used for data collection, the software used for data analysis and interpretation, the model used for health impact assessment, and other statistical tools used for the study are discussed in this chapter.

Chapter 4 includes detailed results and a discussion section in which the first section contains quantification and measurements of these aerosol particles/ nanoparticles in the urban roadside microenvironments of Delhi, along with their seasonal dynamics. The variation of concentration is due to changes in the vehicular density due to the restrictions. The section also estimates the role of meteorological parameters such as relative humidity, wind speed and direction, temperature, solar radiation, and boundary layer conditions, along with the meteorological parameters of the local emissions in terms of gaseous pollutants such as SO_2, NO_2, CO, O_3, and BC is analyzed in this chapter. The final section of the chapter uses mathematical and computational models for analyzing the health impact assessment of the particles in the human respiratory system along with their deposition fraction. The estimated total particle deposited in the different sections of the lungs is provided.

Chapter 5 describes the detailed conclusion of the experimental studies, its major findings, and a study summary. The results also highlight the effects of the vehicular sources in determining the concentration of the particle's variation.

1.5 Summary

The different chapters of the study will provide detailed discussion about the atmospheric nanoparticle's concentration in the urban roadside microenvironment in the Delhi city.

CHAPTER -2

LITERATURE REVIEW

2.1 Introduction

The atmospheric pollutants differ in their properties and based on their properties the pollutants are classified as particulate matter and gaseous pollutants (Vu et al., 2017). Nanoparticles are a complex mixture of aerosols and small particles suspended in the air with different chemical characteristics (Sly and Schüepp, 2012). The particles size range starts from few nanometres to micrometres (Jayaratne et al., 2015). The nanoparticles are measured and identified using their electrical mobility diameter instead of their chemical composition (Jeong et al., 2021). The nanoparticles are further classified into different size ranges by different researchers and the widely accepted classifications are, Nucleation particles (N_{nuc} – 1 to 30nm), Aitken mode particles 30 to 100nm which are further classified into small (N_{satk} – 30 to 50nm) and large Aitken mode particles (N_{satk} – 50 to 100nm), accumulation mode particles (100 to 1000nm) (Kumar et al., 2011). The particles in the size range of < 100 nm are also referred as ultrafine particles (UFP) and the particles < 300nm are collectively called as atmospheric nanoparticles (ANP) (Kumar et al., 2012). The particles in the range of 250 to 500nm are referred widely as quasi- ultrafine particles(qUFP) (Yadav et al., 2022a). Current air quality standards don't monitor the concentration of these nanoparticles but these particles influence around 80 to 90% of the total nanoparticle's concentration (Sabaliauskas et al., 2013). However, the nanoparticles contribution for the mass of the particles such as Particulate matter ($PM_{2.5}$ and PM_{10}) (Mishra et al., 2015).

The nanoparticles are measured in the particle number concentration and are often referred as PNC (Lin et al., 2022). In urban regions the total PNC of the nanoparticles are dominated by the contribution of transportation sources (Zhu et al., 2002). The modal classifications are primarily used in the aerosol research and later adopted for nanoparticles study to classify anthropogenic emissions (Dallosto et al., 2013). The number concentration and the size distribution of the atmospheric nanoparticles varies significantly based on the sources, geography and climatic conditions of the region (Posselt et al., 2019). The size distribution reveals the secondary transformation

process such as formation (Wang et al., 2011). The number concentration and size distribution of the particles in the urban regions varies based on the source's intensity and its interaction in the atmosphere which determines different process in the atmosphere (Sabaliauskas, et al., 2012). Different mode nanoparticles also indicate the different sources as well. In the urban regions the concentration of the nanoparticles was seen higher at their emission sources and its size distribution increase with respect to time and distance from the sources (Hudda et al., 2012). During the natural process such as new particles formation (Kompalli et al., 2014) the nucleation mode particles concentration was found more whereas during the fireworks emission the accumulation mode particles concentrations were found to be in higher concentration. Fresh engine emissions influence the particles in the Aitken mode particles. Studies refer accumulation mode particles as soot mode particles which are formed due to the combination of nucleation and Aitken mode particles. The aged traffic emissions are found to be in the accumulation mode particles (Xie et al., 2021).

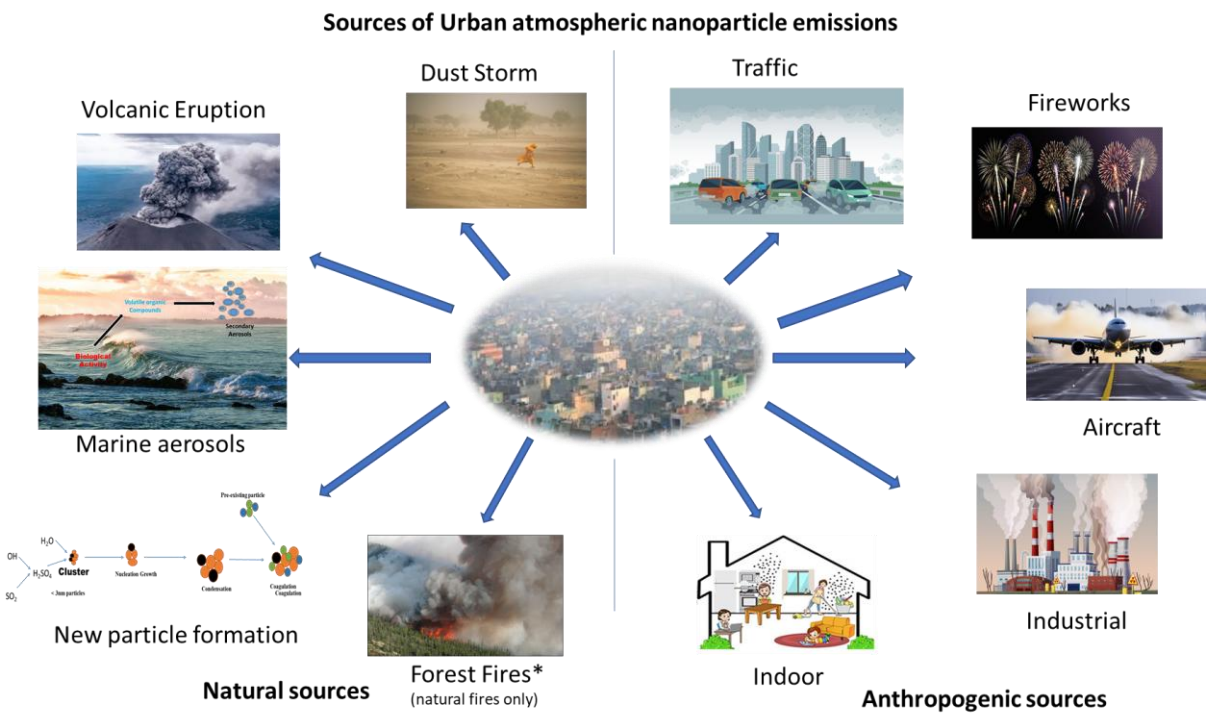

Fig 2.1 Different sources of urban ultrafine particles

The measurements of these atmospheric nanoparticles are done through highly sophisticated expensive instruments which use total particle number concentration

measurements (Machaczka et al., 2021). The upper and lower size range of the detection of these particles' changes from one manufacturer to other manufacture. In general, the condensation particle counter with electrically mobility measurement are the widely used principle for the measurement of these nanoparticles in the atmosphere (Aggarwal et al., 2012). Few instruments use optical measurements for measuring the nanoparticles found in the atmosphere. The scanning mobility particle sizer and differential mobility particle sizers are used by different research throughout the world for the measurements (Hillemann et al., 2014).

2.2 Sources of nanoparticles in urban atmosphere

In urban regions the nanoparticles exist due to both natural and anthropogenic sources (Kumar and Gupta, 2013) (Table 2.1). The natural process which contributes for the nanoparticle's emissions are volcanic eruptions, natural forest fires, marine aerosols, dust storm emissions and new particles formation activities (Fig 2.1) (Masiol et al., 2018). Similarly, the anthropogenic activities include traffic emissions, fireworks, aircraft sources, industrial and indoor sources contribute for the primary nanoparticle's emission from the anthropogenic sources (Meskhidze et al., 2019). The secondary sources of nanoparticles in the atmosphere are due to the condensation and coagulation of the primarily emitted nanoparticles (Saha et al., 2019). The new particle formation events, coagulation and condensation of the nanoparticles are influenced by the atmospheric conditions where the emissions took place and then based on that the frequency and efficiency of the process differs. In general, urban regions nanoparticles concentration are dominated by the emission from the transportation sectors that includes different vehicles such as two, three wheelers, light and heavy motor vehicles (Kumar et al., 2014). The automobiles include aircraft sources and marine traffic sources as well (Zhao et al., 2021).

Several studies revealed that the nanoparticles concentration of ultrafine particles in the total nanoparticle's concentration is around 70 to 95 % due to the transportation sources. Globally several studies about the nanoparticles concentration in the atmosphere is conducted in the developed nations such as USA (Saha et al., 2019), Germany (Giemsa et al., 2021; J. Sun et al., 2020), Europe (de Nazelle et al., 2017;

Garcia-Marlès et al., 2024) and few studies are found in the developing nations such as India (Kompalli et al., 2016; Yadav et al., 2021) , China (Yin et al., 2019; Zhou et al., 2020; Zhu et al., 2002), Japan (Orikasa et al., 2020), and other few south Asian countries (Akteruzzaman et al., 2023). Very few studies are conducted in the developing nations. The European union developed the emission norms for the nanoparticles with a standard of 6×10^{11}/km for the gasoline and diesel engine followed that the World Health Organisation (WHO) emphasized the importance of importance of atmospheric nanoparticles and came up with a guideline for the ambient nanoparticle's concentration as low and high category. The low with a concentration of < 1000 particles/ cm^{-3} (24 hr mean) and high concentrations with (> 10,000 particles/ cm^{-3} for 24 hrs and > 20,000 particles/ cm^{-3} for 1 hr) for having particles size ≥10 nm with no upper limit. The WHO in the year 2021 also stated that the measurements of these nanoparticles are to be done with the existing monitoring systems and also the epidemiological studies should be initiated to for the health impacts assessment.

Table 2.1 Summary of atmospheric nanoparticles around the world

S.no	Country, city	Environment	Concentration (cm-3 $\times 10^3$)
1.	Australia	Urban Region	26
2.	Bangladesh	Urban background	25
		Urban Region	60
		Urban Roadside	82
3.	Belgium	Urban Region	13
4.	Canada	Urban Region	26
5.	China	Urban Region	33
6.	Denmark	Urban Background	18
7.	Europe	Urban Background	8
		Urban Roadside	19
		Urban Region	17
8.	Finland	Urban Region	35
		Urban Roadside	40

9.	France	Urban Background	8
		Urban Roadside	27
10.	Germany	Urban Background	17
		Urban Roadside	60
		Urban Region	31
11.	India	Urban Background	12
		Urban Roadside	45
		Urban Region	27
12.	Italy	Urban Region	45
13.	Jordon	Urban Region	35
14	Malaysia	Urban Region	153
15.	Netherlands	Urban Region	35
16.	Singapore	Urban Region	12
17.	Sweden	Urban Roadside	65
18.	Taiwan	Urban Roadside	120
19.	United Kingdom	Urban Background	7
		Urban Roadside	71
		Urban Region	17
20.	United states of America	Urban Background	8
		Urban Roadside	15
		Urban Roadside	30
		Urban Roadside	22

2.3 Urban roadside microenvironment nanoparticles

In urban regions, roadside microenvironments are hubs for the nanoparticle's emission (Zhu et al., 2004). The concentration observed in the roadside is combination of both vehicular and ambient background emissions in the region (Zhu et al., 2004). The concentration in the roadside microenvironment can be as high as 25 times compared to the urban background conditions. The traffic density is another one deciding factor for the nanoparticle's concentration. The developing countries vehicle population is

increasing at an alarming rate, especially in Delhi the vehicle population will increase from 4.74 million in 2010 to 25.6 million in 2030 as projected. The traffic intersections such as red signal region revive more concentration of about 3.5 times higher than the green signal intersections (Y. Wang et al., 2008). The roadside microenvironment has significant impact on human health due to the location of residential areas adjacent to the roadside microenvironments in urban regions (Hagler et al., 2010; Sabaliauskas, Jeong, et al., 2012). The concentration of the nanoparticles in the urban street canyon is much higher than the urban roadside microenvironment due to the vortex effect (Kumar et al., 2008a). Majority of the global urban cities experience this canyon effect due to their built environment in urban regions (Weichenthal et al., 2014). The concentration of the nanoparticles in the urban microenvironment also depends on the driving pattern (Goel and Kumar, 2014). The nanoparticle emission is found to be high during low speed conditions and waiting period. The waiting period concentration increases around 14 times compared to the normal condition and also the accelerating conditions are found to have 6 times higher concentration of nanoparticles compared to the idling conditions (Argyropoulos et al., 2016).

The nanoparticles concentration in the roadside environment also changes during the different hours of the day such as peak and non-peak hours (Farrell et al., 2016). The particle number concentration of the nanoparticles is found similar to the traffic pattern and the size distribution exhibit bimodal distribution of the particles (Agudelo-Castañeda et al., 2013). The concentration of the nanoparticles in the tailpipe can reach up to 10^7 to 10^9 cm^{-1} whereas, the new particle formation can add particles up to 10^3 to 10^4 cm^{-1} under high condensation sink and growth rate so in urban region the vehicular sources dominate the total particle number concentration (Goel and Kumar, 2016). Asian countries report the higher concentration of urban nanoparticles compared to the Europe. with a mean concentration of about as $6.65 \pm 2.88 \times 10^4$ cm^{-3}, $4.81 \pm 2.61 \times 10^4$ cm^{-3} and $3.78 \pm 2.01 \times 10^4$ cm^{-3} (Nabizadeh et al., 2018). Congested traffic, a common phenomenon in urban cities can increase the nanoparticles concentration in roadside microenvironments when the vehicle constantly accelerating and deaccelerating (Joerger and Pryor, 2018). The urban regions in developing nations experience soaring levels of atmospheric nanoparticles but lack of scientific studies

and un availability of data base makes it hard to provide necessary mitigation measures (Belkacem et al., 2020). The nanoparticles emissions vary based on vehicle types, fuel quality, different driving patterns and in cabin measurements are still a grey area which needs to be focused (Belkacem et al., 2022).

The background concentration in the roadside environment also varies based on the location, surrounding industrial emission which also influences the concentration in the roadside environment (Zheng et al., 2022). Studies showed that the exposure of nanoparticles in the vicinity of road is a magnitude higher that the ambient levels (Yao et al., 2022). The exposure occurs during transportation, waiting for transit, walking, residing in homes near road environments, working in vicinity of road (Rajagopal et al., 2023).

2.4 Different urban microenvironments

In urban regions apart from roadside microenvironments, tunnel environments are another important region where the concentration of the nanoparticles increases significantly (Y. H. Cheng et al., 2010). A study conducted in Taiwan in a tunnel environment shows that the concentration of the nanoparticles inside the tunnel were 19 to 70 times higher than the roadside environment (S. C. Chen et al., 2010; Cheung et al., 2016). When the vehicle fleet inside the tunnel increases from 100 to 2000 then the concentration of the nanoparticles also increases from 49×10^3 cm^{-3} to 125×10^3 cm^{-3} (Kearney et al., 2011).The study measures the nanoparticles concentration during different vehicle density conditions and the found that the traffic volume has a significant impact on nanoparticles concentration and also the concentrations are imprisoned inside the tunnel due to the confined space (Zhao et al., 2020). Similarly, another study found the concentration in the peak hours and how the fresh emissions vary its size modal distribution inside the tunnel due to the atmospheric activity with respect to the time (Skuland et al., 2022). The size distribution study reveals that outside the tunnel nucleation mode particles contributes more due to the fresh emissions and inside the tunnel Aitken mode particles due to the coagulation of particles (Skuland et al., 2022).

Urban residential areas are another microenvironment where more studies need to be conducted (Chen et al., 2020). Preliminary study by researchers found that the concentration in the urban residential areas are high during the winter periods with a concentration of about 10 $\times 10^3$ cm^{-3} and less during summer 7 $\times 10^3$ cm^{-3}. In the residential regions the concentration of 10 to 100 nm particles is found more than 100 to 800 nm particles and the influence of outdoor concentrations are also found more in the residential zones (Hussein et al., 2019). Urban street canyons are another major microenvironment in the urban regions where the higher levels of atmospheric nanoparticles are found (Weber et al., 2013). The concentration increases due to the recirculation and vortex formation of the exhaust emission due to the infrastructure (Gerling and Weber, 2022). The study in different countries reveals that urban street canyon concentration in Spain is 13×10^3 cm^{-3}, 17×10^3 cm^{-3} in Germany, 40×10^3 cm^{-3} in Finland and 60 to 70×10^3 cm^{-3} in Sweden. Metro corridors are another major microenvironment in the urban regions where large number of people's commute (Yang et al., 2021). In Barcelona the metro station study revealed a concentration of about 23×10^3 cm^{-3} similarly, in USA- 25×10^3 cm^{-3}, Helsinki - 31×10^3 cm^{-3}, 10 to 29×10^3 cm^{-3} in UK, 11×10^3 cm^{-3} in chez Republic and 12×10^3 cm^{-3} in Spain are the globally reported concentrations in the metro stations (H. Patel et al., 2023). The literature suggests that in the urban regions there are different microenvironments where the concentration of the nanoparticles is extremely high compared to the ambient concentration (Bergmann et al., 2022).

2.5 Nanoparticles concentration in airport regions

Aircraft sources are one among the major source of atmospheric nanoparticles (Table 2.2) apart from vehicular sources (Ren et al., 2016). The concentration of nanoparticles is found high during the time of take-off and landing in the airport region (Pirhadi et al., 2020). The concentrations in the airport are highly influenced by the wind parameters. The concentration of the nanoparticles in the airport also varies based on the distance of measurement away from source (runway) and also in the UP/Down wind condition (Pirhadi et al., 2020). Few global studies are conducted to measure the concentration of these nanoparticles in the airports (Stafoggia et al., 2016). A study conducted in Tianjin international airport china reports that the concentration of

particles peaks between 25 to 50 nm during the take-off and landing of aircrafts and also the concentration also increases to 4×10^5 cm-3 whereas during normal period it was 2.2×10^5 cm^{-3}. During take-off the concentration increase was ~ 25×10^3 where as during the landing the increase in concentration was ~5×10^3. The geometric mean diameter of the aircraft nanoparticles is found lesser than the diameter of the particles found in the roadside microenvironments. The aging process of the aircraft emitted nanoparticles are less compared to the other vehicular sources due to their high dilution rate (Yadav, Mishra, et al., 2019). The airport concentrations are influenced by different events in airport such as take-off, landing, ground operations, background existing concentrations and meteorological conditions(Chen et al., 2010). The airport regions receive a mean of ~20% of the concentration contribution from the road traffic sources (Ragettli et al., 2014). The lubrication oil used in Jet engines also emit particles in the range of 10 to 30nm. The percentage contribution of sub10nm particles in the total particle number concentration is high compared to the other urban regions. Heal impacts due to the exposure of these nanoparticles are significant even if their exposure time is low (Moreno-Ríos et al., 2022). Health subjects exposed to atmospheric nanoparticles are found to have change in their forced vital capacity reported in the study conducted by the researchers in the airport environments (Junkermann and Hacker, 2022). The studies also found that the concentrations are time resolved. The different concentration of the atmospheric nanoparticles measured in the different international airports are reported in the table given below.

Table 2.2 Summary of atmospheric nanoparticles in different airports

S.no	**Airport name**	**Country**	**Concentration (cm^{-3})**	**Author**
1.	Tianjin	China	22×10^4	(Ren et al., 2016)
2.	Ciampino	Rome	1.9×10^4	(Stafoggia et al., 2016)
3.	Los angles, Hartsfield-Jackson	USA	1.9×10^4, 0.7×10^4	(Riley et al., 2016)
4.	Schiphol	Netherlands	5.3×10^4	(Lammers et al., 2020)
5.	Narita	Japan	3.4×10^{17} (kg per fuel)	(Takegawa et al., 2021)

6.	Gatwick	London	9.4×10^4	(Tremper et al., 2022)
7.	Frankfurt	Germany	2.4×10^4	(Dröge et al., 2024)

2.6 Role of new particle formation events in urban regions

New particle formation events are observed in different regions such as urban regions (Fig 2.2) , rural, free tropospheric, forest areas and coastal zones (Kulmala et al., 2021). In urban regions the new particle formation events usually occur during the late morning and grow throughout the day (Wu et al., 2024). The growth rate of the nanoparticles due to the new particle formation events ranges from 1 to 20nm/hr (Zimmerman et al., 2020). The new particle formation events are occurs based on four main mechanisms (Dinoi et al., 2023). The mechanism includes homogenous binary nucleation, heterogeneous binary, homogeneous ternary nucleation, ion-induced nucleation of binary, ternary based on the environmental conditions (Cheung et al., 2010). New particle formation events are initiated with the help of photochemical reactions and the activity is enhanced by the gaseous precursors such as H_2SO_4, NH_3 and other volatile organic compounds (VOC) (Dinoi et al., 2021).

The low volatile vapours in the atmosphere nucleates into neutral molecular clusters which are stabilized by amines, ammonia and organic vapours that are activated by condensation of the low VOCs (Tanda et al., 2019). The factors such as low relative humidity, presence of SO_2 and lesser pre-existing particle concentration, surface area of particles, high insolation and wind speed of the region (Kerminen et al., 2018). The NPF events increases the concentration of nucleation mode particles and it grows subsequently for other modes under favourable conditions in the urban regions (Bousiotis et al., 2021). Urban NPF events can interact with the regional NPF events under certain conditions and grow horizontally in the city regions (Das et al., 2021; C. Deng et al., 2020; Kanawade et al., 2022). The nanoparticles in the urban regions are highly affected by the temperature of the emission sources such as household activities, domestic heating, power production and industrial process and vehicular road emissions flume temperature (Carnerero et al., 2018; Rosati et al., 2021). The cloud condensation nuclei can initiate the NPF events and growth of particles by 40 to 50%

which relates the process of climatic systems which is of global importance (Cheung and Chou, 2013; Zhang et al., 2017).

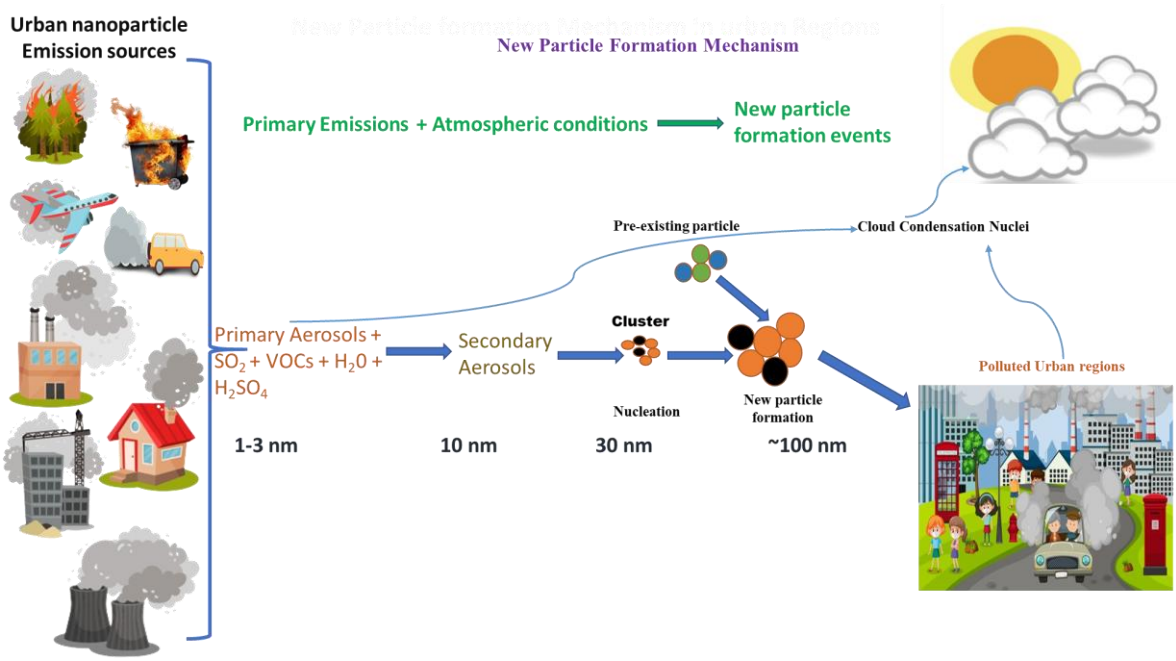

Fig 2.2 New particle formation mechanism in the atmosphere (Yadav et al., 2021)

The global tropospheric aerosol particles are responsible for their contribution to air quality and climate change patterns emphasis the necessity for understanding the particles in a detailed manner including their transformation in the atmosphere (Okuljar et al., 2021). New particle formation events also undergo transformation in size causing increase in concentration of the atmospheric particles in the atmosphere (Wang and Oliver Gao, 2011). Over the years the understanding of the NPF events are evolved due to various breakthroughs in the field and the theoretical prediction of molecular clusters through the Kohler type process (Yu et al., 2020). Previous studies are detected the NPF events in the rural and background regions but the recent several studies in urban regions proved the NPF events in a highly polluted urban region (B. Sarangi et al., 2018). This is due to the low condensations sinks exists in the cleaner regions assist the new particle formation process. However, the highly polluted urban regions with high condensation sinks affects the frequency of the NPF events (Yadav et al., 2021). The nucleation of gaseous precursors as nanoparticles in the atmosphere are one of the sources for urban nanoparticle concentration (Wu et al., 2021).

Several studies recommend to investigate the NPF events through micrometeorological perspective including the turbulent fluctuations (Ou et al., 2021). It is estimated that the global tropospheric cloud condensation nuclei are formed through NPF events (30 to 50%) (Chen et al., 2022). Because NPF events are globally phenomenon and it has huge impact on global climate (Blanco-Alegre et al., 2022). The literature suggests that there is a need of further research that includes filed observations that includes different microenvironments of urban regions and different other aspects such as frequency, strength and related meteorology also has to be considered for the study (Rajagopal et al., 2023, 2024). The basic nucleation starts clustering at sub 3nm particles which is also important parameter for measurement in the urban environments for detecting the NPF events and their role in ambient nanoparticles concentration in the urban regions (Jose et al., 2021).

2.7 Nanoparticles emission from fireworks

Firework emissions are considered as the short-term air quality degradation events (Garg, 2018). The most unusual anthropogenic activities that create notable short-term air pollution events are the firework events for celebrating events and festivals throughout the world (Tanda et al., 2019; Zhang et al., 2010). Firecrackers are used to celebrate certain festivals like new year eve, Diwali, spring festivals, Guy fawkes night were extensive fireworks were used for the celebrations (Hoyos et al., 2020; M. Zhang et al., 2010). Literatures reports emission of trace metals, suspended particles, organic compounds, sulphur dioxide and nitrogen oxides but the recent studies revealed that the nanoparticles are also emitted during the firework event and the impact of these emission lasts for few days causing series threat to human beings (Yerramsetti et al., 2013). The studies measured the temporal concentration of the particle concentration which always showed a peak concentration during and after the firework events (Yadav et al., 2022b). Studies conducted during the Chinese New Year firework events concentration of the nanoparticles attains a peak concentration of 3.8×10^4 cm^{-3} and also the particles in the size range of 100 to 500 nm are found to have more contribution in the total nano particle's concentration (Yao et al., 2022; Yu et al., 2017; Thakur et al., 2010). The Indian subcontinent where Diwali festival is celebrated throughout the country and many studies are conducted during this period for the measurement of the

nanoparticles emitted during this period (Chhabra et al., 2020). In the year 2012 the measurements of nanoparticles during Diwali period was reported with a concentration of about 1.2 $\times 10^5$ cm^{-3} particles (Saxena et al., 2020). Similarly, several studies were conducted during the different phases of the Diwali where the normal crackers were used then green crackers were used for emission reduction, restriction of crackers bursting and finally banning of crackers bursting in the country (Rajagopal et al., 2024). Series of studies conducted to explain the different concentration of the nanoparticles in the national capital of the India (Yadav, et al., 2019). Studies revealed that during the Diwali the concentration of emission increases by 139 percent comparted to the previous period with a concentration of about 1.7 $\times 10^5$ cm^{-3} particles (Prabhu et al., 2019). During the Diwali emissions the shift in the particle's emissions are clearly found in the GMD of the particles which shows a peak of around 180 nm during the fireworks emissions (Vaghmaria et al., 2018). While comparing the green crackers with the traditional crackers the emission of smaller size particles is more compared to the traditional crackers (Izhar et al., 2018; Yadav et al., 2022c). The UFP/N_{total} ratio of green crackers are 0.7 where the traditional crackers ration lies between 0.45 to 0.6. Delhi being one of the highly polluted urban regions during Diwali period the concentration of the nanoparticles reaches to a peak of 2.7 $\times 10^5$ cm^{-3}. Studies that even tough the emission are for short period but the sudden spike in concentration during the Diwali period causes severe health impacts in short and long term (Ghei and Sane, 2018; Sateesh et al., 2018). The emission increases the concentration of inhalable particle concentration in the atmosphere and they may reach up to 10 million particles/day. Whereas the inhalable particle concentration varies based on the different inhalation rates. The concentration may further increase when the individual does any heavy physical activity. The results reveal that the nanoparticles in the atmosphere are causing different illness irrespective of the short term and long-term emissions.

2.8 Nanoparticles emission from Non-Exhaust sources

Several studies revealed that the vehicular sources especially exhaust sources are vital sources for the atmospheric nanoparticle's sources in the urban regions (Kumar et al., 2013). But there are several other non-exhaust sources which are also acts as a

mandatory source in the urban regions. The major non exhaust sources for nanoparticle emissions are construction and demolition sources, forest fires/waste burning, powerplants, cigarette smoking, cooking, break and tyre wear and long-range transportation sources are also some of the other major sources in urban regions where the nanoparticles are emitted into the atmosphere (Vu et al., 2015).

2.8.1 Construction and demolition sources

The construction sites were the crushing, drilling, usage of machineries, soil excavation, usage of fine sand and cement are the major sources which induce the nanoparticles concentration in the atmosphere (Zhu et al., 2022). Similarly, during the demolition activities usage of different cutters and demolishing activities produces nano emissions. The ambient measurements of nanoparticles during demolition activities reports a concentration 1.6 times higher than the normal back ground concentration (Hopke et al., 2022). Similarly, other studies (Li et al., 2023; Ridolfo et al., 2024) are conducted in a controlled environment for measuring the nanoparticles emissions and the net emissions received during the slab demolition is around 1.8×10^4 cm^{-3}. The studies also revealed that the nanoparticles emitted during the different demolition process are in the range below 100nm i.e in the range of ultrafine particles (Li et al., 2023). The nanoparticles emitted from the construction and demolition activities are non-volatile in nature whereas the transportation sources emits particles of volatile origin (Ridolfo et al., 2024). The non-volatile nature of the nanoparticles is capable of having longer atmospheric lifetime which is even more vulnerable due to the dispersion in the receptor regions (Teknologi et al., 2016). However, the concentration fluctuates based on the parameters such as the distance of the sampling location from the source.

2.8.2 Forest fires and agricultural waste burning

Forest fires and agricultural waste burning emits significant number of nanoparticles in the atmosphere (Lv et al., 2020). The emitted nanoparticles not only cause health impacts but also alters the radiation of the atmosphere due to their property to act as a cloud condensation nuclei (Banerjee and Christian, 2018). In recent years the frequency of the forest fire events increases and it emits fine particles, trace gases and

the emission from the forest fires causes effects in local and regional boundaries due to their transboundary nature (Bhardawaj et al., 2017). Biomass burning for cooking and surface heating also emits nanoparticles into the atmosphere (Marval and Tronville, 2022). The fresh smoke emissions from the biomass burning emits particles in the size range of 100 to 160 nm with a peak concentration at 130nm (Phairuang et al., 2021). Similarly, the aged forest fire smoke emits particles are detected at 250 to 300 nm size ranges (Li et al., 2023). Majority of the studies developed emission factors for the different types of biomass fuels such as savanna fire plumes emit 3.4×10^{15} kg^{-1} and tropical forest fires emits 1.5×10^{15} kg^{-1} (Audignon-Durand et al., 2023). Buring of agricultural residue also emits nanoparticles and their concentration and size distribution also varies from other sources (Li et al., 2017). Studies are conducted for measuring the particle concentration of different fuels under different emissions conditions (Reche et al., 2017). Rice straw burning shows a unimodal distribution of particle emissions in all the three different modes of burning such as open fire, flaming and smouldering (Zhang et al., 2016). Even though the concentration shows a unimodal distribution but the mean diameter of the particle's changes from 52 nm to 141 nm based on the emission mode (Cusack et al., 2013). Wheat straw also shows a unimodal distribution of particles ranging between 10 to 400nm (Dahari et al., 2022). Flaming produces particles in the range of 200 nm where the smouldering produces particles in 500 nm range (Resmi et al., 2019). The studies also show that the nanoparticles emission from the forest fires and agricultural waste products are not uniform and it changes based on types of measurements, type of fuel used and type of combustion involved as well (Donateo et al., 2021).

2.8.3 Nano emissions from power plants

Powerplants are well known sources for emission of different types of gaseous and particulate matter (Gerling et al., 2020). In similar fashion the powerplants are emitting nanoparticles as well into the atmosphere (Michaelis et al., 2021). Power plants uses different types of fuel, different ratios of fuel quality which emits different types of nanoparticles (Liu and Cui, 2014). Research studies shows that the nanoparticles emission from the coal fired power plants are multimodal in nature and are emitting particles in the range of 10^8 to 10^{10} range before flue gas treatment (Saha et al., 2021).

After flue gas treatment the concentrations reaches to 10^5 which is still a higher concentration compared to the background conditions concentrations 10^3 (Shrestha et al., 2016). In china a full scaled coal fired power plants were chose for the study and found that the concentration of emission which was 6.8 $\times 10^8$ cm^{-3} which 2 order magnitude higher concentration than the higher background PNC concentration 3.1 $\times 10^6$ cm^{-3} (Borsós et al., 2012). The electrostatic precipitator used in the cola fired power plants are capable of removing nanoparticles emission concentration from 10^8 to 10^5 due to their higher performance efficiency of PM removal (Hussein et al., 2022). Cola combustor plant indicates two or three modal concentration mainly sub 100 nm indicates that majority of the particles emitted are in the UFP range (Davulienė et al., 2022). In pre-treated flue gas the bimodal peaks are observed at 9.31 nm and 60 nm. Similarly, peak between 40 to 50 nm, for sulphur bituminous coal and ~80 nm for subbituminous coal are found in different studies(Liu et al., 2021).

2.8.4 Nanoparticle emission from cigarette smoking

Tobacco smoking emits different types of toxic substances and pollutants which causes serious health effects for active and passive smokers (Mosonik et al., 2019). In Italy the concentration of the nanoparticles reduced from 7.7 $\times 10^4$ cm^{-3} to 3.8 $\times 10^4$ cm^{-3} when smoking was banned in a public building (Wu et al., 2021). Water pipe smoking emits particle numbers 5 times higher than the normal cigarette (Fawzy et al., 2024). Detailed study reveals that one cigarette can typically produce particles of about ~ 10^{11} to 10^{12} cm^{-3} particles min^{-1} or ~10^{12} cm^{-3} particles $cigarette^{-1}$(Schraufnagel, 2020). The mean concentration of particle number emitted during the smoking of five different brands of cigarette were 3.36 ±0.34 $\times 10^{11}$ cm^{-3} and similar studies also reports the concentration of about 3.8 $\times 10^{11}$ cm^{-3}. Total particles emitted by a single cigarette concentration ranges from 0.64 ±0.19 $\times 10^{12}$ particles $cigarette^{-1}$. Few studies report elevated concentration of nanoparticles in the indoor environment which is 2.7 $\times 10^4$ cm^{-3} which is 1.5 times higher than the background concentrations. Another study (Dijk et al., 2011) reports elevated concentration of 2 $\times 10^5$ cm^{-3} to 3.5$\times 10^6$ cm^{-3}. Studies also found that the peak concentration attained during smoking lasts for 20 minutes and it takes 300 minutes to attain the original background concentration (R. Fuller et al., 2022). The results suggest that the smoking nanoparticles emission not

only releases different types of toxic substance into the atmosphere but also, they emit higher concentration of atmospheric nanoparticles which are very harmful especially in the indoor environments.

2.8.5 Nanoparticle emissions from cooking

Cooking activities are found in residential areas, commercial restaurants and open cooking(Xiang et al., 2021). Cooking activities with solid fuels and biomass are know from emission of different types of pollutants but the gas fuels and electric stoves are used widely globally and their emissions are known less (Tang and Pfrang, 2023). During cooking process, the nanoparticles are formed due to the incomplete combustion of food, oil and fuel. Studies revealed that during cooking process the concentration of the PNC increases around 1 to 30 times compared to the background which influences the indoor PNC concentration by 15 times (Pokhrel et al., 2015). During cooking process such as steaming, frying, boiling and type of meal cooked such as vegetables, rice and meat also influences the particle number concentration. Stir frying increases particle concentration about 85 times higher than the normal concentration (Lenz et al., 2023). During cooking process, the concentration increases from 9.1×10^{3} cm^{-3} to 7.7×10^{5} cm^{-3}. Frying of chicken increase particle concentration from 3.7×10^{3} cm^{-3} to 3.6×10^{5} cm^{-3} rapidly (Sun and Singer, 2023). The concentration of the nanoparticles changes also based on the different cooking styles such as Indian, Italian, Chinese and American cooking activities (Kang et al., 2023). The stir-frying method is considered to be the most nanoparticle emission cooking methods (Zhang et al., 2021). During cooking hours, the concentration in households increases by 10-fold times in living room and 20 to 40 times in kitchen (Kuye and Kumar, 2023). Summary of different cooking related studies shows the concentration of the cooking activities varies between a concentration of 1.5×10^{6} cm^{-3} to 5.6×10^{6} cm^{-3} concentration of particles (Gabdrashova et al., 2021). The emission rates during cooking varies between 0.35×10^{11} min^{-1} and 7.3×10^{11} min^{-1}. Emission rates for stoving activity is 51.4×10^{11} min^{-1} and for toasting it was 16.7×10^{11} min^{-1}. During cooking activity, the nanoparticles emissions are varies based on the type of fuel used, food type, cooking method and type of cooking stoves (Delapena et al., 2018). Gas based cooking and electric stove both produce higher number of nanoparticles at high temperature

cooking (Gould et al., 2020). Compared to frying technique, boiling way of cooking was found to emit lesser particles. All the different types of cooking emit particles in the size range of particles < 100nm (Kota et al., 2022). The cooking activity in urban regions are also one of the major sources of urban nanoparticles concentration from the non-exhaust sources which has influence on both indoor and outdoor nanoparticles concentration (Zhang et al., 2022).

2.8.6 Break wear and tyre wear nanoparticles emissions

Tyre wear and break wear are important non exhaust sources of emissions from the transportation sector (Kumar et al., 2013). In urban regions the concentration of these emission contributes significant amount of emissions to the total emission. The nanoparticles emission from the tyre wear is based on the speed of the vehicle, type of tyre and road condition. In laboratory condition at a fixed speed of 50km/hr and 70 km/hr the nanoparticles emission ranges from $4\text{-}30\times10^{11}$ km^{-1} for studded and non-studded tyres. The break wear emission emits heavy metal particles such as Fe, Cu, Pb and Zn nanoparticles which are more toxic in nature. The tyre emissions emit highly carcinogenic volatile compounds such as PAHs (Harrison et al., 2018). More break wear emissions are observed in corners, traffic junctions and pedestrian crossing zones. Studies shows that the contribution of wears to the particulate matter is around 16 to 55% in the urban regions and in highways the contribution is ~3%(Kwak et al., 2014). Similar phenomenon will be applicable for the nano emissions from the wear because in urban regions frequent breaking is used compared to the highways. Recent study estimated the payment tyre interface concentration was 2.5×10^{4} cm^{-3} which is ten times higher than the background concentration ($1\text{-}2\times10^{3}$ cm^{-3}). The mean particle emission ranges from 15 to 50nm which is similar to the exhaust emissions of light motor vehicles. The size distribution showed a peak concentration between 20 to 50nm. The exhaust emission is reducing in urban regions due to change in combustion methods, increasing fuel quality and EV vehicles whereas for non-exhaust the wear emissions are unregulated and keep on increasing due to the increase in vehicle density and congestion.

2.9 Urban Indoor Nanoparticles concentration

Nanoparticles emissions in indoor is more vulnerable than the ambient nanoparticles concentration (Nazaroff, 2023). Majority of the time is spent in indoors compared to the outdoors. The major indoor sources include cooking, smoking, hair dryers, use of incense sticks and photo copiers (Kulshreshtha et al., 2008). The detailed summary of cooking and smoking are mentioned in the above sections and in this section other indoor sources are discussed (Okam et al., 2024). In indoor cleaning activity also contributes for indoor nanoparticles exposure (Vicente et al., 2024). After smoking and cooking usage of air fresheners were considered to be the highest particle number concentration contributor (Datta et al., 2017). Burning of candles increases a concentration of particles 10^6 cm^{-3} (Zou et al., 2024). Cleaning produces concentration of about 10^5 cm^{-3} (Jeong et al., 2023). Steam ironing activity emits more particles compared to ironing without steam (Kulshreshtha and Khare, 2010). In Indoor heating activity was the least nanoparticle emitter in indoor sources (Chen et al., 2020). Fire places have a mean concentration of about 68.5×10^3 cm^{-3} during closed fires and 128×10^3 cm^{-3} during open fires (Pipal et al., 2021). In case of electric heaters different peaks were observed for different manufactures and among them higher concentration was observed for air blow heaters and lower particle concentration was for oil filled heaters (Madureira et al., 2020). Usage of hair dryers generates concentration of particles around 5.3×10^4 to 2.5×10^5 cm^{-3} with a particle peak attaining between 10 to 25 nm (Kulshreshtha and Khare, 2011). Printing activity in indoor emits mean particle concentration of about 10^4 cm^{-3} for 3D printers and for laser printing in indoors for more than 10 pages results in emission concentration of 0.6 to 1.9×10^5 cm^{-3} particles and the concentration decreases when measured at a distance more than 2m from the printers. The domestic activities in indoors also emits different types and concentration of nanoparticles and their size distribution also varies based on their source.

2.10 Role of vegetative barriers on nanoparticle concentration

The fate of nanoparticles from the roadside environment is effectively prevented by the existing topography of the region (Cusack et al., 2013). The topography includes

natural and artificial means such as vegetative and building environment. The vegetative barrier is the cost-effective method and showed a significant reduction of particle number concentration in the nearby micro environment (Nøjgaard et al., 2012). Various research studies found that the vegetative barrier in the roadside microenvironment acts a barrier for the air pollutants preventing it from dispersing in the nearby environment (Mohan et al., 2024). The role of vegetative barrier on nanoparticles reduction is still a grey area to research and having lot of potential scope in future. Very few studies are conducted in this direction and found interesting results (Dasappa and Camacho, 2021). During a low wind condition of <0.5 m/s the concentration of the particle number concentration reduced to around 37.7 to 63.6 % due to the vegetative barriers in the downwind condition (Ghei and Sane, 2018). Similarly, another study found that the efficiency of the vegetative barrier depends on the thickness of the vegetative barrier (Kanawade et al., 2014). Based on the wind direction and speed the efficiency of the vegetative barrier varies and it not only helps in reducing the concentration of the nanoparticles but also plays a major role in reducing the Respiratory Deposition Dose of an individual from 36 to 80% (Zheng et al., 2021). The results of all the studies suggest that the efficiency of the vegetative barrier increase when they are placed at the downwind condition (Fangqun, 2010). The performance efficiency of the vegetative barriers is found high when compared with the solid barriers such as buildings due to the higher surface area of the vegetation which helps in dry deposition of the nanoparticles (Fatima et al., 2022). Studies revealed that the vegetative barriers installed on the roadside environments are not only successful in reducing the particle number concentration of the nanoparticles but also useful in reducing the co pollutants such as BC which also emitted in higher concentration from the transportation sector in the urban regions(Mohtar et al., 2018).

2.11 Nanoparticle measurement and detection techniques

Nanoparticles emitted in the atmosphere have wide range of shape, structure, size distribution and composition (Manigrasso et al., 2020). Measurement of this nanoparticles are challenging but due to the recent advancements in instrumentation there are several instruments with different principles are found for the measurement of these nanoparticles (Hu et al., 2017). The concentration of the nanoparticle's

changes with distance from the source in this regard the concentration of the nanoparticles inside the engine exhaust is more and the temperature of the plume will be high even the measurement of PNC in that condition is also possible due to the advance instruments (Almeida et al., 2015). The European commission provides the regulation for the vehicle exhaust emission standards (Gómez-Moreno et al., 2011). In nanoparticle measurement techniques measurement through aerodynamic diameter and electrical mobility are the two most commonly used measurement technique by the researchers globally (Jianhua et al., 2005). However, the efficiency of the measurements changes from manufactures to manufactures and from one principle to different principle (M. Tiwari et al., 2014). There major parameters of the nanoparticles which needs to be measured are concentration, size distribution and physiochemical properties (Casquero-Vera et al., 2022).

2.11.1 Gravimetric Concentration measurement

The concentration measurement of the nanoparticles in the urban regions are done for both mass and number concentration (Kumar et al., 2008b). The mass measurements of the nanoparticles are done using a different types of cascade impactors where the filter papers are used for the collection of the dust particles (Herr et al., 2021). The mass measurement provides a specific size cut off range for a different range of size bins which are arranged stage wise allowing air particles to enter each stage and get collected on the impactor (Patel et al., 2021). The instruments use a different size cut off range based on the different manufacturer and the even customisable size ranges and a single pump for maintaining the air flow in the impactor (Dumka et al., 2018). The cascade impactor provides non-real time data and statistically not significant for lesser sampling period (Sarangi et al., 2018). Conventional impact factors are not favourable for the measurement of particles < 0.4 µm. Dekati Low pressure impactors are used for the measurement of particle size ranges from 10 nm to 10µm. Micro orifice uniform distributed impactor with a wide sample flow rate of 10 to 100L/min are capable of measuring particles from >30 nm to <2500 nm. The impactor collects the dust on a quartz plate which can be further used for physiochemical analysis (Li et al., 2013).

2.11.2 Optical measurement

In the detection technique of atmospheric nanoparticles employ light beam scattering, absorption principles (W. C. Lee et al., 2014). The light scattering and absorption measurements are used for real time measurements. The light scattering method in which the scattered light is absorbed at the receiver (Buonanno et al., 2014). The deviation of the light sources in the receiver end is based on the particle size present in the pathway (Baldauf et al., 2013). When the light source is emitted in the measurement chamber the particles present in the chamber scatters the light the angle of scatter and the photometer detects the scattered light (Ma and Birmili, 2015). The number concentration of the particles is detected through the count rate and the size is determined through the pulse height variation(Weichenthal et al., 2016). Commercially available light scattering based instruments can detect particles from few nanometres to several hundred micro meter particles with different measuring angles such as 30º, 45º, > 90º based on the technology used (Tiwari et al., 2018). The instruments require proper maintenance and cleaning of the particle counting chamber for more reliable data (Babu et al., 2016). The optical particle counters and condensation particle counters are widely used light scattering technique instruments in atmospheric nano particle measurement instrument. The condensation particle counters (CPC), based on this light scattering principle is the most commonly used instrument for the lower size nano particle measurements such as ultrafine particles. However, the atmospheric nanoparticles have a detection limit due to its lower size so there is a condensation chamber is used to grow the size of the nanoparticles using a condenser (Cong et al., 2017). The condensation solution such as butanol or distilled water is used for condensation. The other size ranges such as quasi-ultrafine particles are measured through the optical particle counters (Ezz et al., 2015). The CPC combined with a differential mobility analyser (DMA) is used for the effective size distribution measurement of the atmospheric nanoparticles (Reggente et al., 2015). The light absorption techniques are used for black carbon (BC) based ultrafine particles due to their strong correlation. The instruments such as Photoacoustic Soot Sensor (PASS) and laser induced incandescence (LII) are advanced instruments for measuring the BC based nanoparticles from exhaust or tailpipes.

2.11.3 Microbalance techniques

The ultrafine particles collected through the mass measurements are collected on surface of an oscillating element that occurs due to the change in resonance frequency (Meier et al., 2015). The microbalance is designed for the measurement of the sampled nanoparticles through quartz (Simon et al., 2017). The sampled particles are deposited on the thin quartz crystal resonator. The decrease in resonance frequency is used for the measurement of particle mass. The ambient temperature and humidity influence the concentration of the measurement (Padró-Martínez et al., 2012). The instrument mostly uses different size stages for the collection of these particles. The measured nanoparticles are further used for physiochemical analysis (Lee et al., 2012).

2.11.4 Microscopic technique

Microscopy techniques are used for examine the morphology of the measured particles (Gordon et al., 2012). The particles are collected on specific filter paper in the cascade impactor or MOUDI instruments are then magnified for microscopic analysis (Carpentieri and Kumar, 2011). The instruments such as TEM, SEM and TCP-MS are used for the wide range detection of particle morphology, radius, dimensions, and other morphological property of the particles (Fuller et al., 2012). In recent technological development there are few real-time measurements of nanoparticles coupled with TEM are also available(Cheng et al., 2019). The drawback of this technique is that this technique is suitable for solid particle analysis but not suitable for semi volatile particles due to the particle evaporation or loss during vacuum and electron beam heating.

2.11.5 Impactors technique

The cascade impactors woks of the principle of particle inertial classification. The nanoparticles are passed through series of stage filters through an array of nozzles above a solid substrate. The nanoparticles which are having aerodynamic diameters greater than the design cut point are impacted where the smaller particles follow the air flow and got deposited on different stages of impactor based on the cut diameter. The impactors efficiency is proportional to strokes number. Due to the inertia the smallest particles which pass through the final stage of the cascade impactors are not

collected. The advanced cascade impactor can collect nanoparticles from 30 nm to 10 µm. some of them are low pressure cascade impactors, Dekati low pressure cascade impactors are fee examples. The Electrical low-pressure Impactor (ELPI), is a real time high-tech impactor in which unipolar corona charges are used along with inertial classification and electrical detection. The Dekati electrical low-pressure impactors have minimum scale time of 1s with a capacity to measure particles from 7 nm to 10 µm.

2.11.6 Mobility analyser

The differential mobility analyser and scanning mobility particle sizer are the two majorly used mobility. In differential mobility analyser the sampled air is passed through a central rods outer boundary which is made up of a series of electrically isolated rings that's are linked to electrometers (Noble and Hudson, 2019). The size distribution of nanoparticles is measured by the deposition of charged particles in the ring electrode. The DMS has lower particle sensitivity than the scanning mobility particle sizer (SMPS). The sampling time resolution od DMS is (0.1 to 1Hz) so it is more commonly used in vehicle exhausts emission monitoring and dilution.

The Fast-integrated mobility spectrometer consists of a charger, size classifier, condenser and detector. The sampled particles pass through a neutralizer thereby receiving a charge distribution of bipolar equilibrium. Based on the electrical mobility charge the particles are separated into different paths. These particles are then passed through a supersaturated butanol vapor where the particle size increases their size by condensing over them (Jbaily et al., 2022).

2.12 Modelling of nanoparticles

Land use regression (LUR) models are widely used model for distribution of spatial variation of nanoparticles and aerosols (Tawiah et al., 2022). This model uses the air pollution concentration of different pollutants at different locations which spread over a larger area and they develop stochastic models through prediction functions available in GIS (Farmer et al., 2019). AERMOD is another widely used model for simulating simultaneously different shapes, characteristics and elevations based on the gaussian dispersion theory. The ADMS5 models are widely used models by researchers, which

is capable of calculating concentration of pollutants generated from all the three different sources (point, line and area sources) and maximum of 300 sources can be handles through this model at a time (Benka-Coker et al., 2020). ADMS and AERMOD have similar algorithm and the dedicated roadside pollutants are modelled using ADMS-Roads software (Singh et al., 2021). OSPM is the dedicated model used for ultrafine particles in Denmark developed by the National Environmental Research Institute. The OSPM model is used for modelling the ultrafine particles in the urban street canyon based on the turbulence and meandering effects of winds (Pokhrel et al., 2015). WRF-Chem is another widely used atmospheric chemistry models in the aerosol science for simulation of aerosols, trace gases and particulate matter. The model has two modules such as weather module and chemistry module which can be used for stimulating meteorological and chemical parameters on the different pollutants simultaneously (Kumar et al., 2022). The WRF-Chem models provides the more realistic and accurate results for aerosol prediction. During the year 2000, MONO-32 and MULTIMONO model are developed for the nanoparticle modelling. It was developed to study their properties and the use of this model is that, it can investigate the role of different emissions in determining the composition of the different sources. The model considers both gaseous and particulate emissions including the gas phase chemistry for modelling (Kesarkar et al., 2007). The model include parameters such as dry deposition loss, nucleation, condensation and inter-intra molecular coagulation parameters also. The models can be used in combination with the computational fluid dynamics (CFD) models to form an advance sophisticated model such as MPPD (Manojkumar et al., 2022). USEPA developed different models to determine the concentration of the atmospheric nanoparticles specially the R-line models are used for the roadside emissions (Zou et al., 2024). The R-line model helps in estimating the near road emission dispersion and its exposure to humans. This model is most suitable for the exposure risk assessment and also designed to predict pollutant concentration at the receptor side which is located adjacent to the road. The main advantage of this model is that this model have an embedded wind meander algorithm that helps to predict the dispersion of the pollutants in all the different directions based on the light and variable winds (Estévez-García et al., 2020). The GAM models are widely used model the prediction of atmospheric nanoparticles. The GAM model was

developed by Hastie and Tibshirani which was latter modified by the Wood (Steenland et al., 2018). This model is a hybrid model which have features of both LUR and R-line model. In this model the time series estimation and spatial characteristics while representing the nonlinear relations are widely used by different researchers (Lorelei de Jesus et al., 2020). Previously the GAM models are used for the single point sources and mobile monitoring sources with less temporal coverage but in recent days with the advancements in the model helps to estimate the different process of the atmospheric nanoparticle process such as nucleation, deposition, dilution and long-range transportation. The Artificial Neural Networks and machine learning tools are used for modelling large data sets with different parameters along with the atmospheric nanoparticles (Jung et al., 2023; Xu et al., 2020; Wu et al., 2024).

2.13 Health impacts of nanoparticles

The health impacts due to the exposure of atmospheric nanoparticles are developing research area (Salvi and Apte, 2016). Very few epidemiological studies are done in examining the mortality and morbidity of the atmospheric nanoparticles (Kwon et al., 2020). The atmospheric nanoparticles are smaller in size, mass and their deposition and clearance are totally different from larger size particles (Figure 2.3) (Singh et al., 2019). The deposited particles in the human body is governed by diffusional mechanism and the atmospheric nanoparticles are expected to translocate within the body due to their smaller size (Deng et al., 2019). The deposition estimation of the atmospheric nanoparticles is expected to be in the alveolar region and they are potential to enter the blood stream (Shupler et al., 2024). Very few experimental studies proved the translocation of atmospheric nanoparticles in the blood streams of the human body. Based on the exposure time the health impacts of the atmospheric nanoparticles are determined (Saha et al., 2024). Short term exposures to atmospheric nanoparticles can cause cardiovascular health problems as well. The atmospheric nanoparticles after inhalation can penetrate deep into the respiratory system such as lung tissues. Recent studies revealed that the human alveolar macrophages can’t able to remove the particles less than 70 nm causing the particles to translocate in the blood streams (Rentschler and Leonova, 2023). The translocated nanoparticles are transferred from the lungs to the liver and their depositions are found in the liver after

the exposure. The exposure to these atmospheric nanoparticles also causes sequential lung inflammation (Velasco and Tan, 2016). Few epidemiological studies (Kwon et al., 2020; Xu et al., 2021; Yu et al., 2022) showed inconsistent results on comparing the particle exposure and mortality rate.

Recent study in UK estimated an average loss of about 6 months life expectancy occurs due to the resident's exposure to $PM_{2.5}$ and such studies are not found extensively for the nanoparticle's exposure (Morales Betancourt et al., 2017). The toxicity of the atmospheric nanoparticles due to their characteristics such as shape, concentration, size distribution, surface area, volume and other characteristics such as chemical composition, surface chemistry, surface charge and crystal structure are hard to find the suitable metric to quantify the human exposure (Joodatnia et al., 2013). Few studies suggest the surface area is the suitable metric for health impact assessment and few suggest the concentration (Bouma et al., 2023). The particles with higher surface area to mass ratio have great contact area for materials to interact with biological surfaces (Manojkumar et al., 2021). Majority of the toxicology studies proved that the number and surface area pose a great effect on human health.

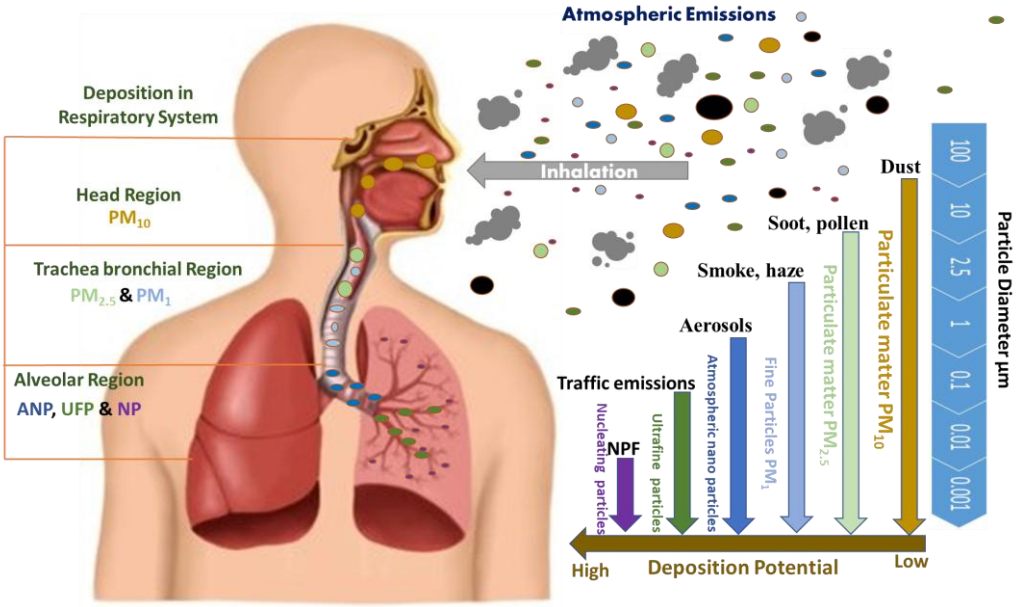

Fig 2.3 Deposition of different size pollutants in the respiratory system

Due to lack of long-term studies such as $PM_{2.5}$ there is very less evidence of nanoparticles health effects. The atmospheric nanoparticles have great potential for

harming health but its precise function is still unknown for many diseases (Goel and Kumar, 2015). The roadside environment in the urban region is one of the major hotspots for atmospheric nanoparticles which is having higher concentrations compared to the background regions. Many developing cities are found in the Asian regions compared to Europe and united states, that have higher potential risk due to their high number concentration. The children's and old age people are more vulnerable to the exposure of these nanoparticles which causes respiratory and cardiovascular illness (Gould et al., 2020).

The deposition efficiency of the nanoparticles in the human respiratory system are not uniform due to their different particle sizes. The higher size particles are deposited in the head air way region and the lower size particles are deposited in the alveolar region (Manojkumar and Srimuruganandam, 2021b). The atmospheric nanoparticles from the traffic emissions are deposited in the epithelium cells and then transported to the central nervous system such as olfactory bulb which can cause Alzheimer's disease and other brain disease (Gabdrashova et al., 2021). The transport emissions are responsible for the decreased cognitive function in elderly people (Zhu et al., 2016). The reduced particle size and increased surface area has adverse toxicity in air pollution related health effects (Delapena et al., 2018). Due to their higher surface area the atmospheric nanoparticles can have high capacity to absorb the organic gases and heavy metal elements as well which grows further due to the agglomeration. The particles with low mass, high surface area ratio show different physiochemical properties (Bergmann et al., 2021). The unique properties of the atmospheric nanoparticles make its toxicity more complicated compared to the toxicity of other materials (Manojkumar and Srimuruganandam, 2021a). The nanoparticle exposure in the human body is mainly governed through the respiratory exposure. Respiration and adsorption are possible ways of exposure. The other ways of exposure to atmospheric nanoparticles are Respiratory tract, Derman exposure and ocular Exposure.

The atmospheric nanoparticles enter through the nasal cavity through inhalation. The inhaled nanoparticles enter the downstream airway of the lungs therefore the UFP get more interaction with lungs including trachea, bronchia and alveolus (Arub et al., 2021). The interaction of these particles goes beyond the tissue cell with mucosa. The

lungs do not have the ability to clean or filter the fine or ultrafine particles through its filtering mechanism. The human nose has a limitation for filtering atmospheric nanoparticles (Schwarz et al., 2023). The filtering capacity of the human lungs is 80% for the 1µm particles and less than 5% for particles having diameter around 100 nm during the resting period (Mosonik et al., 2019). The lungs are the most important part of the respiratory system which have direct contact with the atmosphere. The two major parts of the lungs are the airways and the alveolar structure. The alveolar region contains a monolayer epithelial cell which can increase the possibilities of the atmospheric nanoparticles entering into the blood gas barrier (Badami et al., 2024). The nanoparticles are not capable of penetrating the light junction of the cells due to their size but can enter through the epithelial cell body. It can also be transported into the cell cytoplasm due to the passive diffusion. For higher size particles the particles enter into the cell directly. The nanoparticles after crossing the blood-gas barrier enters the blood circulation and gets contacted with the extra pulmonary tissue cell. The cell interaction or deposition of the nanoparticles can cause reactive oxygen species (ROS). The circulation of the nanoparticles in the human body increases it toxicity and inflammation compared to the other size particles (Klemm et al., 2022).

The alveolar region has the highest deposition efficiency for the smaller size particles. The particles with diameter 20nm are found to have deposition potential of about 50% and the particles having concentration > 100 nm to 2.5µm are found to have 10 to 20% efficiency (Vu et al., 2017).

Multiple path particle dosimetry model is one of the sophisticated models for the estimation of nanoparticles deposition in the different regions of the lungs (Ma et al., 2022). The model is useful for estimating the dose of deposition. Ocular exposure is another possible way of nanoparticles exposure in the human body. The exposure occurs due to the floating of particles or through rubbing of eyes in the area. The nanoparticles can reach to the brain cells. Apart from alveolar deposition the olfactory bulb deposition is another issue for the human health risk assessment through the atmospheric nanoparticles.

2.14 Studies related to the proposed study area

Table 2.3 Summary of the works done so far in the proposed study area

Location	Type	Size range (nm)	Num. Con. ($x10^3$ #/cm^{-3})	Reference	Summary
New Delhi, India	Urban roadside	10-1000 nm	42 to 24	Rajagopal et al., 2023	This study measured the atmospheric nanoparticles concentration in the roadside environment during different emissions scenarios which shows the direct impact of transportation sector in the atmospheric nanoparticles in the road side microenvironments.
New Delhi	Urban roadside	10-1000 nm	41 to 24	Rajagopal et al., 2024	The study measured the concentration of the atmospheric nanoparticles in the roadside environment for different seasons showing winter season as the highly polluted season comparted to others.
New Delhi	Urban roadside	10-1000 nm	26-day time 24 night time	Mohan et al., 2024	The study conducted for the different hours of the day such as day time and nigh time based on the

					vehicular intensity and source variation.
New Delhi and Rani-chouri	Urban region and background region.	10-1000 nm	2.9 in background and 25 in urban regions	Mohan et al., 2024	The study conducted in different geographical variation such as urban region and background conditions.
New Delhi, India	Inside urban area	5 nm to 32µm	14.8	Jose et al., 2021	This study site is dominated by the Aitken mode particle, which follows a bimodal diurnal variation pattern, with peaks during morning and evening traffic hours. Accumulation mode particles are scarce over the study location except during the winter and post-monsoon days, when it shows a bimodal secondary peak along with the primary Aitken mode particle.
New Delhi, India	Inside urban area	10 to 800	25.52	Kanawade et al., 2020	New particle formation events study was conducted and reported higher GR rate with a

					higher concentration in Aitken and accumulation mode particles.
IITK, Kanpur, India	Inside urban area	4.45 to 736.5	10.195	Kanawade et al., 2020	The study emphasis the secondary aerosol formation process in the highly polluted urban regions.
New Delhi, National Physical Laboratory	Inside urban area	4 to 661	-	Sarangi et al., 2018	New particle formation or gas to mparticle conversion process observed during the night time in Delhi city. Which is a first of its kind in the study region.
Ooty, India	Topographically 300 m above the valley	10.9 to 461.4	2.845 ±1.184	Kompalli et al., 2018	The study analysed the concentration of the aerosol particles in the background region in the country and its size distribution.
Mahabaleshwar, India Physics Laboratory	Background 1348 m above mean	5 to 1000	21.800	Leena et al., 2017	In tropical regions, such studies are limited, especially in the Indian region

	sea level				
Trivandrum, India	Background (10KM from urban area)	15 to 15,000	~5.119 (±3.139)	Babu et al., 2016	The study identified the UFP particles burst during two different periods. First period is during the onset of land breeze event in evening or midnight. The seond event during the sunrise hours in the seas breeze.
New Delhi, India National Physical Laboratory	Inside urban area	9 to 425	37.2(event day 24.9(Non-event Day)	Sarangi et al., 2015	New particle formation study
Trivandrum, India	Background (10KM from urban area)	10 to 875	~15.900	Kompalli et al., 2014	New particle formation study during late evening and nigh hours
Hanle, India	Background	16 to 1364	~2.700	Kompalli et al, 2014	New particle formation event studies

	(~300m above the surrounding				
IITK, Kanpur, India	Inside urban area	4 to 750	-	Kanawade et al., 2014	The particle number concentrations were found to be less in Kanpur resulted in larger particle sizes creating higher condensation sinks. The mean particle mode diameter at Kanpur was larger by a factor of ~1.8 than at Pune. Generally, the particle growth rates were higher at Kanpur, whereas the formation rates were higher at Pune.
IITM, Pune India	Outskirt of Urban area	14 to 750	-	Kanawade et al., 2014	
IITM, Pune	Outskirt of Urban area	0.46 to 50	-	Siingh et al., 2013	Positive and Negative ions measurement

2.15 Summary

The detailed literature review provides information about the global studies and also the research gaps which needs to be addressed in further studies.

CHAPTER-3

METHODOLOGY

3.1 Introduction

The air quality in the global south region are deteriorating at an alarming rate. The majority of the growing urban region are located in the global south region especially in the Asian subcontinent. The rapid urbanization in these regions are responsible for the poor air quality which are generated through various process such as emission from industries, transportation sources and other sources. The air pollution in the urban regions is a complex mixture of different sources, among them transportation sources is one of the major emission sectors. The current study was conducted in the Indian subcontinent which is one of the highly populated country. Delhi city is capital of India with a population of about 33.81 million people. The population in Delhi increases at a rate of 2.63% compared to the previous year (2023). The city experiences severe pollution events and ranked among the highly polluted city globally is the proposed study region (Sharma et al., 2025). Due to its geographical location and climatic conditions the capital city experiences different pollution events. The air pollution related human health risks in the city is estimated to be around 7 million premature deaths. The Delhi city having an area of around 1483 km^2. The vehicle population in about 11 million and it is predicted to increase to 25.6 million by 2030. The personnel vehicle population in Delhi accounts for 2.9 million for cars/jeeps and 6.1 million two-wheelers. Two wheelers and cars alone contribute for around 93% of the total vehicle population in Delhi (Rajagopal et al., 2023). So, the emission from the transportation sector is one of the major sectors for the atmospheric nanoparticles emission in the Delhi city which is considered as the study region for the study.

3.2 Study location characteristics

The monitoring site is located in the North West region of Delhi city (28.75° N, 77.12° E). The region geographically falls under the Rohini District (Fig. 3.1). The measurements are done using a real-time air quality monitoring station which is located adjacent to the Delhi Technological University campus. The study aims to measure the emissions from the transport sector in the road environment so the monitoring station is placed adjacent to the road. The road where the measurements

are done is classified as state highway without central meridian. The road is a major connecting road for Delhi and Rohtak city which is located in the nearby state Haryana. The vehicle density in the selected road is around 1300 vehicles/ hr with a daily average of about 3500 vehicles. The vehicle density in the road includes different types of vehicles such as cars personnel and commercial, three wheelers, E-rickshaws, light motor vehicles, heavy motor vehicles, two wheelers, E-busses. The major commercial fuels used by the vehicles are petrol, diesel compressed natural gas and electricity.

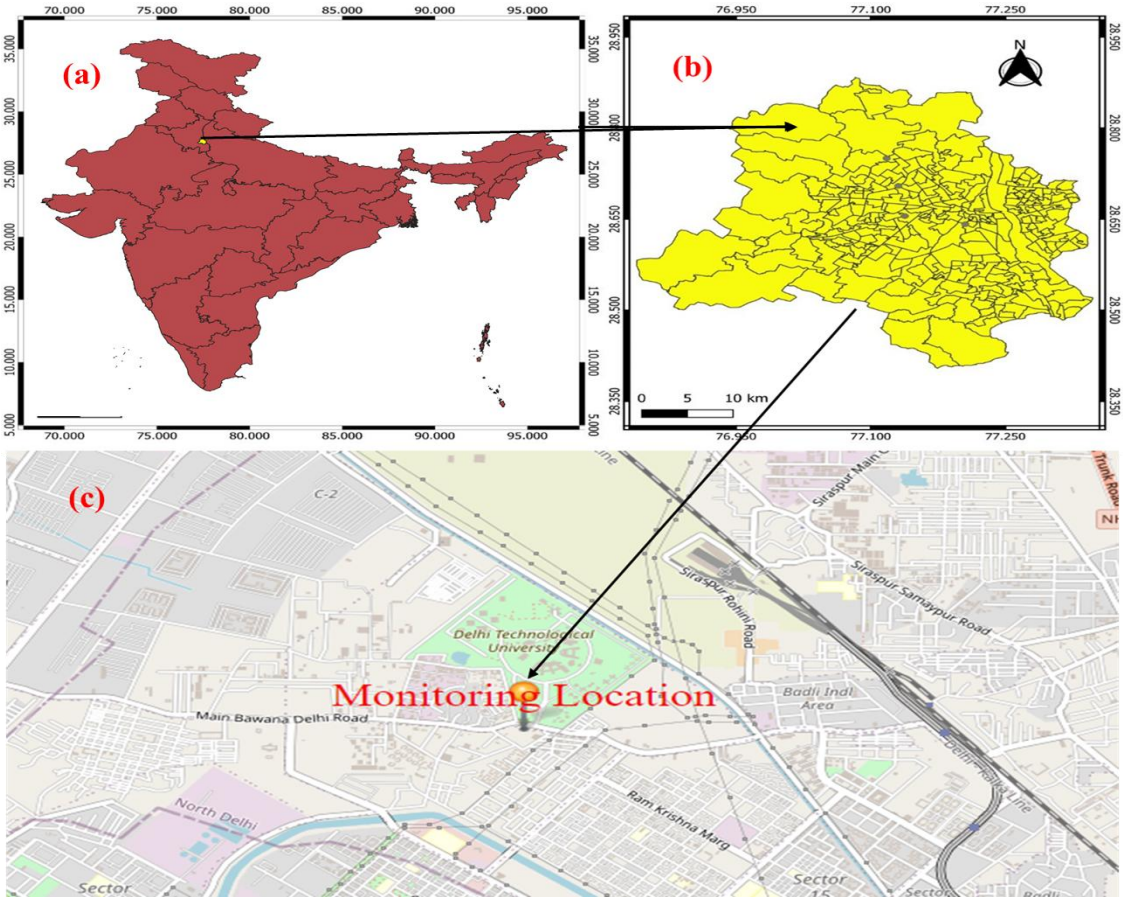

Figure 3. 1: (a) map of India with all the states of the country, (b) map of Delhi city with major road network, (c) geographical location of the study area

The sampling of the nanoparticles is done at distance < 2m from the road. The sampling was done adjacent to the pedestrian way in the road. The major sources of pollution in the study region includes waste burning, transport emissions, road dust and other sources. The location of the monitoring station provides way for the monitoring station to receive the emission from the transportation sector majorly. The study region is surrounded by different types of primary and tertiary roads.

The study region is surrounded by educational institutions, residential areas and road networks.

The region is well connected through road, rail and metro connectivity. The metro station and the railway station are located in the south east direction of the monitoring station with an aerial distance > 2km (Figs. 3.2, 3.3). Within the aerial distance of 1 km a major bus depot is located and the Indira Gandhi international air post located at the southern direction of the monitoring station. The north direction is surrounded by residential area and road network. The study region comes under the Indo Gangetic Plain region. This Indo Gangetic Plain region is known for the highly polluted region with majority of the highly urbanising cities lies in this region. The mighty Himalayan Ranges acts as barrier for the air passage in this region which resulted in accumulation of pollutants in this region.

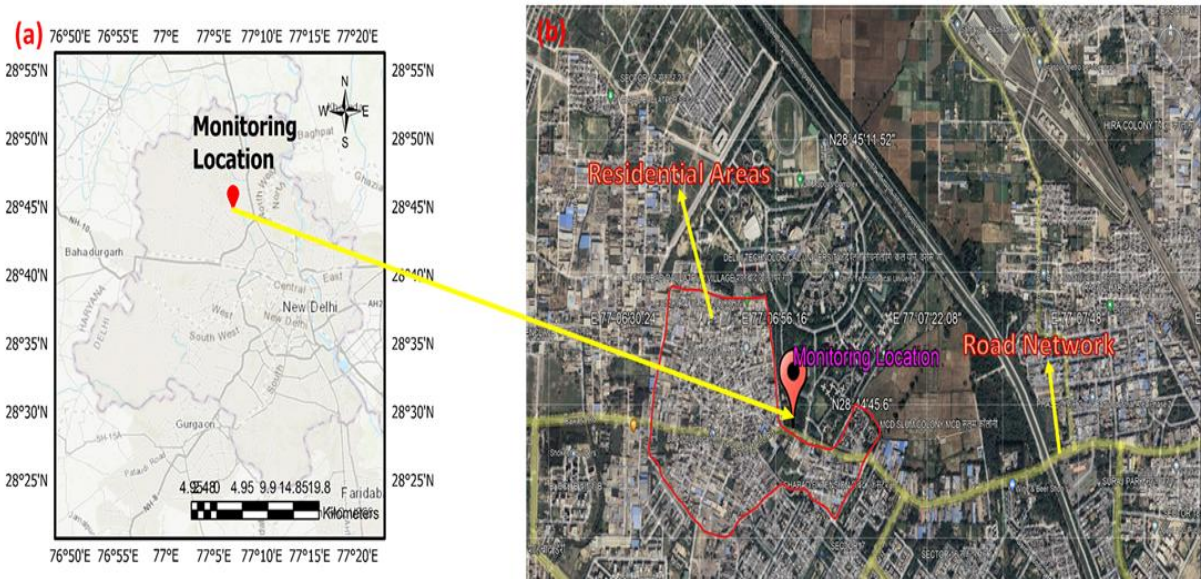

Figure 3.2: (a) Map of Delhi showing the study area, (b) Aerial view of the monitoring site with the surroundings

Figure 3.3. Picture of the monitoring station and its location

3.3 Measurement period

The measurements of the different pollutants are done for a year starting from December 2020 to November 2021 (Fig 3.4). This year long measurement includes all the major seasons of the study area and also the major events in the year. The study period also includes a emission restriction period as well which helps to identify the role of transport emissions in the study area. The data collection was done for 298 days in a year out of 365 days.

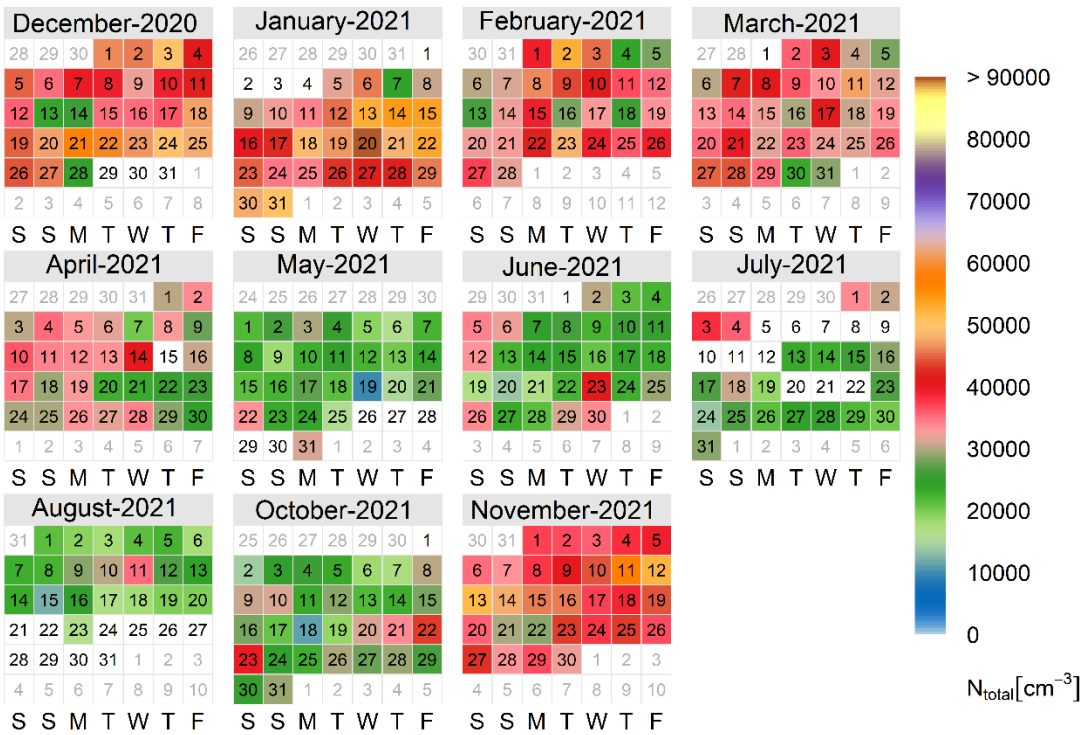

Figure 3.4 calendar plot showing the monitoring days with total PNC concentration on particular day

Based on the objectives, the study period is classified into two different types seasonally and also based on the emission episodes. The episodic classifications are based on the restriction imposed for the movement of public during the outbreak of corona virus in the year 2021. The emission episodes are classified into two major period namely, period I and II. Both the periods have three different phases: phase I will have normal scenario, phase II have an episodic event either less emission or extreme emission and phase III will be the period after the episode. These are the three sub classifications in both the periods. The period I consist of total 91 days in which the first phase consists of 20 days, 47 days in second phase and 24 days of monitoring in the third phase. Similarly, in the period II, phase I consist of 33 days, phase II consists of 8 days and phase III consist of 18 days with an overall data of about 59 days. The detailed classification of episodes and their respective phases are depicted in the Table 3.1.

Table 3.1 Classification of different periods based on the imposed restrictions.

Sr. no	Period	Time period	Phase	Total Days
1	I	1-20 April 2021	BR- Before Restriction	20
2	I	21 April – 5 June 2021	DR- During Restriction	47
3	I	6-30 June 2021	AR- After Restriction	24
4	II	3 October-4 November 2021	BD- Before Diwali	33
5	II	5-12 November 2021	AD- After Diwali	8
6	II	13-30 November 2021	DR-II- During Restriction II	18
Total Days				150

The percentage of vehicular reduction obtained during the period I and II is taken from the google mobility data of this particular region. The google mobility data provides the information about the vehicular density changes during the different phases of the year. The north west Delhi region is selected for the google mobility data analysis.

The measurement period is further classified seasonally based on Indian science academy classification. The study region has five major seasons namely winter, spring, summer, monsoon and autumn. The climatology of the study region varies greatly during different season from extreme hot summers to cold winters. The climatic conditions play a major role in determining the concentration and other secondary transformations of these atmospheric nanoparticles. The detailed time frame and classifications of the season along with the information of data available for the particular period is mentioned in the Table 3.2.

Table 3.2 Seasonal classification of the study period.

Seasons	Time period	Total number of days	Monitored days
Winter	December to mid-February	76	69

Spring	Mid-February to March	45	44
Summer	April to June	91	84
Monsoon	July to mid-September	77	41
Autumn	Mid-September to November	76	60
Total days		298	365

3.4 Instrumentation

Various instruments are used in the study for measurement of different types of the pollutants. All the instruments are kept in a fully airconditioned monitoring station. The monitoring station consist of a separate sampling channel for nanoparticles measurement and gaseous measurement. The monitoring station is equipped with continuous powers supply and the Realtime measurements are done and the collected data are stored in a computer for all the measurement. The pictures of the monitoring station are shown in the figures (Figs. 3.5, 3.6).

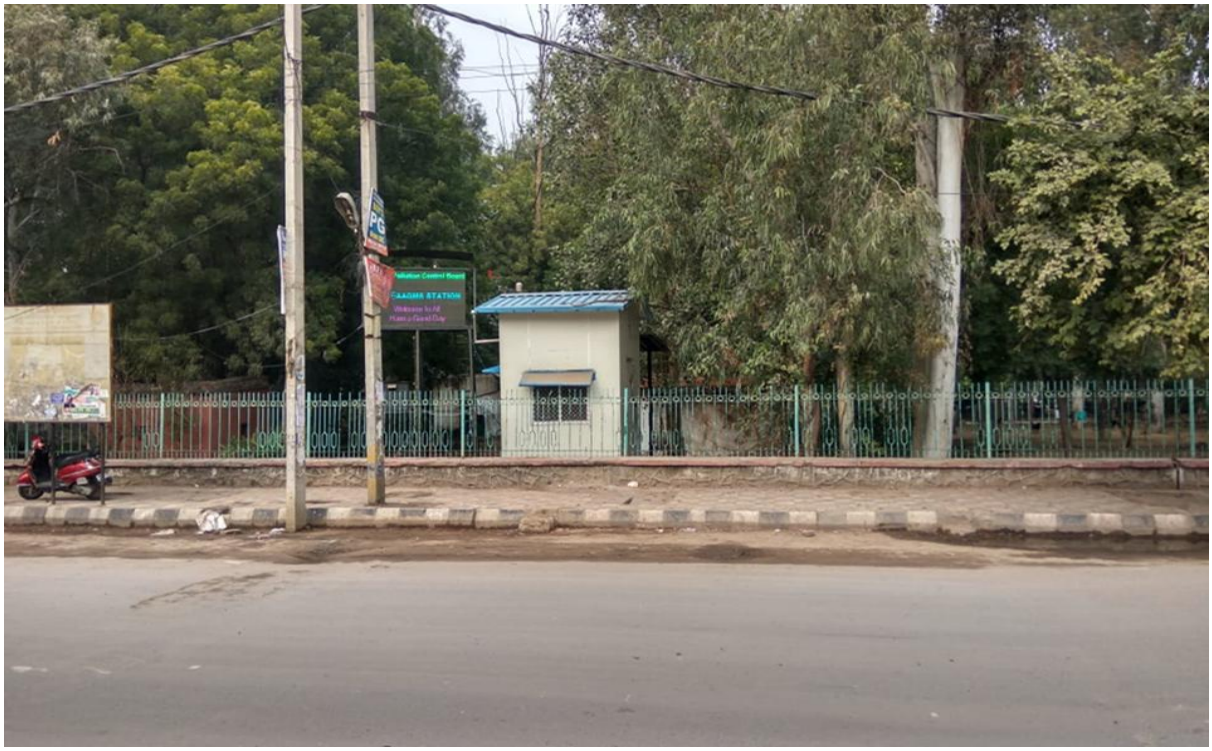

Figure 3.5 Picture of the monitoring station, located adjacent to road

Figure 3.6 Internal view of the monitoring station

3.4.1 Atmospheric nanoparticle measurement.

The atmospheric nanoparticles are measured using a scanning mobility particle sizer (SPMS +C) with condenser. The SMPS+C instrument was manufactured by GRIMM aerosol Technik GmbH & Co company. The serial number of the instrument is 54031801 (Figs 3.7,3.8). The instrument consists of a neutralizer, differential mobility analyzer and a condensed particle counter combined together. The instrument uses a Vienna type L-DMA which has capacity to measure particles from 10nm to 1090nm. The air is sampled through a diffusion dryer which helps to maintain the relative humidity of the air sample and then the sampled air is passed through a neutralizer made of made of radioactive material (Am-241). The air is then passed through a DMA consist of a length of 0.35 m. The inner diameter of the DMA is 0.040 m and outer diameter is 0.026 m. The optimum DMA temperature is 20° C and pressure is 101300 Pa. The slip factor of the instrument used is 2.83 and the effective length of the sampling probe without losses is 0.38m. The time scale for one complete cycle of measurement is ~7 minutes and the different size particles are distributed in a 45 different size segregated channels.

The size distribution calculation of the different size bin calculations is based on the Winklmayr et al. (1991) 9(d) equation and it follows the ISO 15900 standards. The size distribution calculations flows the different mathematical equations that are described below.

$$N_c(D) = \left(\frac{Q_a}{Q_{sh}}\right).\sum_{i=1}^{\infty}[\alpha(D,i).\Psi(D).F(D)]_{D=D_i} \quad - \quad (1)$$

Where, $N_c(D)$ – Total number concentration measured in CPC

D- Diameter of single charged particle that corresponds to voltage of DMA.

D_i- Diameter of the particle with i charges that correspond to voltage of DMA.

Q_a – Volume flow rate of the sample airflow.

Q_{sh} – Volume flow rate of the sheath airflow.

i- Number of elementary charges carried by the particle.

α (D_i, i)- probability of the particle to carry i elementary charges (Fuchs-Wiedensohler values).

ψ D_i – function converts diameter interval into mobility interval.

F(D)- Number size distribution at the inlet of DMA (Rajagopal et al., 2023).

Two factors are added to this formula, one is eff CPC (D) which is accountable for the efficiency of the CPC particles having size lesser than 10nm; and the second one is eff CPC (D) which considers the particle loss in the DMA. The particles with 10 different charges can be neglected for the practical assumption. Then the calculation is as follows

$$N_c(D) = \left(\frac{Q_a}{Q_{sh}}\right).\sum_{i=1}^{10}[eff\ CPC\ (D).\ eff\ DMA(D).\alpha(D,i).\psi(D).F(D)]_{D=D_i} \text{ - (2)}$$

By solving this equation F(D) is

$$F\ (D) = \frac{1}{eff_{CPC}\ (D).\ eff_{DMA}(D).\alpha(D,i).\psi(D)} \quad - (3)$$

$$\{\frac{N_c\ (D).Q_{sh}}{Q_a} - \sum_{i=2}^{10}[eff_{CPC}\ (D).\ eff_{DMA}(D).\alpha(D,i).\psi(D).F(D)]_{D=D_i}\} - (4)$$

The standard stepping mode $F(D)_{D=Di}$ can be exactly calculated for i =2 from the previously measured size channels.

Figure 3.7 Picture of the scanning mobility particle sizer

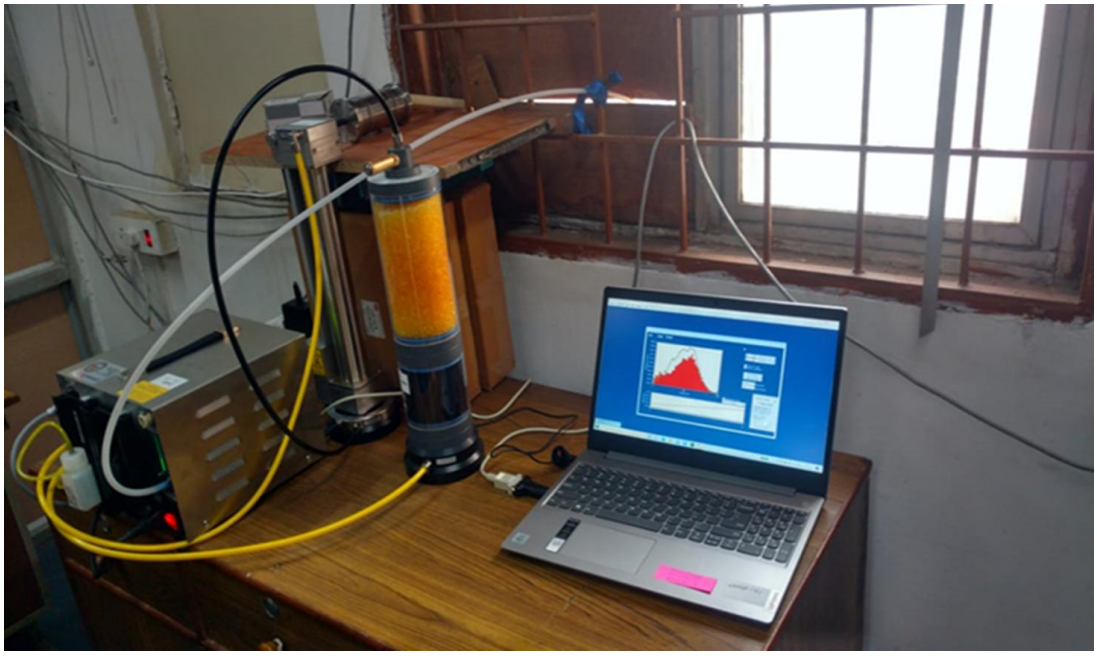

Figure 3.8 Picture of the scanning mobility particle sizer

3.4.1.1 Number distribution calculation

The different size distribution calculations are based on the following mathematical calculations given below.

The values of the size distribution of the particles (n_i) for the size interval ($_i$) was expressed in the ratio of the absolute concentration. N_i of this interval and the different size range ΔD_p. Then the equation is

$$N_i = n_i \Delta D_p - \ (5)$$

The smaller size bin taking the limit $\Delta D_p \longrightarrow$ 0 the limit ΔD_p becomes small and the values equals to dD_p. Then the size distribution are as follows $n_{\mathrm{N}}(D_p)$.

$$n_N(D_p)dD_p = \text{number of particles per cm}^3$$
$$D_p \text{ to } (D_p + dD_p) \ - (6)$$

The units of $n_{\mathrm{N}}(D_p)$ are μm^{-1} and the total particles measured in per cm^3. Then N_t is then

$$N_t = \int_0^{\infty} n_N(D_p)dD_p - (7)$$

The cumulative size distribution function $N(D_p)$ is defined as

$$N(D_p) \quad = \text{number of particles per cm}^3.$$

The actual particle in the size range

$$N(D_p) = \int_0^{D_n} n_N(D_p^*)dD_p^* \ - (8)$$

Finally, the size distribution can be expressed as

$$n_N(D_p) = dN/dD_p - (9)$$

3.4.1.2 The surface area, volume and mass distributions calculation

The properties of the measured particles properties changes based on the particle surface area, volume and mass distributions of the particles.

The total surface area of the particle measured are obtained from the equation

$$S_t = \pi \int_0^\infty D_p^2 n_N(D_p) dD_p = \int_0^\infty n_S(D_p) dD_p \quad (\mu m^2\ cm^{-3}) \text{ - (10)}$$

Similarly, the volume concentrations are based on the

$$V_t = \frac{\pi}{6} \int_0^\infty D_p^3 n_N(D_p) dD_p = \int_0^\infty n_V(D_p) dD_p \quad (\mu m^3\ cm^{-3}) \text{ - (11)}$$

The mass of the measured particles is obtained using the following calculation.

$$n_M(D_p) = \left(\frac{\rho_p}{10^6}\right) n_V(D_p) = \left(\frac{\rho_p}{10^6}\right)\left(\frac{\pi}{6}\right) D_p^3 n_N(D_p) \quad (\mu g\ \mu m^{-1}\ cm^{-3}) \text{ – (12)}$$

The mean values used in the size distribution are as follows (Table 3.3)

Table 3.3 Different calculations of the nanoparticles based on number measurements

Property	Defining relation
Number mean diameter $\bar{D}_p$	$\bar{D}_p = \frac{1}{N_N} \int_0^\infty D_p n_N(D_p) dD_p$
Median diameter D_{med}	$\int_0^{D_{med}} n_N(D_p) dD_p = \frac{1}{2} N_t$
Mean surface area $\bar{S}$	$\bar{S} = \frac{1}{N_p} \int_0^\infty n_S(D_p) dD_p$
Mean volume $\bar{V}$	$\bar{V} = i_{N_1} \int_0^\infty n_v(D_p) dD_p$
Surface area mean diameter D_S	$N_t \pi D_S^2 = \int_0^\infty n_S(D_p) dD_p$
Volume mean diameter	$N_t(\pi/6) D_V^3 = \int_0^\infty n_V(D_p) dD_p$

Surface area median diameter D_{S_m}	$\int_0^{D_{Sm}} n_S(D_p)dD_p = \frac{1}{2}\int_0^{\infty} n_S(D_p)dD_p$
Volume median diameter Dv_{m}	$\int_0^{D_{vm}} n_v(D_p)dD_p = \frac{1}{2}\int_0^{\infty} n_v(D_p)dD_p$
Mode diameter D_{mode}	$\left(\frac{dn_N(D_p)}{dD_p}\right)_{D_{\mathrm{mat}}} = 0$

3.4.1.3 Properties of lognormal distribution

The lognormal distribution of the particles is based on the following calculations.

$$n_S(D_p) = \frac{\pi D_p^2 N_t}{(2\pi)^{1/2} D_p \ln\ \sigma_g} \exp\left(-\frac{(\ln\ D_p - \ln\ \bar{D}_{\mathrm{RS}})^2}{2\ln^2\ \sigma_g}\right) - \quad (13)$$

$$n_S(D_p) = \frac{\pi N_1}{(2\pi)^{1/2} D_p \ln\ \sigma_g} \exp\ (2\ln\ \bar{D}_{PS} + 2\ln^2\ \sigma_s) \times \exp\left(-\frac{\ln\ D_p - (\ln\ \bar{D}_{PS} + 2\ln^2\ \sigma_g)]^2}{2\ln^2\ \sigma_g}\right) \quad - (14)$$

3.4.2 Gaseous pollutant measurement

The gaseous pollutants such as carbon monoxide (CO), ozone (O_3), Sulphur dioxide (SO_2) and different oxides of nitrogen (NO_x) are measured using instrument such as Horiba and 2B technologies.

3.4.2.1 CO Monitor

Horiba AP370 ambient CO monitors are used for the measurement of CO (Fig 3.9). This monitor uses the non-dispersive infrared analysis method as its principle of operation (Fig. 3.10). The instrument is capable of measuring continuously. The instrument can measure the concentration such as rolling average and momentary values. The measured data can be collected through the RS232 cable. The instrument can detect the CO concentration in the air sample having temperature from 5°C to 40°C. The flow rate of the instrument is 1.5L/min for air sample and for calibration

gas it was 2.5L/min. The response rate of the instrument is 60s. The minimum detection limit of the instrument is 0.05 ppm, zero drift varies from ±0.1ppm/24hr. The linearity of the instrument is ±1.0% with a minimum time scale of 3 minutes.

Figure 3.9 Picture of the Horiba AP370 CO monitor

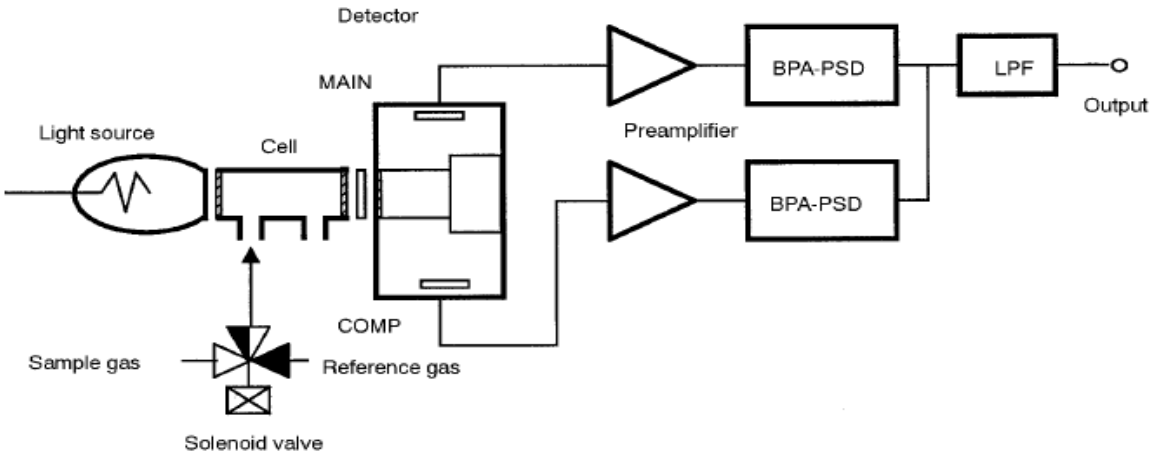

Figure 3.10 Circuit diagram of the instrument Horiba AP370 CO monitor

3.4.2.2 SO_2 Monitor

Horiba AP370 ambient SO_2 monitors are used for the measurement of SO_2 (Fig 3.11). This monitor uses the ultraviolet fluorescent and non-dispersive infrared analysis method as its principle of operation (Fig 3.12). The instrument is capable of measuring

continuously. The instrument can measure the concentration such as rolling average and momentary values. The measured data can be collected through the RS232 cable. The instrument can detect the SO_2 concentration in the air sample having temperature from 5°C to 40°C. The flow rate of the instrument is 1.5L/min for air sample and for calibration gas it was 2.5L/min. The response rate of the instrument is 60s. The minimum detection limit of the instrument is 0.05 ppb, zero drift varies from ±0.1ppm/24hr. The linearity of the instrument is ±1.0% with a minimum time scale of 5-minutes.

Figure 3.11 Picture of the Horiba AP370 SO_2 monitor

During measurement when the sampled air is irradiated with UV ray (215nm), the SO_2 pollutant emits light of different wavelengths such as 320, 240 and 420nm) from the irradiated light. The irradiated light is referred as excitation light and the emitted light is referred as fluorescence. This method of absorbing the fluorescence intensity is known as fluorescence method. The fluorescence is usually detected at right angles to prevent interface from the excitation light which emits in all the direction.

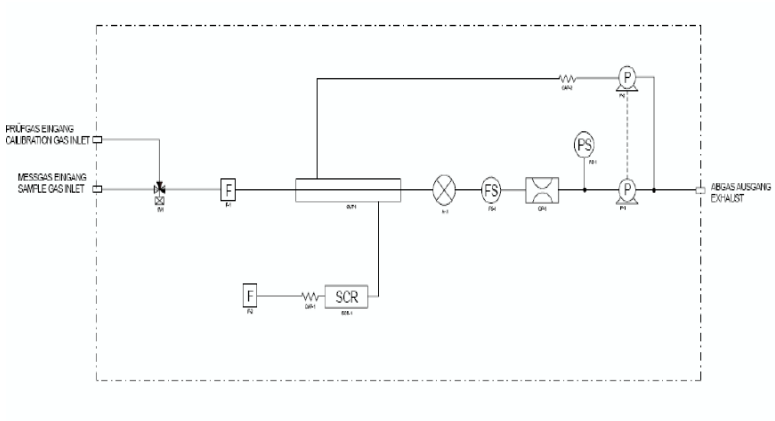

Figure 3.12 Circuit diagram of the instrument Horiba AP370 SO_2 monitor

3.4.2.3 $NO/NO_2/NO_X$ Monitor

The model 405nm NO_x monitor is an instrument used for the direct measurement of atmospheric nitrogen dioxide, nitric oxide and as well as the total reactive oxides of nitrogen ($NO_x = NO+NO_2$) (Fig 3.13). The concentration ranges from 0 to 10 ppm for NO_2 and 0 to 2 ppb for NO (Fig. 3.14). The instrument can measure the pollutants with high precision and accuracy. The NO_2 measurement is based on the direct absorbance at 405 nm. NO is measured by selective conversion with ~ 100% efficiency with a highly selective reaction of NO with Ozone (O_3). Total NO_x is obtained by addition of NO and NO_2. The long-life pump of the light source is ~15,000 hours with an internal data logger. The operating temperature of the instrument is 10° to 50° C. The minimum flow rate of the instrument is 1.4 L/Min with a maximum flow rate of 1.6 L/min. The data can be obtained for 5s, 1min, 5min and 1-hour interval.

Figure 3.13 Picture of the $NO_2/NO/NO_x$ monitor

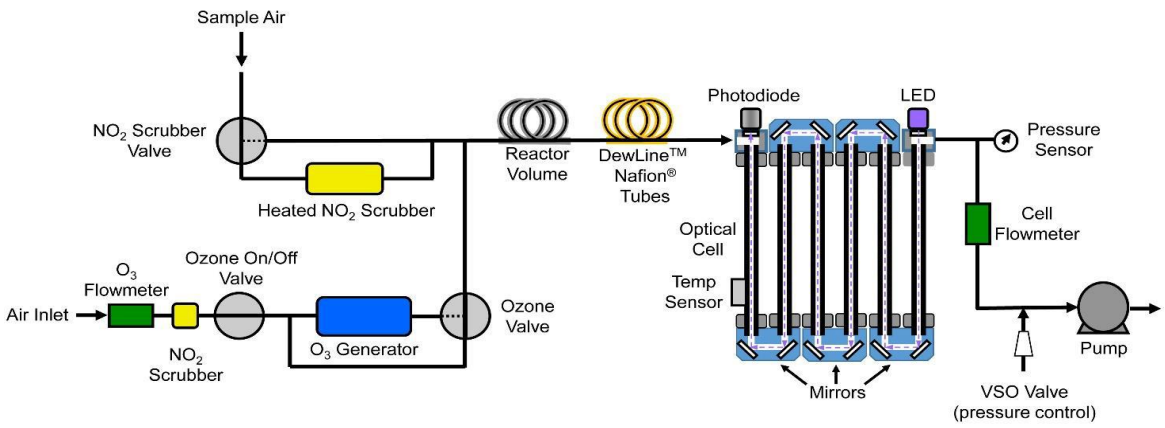

Figure 3.14 Circuit diagram of the $NO_2/NO/NO_x$ monitor

3.4.2.4 Ozone Monitor

Figure 3.15 Picture of the 2B Technologies O_3 monitor

The 205 2B technologies O_3 monitor makes use of dual beam technology (Fig 3.15). In this dual beam technology, the UV light measurements are made simultaneously with both ozone-scrubbed air and un scrubbed air. The instrument uses UV based O_3 measurements are one of the fastest measurement techniques available in the market.

The operating temperature of the instrument is 10° to 50° C (Fig 3.16). The Nominal flow rate of the instrument is 1.8 L/Min. The data can be obtained for 10s, 1min, 5min and 1-hour interval.

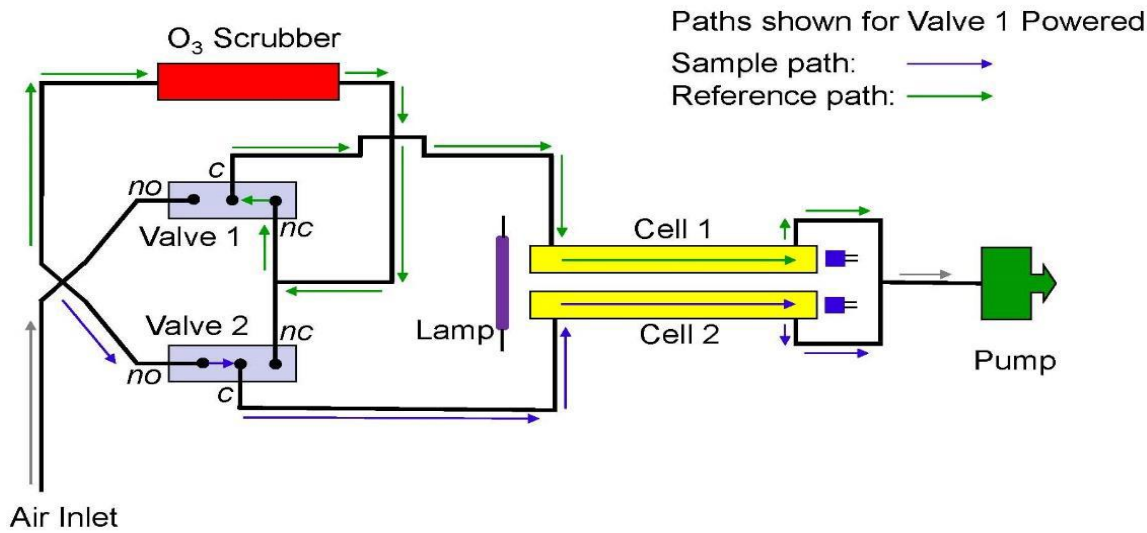

Figure 3.16 Circuit diagram of the 2B Technologies O_3 monitor.

3.4.3 Meteorological measurement

The meteorological parameters such as wind speed, wind direction, relative humidity and temperature are measured using the Amil make sensor which has an accuracy of ± 5% and sensitivity 0.5% (Fig 3.17). The weather station is fully automated and real-time instrument.

Figure 3.17 Picture of the automated weather station

3.4.4 Secondary data collection

The secondary data's such as solar radiation, planetary boundary layer is taken from the open source data sets. The solar radiation is taken from the central ambient air quality monitoring station which is located at an aerial distance less than 500 m from the study region. Similarly, the planetary boundary layer height for the study region during the different season is taken from the ERA5 reanalysis data with an interval of 1-hr with a resolution of 0.25º × 0.25º. The both primary and secondary data are taken from well validated sources for minimal errors and used in the study.

3.5 Data analysis and visualization

Data analysis is done using different software such as R Software, Origin software, MATLAB software and the health impact assessment are done using the mathematical and computational models.

3.5.1 R software

R software (version 5.12.8) is one of the widely used programming language used for statistical analysis and data visualization (Fig. 3.18). This is an open source software which is freely available under general public license. The software has excellent

features in data mining, calculation, graphical display of the data, handling of multiple data sets parallelly. This software has a wide range of libraries in which different libraries are used for various different functions. The most widely used library for the air pollution data analysis is the open-air package. This software is available for different operating system and it has a good community support. The software has different types of resources available for the learning and troubleshooting the issues. This salient feature makes it a versatile software for usage (https://cran.r-project.org/doc/contrib/Paradis-rdebuts_en.pdf).

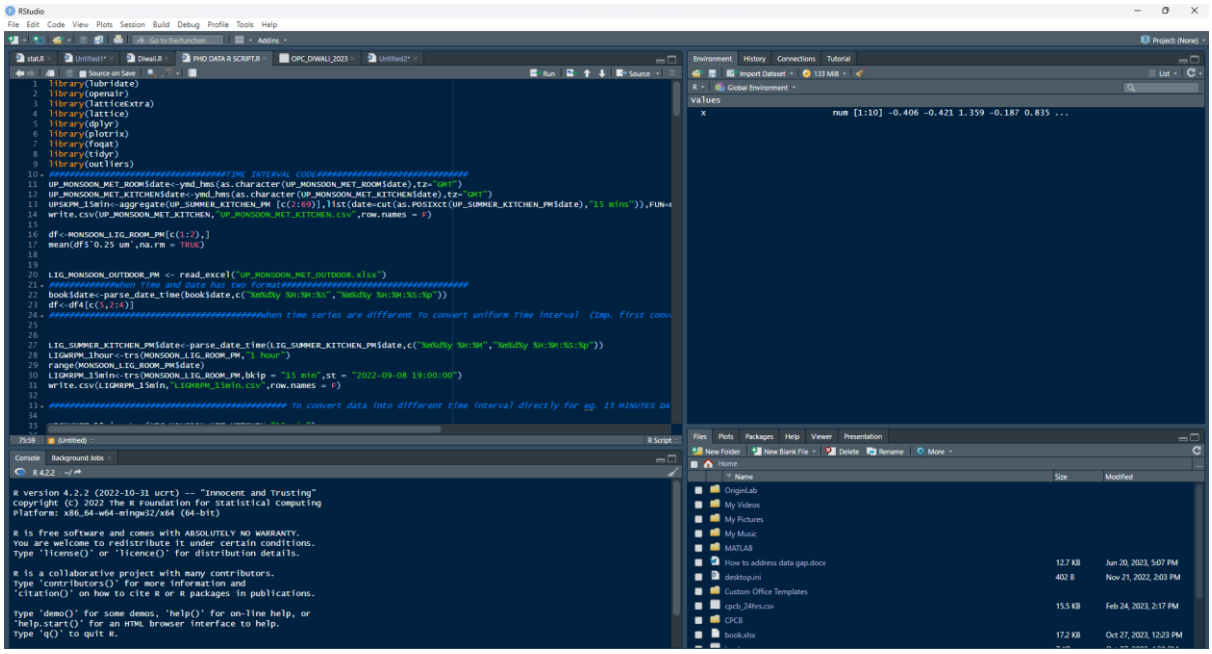

Figure 3.18 Picture of R software platform

3.5.1.1 Open air package

Open air package was developed by Carslaw D.C. and K. Ropkins for analysing the different air pollutants for multiple data (Fig 3.19). The open-air package provides sophisticated analysing tools such as wind rose, pollution rose. The advance tools such as bivariate polar plots and condition probability functions for identifying the different pollution sources. The package provides access to the NOAA trajectories as well for the analysis. The detailed manual for the open-air package are found in (https://davidcarslaw.com/files/openairmanual.pdf).

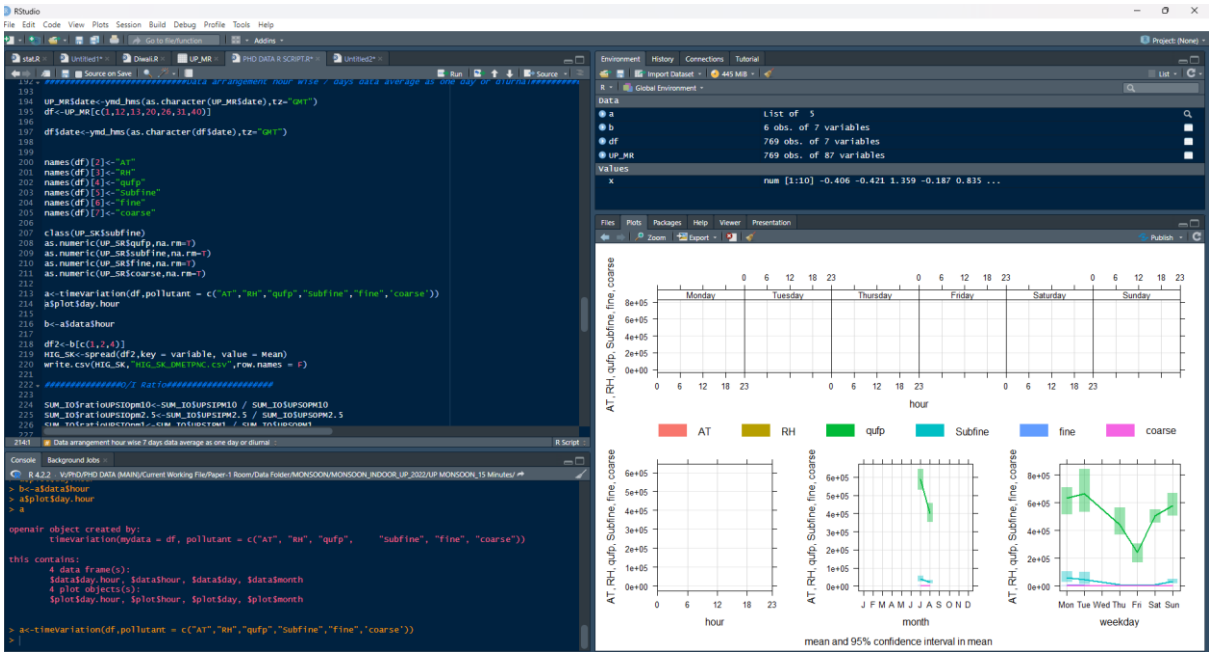

Figure 3.19 Data visualization in R platform

3.5.2 MATLAB software

MATLAB is a tool used to analyses, visualize and handle different types of air quality data (Fig 3.20). The software can be used for creation of plots, dashboards etc (Fig 3.21).

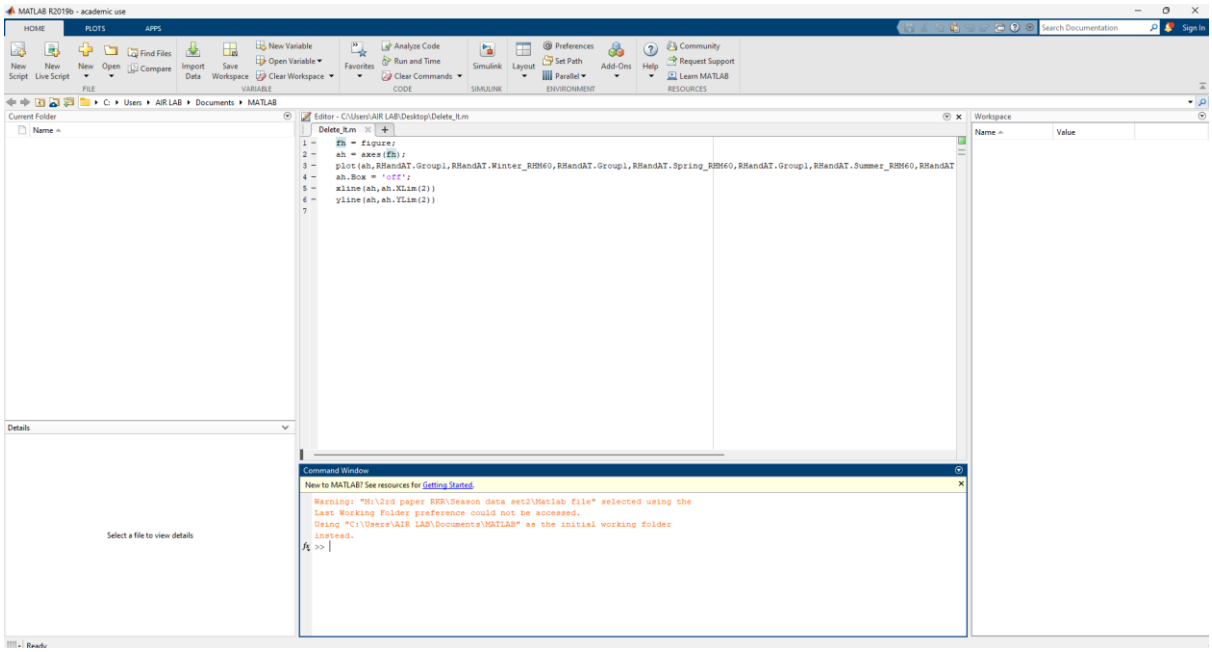

Figure 3.20 Picture of MATLAB software with data feeding window

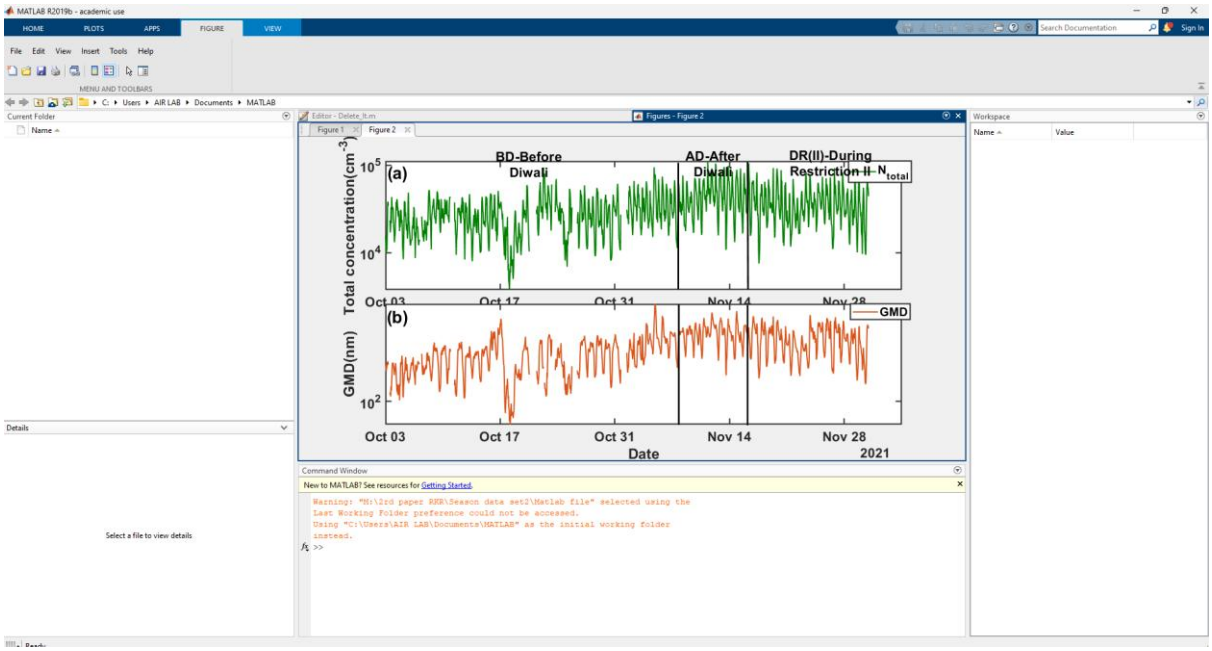

Figure 3.21 MATLAB data outputs and visualization

The timeseries data analysis, heatmaps can be created using the air quality data in MATLAB. MATLAB can be integrated with IOT platforms to analyze data real time using the sensors. The software can be used for prediction of air quality using machine learning tools. Regression analysis can also be performed using the MATLAB. This software is used for data analysis and visualization in the study. The version used in the study is 2016a.

3.5.3 ORIGIN software

Origin is a data analysis and graphing software which was developed by Origin Lab corporation (Fig 3.22). Origin software is helpful in plotting 2D and 3D plots. This software is useful in data analysis such as statistical analysis, signal processing and curve fitting. Curve fitting uses Levenberg-Marquard algorithm in this software. In origin programming languages such as python and R functions are enabled and also scripting language like Lab Talk. In origin different data formats such as Net CDF, excel and ASCII text formats. The output of the origin can be taken in formats such as JPEG, PNG and TIFF files. This study used Origin 2022 version for analysis (Fig 3.23).

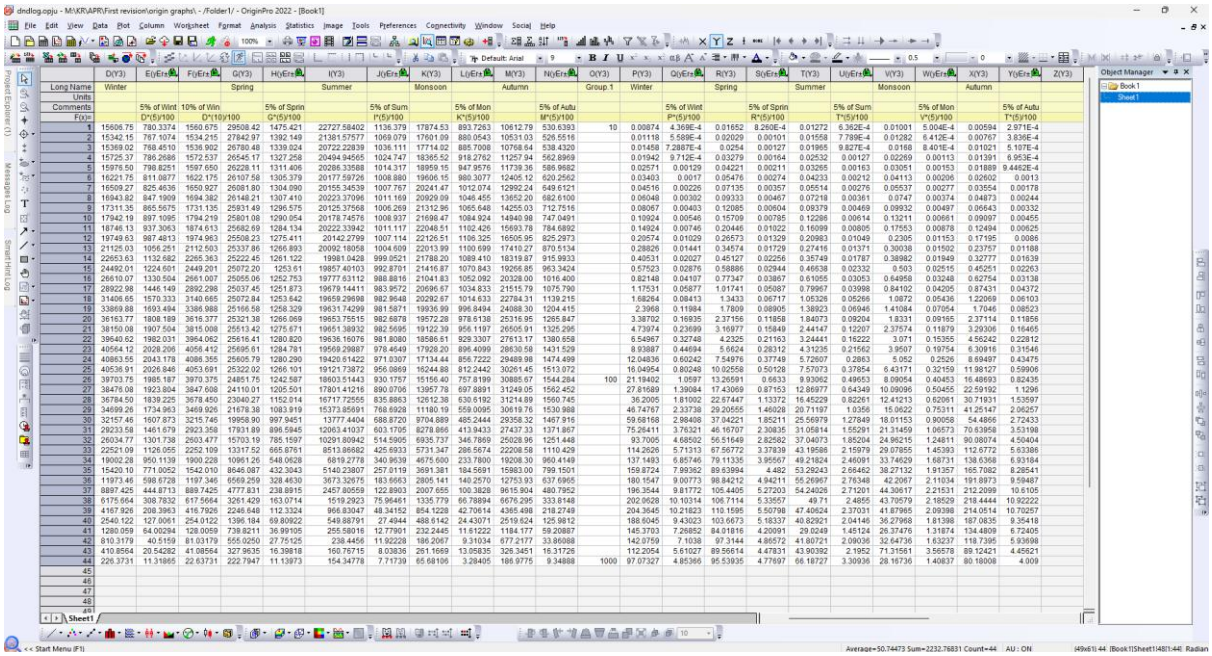

Figure 3.22 Picture of data feeding platform in the origin software

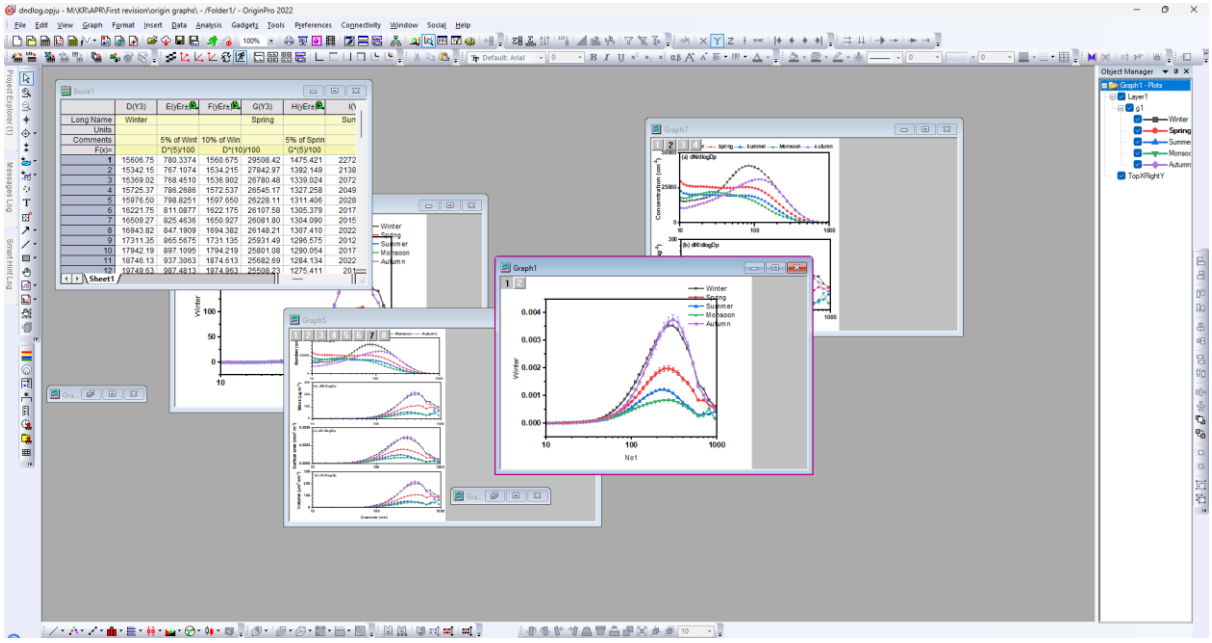

Figure 3.23 Output of the data visualization in the Origin software

3.5.4 IBM SPSS software.

The IBM SPSS software in the study is used for conduction different statistical tests (Fig 3.24). The air quality data is tested for its significance using the IBM SPSS

software (Fig 3.25). The Levene test was conducted for testing the variance equality during the different emission periods of the study and found that the p value is found to be < 0.05. The other statistical tests such as F test are also utilized. The variances at 95% confidence interval level are also applied in the study. The outliers in the data were statistically tested and removed using the z ± 3 score values. The Kruskal-Wallis test is used for determining the differences of the data between the different periods. The Kruskal-Wallis test is a non-parametric test. The Mann-Whitney U (non - parametric test) is used for testing the variation of independent groups especially season in our case. The statistical tests reveal that the concentration of the nanoparticles in the study area is statistically significant based on the sources and seasons. The p-value shows < 0.05 and the null hypothesis is rejected.

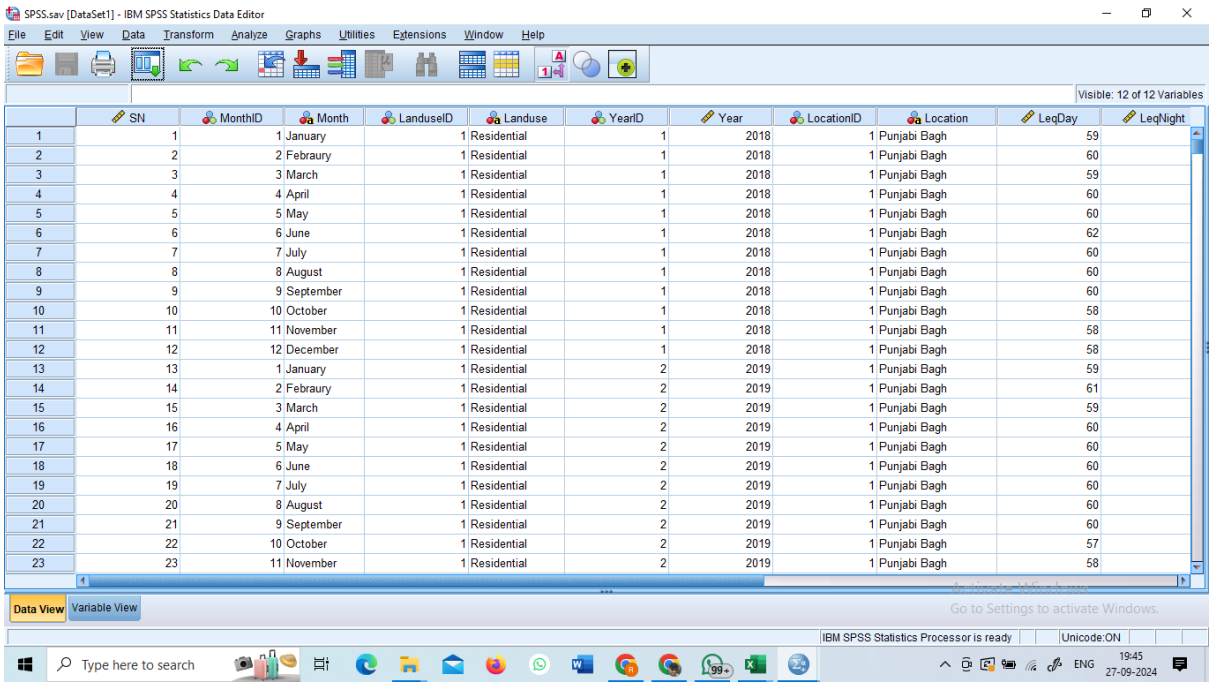

	SN	MonthID	Month	LanduseID	Landuse	YearID	Year	LocationID	Location	LeqDay	LeqNight
1	1	1	January	1	Residential	1	2018	1	Punjabi Bagh	59	
2	2	2	Febraury	1	Residential	1	2018	1	Punjabi Bagh	60	
3	3	3	March	1	Residential	1	2018	1	Punjabi Bagh	59	
4	4	4	April	1	Residential	1	2018	1	Punjabi Bagh	60	
5	5	5	May	1	Residential	1	2018	1	Punjabi Bagh	60	
6	6	6	June	1	Residential	1	2018	1	Punjabi Bagh	62	
7	7	7	July	1	Residential	1	2018	1	Punjabi Bagh	60	
8	8	8	August	1	Residential	1	2018	1	Punjabi Bagh	60	
9	9	9	September	1	Residential	1	2018	1	Punjabi Bagh	60	
10	10	10	October	1	Residential	1	2018	1	Punjabi Bagh	58	
11	11	11	November	1	Residential	1	2018	1	Punjabi Bagh	58	
12	12	12	December	1	Residential	1	2018	1	Punjabi Bagh	58	
13	13	1	January	1	Residential	2	2019	1	Punjabi Bagh	59	
14	14	2	Febraury	1	Residential	2	2019	1	Punjabi Bagh	61	
15	15	3	March	1	Residential	2	2019	1	Punjabi Bagh	59	
16	16	4	April	1	Residential	2	2019	1	Punjabi Bagh	60	
17	17	5	May	1	Residential	2	2019	1	Punjabi Bagh	60	
18	18	6	June	1	Residential	2	2019	1	Punjabi Bagh	60	
19	19	7	July	1	Residential	2	2019	1	Punjabi Bagh	60	
20	20	8	August	1	Residential	2	2019	1	Punjabi Bagh	60	
21	21	9	September	1	Residential	2	2019	1	Punjabi Bagh	60	
22	22	10	October	1	Residential	2	2019	1	Punjabi Bagh	57	
23	23	11	November	1	Residential	2	2019	1	Punjabi Bagh	58	

Figure 3.24 Data feeding in SPSS for statistical analysis

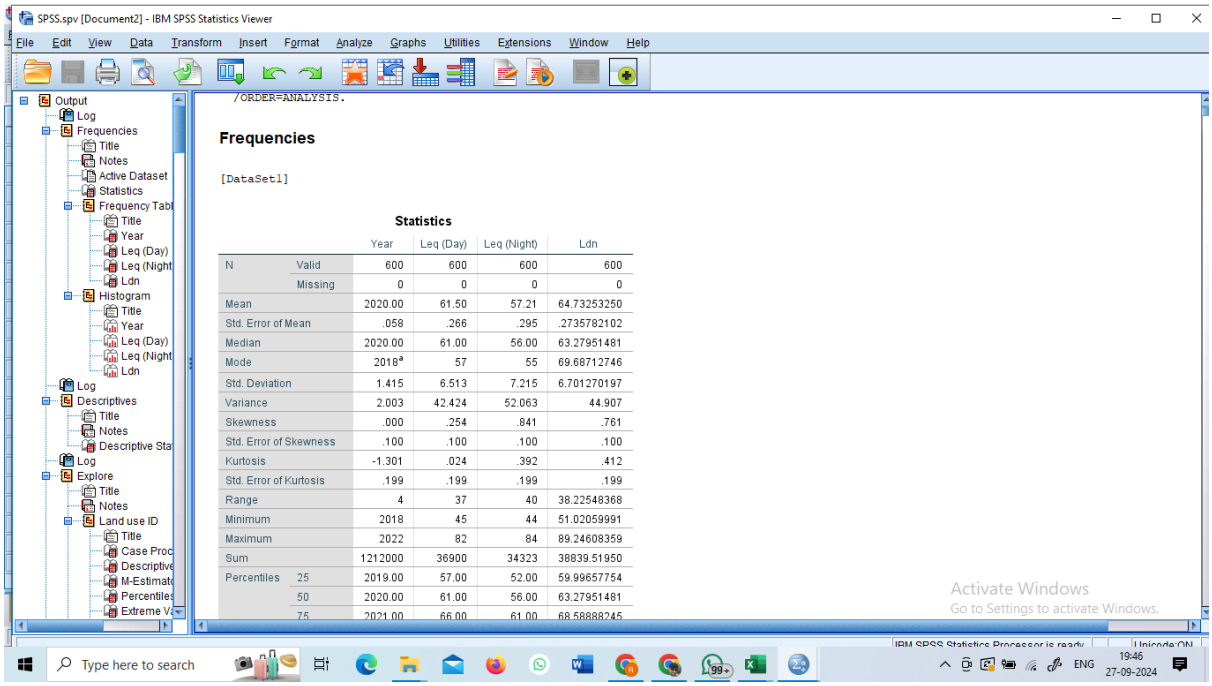

Figure 3.25 Results of the statistical analysis in SPSS

3.5.5 Inhalable nanoparticle concentration.

The inhalable particle number concentration is a mathematical method of analyzing the probable inhalable concentration of the nanoparticles in the atmosphere based on the concentration of the nanoparticles and also the different breathing rate associated inhalation volume. Different physical activities of human will have different inhalation volumes which influence the exposure of the air pollution as well (Prabhu et al., 2019; Qiu et al., 2019) (Table 3.4). This mathematical method is considered as the reliable method and also one of the easiest methods for analyzing the probable inhalable particle number concentration. The analysis shows the number of particles which can be penetrated into the human respiratory systems. The nanoparticles are believed to have deposition in the deeper regions of the lungs such as alveoli and bronchioles (Kim et al., 2017; Koehler and Peters, 2015).

The equation which is used for the analysis of the inhalable particle number concentration is given below. where IPN represents the inhalable particle number concentration, PNC is particle number concentration (concentration of the

nanoparticles) and the IR represents the Inhalation rate of that particular physical activity.

$$IPN(min^{-1}) = PNC(cm^{-3})\ x\ IR(cm^3 min^{-1}) \qquad -(15)$$

The different IR rates used in the study is based on the guidelines of the US EPA exposure guideline handbook.

The IR values will be more for heavy physical activity such as running, weightlifting, heavy exercise. During the heavy exercise period the concentration of the particles gets deposited in the respiratory system will be 4.5 times higher than the normal mode of deposition during the resting position. (Ma et al., 2022). The walking activity is found to have less IR value and the long distance or cross-country running is found to have the higher IR which is used in our study. The detailed IR of the different physical activity is provided in the Table 3.4. The advantage of this method is that it requires very less inputs, i.e. only concentration of the nanoparticles is sufficient for estimation. This is the simplest mathematical calculation method for exposure estimation. The limitation of this method is that this method provides only the probable number concentration which can gets deposited in the respiratory system. The actual deposition in the respiratory system may vary in real which is not estimated by this method.

Table 3.4. Table showing different Inhalation rates and physical activity associated with it.

Category		**Associated activity**	**Inhalation volume (cm^{-3}/min)**
Light	Level 1	Walking, cloth washing.	13
	Level 2	Scrubbing floors, bowling.	19
	Level 3	Dancing, pushing, wheelbarrow, construction activities.	25
Medium	Level 1	Easy cycling.	30

	Level 2	Climbing stairs, playing tennis.	35
	Level 3	Fast walking and digging trenches, potholes.	40
Heavy	Level 1	Climbing stairs with load, playing squash and handball.	55
	Level 2	Wood cutting with an axe.	63
	Level 3	Activities in level 1 and 2 simultaneously.	72
Very Heavy		Running, competitive cycling.	85
Severe		Long-distance running, cross-country skiing.	100

3.5.6 Particle dosimetry model

The nanoparticles deposition in the different regions of the human respiratory system can be evaluated using a highly sophisticated model called Multiple Path Particle Dosimetry model (MPPD 3.04) (Fig 3.26). The MPPD model was developed by Owen price along with the Hammer institute of health science and Applied Research Associates. In the MPPD model calculates the deposition and also the clearance of monodisperse and polydisperse particles in the respiratory tracts of humans and different animal species. The model can predict deposition of particles from 1 nm to 100 µm. The model is also useful for toxicology studies of different laboratory animals such as rat, mouse pigs and rabbit. The model depositions prediction uses both single and multiple path flow analysis. In single path model specification, the deposition analysis of the nanoparticles is done using typical airway path generation but in multiple path method the deposition is analyzed in lobar specific and airway specific information. The deposition of the exposed particles is calculated using the theoretically derived efficiencies such as deposition by diffusion, sedimentation, and also the impaction within the airway. The filtration of the nanoparticles by the

defensive mechanism of nose and mouth are also determined using the empirically derived efficiency equations. This model is considered as one of the most accurate models for dosimetry analysis. The model works on the basis of computational fluid dynamics. The more general details of the model can be found at (https://www.ara.com/mppd/).

This model is a well validated model and it is tested and widely used in research and education purpose for the nanoparticle deposition in the human respiratory tract (Khan et al., 2022; Manojkumar and Srimuruganandam, 2021b, 2022b). This model is considered to be one of the best models available for the dosimetry studies due to the features and updated functions of the model. The major input parameters of the model include, particles feature such as size, density and then lung features such as breathing frequency (BF), tidal volume (TV), upper respiratory tract volume (URT), and the different orientation of exposure conditions. The different exposure orientation conditions available in the model are particles recaching the respiratory system through respiratory tract through nose and the body in upright orientation and dispersion. This model also uses certain assumptions and constant as per the different global study suggestions. In the model the deposition of the nanoparticles in the different regions of the respiratory system can be analyzed such as pulmonary, tracheobronchial, and alveolar regions. The depositions in the alveoli, bronchus and bronchiole. The input of the model uses size segregated measurement for better accuracy which is one of the drawbacks of the model. Another limitation of this model is that this model uses theoretical and computational functions for the deposition analysis but in real the deposition may vary in the respiratory tract. The variation of deposition is due to the water vapor present in the respiratory tract which causes particle to grow its size in the respiratory tract due to the humid conditions.

Figure 3.26 Data feeding in the MPPD model

The model contains the ideal lung geometries and lung assumptions which mimics the exact function and structure of the human lungs. This model has lung geometry for different age groups of humans such as infants, children and adults. The three different regions of the human respiratory tract such as head/throat, tracheobronchial and alveolar/ pulmonary. While estimating the lung deposition the density of the particle inhaled, mono or poly dispersed particles, exposure time, breathing routes are some of the major basic model requirements which has to be provided as input parameters. In this study the advanced version of the MPPD model (3.04 version) is used. This version has several advantages compared to the other previous version (Miller et al., 2016). This version of the model can calculate the both single and multiple flow deposition. This model geometry resembles the most realistic human lung structure and this can handle different distributions of the particles at a time (Fig. 3.17).

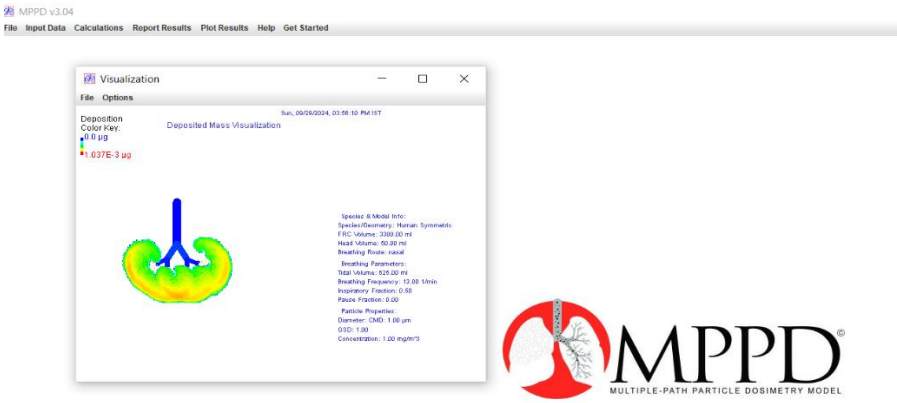

Figure 3.27 Demo output in the MPPD model

In the study the nanoparticles measurements are done extensively for a year. The deposition occurred during the different seasons are analysed. The seasonal mean concentration of the nanoparticles is used for the estimation deposition in the different regions of the human lungs. The deposition dose of the particles inhaled for different size ranges are analysed using the equation given below.

$$Dose\ Rate = \int_{Dp1}^{Dp2} V_E . DF(D_P) . n_N^0(D_P) . f dlog(D_P) \ - \ (16)$$

The step by step model execution is provided in the Figure 3.28 and the basic assumptions and functions of the model are also provided in the schematic diagram.

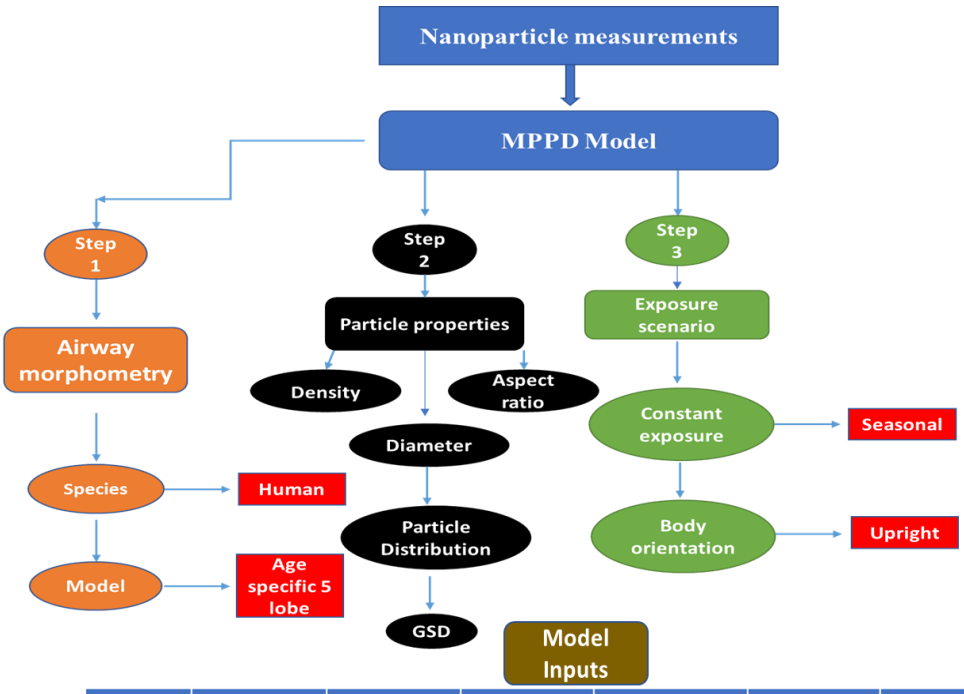

Model value	Infant(3 months)	Toddler 28 months	Children 8 years	Adolescence 14 years	Adult 18 years	Adult 21 years
URT	2.45	7.92	21.03	30.63	37.38	42.27
FRC	17.97	30.81	501.32	987.56	1159.38	2123.75
TV	30.44	100.1	278.2	388.1	446.7	477.2
BF	39	26	17	16	15	14

Figure 3.28 Schematic diagram of the MPPD model

*URT- Upper respiratory tract volume, FRC- Functional residual capacity, TV- Tidal volume, BF- Breathing frequency.

3.6 Summary

The detailed methodology of the study provided different information about the study area, types of instrument used and different types of software's used for data analysis and data interpretation.

CHAPTER – 4

RESULTS AND DISCUSSION

4.1 Introduction

The measured atmospheric nanoparticles are classified into four different categories based on the size fractions. The classifications are N_{nuc} (10 to 30 nm), small Aitken N_{satk} (30 to 50 nm), large Aitken N_{latk} (50 to100 nm), N_{acc} accumulation mode (100 to 1000 nm). The overall size fractions (10 to 1000 nm) is referred to as N_{total} PNC. The small Aitken and large Aitken can be combinedly referred as simply Aitken mode and the size fractions starting from the 10 to 100 nm are globally referred as Ultrafine particles (UFP 10 to 100nm). The geometric mean diameter for the entire size range is referred as GMD. The aim of the study is to measure and quantify the nanosized particle concentration in the road side microenvironment. The measurements are done in the road side environment in different emission conditions. The different emission scenarios are classified into different phases to quantify the role of transport emissions in the urban roadside regions. Similarly, the study aims to analyse the seasonal factors influence on these atmospheric nanoparticle's concentration along with the role of meteorological conditions. The measurements are done for a yearlong period in the study region which covers all the seasonal classifications in the study area. The study period includes winter, spring, summer, monsoon and autumn. Along with this the meteorological parameters such as temperature, humidity, wind direction wind speed is also measured in the study region for analysing the role of the meteorological parameters in the atmospheric nanoparticle's concentration. The dynamics of the atmospheric nanoparticles in the road side based on the emission sources variation that are classified on the basis of restrictions which was imposed to tackle the spread of Corona Virus (COVID -19). And also, the extreme pollution event in the study area was selected during the Diwali period. During this along with regular emissions the emissions from the fireworks also contributed to for higher number of atmospheric nanoparticles emissions in the study area. These scenarios were classified in to two periods namely, period I and period II. Both the period has three different phases one is before the event, another one is during the event and one is after the event. This

gives a detailed information about the role of these emissions sources in the study area. The first period is classified into three phases namely, Before Restriction (BR). During restriction (DR) and After Restriction (AR). The BR phase lasts for 20 days from 1st to 20th April 2021 in the study area, followed by DR phase which lasts for 47 days from 21st April to 5th June and the AR phase lasts for 24 days (6th June to 30th June). Totally period I covers 91 days of data measurements. Similarly, in period II the BD phase last for 33 days (3rd October to 4th November), AD period lasts for 8 days (5th to 12th November and DRII phase lasts for 18 days (13th to 30th November). Period II covers a monitoring period of 59 days. In total both the period I and period II cover a total monitoring period of 150 days. The seasonal classification in the study area includes winter, spring, summer, monsoon and autumn. The winter seasons starts from the month of December to the mid of February accounting for 76 day out of which 96 days of data is available for analysis. Similarly, for spring from mid-February to March accounting for 45 days (44 days data available). The summer seasons starts from April and ends at June which lasts for 91 days. The summer season is the longest season in the study region and during this season 84 days of data is available for analysis. The monsoon season starts in the month of July to mid-September and 41 days of data is available out of 77 days. Autumn season starts from mid-September to November consisting of 76 days and 60 days of data are available during this season. In a year out of 365 days the measurement campaign lasts for around 300 days of data in all the different periods. The study used the measured concentration for analysing the exposure to these nanoparticles using different mathematical and computerized models.

4.2 Analysis of particle dynamics based on the emission sources variation

4.2.1 Temporal variation PNC during different periods

The particle number concentration and associated GMD concentration during the different periods are analysed using the temporal variation of the concentration. During the both the periods the lowest concentration of the total PNC (1.7 x 10^3 cm^{-3}) was found during the DR phase in period I in which the vehicular movement in the study region reduced to around 45%. The study region is in the roadside microenvironment

where the majority of the emission sources are from the transportation sectors. The engine exhaust emissions release wide range of pollutants. Comparted to the normal scenario in the BR phase the concentration of the particles reduced to around 31% (Fig 4.1). This shows the role of vehicular sources in the nanoparticle's emission in the study region. The study region represents the urban roadside micro environment which represents similar conditions the road microenvironments in the city. During the AR phase when the vehicular activities resumed, the particle number concentration also starts to increase and reached peak concentration of 1.3 x 10^5 cm^{-3} (Fig 4.1). This concentration is the highest recorded hourly mean concentration during the period I. During the BR and AR phase, there was no restriction for vehicular activity revealed that the reduction obtained in period I was associated with the vehicular sources. The period I analysis shows that the reduction in vehicular sources directly proportional to the number concentration.

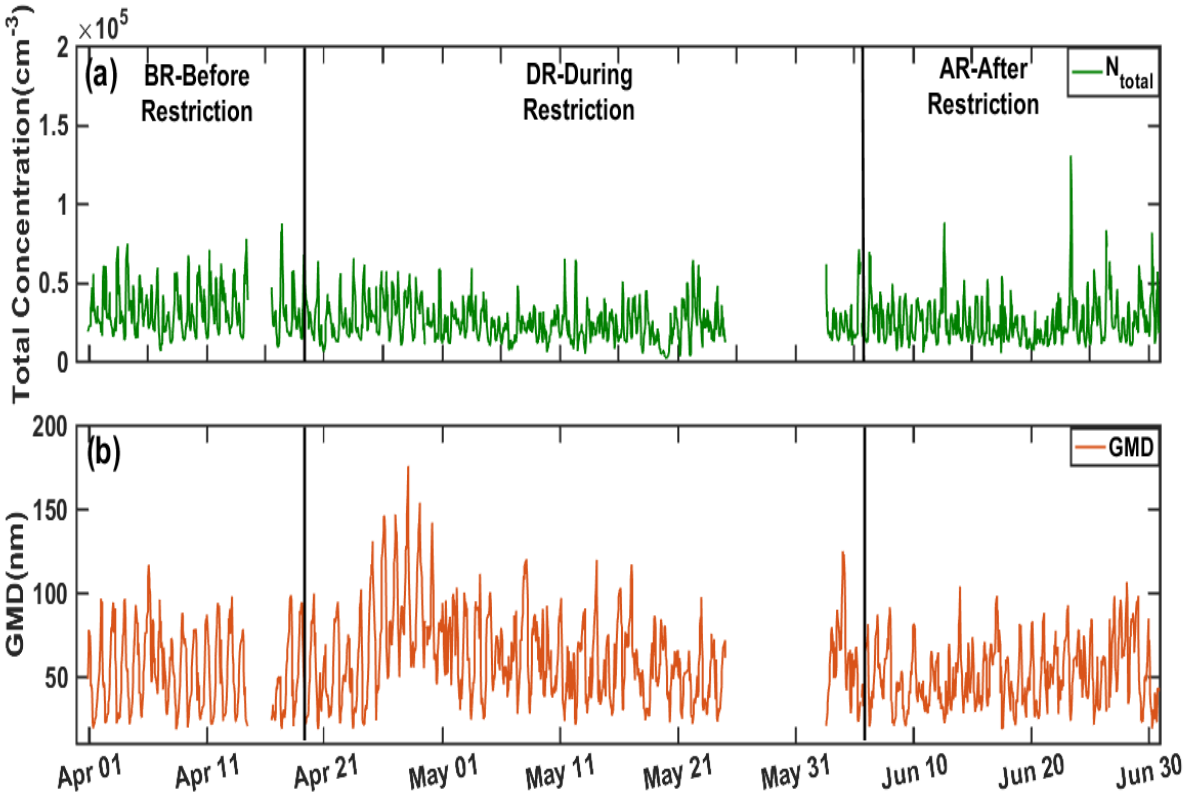

Figure 4.1: Temporal distribution of hourly average concentration of (a)N_{total} (b) GMD during Period I (1st April 2021 – 30th June 2021)

During period II (Fig 4.2) the highest mean concentration of the total PNC is found during the AD phase with a concentration of about 4.2 x 10^4 cm^{-3} which is around 35% increase in concentration compared to the BD phase (2.7 x 10^4 cm^{-3}). However, the concentration during the AD phase decreases gradually compared to the previous year (2.19 x 10^6 cm^{-3} in 2021) due to the implementation on restrictions to the cracker's usage (Yadav et al., 2022). The concentration received during the AD phase is the highest found concentration in the both periods. The period I and II shows that the concentration of the atmospheric nanoparticles in the urban atmosphere id directly proportional to the emission sources. Higher emission sources lead to higher concentration of the particles (AD phase, period II) and lower sources leads to low emissions (DR phase, period I). The concentration received during the AD phase is 25% higher than the period I maximum concentration and 57% higher than the period I lower concentration. The concentration of the atmospheric nano particles in the study area are also driven by the local meteorological conditions and the precipitation process in the region.

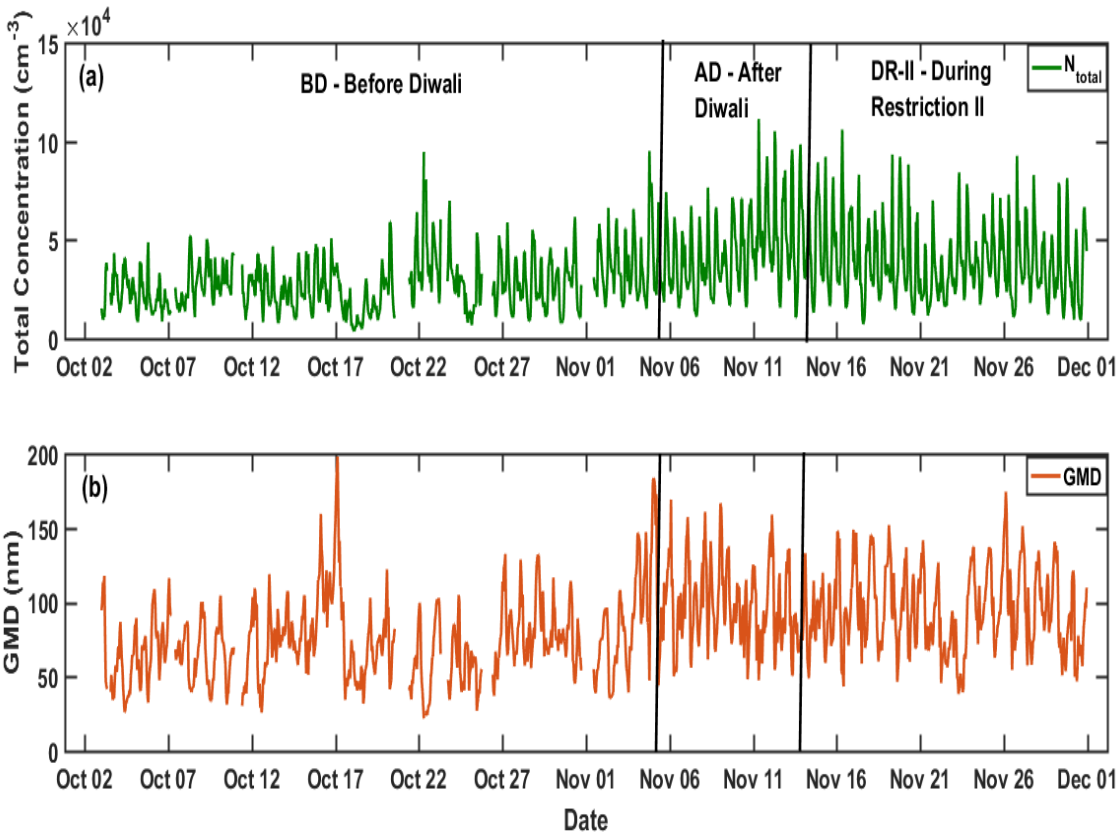

Figure 4.2: Temporal distribution of hourly average concentration of (a)N_{total} (b) GMD during Period II (3rd October 2021 – 30th November 2021)

The gaps in the figures represents the data missing. In the study region the during period I and II rainfall of 116 and 80mm received respectively. The precipitation received during this phase helps in the wet removal of the particles. Global studies found that the nanoparticle concentration in the study region varies from 10^2 to 10^6 particles cm^{-3} (Kumar et al., 2014). In our study the concentration varies from10^3 to 10^5 particles cm^{-3}. During different periods the order of concentration of the total PNC varies as BR> AR> DR phase in Period I and DR II>AD>BD in period II (Table 4.1). The minimum concentration of the atmospheric nanoparticles increases in urban regions in the recent years especially in the south Asian region due to the intense anthropogenic emission activities in these regions and many globally polluted urban regions are found in these Global south regions which a serious concern (Ramachandran and Rupakheti, 2022).

Table 4.1: Statistical summary of the different size range concentration during different periods

Phase	Size (cm^{-3})	Minimum	Maximum	Mean ± S. D	Median
Before Restriction (BR)	N_{nuc}	534	74375	14054 ±13242	10317
	N_{satk}	905	19581	4768 ±2791	4127
	N_{latk}	1654	18248	6256 ±3189	5830
	N_{acc}	705	20206	6521 ± 3952	6040
	N_{total}	6362	87343	31599 ± 15028	28220
	GMD (nm)	18	117	52 ± 23	49
During Restriction (DR)	N_{nuc}	106	54471	8131 ± 8691	111
	N_{satk}	305	19245	3399 ± 2393	12
	N_{latk}	498	19316	5604 ± 3153	5283
	N_{acc}	418	33838	7346 ± 5946	2801
	N_{total}	1752	70927	24481 ± 12034	4766
	GMD (nm)	18	176	77 ± 16	7
After Restriction (AR)	N_{nuc}	565	90646	10816 ± 10927	7537

	N_{satk}	727	25546	4123 ± 2991	3262
	N_{latk}	966	19861	5382 ± 2901	4700
	N_{acc}	709	15093	4912 ± 2541	4424
	N_{total}	5022	130433	25235 ± 14173	22034
	GMD (nm)	18	106	50 ± 18	47
Before Diwali (BD)	N_{nuc}	161	71873	6917 ± 7070	4741
	N_{satk}	498	14646	3822 ± 2513	3252
	N_{latk}	897	21177	6447 ± 3893	5196
	N_{acc}	1012	58056	10236 ± 6460	9086
	N_{total}	3774	95021	27423 ± 13498	2554
	GMD (nm)	22	198	73 ± 26	70
After Diwali (AD)	N_{nuc}	504	46986	7823 ± 7713	5273
	N_{satk}	530	14008	4343 ± 3145	3590
	N_{latk}	2091	28951	8947 ± 6527	6858
	N_{acc}	6513	45886	21315 ± 7874	21016
	N_{total}	11256	111316	42429 ± 19320	39260
	GMD (nm)	44	184	100 ± 28	97
During Restriction II (DR II)	N_{nuc}	204	37291	5862 ± 6363	295
	N_{satk}	479	17876	4384 ± 3373	655
	N_{latk}	1565	36062	10197 ± 7144	1117
	N_{acc}	3813	48752	19065 ± 8909	885
	N_{total}	7505	105887	39510 ± 19717	35039
	GMD (nm)	38	174	94 ± 27	91

4.2.2 Geometric Mean diameter analysis in different periods

The geometric mean diameter of the particle's concentration based on the types of sources. The concentration of the GMD shows more deviation when the sources are complex and it shows very less deviation when the source present in the region is not complex possibly from one or two sources with similar pattern of the emission.

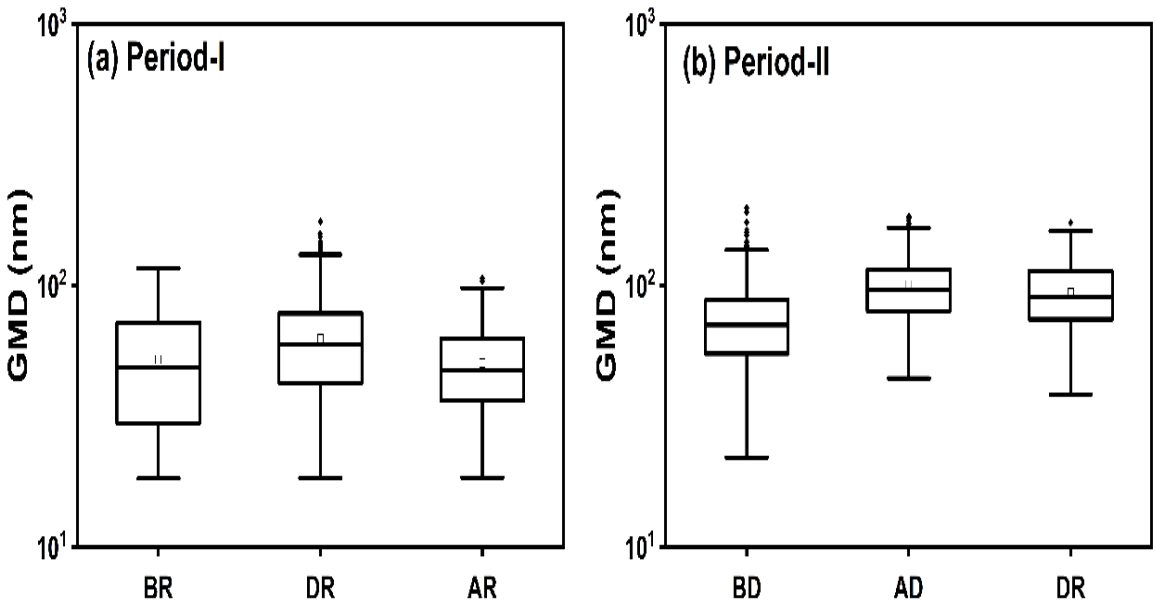

Figure 4.3: Box whisker plot for an hourly average concentration of GMD during Period I (1st April 2021 to 30th June 2021) and Period II (3rd October 2021 to 30th November 2021)

The GMD represents the emission source of the particle. The literature suggests the different size range of the particles are based on the fuels. The CNG fuelled vehicles emits particles in the size ranged from 20 to 60 nm and the diesel-powered vehicles can emits particles in the range of 20 to 130 nm. The natural new particle formation process shows the GMD of particles < 30nm. The reduction in vehicular sources emission in period I can be clearly seen from the size range of the GMD particles measure during that period (Fig 4.3, Table 4.2). During the period I of the study, the size range of the GMD ranges from 15 to 200 nm in all the three different phases. During the restriction phase (DR phase) the movement of HCV (heavy commercial vehicles) is found more compared to the LCV (light commercial vehicles). The vehicle density of the study area is more dominated by the LCV but during the DR phase due to the restriction imposed the personnel cars (LCV) movement is observed less and the movement of HCV (goods carriers) are found more. The LCV utilizes CNG as fuel which emits particles in the size range of 20 to 60 nm and the diesel-powered HCV emits particles in higher size ranges. Apart from the source, the existing meteorological conditions also plays a major role in size of the particles as it undergoes transformation

such as coagulation and condensation in the atmosphere. During the period I the GMD was less than 100nm shows that the sources in the study region is probably vehicles. In the study region the hourly peak vehicular movement was around 1300 vehicles includes all the major types of vehicles. In a day around 35000 vehicles cross the study region. During period II the GMD was in the range of ≥ 100 nm. The study period GMD was the highest mean GMD recorded during the study period. This was due to the presence of different sources such as Diwali Sources (crackers) apart from the vehicular sources. During the period I, the deviation of the GMD concentration was less and it was higher during the period II. In period II, the GMD of 100 nm was obtained during the AD phase and on DRII phase, the GMD ranged from 75 to 100 nm. The percentage change of the vehicular density in the different zones of the study region is obtained from the google mobility data. The data is used to identify how the vehicle fleet in the study region varies during the different periods of the study.

Table 4.2: Percentage reduction of vehicles in different zones of the study area

Phase	Retail Centre	Local markets	Local Parks	Transit stations	Work places	Residential areas
BR	-38.6	4.9	-21.6	-16.9	-29.6	11.6
DR	-71.4	-34.5	-56.3	-60.4	-66.7	25.9
AR	-34.0	10.2	-24.4	-20.7	-34.9	11.1
BD	-11.3	39.8	-10.2	-0.9	-15.5	6.8
AD	-12.6	34.1	-10.2	-3.4	-25.7	7.4
DR II	-11.2	33.5	-9.3	1.8	-16.3	5.2

The google mobility data reveals that the restriction imposed for the vehicular movement in the study region results in the reduction of vehicular fleet in the public areas. The residential zones in the study region sees an increase in the vehicular movement due to the gathering/flocculation of the people in their residence itself. The DR Phase in the study regions shows a maximum vehicle fleet reduction. In DR phase the maximum vehicular fleet reduction was seen in the retail centres (-71.4) followed

by work places (-66.7), transit stations (-60.4), local parks (-56.3) and local markets (-34.5%). The least reduction was seen in DRII phase (period II) in the transit stations.

4.2.3 Particle size distribution of the different size particles during different periods

The size distribution of the entire particle size ranges during different periods also signifies the size profiling of the atmospheric nanoparticles. The ultrafine particles are found to have more association with the engine exhaust emission in the urban regions and about 80 to 90% of the total PNC emission can be from the UFP size ranges (Rönkkö and Timonen, 2019). During period I, the vehicular sources are found less especially during the DR phase which resulted in less particle number size distribution. During the AD phase when the Diwali emissions are found the concentration and size distribution of the particles increased and peak concentrations was found in the accumulation mode. This shows that the different emissions sources such as engine exhausts and Diwali fireworks emits particles in the different size ranges namely ultrafine and accumulation mode particles. During the AD phase the study region climate falls under the winter season where the coagulation of the emissions was found more (Sabaliauskas, et al., 2012; Schneider et al., 2015). This phenomenon also contributed to a certain extent for the higher accumulation size particles during the AD phase. The size distribution profiles of the size ranges 10 to 1000 nm during the different periods and phases of the monitoring period is shown in the Figure (4.4).

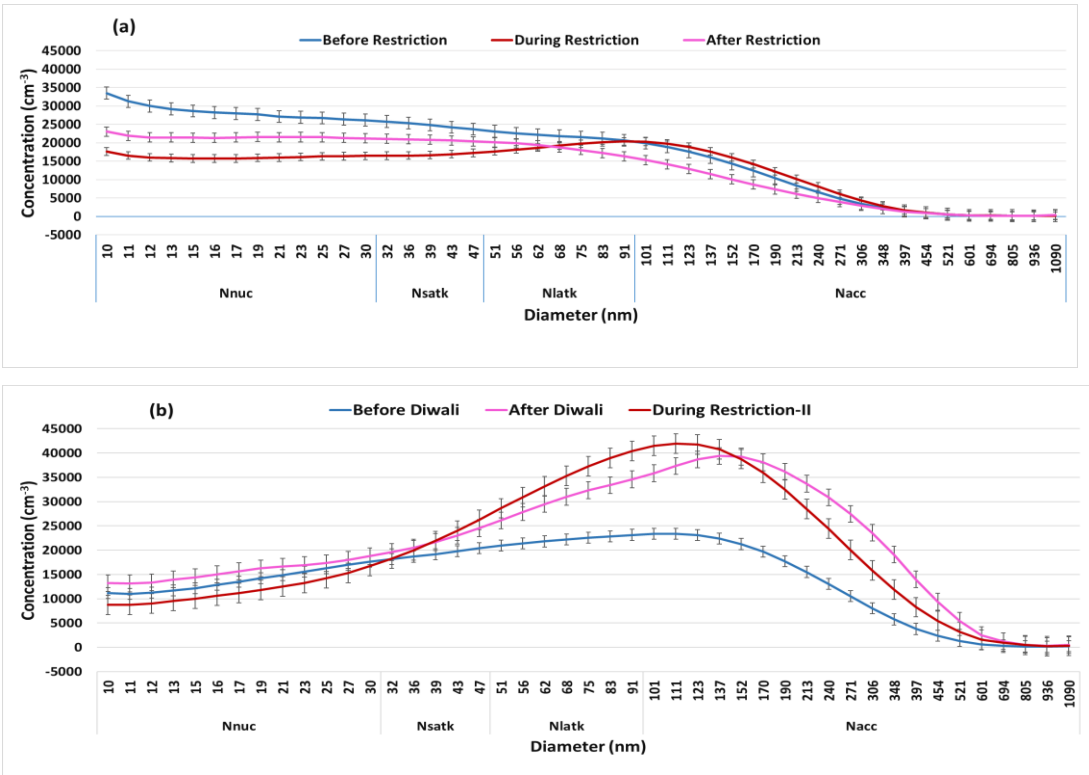

Figure 4.4: Particle number size distribution of hourly average size concentration ranges from 10 to 100 nm during Period I (1st April 2021 – 30th June 2021) to Period II (3rd October 2021 – 30th November 2021)

The size distribution clearly shows that the concentration of the lower size particles (< 100 nm) is high during the period I where the climate is hot and less humid. The particles concentration gradually starts to reduce from higher size to lower size. In period II the complex sources lead to the lesser concentration of the UFP particles then flowed by higher concentration of accumulation mode (100 to 500 only) and gradual reduction of the particles having diameter > 500nm. The maximum concentration of the particles during the period I is ~ 3.5 $\times 10^3$ cm^{-3} which is recorded for the particle having diameter ~10 nm. Similarly, in the period II the concentration of the particles around 100 to 200 nm diameter reaches a peak concentration of about 4.5 $\times 10^3$ cm^{-3}. The order of concentration from higher to lower for particles till 10 nm in the period I is BR > AR > DR and in period to for the particles having diameter 100 to 200nm the order is DR II> AD > BD.

4.2.4 Time series measurements of meteorological parameters during different periods

During period I and period II the meteorological parameters such as temperature, relative humidity, wind speed and solar radiation is also measured along with the nanoparticle's concentration. The temperature and humidity play a role in condensation of the particles whereas wind speed and direction play a role in ventilation or dispersion of the particles (Kozawa et al., 2012b; Mehel and Murzyn, 2015). During the period I the seasonal condition in the study region is summer where the temperature ranges from 30 to 36 ºC and relative humidity ranges from 30 to 55%. During this period the PNC concentration shows that the particles under 100 nm are high due to emission as well as due to the unfavourable condition for coagulation of the particles. During this period, the wind speed was also >2m/s which is favourable for the particle's dispersion. During period I (Fig 4.5, Table 4.3) along with emission source reduction in the emission sources the climatology of the study area also played a major role in the concentration of the atmospheric nanoparticles. During period II (Fig 4.6, Table 4.3) the concentration of the nanoparticles was found to have more due to the complex emissions and also the particles are found in the accumulation mode range. During that period the relative humidity in the study region varies from 60% to 80% and also the less favourable wind speed (< 2m) for dispersion. The seasonal factors such as winter and summer climatic conditions also catalyzed the atmospheric nanoparticles concentration of a region apart from the intensity of the sources (Hagler et al., 2012). The solar radiation received during the period I was more when compared to the period II. It is evident from the study that the nanoparticle concentration of a region should be measured along with the regional meteorological conditions. This provides a detailed information about the dynamics of the atmospheric nanoparticles in that particular study area. The role of the meteorological conditions is discussed in detail in the later part of the thesis.

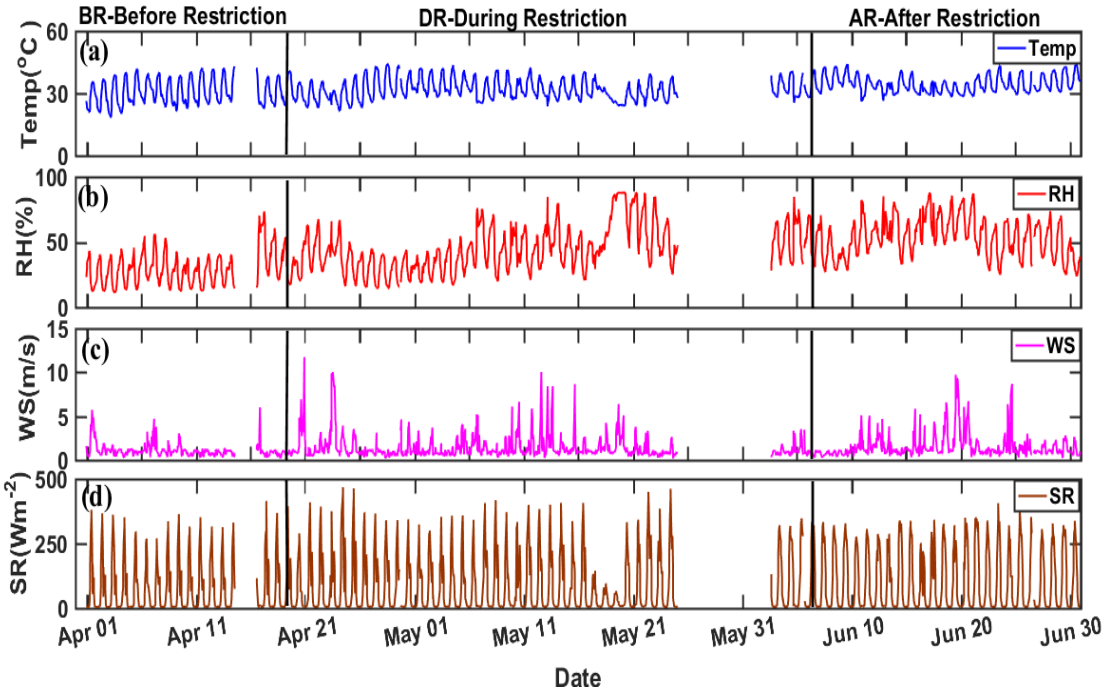

Figure 4.5: Temporal distribution of hourly average concentration of different parameters (a) Temp, (b) RH, (c) WS & (d) SR during Period I (1st April 2021 – 30th June 2021)

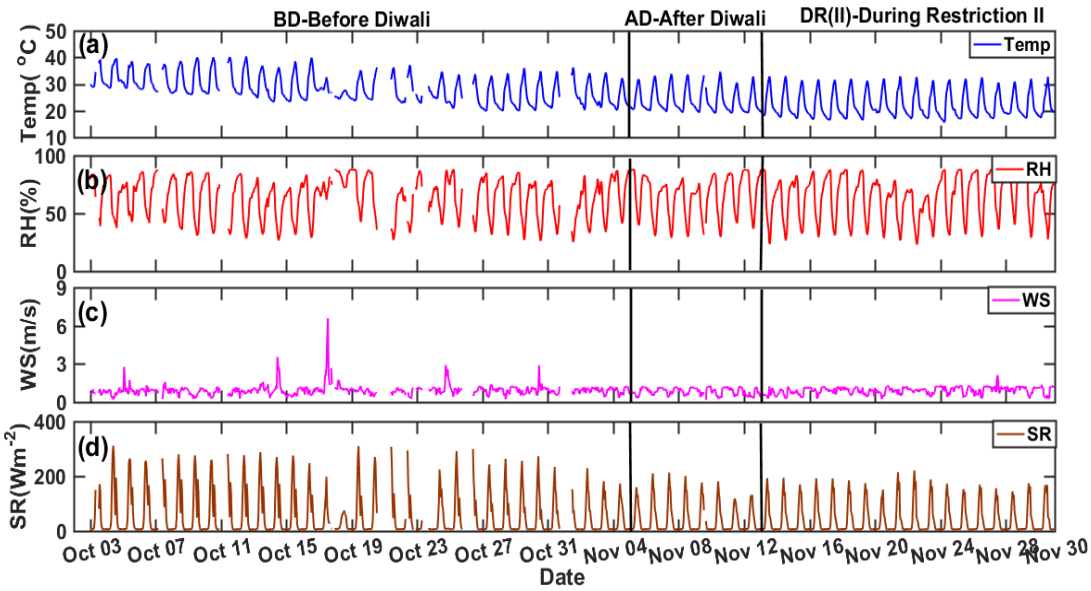

Figure 4.6: Temporal distribution of hourly average concentration of different parameters (a) Temp, (b) RH, (c) WS & (d) SR during Period II (3rd October 2021 to 30th November 2021)

Table 4.3: Statistical summary of different meteorological parameters – air temperature (AT), relative humidity (RH), wind speed (WS) and solar radiation (SR) during different study phases

Phase	**Parameter**	**Minimum**	**Maximum**	**Mean ± S. D**	**Median**
Before Restriction (BR)	AT (ºC)	19	43	31 ± 6	29
	RH (%)	11	73	29 ± 13	28
	WS (m/s)	0	6	1 ± 0	1
	SR (W/m^2)	3	415	79 ± 104	12
During Restriction (DR)	AT (ºC)	21	44	32 ± 4	31
	RH (%)	14	88	44 ± 18	42
	WS (m/s)	0	12	1 ± 1	1
	SR (W/m^2)	4	468	88 ± 11	17
After Restriction (AR)	AT (ºC)	26	44	34 ± 4	34
	RH (%)	24	88	54 ± 15	54
	WS (m/s)	0	10	1 ± 1	1
	SR (W/m^2)	4	406	104 ± 118	29
Before Diwali (BD)	AT (ºC)	20	40	28 ± 5	28
	RH (%)	25	88	63 ± 17	68
	WS (m/s)	0	7	0 ± 0	1
	SR (W/m^2)	4	311	57 ± 77	9
After Diwali (AD)	AT (ºC)	19	35	23 ± 4	22
	RH (%)	29	88	64 ± 17	69
	WS (m/s)	0	1	0 ± 0	1
	SR (W/m^2)	5	213	41 ± 53	7
During Restriction II (DR II)	AT (ºC)	16	33	22 ± 4	20
	RH (%)	23	88	63 ± 18	68
	WS (m/s)	0	2	1±0	1
	SR (W/m^2)	5	221	41 ± 55	7

4.2.5 Diurnal Behaviour of particle number concentration

The diurnal variation of the different size range pollutants shows various profiles and pattern in different seasons as well as in different hours of the day.

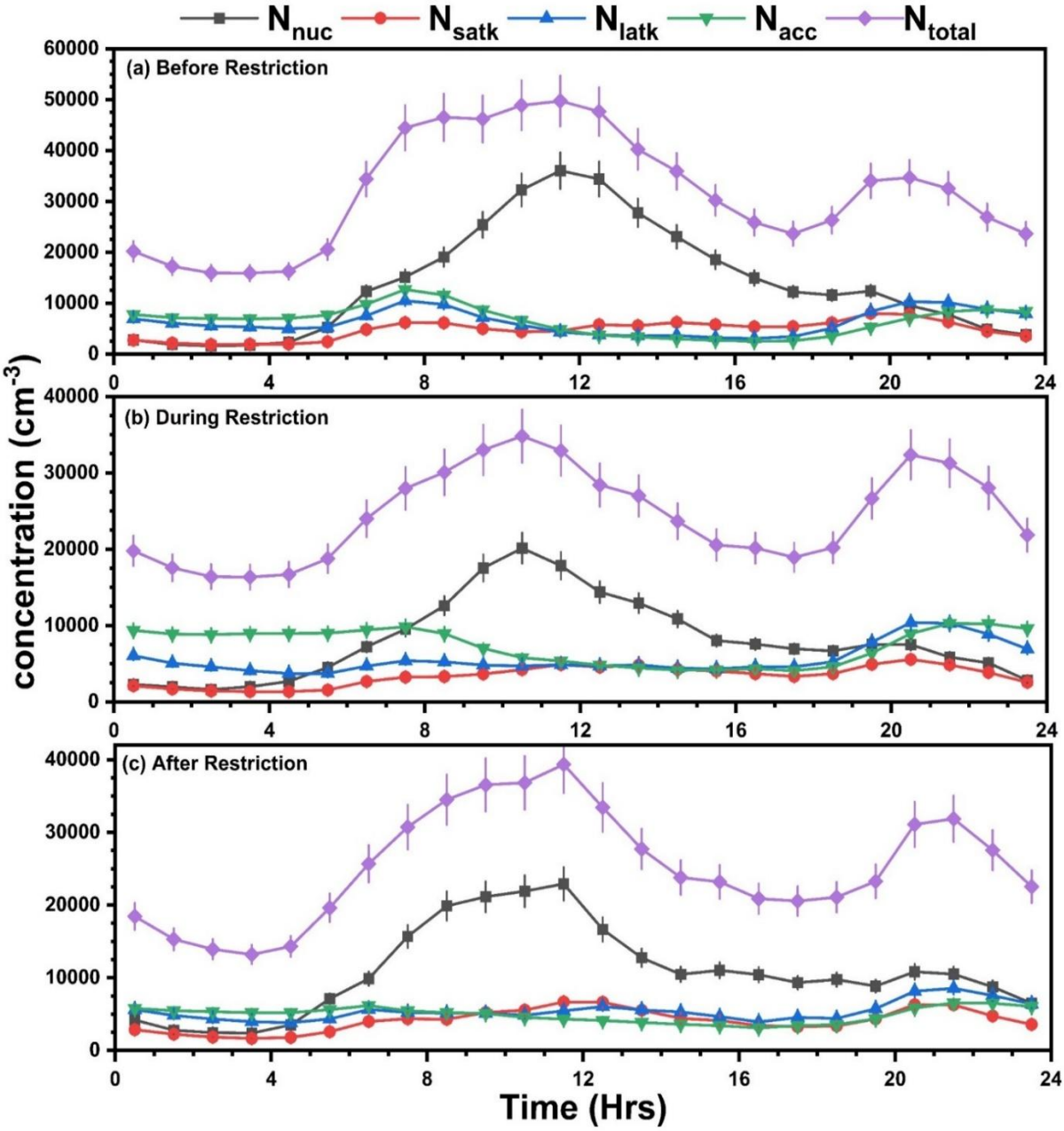

Figure 4.7: Diurnal behaviour of different size range particles during different periods, (a) Nucleation, (b) Small Aitken, (c) Large Aitken, (d) Accumulation and (e) N_{total} Concentration for different phases in period I (1st April 2021 to 30th June 2021)

During the period I, diurnal concentration of the particles shows that the concentration during the vehicle rush hours namely morning and evening peak hours are not clearly

visible due to the reduced vehicular sources (Fig 4.7). The increase in concentration during the peak hours is a common phenomenon in the urban regions especially in the roadside microenvironments. The afternoon hours in the period I received a higher concentration of the particles in the lower size (N_{nuc}) due to the natural new particle formation process (Fig 4.7). The seasonal conditions during the period I was favourable condition for the new particle formation process/UFP burst due to the optimum amount of relative humidity and solar radiation. This can be clearly seen between the morning to afternoon hours in the period I (Fig 4.7).

The diurnal variation during different periods are not uniform and it changes during different phases based on the emission and meteorology. During period II when there was no restriction for the vehicular sources, the diurnal concentration increased during peak hours. The diurnal concentration increases during peak hours 10hrs to 12hrs as well as during the evening peak hours (16 to 20 hrs) (Fig 4.8). The hours are considered as the peak hours where the vehicular flow is more compared to the normal hours of the day. The contribution of the different size ranges also varies during the different hours of the day. The N_{nuc} concentration was found high during both BR and AR phases (37.7 % and 37.6%) which was directly influenced from the vehicular sources. In similar fashion there is another peak found during the evening peak hour due to the vehicular movement. During period II the diurnal variation throughout the period shows a double hump model pattern which is aligning with the peak hours. This shows that the vehicular sources played a major role in the atmospheric nanoparticle concentration in the study area (Kompalli et al., 2018). During the DR phase of Period I, the smaller size particles N_{nuc} and N_{satk} contributes to around 30 % and 14% in the N_{total} PNC concentration. During the same period N_{latk} and N_{acc} contributes around 29% and 28% during the DR phase. N_{nuc} contributes to around 30 to 40% during the different phases of period I, N_{satk} concentration lies between 10 to 15%, N_{latk} ranges from 25 to 30% and the N_{acc} particles concentration contributes for 20 to 30% in the period I irrespective of the phases. Similar to the diurnal concentration the percentage contribution also varies during the different periods. The percentage contribution during the period II of different size range particles are as follows: 15 to 25% for N_{nuc} particles, 20 to 30% for N_{latk} particles, 35 to 50% for N_{acc} particles.

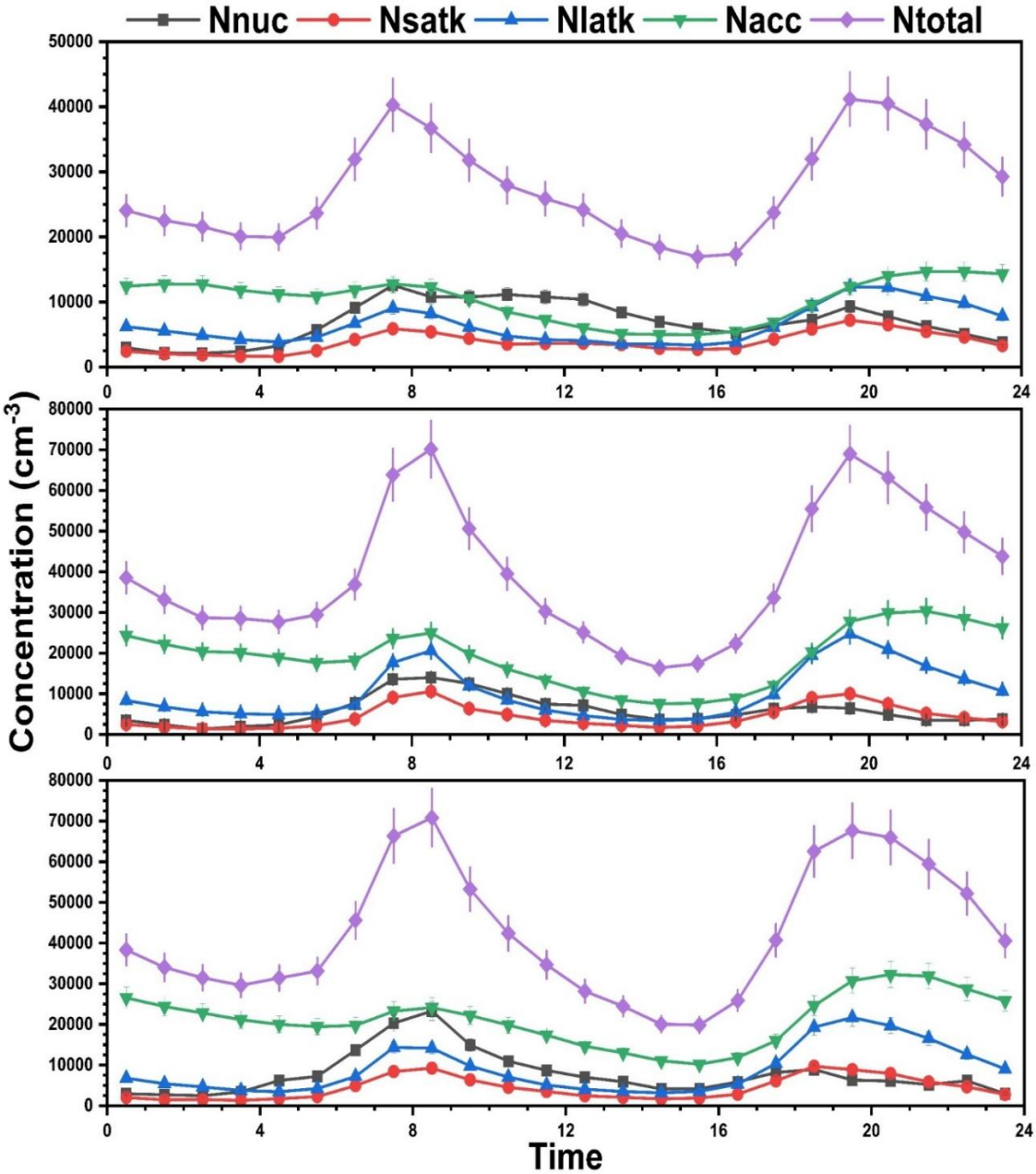

Figure 4.8: Diurnal behaviour of different size range particles during different periods, (a) Nucleation, (b) Small Aitken, (c) Large Aitken, (d) Accumulation and (e) Ntotal Concentration for different phases in period II (3rd October 2021 – 30th November 2021)

The vehicular reduction during period II was only 1% compared to the previous year and also the Diwali sources contributed for more contribution of N_{acc} sources. N_{acc} contributes to around 50% in the AD phase and 46% in DRII phase to the N_{total} concentration. The diurnal analysis reveals that the increase or decrease in

concentration in day also varies in different hours of the day. Based on the source's variation the atmospheric nano particles concentration increases or decreases. The variation is not only seen in the concentration but also seen in the size proportion. The size proportion also varies based on the nature of the emission and their contribution in the atmospheric nanoparticle's concentration.

4.2.6 Impact of meteorology on particle number size concentration

The meteorological parameters of a region are another influencing parameter for determining the particle number concentration in a region. The major meteorological parameters which influences the concentration are wind speed, solar radiation and the relative humidity. These parameters help the nanoparticles to get dispersed or influenced them to undergo secondary transformations in the atmosphere (Nicolás et al., 2009; Shrestha et al., 2016; Väkevä et al., 2000b).

The relative humidity plays an important role in particle coagulation process in the atmosphere (Kumar et al., 2008b). The agglomeration of the nanoparticles causes the particles to get agglomerate from one size to another size majorly from lower to higher size under the favourable relative humidity and temperature (Cusack et al., 2013). The weather pattern in the study area varies during the different periods based on the seasonal changes of the study location (Fig 4.9). During period I the climatic condition of the study area was summer where the temperature (44.5°C) attains peak but in period II the temperature varies largely from 15.6 °C to 40.34°C (Fig 4.9). During period II the relative humidity was found high throughout the day compared to period I. The period I records maximum sunshine hours among the both periods and the maximum solar radiation was observed during the period I with an irradiance of 468 Wm^{-2}. The diurnal analysis clearly indicates that the solar radiation and RH are inversely proportional to each other. The diurnal analysis on temperature coincides with the seasonal changes and it clearly shows that the AR phase is found to have more concentration of the temperature which occurred during the month of June which is the peak summer season in the study area. Similarly, DRII phase the period falls under the winter season which is the coldest period throughout the monitoring period. The diurnal pattern of the temperature and relative humidity are directly opposite to each other.

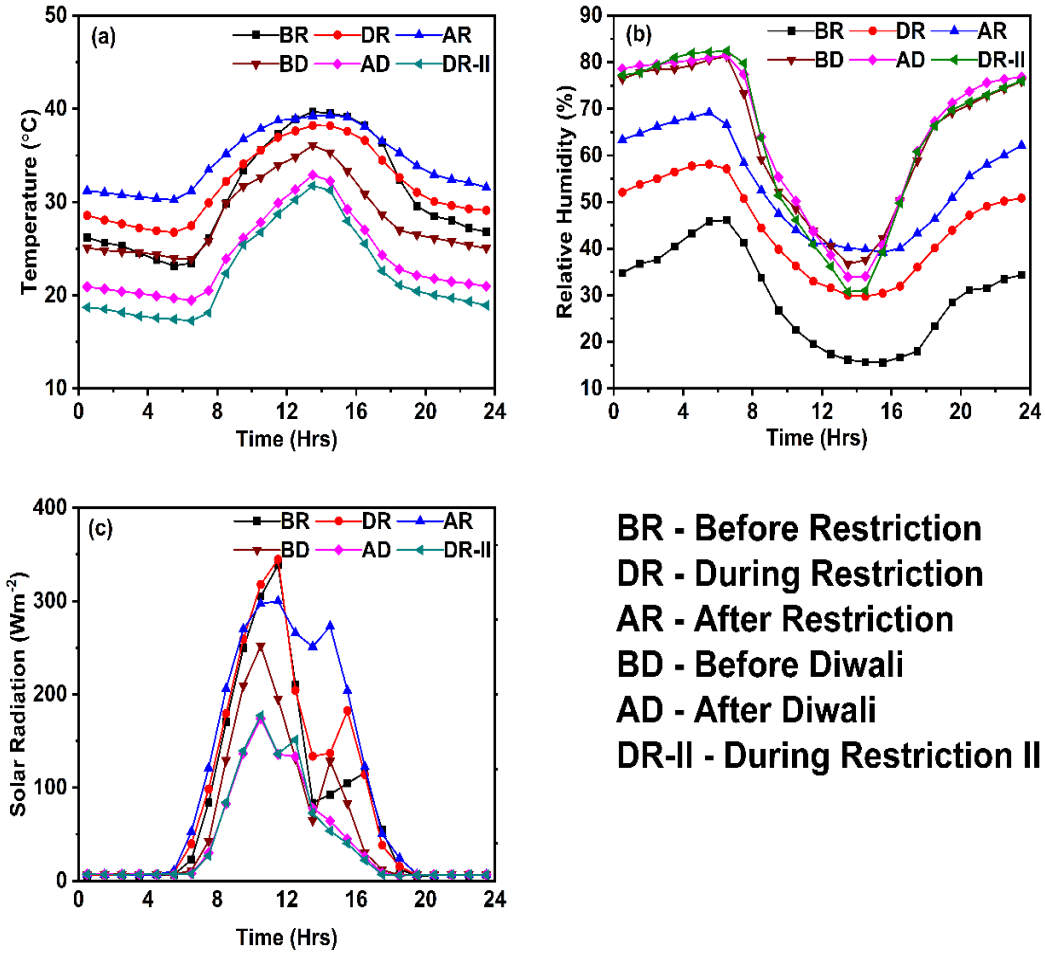

Figure 4.9: Diurnal variation of (a) Temperature (Temp), (b)Relative Humidity (RH), and (c) Solar radiation (SR) of different phases during period I (1st April 2021 to 30th June 2021) and period II (3rd October 2021 to 30th November 2021)

4.2.7 Influence of wind speed on measured particle number concentration

The wind speed and direction are other major factors which helps the particles to undergo dispersion or dilution. In the urban regions that to in the road microenvironment the dispersion is mainly based on the two major factors. The first one is traffic condition, where the turbulence is created by the flow and the second one is the wind dependent where the turbulence is created by wind speed and direction. The wind direction along with the windspeed can form a vortex formation in the urban street canyon. In urban regions the wind flow can be either recirculating flow or along

with the street flow (Liu and Cui, 2014). Wind parameters can contribute for the different spatial variation in particle number concentration (Hofman et al., 2016; Kozawa et al., 2012a). In the study region the majority of the wind flow is from south west to north east due to the vehicle induced turbulence. A busy road surrounds the study area in south direction. During period I the maximum wind speed recorded in the study area was 11.7 m/s and in period II it was 6.5 m/s (Fig 4.10). Bivariate polar plot analysis reveals that the pollutants are dispersed on the receptor site. The mean concentration of N_{total} observed during the BR phase of period I found to have more concentration in the region when the wind speed was less (< 6m/s). The winds travelling from the southwest to northeast is the major reason for the higher concentration from the roadside. During the DR and AR phases of period I, the wind speed in the study region was higher than the BR phase which varies from >6 m/s to < 12 m/s. During period I the wind created turbulence was more compared to the traffic induced turbulence due to the restricted traffic movement and also the recorded wind speed received was > 1.5 m/s during all the three phases. The vortex formation possibilities increase when the wind speed increases and also the exchange of particles occur from the wind induced turbulence instead of traffic induced turbulence (Kumar et al., 2008a).

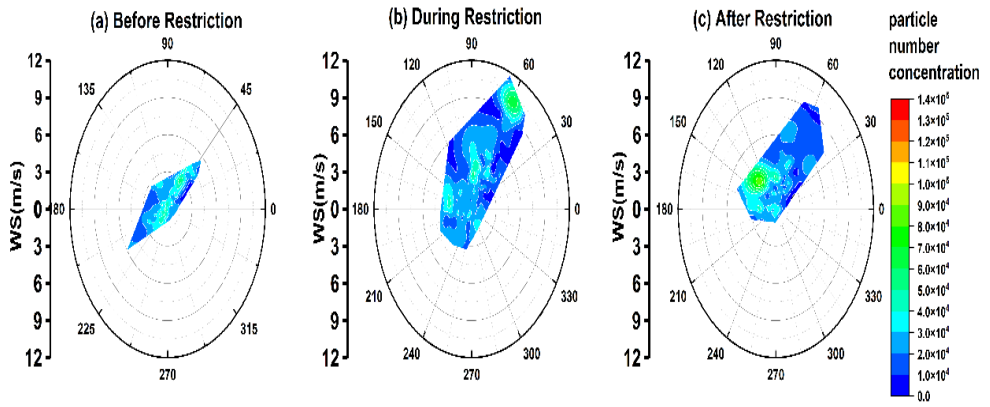

Figure 4.10: Polar plots of N_{total} with windspeed and direction during (a) BR-Before restriction, (b) DR – During restriction, (c) AR- After restriction during Period I (1st April 2021 to 30th June 2021)

Based on the velocity of the wind speed the dispersion also varied. However higher the wind speed more will be the dispersion of the particles. High dispersion of the particles resulted in less concentration (Hagler et al., 2012). Similarly, way during period II when the windspeed was less (<2 m/s) the concentration of the N_{total} concentration of the particles were found to have higher concentration and this occurs during the AD phase. During this period the recorded windspeed recorded was from the southwest to northeast direction due to the traffic induced turbulence created in the study area. During the AD phase the vehicular sources and Diwali activities were the major emission source. The wind direction in all the different directions reveals that the PNC decreased with increase in windspeed and vice versa. The observations during the period I and period II indicates that the regions located on the leeward side of the study region was found to have more concentration due to the transport of pollutants from windward side (Kozawa et al., 2012b). This indicates that the local emissions played a significant role in PNC concentration.

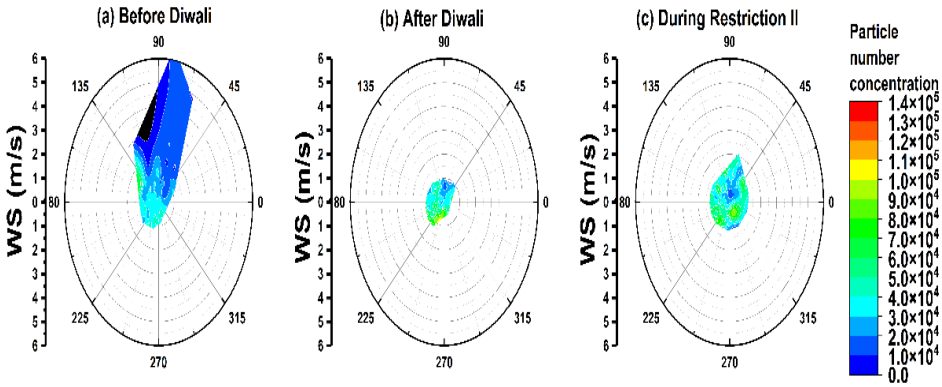

Figure 4.11: Polar plots of N_{total} with windspeed and direction during (a) BD-Before Diwali (b) AD – After Diwali (c) DR- During Restriction II during Period II (3rd October 2021 to 30th November 2021)

4.3 Seasonal analysis of particle number concentration

4.3.1 Seasonal temporal variation of particle number concentration (PNC)

The monitoring location in Delhi experienced widely varying concentration levels of particles in different seasons. The average concentration of total PNC was higher during winter, followed by spring, autumn, summer, and monsoon (Fig. 4.12). The average total PNC was found as >10^4 cm^{-3} during the year. The total PNC or N_{total} corresponds to the sum of Nucleation - N_{nuc}, small Aitken - N_{satk}, large Aitken - N_{latk}, and accumulation - N_{acc} modes (total PNC/ N_{total} = N_{nuc} + N_{satk} +N_{latk} +N_{acc}). The number concentration was higher during colder seasons (higher relative humidity and calm wind conditions) due to less dispersion when compared to hot seasons when wind speeds and ventilation coefficients were higher, which promoted higher dispersion resulting in comparatively lesser concentrations (Fig. 4.12, Gani et al., 2021).

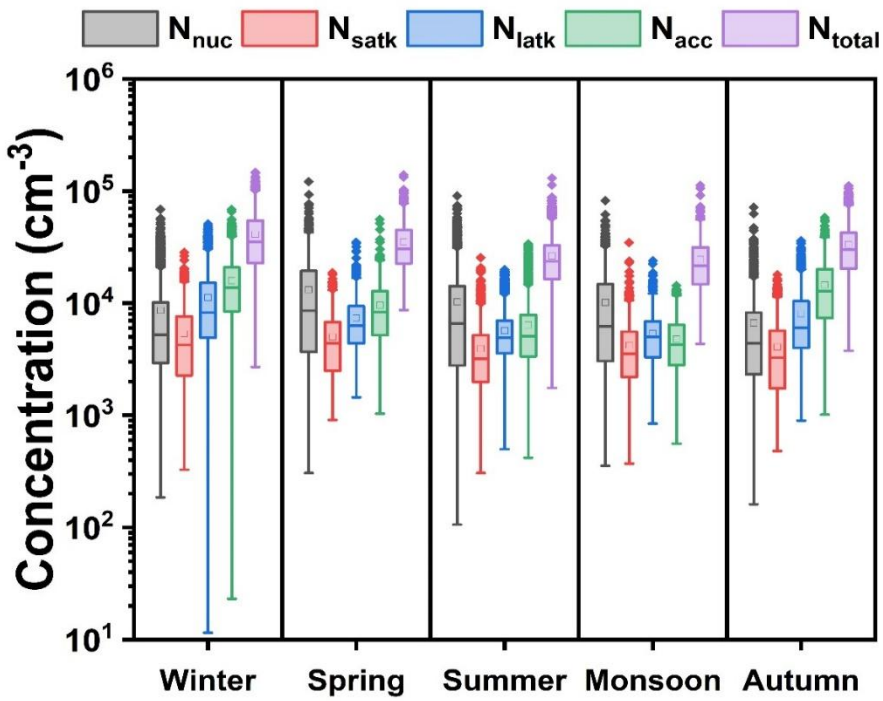

Figure 4.12: Seasonal mean concentration (cm^{-3}) of particles in the nucleation (N_{nuc}, 10 to 30 nm), small Aitken (N_{satk}, 30 to 50 nm), large Aitken (N_{latk}, 50 to 100 nm), and accumulation (N_{acc}, 100 to 1000 nm) size range and their total (N_{total}, 10 to 1000 nm) in different seasons in Delhi

The minimum and maximum PNC in different sizes varies in the range of 10^3 particles cm-3 (lowest in monsoon) to >10^5 particles cm^{-3} (highest in winter) (Table 4.4).

Results on a global study showed that particle concentrations may vary from 10^2 to 10^7 in highly polluted megacities such as Delhi and Beijing (Kumar et al., 2014), which are consistent with the present study. The seasonal mean PNC in different size bins of N_{satk} (5.3 x 10^3 cm^{-3}), N_{latk} (11.2 x 10^3 cm^{-3}), and N_{acc} (15.9 x 10^3 cm^{-3}) are the highest during the winter season giving rise to the highest N_{total} in winter (exceeding 40,000 particles cm^{-3}); interestingly, the seasonal behavior of N_{nuc} was different than the other sizes and exhibits a peak during the spring season with a concentration of about 13.2 x 10^3 cm^{-3}. The higher N_{nuc} in spring occurs due to prevalent atmospheric conditions of moderate relative humidity and solar intensity, which facilitate the new particle formation process. The new particle formation process increases the concentration of N_{nuc} particles significantly as only very few anthropogenic sources directly emit particles in this size range. The N_{total} concentration in winter is ~2 times higher than monsoon and 1.6 times higher than summer (Table 3). A comparison of day and night time concentrations in different size bins reveal that the lower size range particle, N_{nuc}, is higher during the daytime (Fig. 4.13). Higher N_{nuc} concentration in urban regions represents fresh emissions and particle formation process during the daytime, whereas higher N_{acc} mode particles in the nighttime occurs due to coagulation and emission from the traffic sources, especially heavy vehicles. The pattern and magnitude of N_{satk} and N_{latk} do not vary significantly between day and night (Fig. 4.13). The N_{total} is ~1.3 times lower in autumn and spring than winter. The lowest and highest concentrations in different sizes in seasonal scales are not uniform (Table 4.4). The PNC in bigger size range, N_{acc} and N_{latk}, are lower during the monsoon season due to wet removal leading to lower N_{total}, whereas PNC in smaller (N_{satk} and N_{nuc}) is relatively lower during the summer, monsoon and autumn seasons compared to spring due to new particle formation process and UFP bursts that occur during spring giving rise to higher N_{nuc} (Table 4.4).

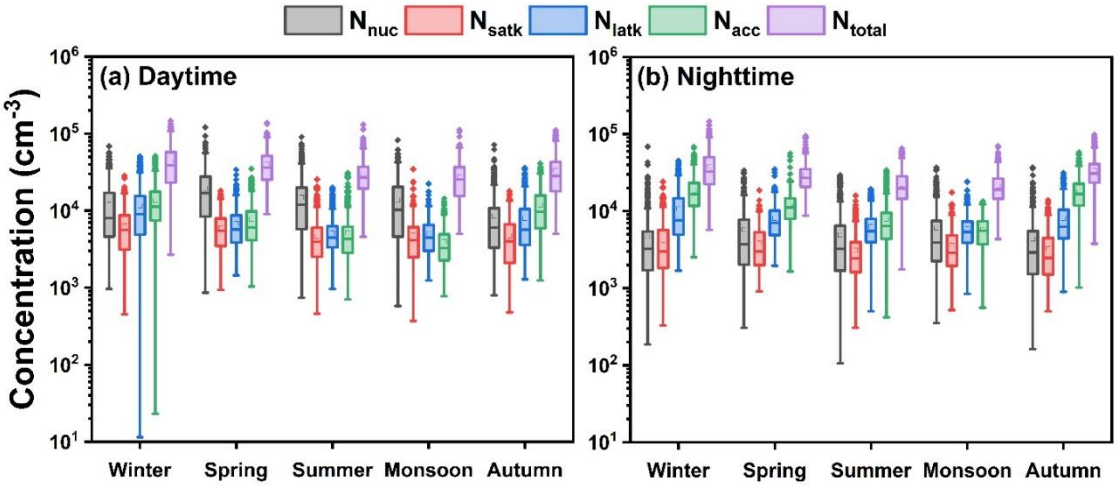

Figure 4.13: (a) Daytime and (b) nighttime variation in the number concentration of particles (cm^{-3}) in the nucleation (N_{nuc}, 10 to 30 nm), small Aitken (N_{satk}, 30 to 50 nm), large Aitken (N_{latk}, 50 to 100 nm), accumulation (N_{acc}, 100 to 1000 nm) and total (N_{total}, 10 to 1000 nm) during different seasons in Delhi

Table 4.4 Statistical summary of particle number concentrations (PNC) classified as a function of size into nucleation (N_{nuc}), small Aitken (N_{satk}), large Aitken (N_{latk}), accumulation (N_{acc}) and total (N_{total}) in different seasons over Delhi from the measurements made in 2020-2021

Season	Parameter	Minimum (cm^{-3})	Maximum (cm^{-3})	Mean ± 1σ (standard deviation) (cm^{-3})	Median (cm^{-3})
Winter	N_{nuc}	185	68626	8594 ± 9079	5201
	N_{satk}	327	28395	5335 ± 3842	4239
	N_{latk}	11	50832	11236 ± 8719	8248
	N_{acc}	23	68458	15905 ± 9645	13803
	N_{total}	2691	147182	41089 ± 23669	35134
Spring	N_{nuc}	306	121136	13234 ± 13287	8584
	N_{satk}	910	18674	4981 ± 3025	4390
	N_{latk}	1446	35027	7411 ± 4385	6326
	N_{acc}	1039	56033	9599 ± 5832	8337

	N_{total}	8694	139019	35226 ± 17909	30413
Summer	N_{nuc}	106	90646	10284 ± 10803	6556
	N_{satk}	305	25546	3928 ± 2734	3179
	N_{latk}	498	19861	5681 ± 3101	4916
	N_{acc}	418	33838	6411 ± 4808	5076
	N_{total}	1752	130433	26307 ± 13719	23702
Monsoon	N_{nuc}	353	82547	10161 ± 10078	6205
	N_{satk}	370	34664	4225 ± 2932	3546
	N_{latk}	843	23892	5397 ± 2811	5010
	N_{acc}	558	14345	4805 ± 2540	4257
	N_{total}	4337	112587	24590 ± 13256	21459
Autumn	N_{nuc}	161	71873	6667 ± 6955	4398
	N_{satk}	479	17876	4060 ± 2917	3263
	N_{latk}	897	36062	7990 ± 5789	6038
	N_{acc}	1012	58056	14610 ± 8940	12849
	N_{total}	3774	111316	33329 ± 17883	29893

4.3.2 Diurnal Variation of Particle Number Concentration

The diurnal variation of PNC in different size ranges clearly brings out the influence of traffic emissions in the urban curbside environment (Fig. 4.14). The N_{latk} and N_{satk} concentrations (Fig. 4.14 b, c) exhibit a more prominently clear double hump structure during the morning (07:00 to 11:00 h) and evening peak (16:00 to 20:00 h) in all the seasons confirming the dominance of traffic emissions to PNC in these size ranges in all the seasons. The N_{latk} represents the particles in the size range of 50 to 100 nm, and most of the particles emitted from vehicular exhaust lie in this size range. In winter and autumn, N_{latk} is higher than the PNC in the other size ranges throughout the day. Further, N_{latk} is ~2 times higher in winter and autumn than in the other seasons. The N_{nuc} mode particles show a similar emission pattern in all seasons with peaks (Fig. 4.14 a) during the active sunshine hours compared to the other hours of the day. This diurnal emission pattern of pollutants is induced by atmospheric and meteorological

variations in boundary layer height, temperature, wind speed, relative humidity, solar radiation and ventilation coefficient. The peak boundary layer height (BLH) (between 12:00 and 16:00 h) during winter is lowest (~500 m), whereas in summer the peak BLH increases by a factor of 4 going up to more than 2000 m in Delhi. The concentration of particles in different sizes also vary diurnally (e.g., Laakso et al., 2003).

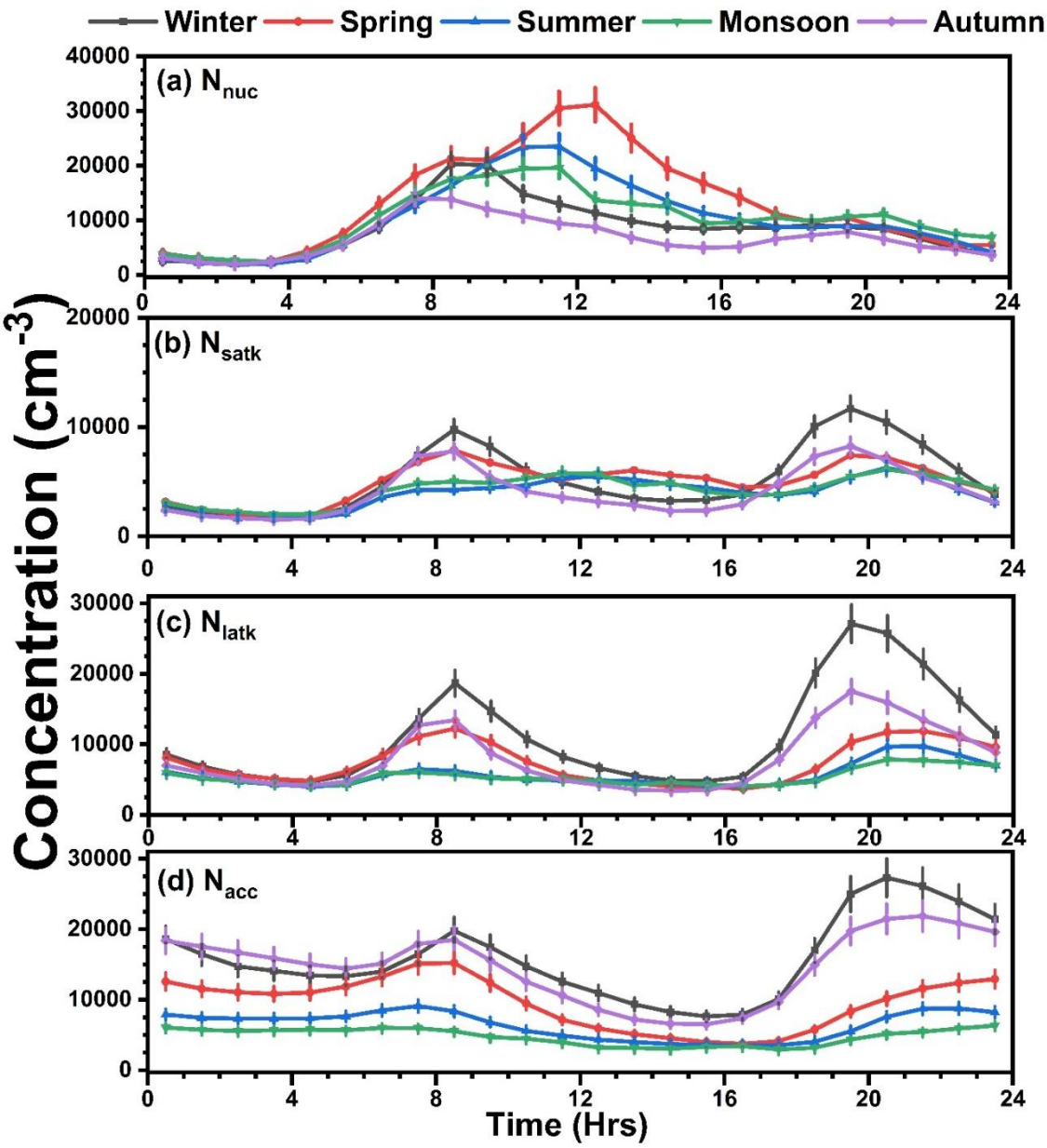

Figure 4.14: Diurnal variation (hourly average) of (a) N_{nuc}, (b)N_{satk}, (c)N_{latk} and (d) N_{acc} (cm^{-3}) during winter, spring, summer, monsoon and autumn seasons in Delhi. Vertical bars correspond to $\pm 1\sigma$ (standard deviation) from the mean

In summer and spring N_{nuc} is higher during the active sunshine hours owing to nucleation burst of particles, and new particle formation events, the details and the processes involved are beyond the scope of the present study. The new particle formation events start as a result of clustering particles in the sub-3 nm size range and oxidative precursor vapors. As the measurements of these events are unavailable, these events could not be probed further in this study. The SO_2 concentration is low during spring as it gets utilized in the formation of H_2SO_4 vapors, which acts as a precursor for the formation of new particle in nucleation mode (Fig. 4.14 a). The concentrations of other pollutants from vehicular emissions, such as nitrogen oxides (NO, NO_2 and NO_x) and carbon monoxide (CO) are also higher in winter. During summer, spring, and monsoon seasons, N_{nuc} increases whereas N_{acc} decreases due to reduced condensation of particles. The microphysical process of aerosol condensation is strongly influenced by relative humidity. Over the study region, RH is lower during summer and spring than winter which leads to lower coagulation of particles. The warmer summer and monsoon seasons are usually more ventilated than the colder winters (lower BLH). The solar radiation (SR) is higher in summer whereas RH is higher in winter.

The average diurnal concentration increases during morning peak hours irrespective of the season; however, in the evening hours, the peak concentration is different in different seasons because of the differences in BLH. During the warmer periods (summer and monsoon seasons), a higher BLH result in good ventilation, enabling dilution of particles resulting in lower N_{total}. A lower BLH, higher RH, lower temperature and lower SR helps trapping the pollutants near surface and result in significantly higher concentrations (>50,000 particles per cm^3) whereas a higher BLH, lower RH, higher temperature and higher SR during summer (and in monsoon) results in at least a factor of 2-lower concentrations than winter. Thus, this synergistic analysis of PNC in different size ranges along with local emissions of gaseous precursors, processes of formation, and meteorological parameters reveals that the PNC is

governed by local emissions of gaseous precursors and meteorological parameters, and the diurnal variations in PNC exhibit seasonal changes due to variations in these parameters.

4.3.3 Seasonal, and temporal variation of ultrafine and accumulation range particles

The diurnal and day to day variation of ultrafine particles (UFP, particles in 10 to 100 nm size range) and accumulation mode (N_{acc}, particles in 100 to 1000 nm size range), and the total particle number concentration (N_{total} particles in 10 to 1000 nm size range) are depicted in Figure 4.15.

The peak/non peak hour changes are analyzed using box whisker plot analysis. The diurnal variation of UFP (Fig. 4.15a) during peak and non-peak hours clearly demonstrates the dominant impact of vehicular exhausts in contributing to nanoparticle concentration (≥60%) in the urban roadside microenvironment. The measurement site is located adjacent to a busy arterial road, which has a higher contribution from traffic sources, resulting in more ultrafine size range particles (<100 nm) compared to N_{acc} (Fig. 4.15 b). Further, the day to day variation in UFP is significantly less than N_{acc} in all the seasons confirming the higher contribution in UFP size range which is more or less constant during the year (Fig. 4.15 d, e).

The UFP concentration is highest in winter followed by spring. The peak time in UFP concentration exhibit a seasonal variation – winter, spring and autumn the peaks occur earlier than summer and monsoon when UFP concentrations are lower. Whereas N_{acc} is highest in winter followed by autumn, spring and summer with monsoon N_{acc} being the lowest. The seasonal mean concentration of UFP is the highest in spring, followed by winter, summer, monsoon, and autumn, whereas for N_{acc} mode, the order of concentration is different, it is high in winter, followed by autumn, spring, summer, and monsoon. The concentrations of particles in different size ranges vary based on the variability and intensity of sources as well as due to the local meteorological conditions of the study area (Table 4.5, Fig. 4.15).

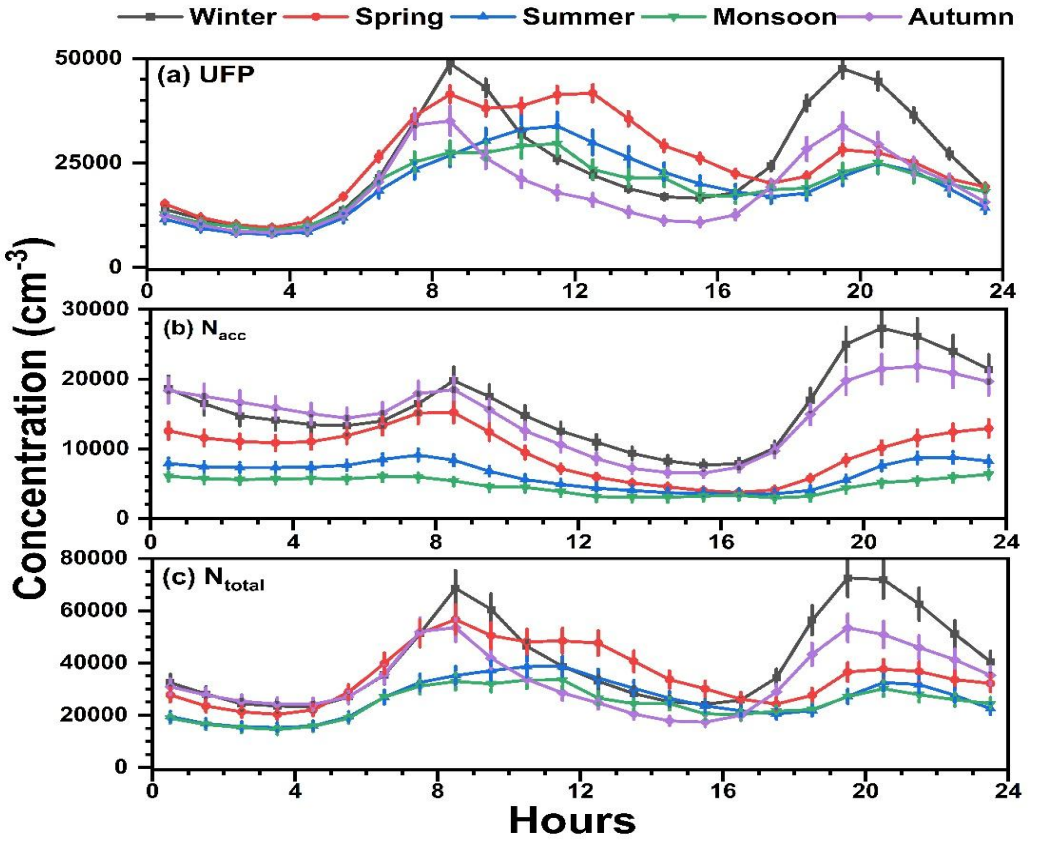
Winter
Spring
Summer
Monsoon
Autumn
(a) UFP
(b) N_{acc}
(c) N_{total}
Concentration (cm^{-3})
Hours

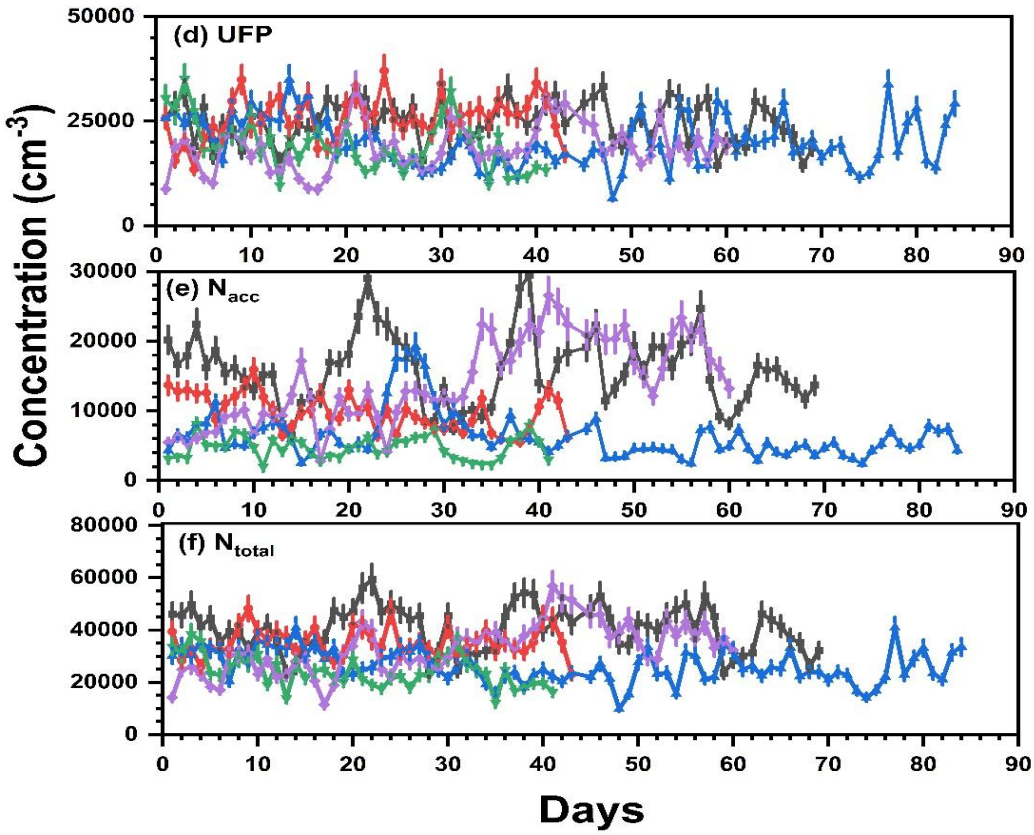
(d) UFP
(e) N_{acc}
(f) N_{total}
Concentration (cm^{-3})
Days

Figure 4.15: Diurnal variation of different sizes (a) UFP, (b) N_{acc} and (c) N_{total} and the temporal variation of daily mean concentration of (d) UFP, (e) N_{acc} and (f) N_{total} in different seasons during December 2020 - November 2021

Table 4.5: Statistical summary of UFP (10 to 100nm) and accumulation mode (N_{acc}, 100 to 1000nm) particles in different seasons and hours of the day over Delhi

Season	**Hour of the day***	**Ultrafine particles** (UFP, cm^{-3})			**Accumulation mode particles** (N_{acc} cm^{-3})		
		Min	**Max**	**Mean ± SD**	**Min**	**Max**	**Mean ± SD**
Winter	MPH	19	101916	41128 ±18959	23	50785	17332 ±9171
	EPH	12472	123505	42869 ± 15875	4661	68458	26135±11303
	NPH	8	121073	22820 ± 14525	3	46505	10498±6141
Spring	MPH	11250	123882	39383 ± 17588	2601	35018	12347±5916
	EPH	13494	677109	26921 ± 8924	1806	30236	10031±4344
	NPH	4411	129904	29836 ± 18099	1039	13578	5044±2157
Summer	MPH	6657	80490	30037 ± 14821	1092	30236	6906±4494
	EPH	3701	52382	23210 ± 8943	1426	13203	7270±4446
	NPH	2281	125935	23202 ± 14809	705	27585	3961±1876
Monsoon	MPH	19	70151	27980 ± 14324	23	13211	4818±2646
	EPH	8419	62950	23354 ± 11635	848	11221	4988±1758
	NPH	5	108793	20926±15693	2	12637	3215 ±1753
Autumn	MPH	5677	82898	27310± 16035	1376	40977	15475±7777
	EPH	6706	64603	20947± 11269	3647	55037	21023 ±1178
	NPH	2969	48912	16182± 10121	1246	31775	8928±5437

4.3.4 Peak and non-peak hour changes

The study region experiences high-ventilated periods during spring, summer and high humid conditions (Table 4.5, Fig. 4.16b) during winter, which influences the physiochemical properties of the nanoparticles (Sabaliauskas et al., 2012). The spring season is marked by frequent new particle formation events and UFP bursts, which

result in higher concentrations of UFP. However, the concentration of the UFP and N_{acc} particles generally show higher concentrations during the peak hours compared to the non-peak hours; during peak hours, most of the UFP concentration ranges are in 25 to 50 × 10^3 cm^{-3} (Fig. 4.16a, Table 4.4), whereas during non-peak hours the concentration decreases and it is <25 × 10^3 cm^{-3} (Fig. 4.16b, Table 4.6) range except in spring season. The concentrations in morning and evening peak hours are not uniform throughout the study period. The UFP and N_{acc} during the evening peak hour is higher than the morning peak hour in winter (42 x 10^3 cm^{-3} (UFP), 26 x 10^3 cm^{-3} (N_{acc})) and in autumn (20 x 10^3 cm^{-3} (UFP). 21 x 10^3 cm^{-3} (N_{acc})) due to less ventilation/lower dispersion, higher rate of coagulation and condensation. The N_{acc} is the lowest in monsoon (3.2 x 10^3 cm^{-3}) due to wet removal of particles in larger size. The analysis shows that the concentration of UFP and N_{acc} mode particles in a region is highly dependent on the sources and the local meteorological conditions of the particular region, and concentration can vary significantly under the influence of these two factors (Fig 4.17). The seasonal mean concentration of total PNC (10 to 1000 nm) in the study region varied from 24 (monsoon, the lowest) to 41 × 10^3 cm^{-3} (winter, the highest) (Table 4.6). The maximum PNC was found range of 111-147 x 10^3 cm^{-3} over Delhi in different seasons; the highest PNC was observed in winter and lowest in monsoon, whereas the minimum PNC was in the range of 1-9 x 10^3 cm^{-3} with minimum value being the lowest in monsoon and highest in spring (Table 4.6).

Table 4.6: Seasonal mean concentration of total PNC covering the size range of 10 to 1000 nm over Delhi. Total PNC is given in units of 10^3 cm^{-3}. Mean ± 1σ (standard deviation), maximum, minimum and median values obtained in different seasons are given

Seasons	Mean ± 1σ (standard deviation) PNC × 10^3 cm^{-3}	Minimum PNC × 10^3 cm^{-3}	Maximum PNC × 10^3 cm^{-3}	Median PNC × 10^3 cm^{-3}
Winter	41.0 ± 23.7	2.6	147.2	35.1
Spring	35.2 ± 17.9	8.7	139.0	30.4
Summer	26.3 ± 13.7	1.7	130.4	23.7

Monsoon	24.3 ± 13.4	1.4	112.5	21.0
Autumn	33.3 ± 17.8	3.7	111.3	29.9

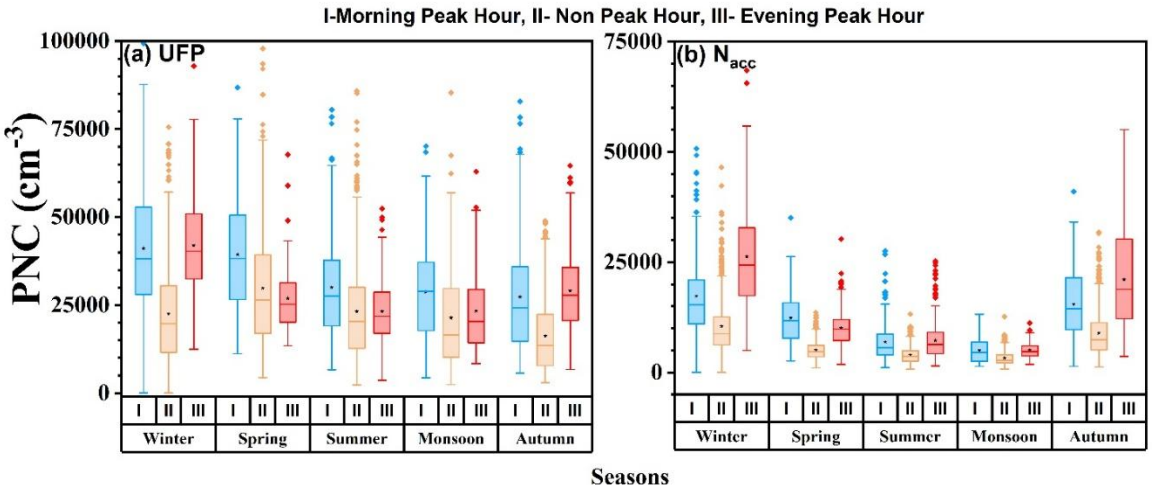

*Figure 4.16: Seasonal mean concentration of particles in the (a) ultrafine range (UFP 10 to 100 nm) and (b) accumulation range (N_{acc}) during different hours of the day – MPH - morning peak hours (7 to 11 h), NPH - non-peak hours (11 to 16 h) and EPH - evening peak hours (16 to 21 h) in different seasons during December 2020 - November 2021. The rectangular box represents data range of 25 to 75% in the box plot. The upper line represents the upper quartile value. The lower line represents a lower quartile value. The centerline of each box corresponds to the median value, and * represents the mean value. The symbol (–I) at the top and bottom of each box denotes the maximum and minimum values*

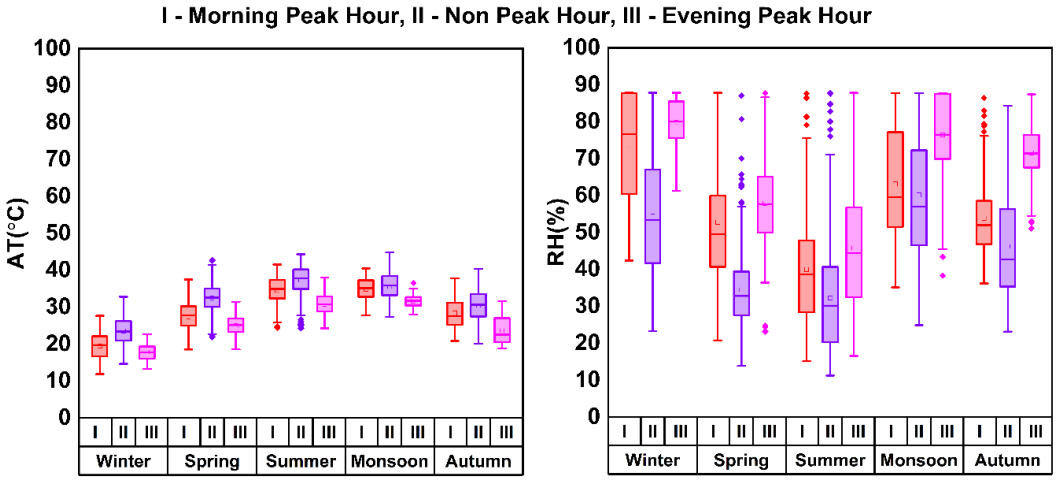

Figure 4.17: Seasonal mean concentration of meteorological parameters (a) air temperature (AT°C) and (b) relative humidity (RH, %) during different hours of the day. MPH - morning peak hours (7 to 11 h), NPH - non-peak hours (11 to 16 h) and EPH - evening peak hours (16 to 21 h) during December 2020-November 2021 over Delhi

4.3.5 Size distribution of ultrafine and accumulation mode particles

The particle number size distribution (PNSD) of measured ultrafine and accumulation mode particles are analyzed during peak and non-peak hours in different seasons to determine the dynamics of the particles (Fig. 4.18). The size distribution determines the precise particle range that dominates the season and identifies the sources similar to the concentration of particles (Fig. 4.18). An analysis of PNSD is significant as it provides quantitative information on the number of particles in different size bins, which is crucial for this study. In winter and autumn, the particle number size distribution during EPH exhibits a single clear peak concentration at around 100 nm size, which is a typical profile of vehicular exhaust sources, especially in urban regions (Sebastian et al., 2021; Yadav et al., 2021). Except for the concentration changes, the MPH follows a similar emission profile as that of EPH during winter and autumn. Besides exhaust emissions, the local meteorology prevalent during winter and autumn influences the concentration of these particles.

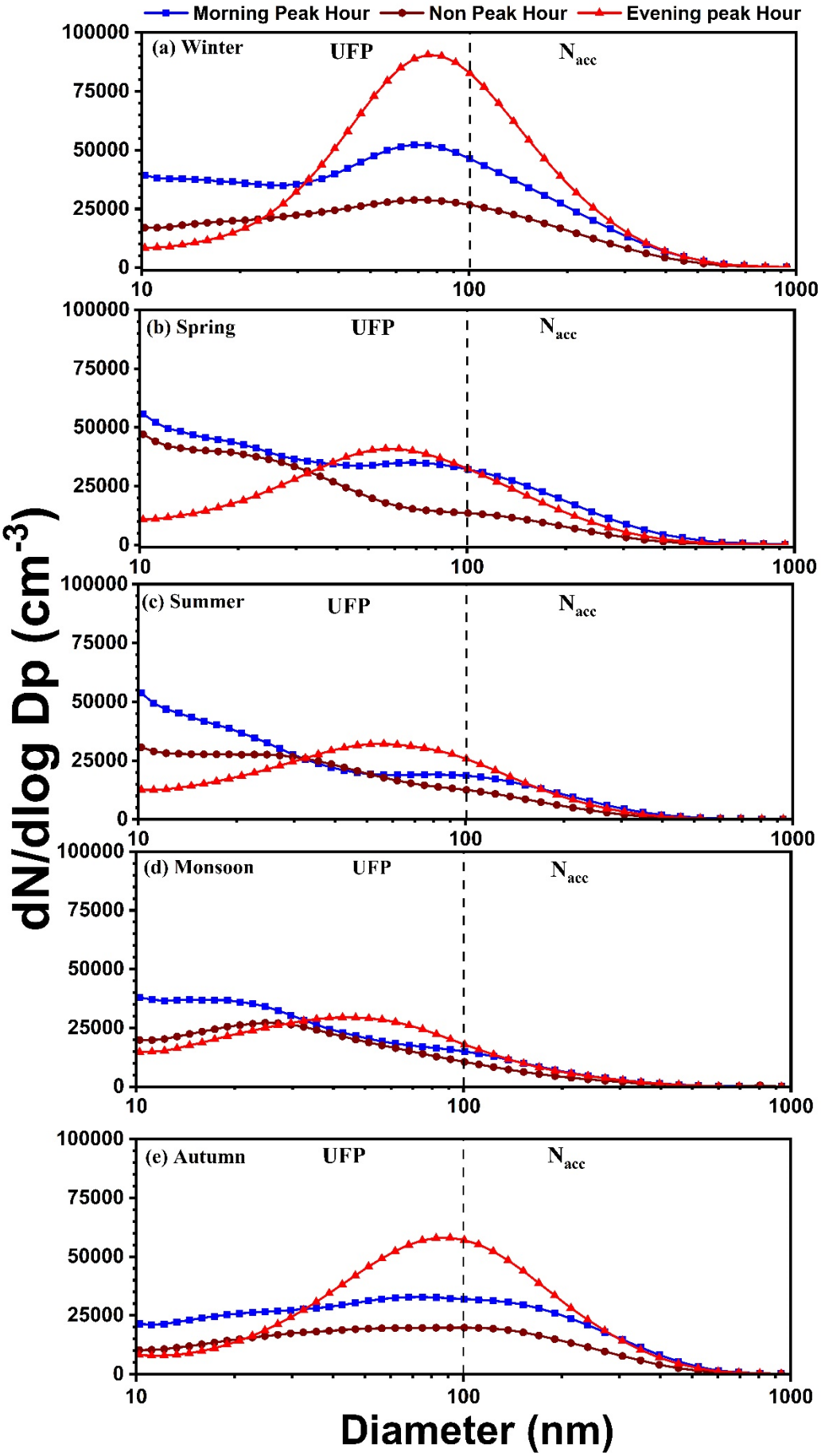
Morning Peak Hour
Non Peak Hour
Evening peak Hour
(a) Winter
(b) Spring
(c) Summer
(d) Monsoon
(e) Autumn
UFP
N acc
dN/dlog Dp (cm-3)
Diameter (nm)
100000
75000
50000
25000
0
10
100
1000

Figure 4.18: Size distribution of Ultrafine particles (UFP) (10 to 100 nm) and accumulation mode particles (100 to 1000 nm) during different hours of the day, such as morning peak hours (7 to 11 h), non-peak hours (11 to 16 h) and evening peak hours (16 to 21 h) over Delhi in (a) winter, (b) spring, (c) summer, (d) monsoon, and (e) autumn, respectively

Whereas during summer and spring (Fig. 4.18), the EPH concentration is not similar to winter and autumn due to different meteorological conditions that prevail during that period, which influences the dispersion of particles (Tyagi et al., 2020). The size distribution in the morning peak hours during summer, monsoon, and spring (Fig. 4.18 b-d) is not similar to winter. Instead, a gradual decrease in concentration from a smaller size to a bigger size occurs, leading to a higher concentration in the UFP range and a lower concentration in Nacc ranges, respectively. The increase in the concentration of smaller size range particles (< 30 nm) during spring (Fig. 5b), especially during non-peak (11-16 h), occurs due to new particle formation events driven by photochemistry, humidity, and solar intensity (which is higher, Table 3) (Deng et al., 2020; Kanawade, et al., 2021; Zimmerman et al., 2020).

4.3.6 Monthly and diurnal variations of particle size distribution

The monthly analysis of particle size distribution during the monitoring period reveals that the concentration of particles <300 nm is the highest in the size range of 10 to 1000 nm, and ranges between 4×10^4 cm^{-3} and 5×10^4 cm^{-3} (Fig 4.19a). During the pre-monsoon months of March, April and May the concentration of particles in the size range <50 nm is higher over Delhi, and exceeds 4×10^4 cm^{-3} which is attributed to gas-to-particle conversion mechanism. These months are found to be favorable for new particle formation process over the study region (Yadav et al., 2021). The annual mean total PNC over the study region is 3.22×10^4 cm^{-3}. The diurnal mean of PNC over the study region exhibits two peaks of higher concentration during the day – one during the morning peak hours and the other in the evening peak hours (Fig 4.19b). The pattern of morning and evening peaks remains constant throughout the year due to the dominance of particle emissions from local sources (vehicles) over the study region. The peak concentration in the evening hours is more prominent, and higher

than the morning peak hour concentration due to the accumulation of particles in the atmosphere over the study region. Though the morning and evening peaks occur due to vehicular emissions predominantly, the evening peak concentration is higher owing to a significant increase in vehicular emissions accompanied with variations in meteorology and atmospheric dynamics (such as shallow boundary layer). This feature in the diurnal mean in PNC is consistent with results obtained over an urban region (e.g., Rajesh and Ramachandran, 2024).

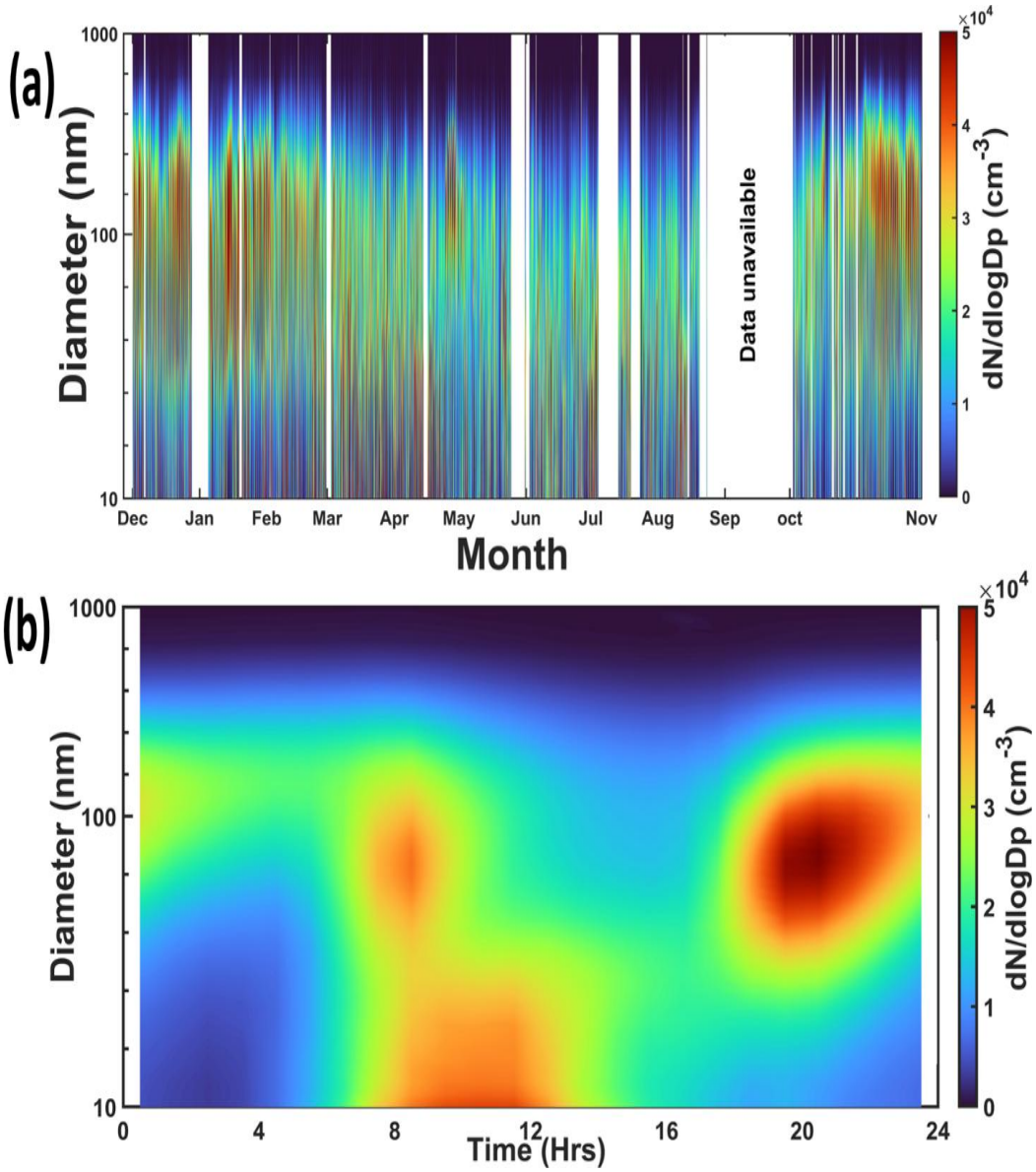

Figure 4.19: (a) Time series of particle size distribution in the size range of 10 to 1000 nm over Delhi during December 2020-November 2021. (b) Diurnal variation of particle number size distribution during the monitoring period over Delhi

4.3.7 Contribution of UFP and Accumulation mode in total PNC

The contribution of UFP and N_{acc} to the total PNC varies seasonally (Fig. 4.20), due to the differences in emission sources and prevalent local meteorological conditions (mainly changes in wind speed, relative humidity, and boundary layer heights).

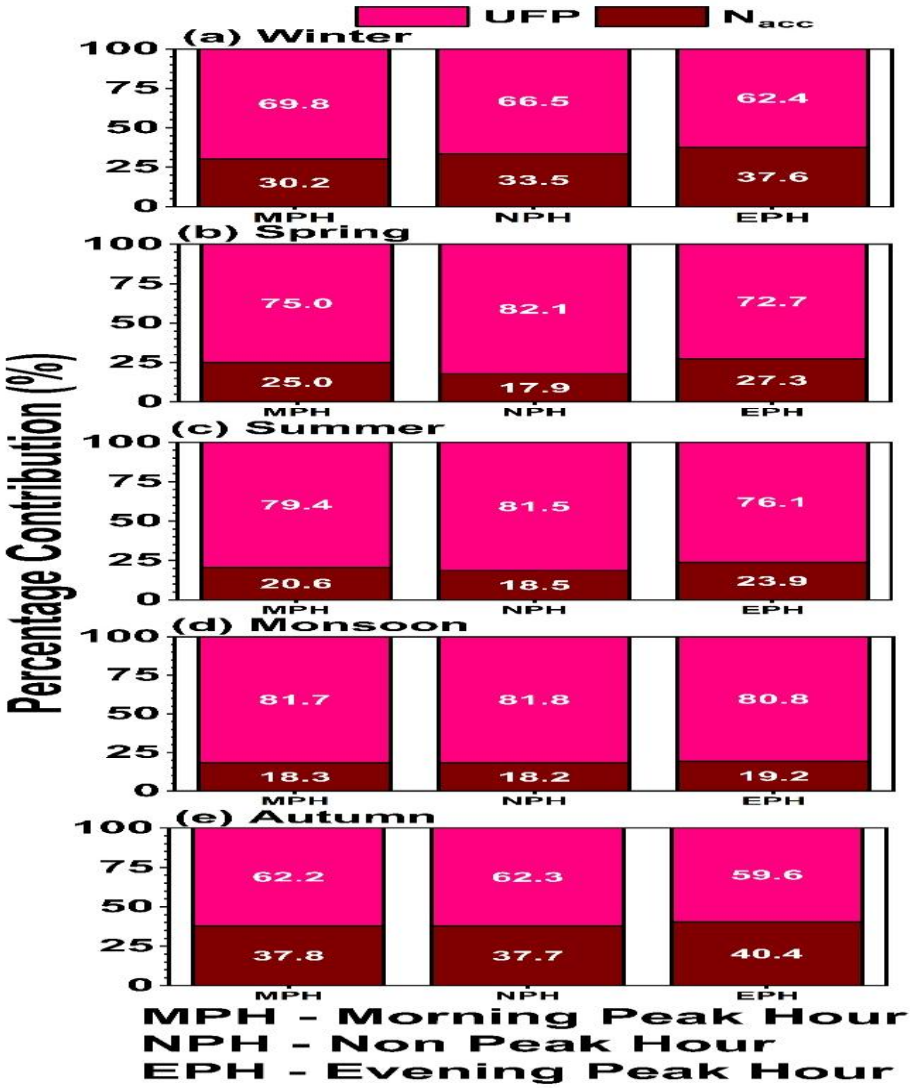

Figure 4.20: Percentage contribution of Ultrafine particles (UFP of 10 to 100 nm size) and accumulation mode particles (N_{acc} of 100 to 1000 nm size) to total concentration in Delhi during morning peak hours (7 to 11 h), non-peak hours (11 to 16 h) and evening peak hours (16 to 21 h) in (a) winter, (b) spring, (c) summer, (d) monsoon, and (e) autumn, respectively

The UFP mode (<100nm) includes particles in the nucleation (10 to 30 nm) and Aitken mode (30 to 100 nm). The majority of vehicular emissions lie in the UFP range. The meteorological factors determine the ventilation rate of nanoparticles or coagulation and condensation of the particles (Wang et al., 2017). The accumulation mode particles contribute about one-third to the total concentration in regions with higher relative humidity and calm wind conditions, such as winter and autumn (Aggarwal et al., 2012), whereas in the urban regions, the contribution of UFP to total particle number concentration is higher. In the present study, the UFP contributes about 59% to 82% to the total particle concentration in different seasons. The contribution of UFP is the highest during monsoon season (80 to 81%) (Fig. 4.20d), highest contribution observed throughout the study period, and this occurs due to the wet removal of N_{acc} mode particles to a large extent.

Similarly, during summer, the contribution of UFP is >80% (Fig. 4.20c), whereas, in summer, the reduction in N_{acc} mode particles is less as condensation and coagulation is less effective because of lesser humidity in summer. During the autumn season, UFP contributes around 59 to 62%, which is the lowest contribution observed throughout the study, and this is due to the influence of higher wind speed, which limits the aging of particles and their growth. During the study period, N_{acc} mode particles during winter and autumn contribute around 30 to 40% to the total concentration of particles, which is the highest average contribution of N_{acc} mode particles compared to other seasons. The winter and autumn seasons and the meteorological conditions are favorable for particle growth through aging and coagulation. In the study region, the sources are the same throughout the year, i.e., mostly engine exhaust sources: However, the variations in the contribution of UFP and N_{acc} to the total PNC are influenced by the variability in local meteorological parameters. The dominance of UFP contribution in the study region occurs due to the direct association with vehicular

exhaust. The monitoring site is located in an urban region, especially adjacent to the road, where the majority of the vehicles use petrol, diesel, and compressed natural gas as fuels, resulting in the dominance of UFP contribution to the total PNC of nanoparticles in the study region.

4.3.8 Size resolved particle contribution

The N_{total} concentration or total PNC is made up of contributions from all the size fractions (Total PNC/N_{total} = N_{nuc} + N_{satk} +N_{latk} +N_{acc}). Apart from changes in concentration, the contribution of different size fractions to N_{total} also varies from season to season due to changes in nanoparticle emission sources, patterns, and regional meteorology (Fig. 4.21). During the winter season, when N_{total} was the highest, $N_{acc,}$ contributes the maximum at 41% followed by N_{latk} 26% to N_{total}. N_{acc} contribution was higher in this season due to higher rate of coagulation in the atmosphere under high relative humidity and lower temperatures. Similarly, in autumn, N_{acc} accounts for 45% of N_{total}. N_{acc} contributes ≥30% during winter and autumn to the total. During spring, summer, and monsoon, the contribution of N_{nuc} is 33%, 34%, and 36%, respectively to N_{total}.

The percentage contribution of N_{satk} and N_{latk} does not varied significantly during the year in Delhi, and their contributions lie in the 12-17% range, and 22 to 26% range, respectively (Fig. 4.21). This indicates that the contribution from the emission sources of particles in the size range of 30 to 100 nm was uniform throughout the year. The smaller N_{nuc} and the larger N_{acc} exhibit a higher variation in their respective contributions to the total, varying from 20% to 36% and 23% to 45%, respectively. Overall, the contribution of N_{satk} (30 nm to 50 nm) particles to total PNC remains more or less the same during all seasons. N_{latk} particles (50 nm to 100 nm) contribute about 25% to the total PNC in all seasons (Gani et al., 2019; Patel et al., 2021).

The percentage contributions by different size particles to N_{total} during daytime and nighttime (Fig. 4.21) vary and the results clearly indicate the distinct role of diurnal variation in emission sources. The % contributions of nucleation mode followed by accumulation contribute >60% to N_{total} during daytime with their sum contribution being the highest in spring season (67%) (Fig. 4.21).

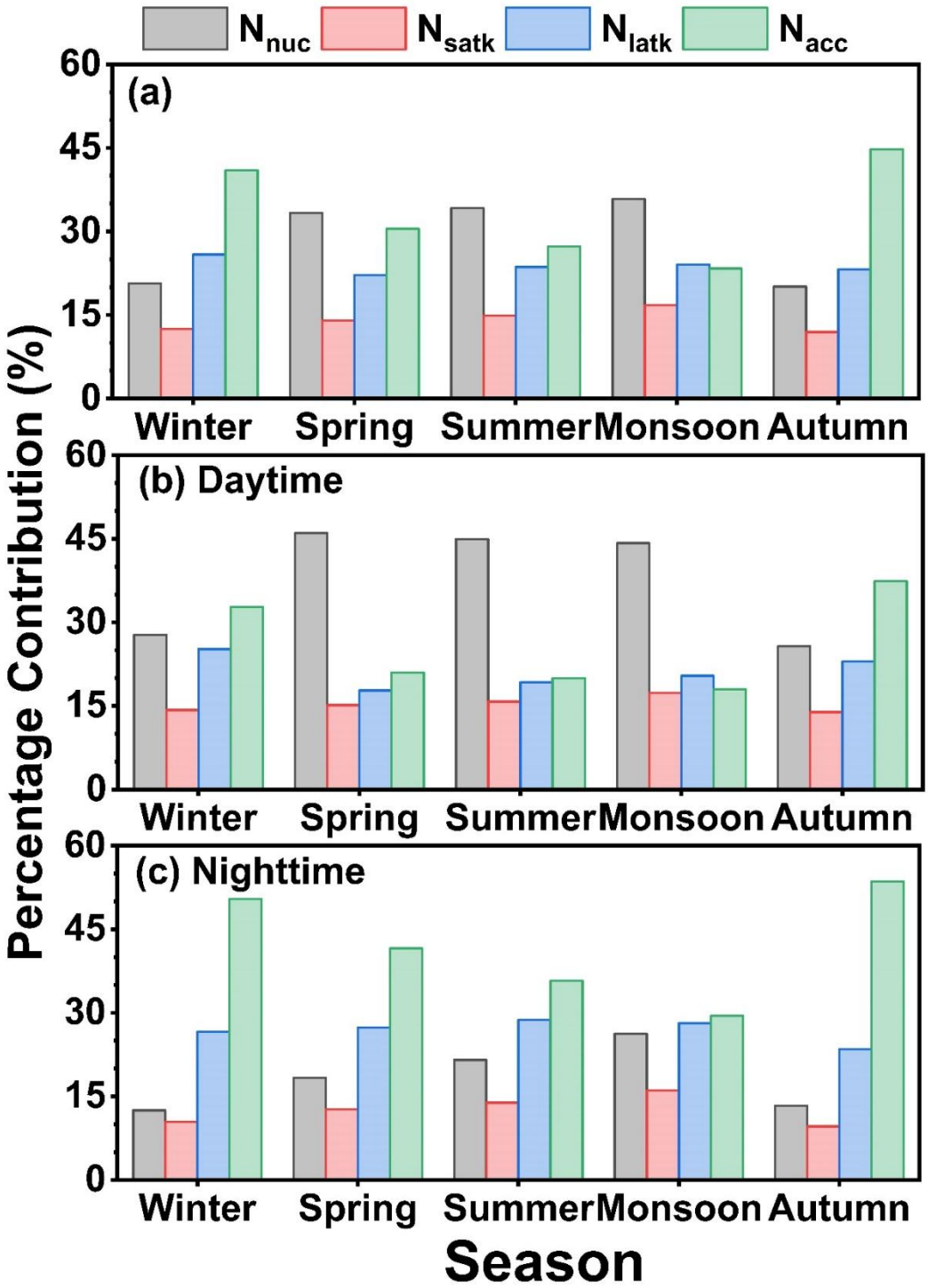

Figure 4.21: Percentage contribution (%) of N_{nuc}, N_{satk}, N_{latk}, N_{acc} to total concentration (N_{total}) from winter to autumn in Delhi (a) throughout the day (24h), (b) in daytime (08:00 to 20:00 h) and (c) in nighttime (20:00 to 08:00 h)

During the warm periods of spring, summer and monsoon, N_{nuc} contributes ~45% to N_{total} during daytime due to the prevalent meteorology conditions which enables freshly emitted exhaust emissions to remain in the atmosphere longer. Whereas in autumn and winter, N_{nuc} contributes <30% to N_{total} in daytime. In stark contrast, N_{acc} dominates the contribution (50% or more) to N_{total} during nighttime in winter and autumn as a result of coagulation of emitted particles as the prevalent atmospheric conditions (higher RH, lower temperature and BLH) favor coagulation (Fig. 4.21b). The N_{satk} contributes <20% during both day and night time in all the seasons.

The contribution from N_{satk} and N_{latk} during daytime and nighttime do not exhibit significant seasonal variabilities – N_{satk} contributes 14-17% (daytime) and 10-16% (nighttime), whereas N_{latk} contributes 18-25% (daytime) and 23-29% (nighttime), respectively. The variations in the contribution of different size particle to N_{total} suggests that the contribution from different sources either enables or inhibits due to the participation of precursor gases and prevailing meteorology, which influence the formation mechanism of nanoparticles in urban regions. Thus, it is clear that the variation in N_{total} concentration on seasonal scales occur as a result of differences in contribution from varied size ranges, sources, and meteorological conditions which vary diurnally and seasonally. Further, such complex mixture of the formation processes in different size ranges makes mitigating poor air quality conditions in these regions difficult.

4.3.9 Heat map analysis of seasonal particle size distribution

A heat map represents the evolution of particle number size distribution with the time in different seasons (Fig. 4.22). In winter, the intensity of accumulation mode particles is high during evening hours, especially from 18:00 to 22:00 h due to coagulation of particles and lower BLH (Fig. 4.22a). In spring, the concentration was found high between 08:00 and 16:00 hours due to gas-to-particle formation mechanism wherein the concentration of particles of size <100 nm attained a peak between 1100 and 1300 hours due to new particle formation events (Sebastian et al., 2021) (Fig. 4.22). The time periods, and favorable meteorological conditions for the new particle formation events reported in earlier studies (e.g., Gani et al., 2021) are similar as in the present

study. The scenario is similar in summer (Fig. 4.22c), however, a complete new particle formation does not occur owing to the emissions from other sources such as vehicular exhaust which suppress the new particle formation process, which was termed a UFP burst. A UFP burst refers to a disturbed or incomplete new particle formation process. During the nucleation process, accumulation mode particle concentration starts increasing gradually from the beginning of the new particle formation event until the end of the process due to the growth of particles from smaller to larger sizes after the nucleation events. This is defined as a complete new particle formation process. The new particle formation process can last for a few hours in a day. In an urban region like Delhi, emissions from different complex sources often disturb/inhibit the above formation process. During the monsoon season, the burst in smaller size particles is interrupted by precipitation events. The particle concentration changes between 08:00 and 12:00 h based on sources and prevailing meteorological conditions. The sources, and the formation of particles by nucleation and other secondary processes govern the magnitude of geometric mean diameter of particles, which was derived by analyzing the particle size distribution and the concentrations. In winter and autumn, the concentration of particles with a diameter >700 nm (that falls in accumulation mode) was higher, whereas the concentration of particles that are ≤100 nm covering the nucleation, small Aitken, and large Aitken sizes are significantly lower (Fig. 4.22). During spring and summer, the concentration of particles <700 nm was significantly higher than the smaller size particles, both of which are consistent with the formation mechanism, sources, and meteorological conditions during these seasons. In summary, the heat map provided a complete picture of formation process and concentrations of particles in different seasons on a diurnal scale, was consistent with the sources of particles and formation, and the prevailing meteorological conditions over the urban region Delhi.

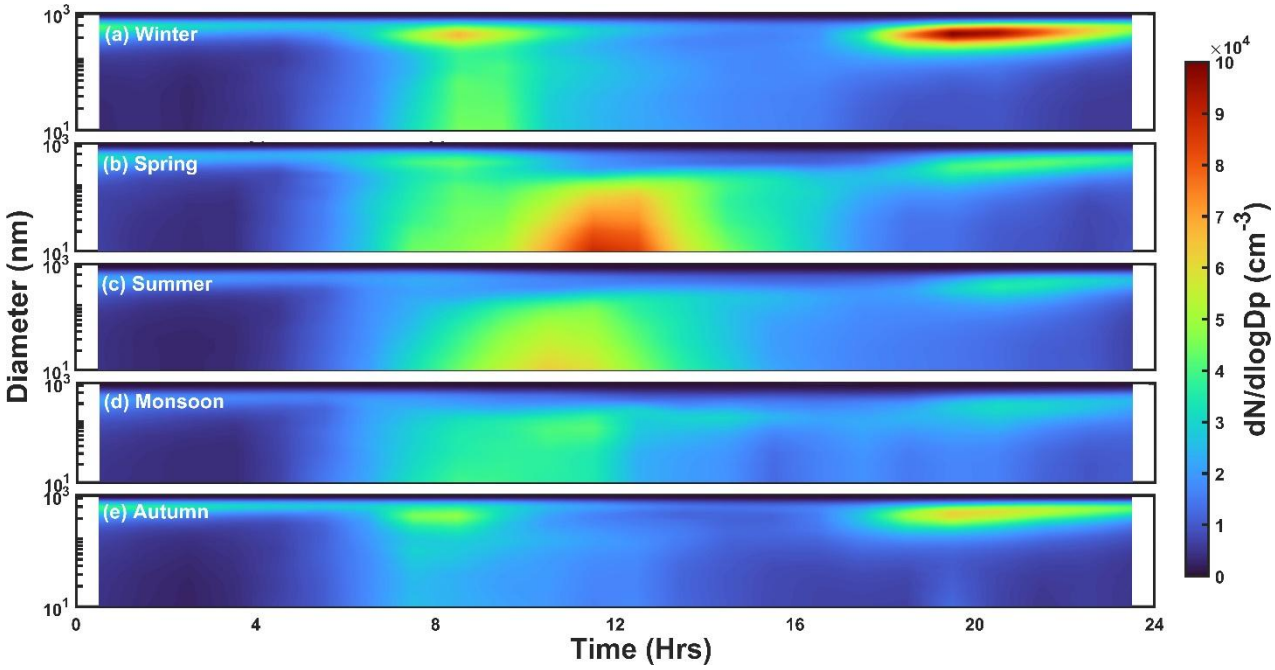

Figure 4.22: Heat map of particles in the 10 to 1000 nm size range (dN/dlogDp, cm^{-3}) as a function of time of the day in different seasons – winter, spring, summer, monsoon, and autumn, respectively over Delhi

4.3.10 Number, mass, surface area and volume distribution during different seasons

The (number, mass, surface area and volume) size distributions from 10 to 1000 nm were used to determine the characteristics of measured particles (Fig. 4.23). The particle number size distribution (PNSD) showed a single clear peak during winter and autumn which was the highest measured concentration compared to other seasons (Fig. 4.23a). The peak concentration was from 100 to 200 nm in almost all seasons, which falls under accumulation mode. Generally, the particle sizes from fresh exhaust emissions of different engines were lower than 100 nm, which showed that in the study area, the emitted fresh particles frequently underwent aging processes in the atmosphere. The peak concentration in the accumulation mode also rose during humid periods due to the evaporation of aqueous droplets (Yao et al., 2007). Mass size distribution showed that the particles in the N_{acc} range were 3 to 4 times higher than other size fractions which further, contributed to the concentration of particulate matter (Şahin et al., 2022; Trechera et al., 2023). The volume of the particle size distributions

looked similar to that of the mass (Fig. 4.23b, d) since they were calculated based on the number concentration, assuming a spherical shape of the measured nanoparticles and the same density.

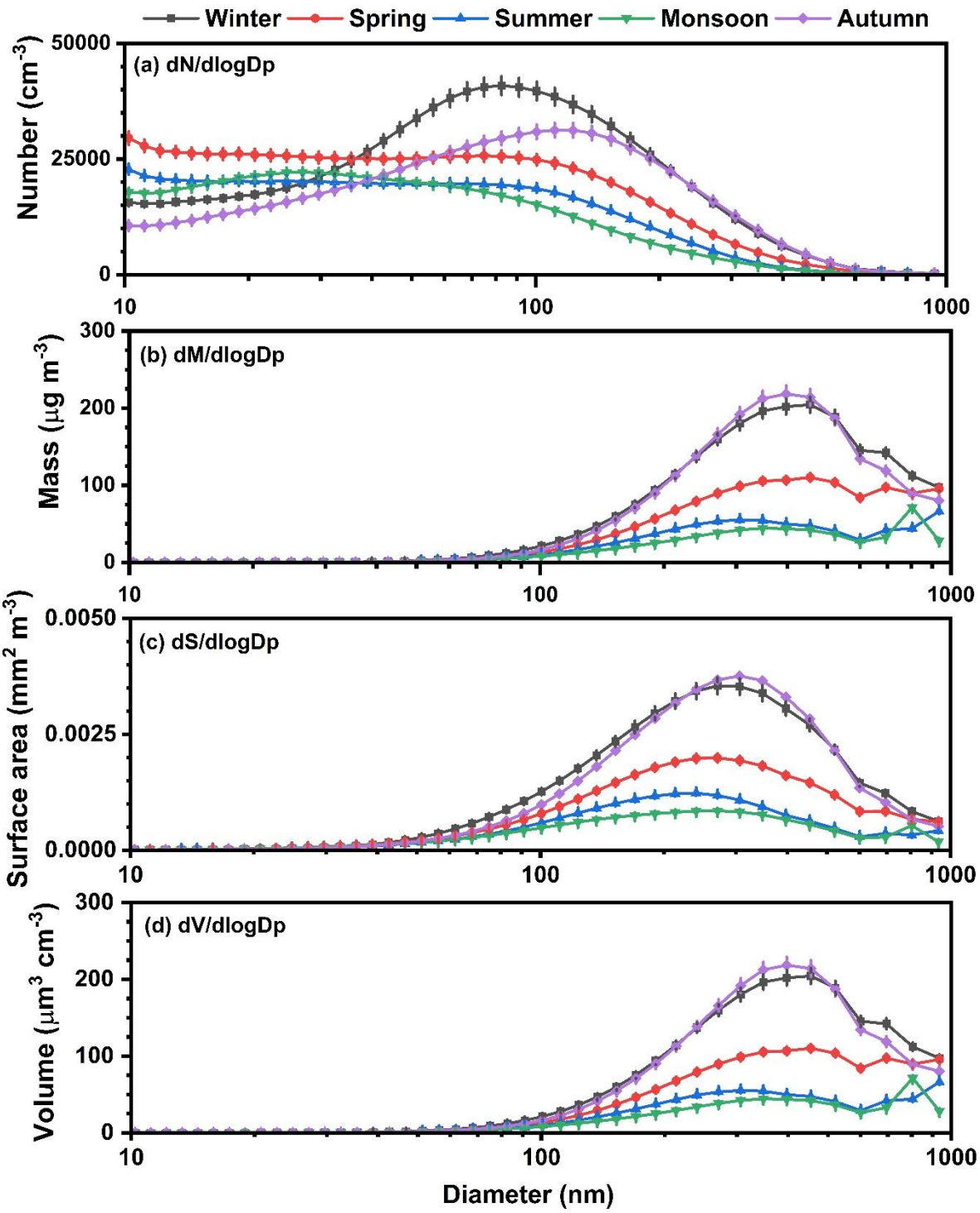

Figure 4.23: The ((a) number, (b) mass, (c) surface area, and (d) volume) size

distribution of aerosol particles from 10 to 1000 nm during winter, spring, summer, monsoon, and autumn in Delhi, a megalopolis (vertical bars represent ± standard deviation from the mean)

Knowing the particle surface area is necessary to evaluate the health impact because the nanoparticles with lower mass and higher surface area possess a higher potential to impact health due to a higher surface reactivity (Qiao et al., 2015), and the generation of reactive oxygen species (ROS). ROS generation is an important factor in analyzing the toxic effects of the inhaled nanoparticles. It develops cytotoxicity, apoptosis, oxidative DNA damage, and cell motility (Chalupa et al., 2004; Ma et al., 2022). The analysis of the particle size distribution showed that the particle surface area was similar during the winter and autumn seasons, peaking at 3.5 x 10^{-3} mm^2 m^{-3} around 300 nm (Fig. 4.23c). In other seasons, even though the concentration of the particle was less, the particle surface area remained more or less the same based on the size and still posed threat to the residents.

4.4 Seasonal variation of gaseous pollutants

4.4.1 Diurnal variation of local emissions in the roadside environment

The major source of nanoparticle emissions over the monitoring location was vehicular emissions. Apart from nanoparticles, various gaseous pollutants are also emitted due to different processes in the urban environment. The gaseous pollutants, such as CO and nitric oxide (NO), are released in the urban environment from combustion processes such as burning fossil fuels and biomass/biofuels.

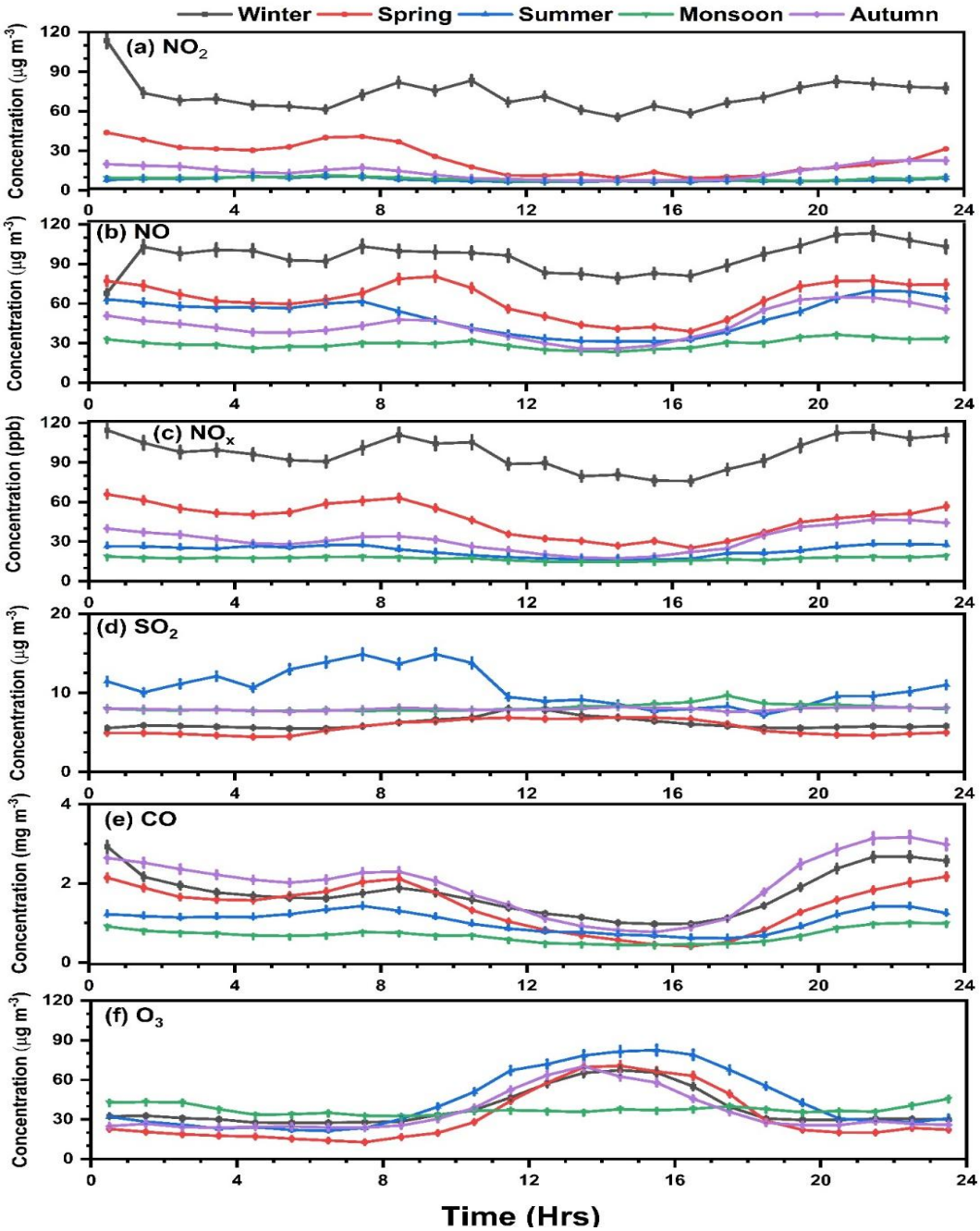

Figure 4.24: Diurnal variation (based on hourly averages) of gaseous pollutants (a) nitrogen dioxide (NO_2 µg/m^3), nitric oxide or (b) nitrogen monoxide (NO µg/m^3), (c) nitrogen oxides (NO_x ppb), (d) sulfur dioxide (SO_2 µg/m^3), (e) carbon monoxide (CO mg/m^3), (f) ozone (µg/m^3) during winter, spring, summer, monsoon and autumn seasons over Delhi. Vertical bars denote ±1σ (standard deviation) from the mean

The diurnal variation of PNC and gases such as CO (and NO) shows a similar pattern, suggesting that the sources of these gaseous and nanoparticle emissions are the same, i.e., transportation sources at the monitoring location. The increase in ozone (O_3) concentration during the sunshine hours in mid-day and afternoon and reduced concentration of NOx in the presence of nitrogen dioxide (NO_2) as a precursor compound due to the photochemical reaction is evident during spring, summer, and autumn when ozone formation by volatile organic compounds (VOCs) and NO_x is a common phenomenon in urban regions (Fig. 4.24, Table 4.7) (e.g., Nelson et al., 2021). In winter, the concentration of SO_2 is relatively higher in the afternoon, suggesting that formation of H_2SO_4 aiding new particle formation process is inhibited during this period due to unfavorable relative humidity and solar intensity (Fig. 4.24). In contrast, during summer, SO_2 concentration is lower due to the use of sulfur compounds as a precursor material for the new particle formation events. During summer and spring, N_{nuc} is also higher, suggesting that higher N_{nuc} occurs due to the emissions and the new particle formation events that contribute to the increase in particle number concentrations in the roadside environment. The particles in the accumulation mode of size range between 100 and 1000 nm occur due to condensational growth and coagulation processes.

The particles in accumulation mode relatively have relatively longer residence times compared to nucleation mode particles. As a result, the contribution of N_{acc} is to particulate matter formation, such as $PM_{2.5}$ and $PM_{10,}$ is proportionately higher (Apte et al., 2011). To explore the relation between the gaseous pollutant emitted due to combustion process over an urban environment and the stable particles in the accumulation mode, carbon monoxide (CO) is correlated with N_{acc} mode (100 to 1000 nm) in all the seasons. CO is found to correlate positively well with Nacc in all the seasons in Delhi, with the coefficient of determination (R^2) between CO and N_{acc} being ≥0.48 in all the seasons (Fig. 4.25), whereas the R^2 between CO and N_{latk} (50 to 100 nm) is ≤0.40, confirming that vehicle-based emissions are the predominant source for PNC and other gaseous pollutants in the study region.

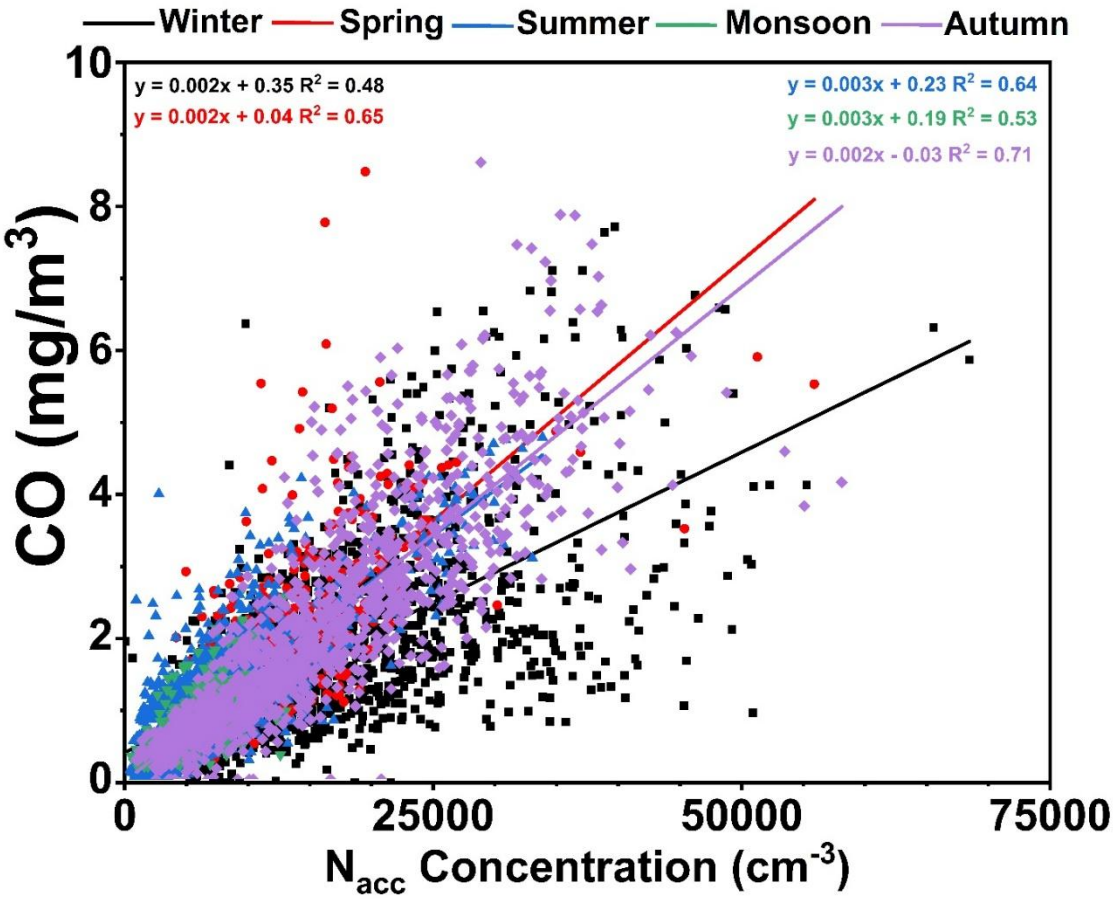

Figure 4.25: Correlation between carbon monoxide (CO, mg/m^3) and particle number concentration in accumulation mode (N_{acc}, cm^{-3}) corresponding to the five seasons over Delhi. The equations of correlation obtained for different seasons are given in respective colors in the figure

Table 4.7: Statistical summary of gaseous pollutants in different seasons over Delhi during 2020-2021

Season	Parameter	Minimum	Maximum	Mean ± 1σ (standard deviation)	Median
Winter	NO_2 (µg/m^3)	5.0	488.0	124 ± 60.3	113.4
	NO (µg/m^3)	0.3	489.0	44.2 ± 55.3	23.5
	NO_x (ppb)	0.3	456.5	97.9 ± 60.4	81.1
	SO_2 (µg/m^3)	1.8	48.0	6.2 ±3.6	4.8

	CO (mg/m^3)	0.2	10.2	1.8 ±1.2	1.4
	Ozone (µg/m^3)	1.1	167.8	37.8 ± 20.6	34.7
Spring	NO_2 (µg/m^3)	0.5	297.0	63.3 ± 36.4	52.2
	NO (µg/m^3)	5.1	291.5	23.6 ± 29.2	12.2
	NO_x (ppb)	11.4	220.0	46.6 ± 30.8	35.9
	SO_2 (µg/m^3)	2.6	41.3	5.6 ± 3.5	4.6
	CO (mg/m^3)	0.05	8.5	1.4 ± 1.1	1.2
	Ozone (µg/m^3)	0.4	172.1	31.6 ± 25.9	20.0
Summer	NO_2 (µg/m^3)	15.5	197.6	51 ± 26	44.6
	NO (µg/m^3)	3.9	175.4	8.1 ± 6.2	6.9
	NO_x (ppb)	6.0	245.5	23.1 ± 10.8	20.6
	SO_2 (µg/m^3)	1.1	127.0	10.6 ± 11.3	7.1
	CO (mg/m^3)	0.1	4.8	1.1 ± 0.8	0.9
	Ozone (µg/m^3)	1.9	196.7	44.3 ± 33.6	34.4
Monsoon	NO_2 (µg/m^3)	10.9	211.7	29.4 ± 16.4	24.8
	NO (µg/m^3)	2.6	36.7	8.7 ± 4.0	7.3
	NO_x (ppb)	4.2	71.9	17.1 ± 5.9	15.5
	SO_2 (µg/m^3)	4.6	49.0	8.1 ± 2.6	7.6
	CO (mg/m^3)	0.16	2.7	0.7 ± 0.4	0.6
	Ozone (µg/m^3)	0.5	184.7	37.4 ± 30.4	24.8
Autumn	NO_2 (µg/m^3)	7.1	319.1	44.1 ± 39.2	32.5
	NO (µg/m^3)	4.8	187.3	13.9 ± 18.2	8.5
	NO_x (ppb)	3.7	318.5	31.7 ± 32.5	19.6
	SO_2 (µg/m^3)	4.3	17.5	7.9 ± 1.7	8.1
	CO (mg/m^3)	0.03	11.5	2.0 ± 1.5	1.6
	Ozone (µg/m^3)	0.8	163.2	35.1 ± 22.6	27.6

* NO_2 - nitrogen dioxide, NO - nitric oxide or nitrogen monoxide, NO_x - nitrogen oxides, SO_2 - sulfur dioxide, CO - carbon monoxide.

The NO_X, CO, and BC peak concentrations in the study region coincided with the nanoparticle's emission (Fig. 4.26, confirming that the source of these pollutants was the same (vehicular sources) (Allen et al., 2009). Studies have revealed that the transportation sector played a major role in the contribution of NO_X and CO in Delhi (Bhandari et al., 2020; Pant et al., 2015; Rizwan et al., 2013). The NO_X concentration was high during the winter (97 ppb) and ~ 5 times higher than in the monsoon season (Fig. 4, Table 2). During the winter period, the concentration of nanoparticles and gaseous pollutants was higher in the study region. However, the concentration of N_{nuc} was found higher in the spring season (1.32×10^4 cm^{-3}) due to the gas-to-particle conversion using SO_2 as precursor molecule for the formation of H_2SO_4. H_2SO_4 vapor acts as SO_2 condensation sink resulting in a lesser concentration (6 µg m^{-3}) in the atmosphere during this season (Fig. 4.26 b). The vapor pressure of the H_2SO_4 depends on the temperature and relative humidity. Therefore, as the spring season experienced a moderate temperature and humidity in the study region (Fig. 2.27), which favored the particle formation process. On the contrary, temperature and humidity were extremely high or low during the summer and monsoon seasons (Fig. 4.27), respectively, inhibiting the SO_2 condensation sink formation. Co-pollutants (O_3, BC) measured in the study region were used to identify the sources and the influence of the atmospheric dynamics on the nanoparticle concentration. The O_3 concentration showed a mid-day peak in almost all the seasons (Fig. 4.26 d) due to the photochemical formation at ground-level from primary pollutants (Nelson et al., 2021; Sharma et al., 2013). BC was used as a tracer for local traffic emissions in the study area, exhibiting higher concentrations during the night than daytime (Fig. 4.26 e) which was consistent with the diurnal variation of N_{acc}.

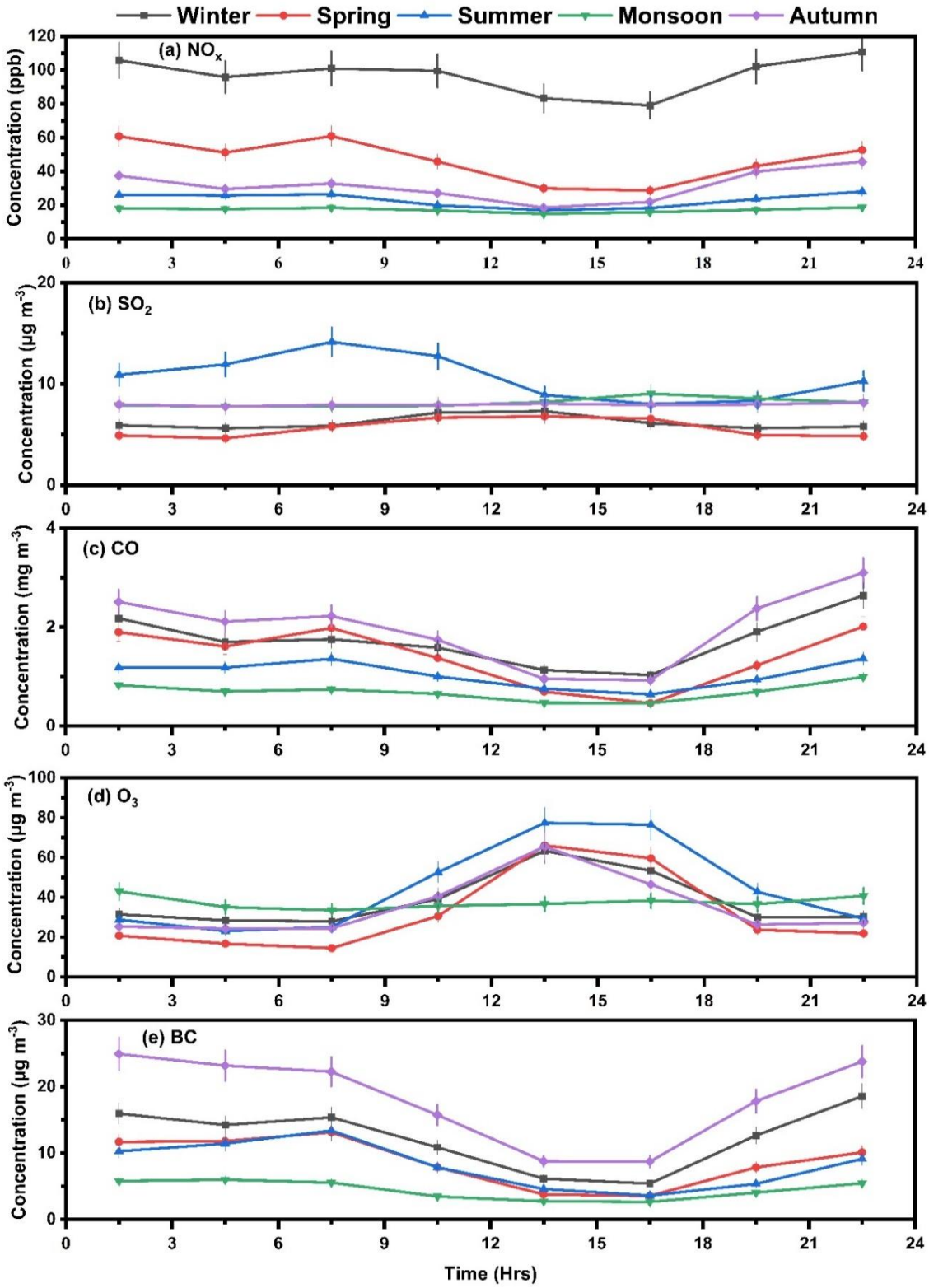

Figure 4.26: Diurnal variation of (a) NO_X, (b) SO_2, (c) CO, (d) O_3, and (e) BC during winter spring, summer, monsoon and autumn seasons in Delhi (vertical bars represent ± standard deviation from the mean)

4.5 Seasonal variation of meteorological parameters and their role in PNC

4.5.1 Diurnal variation of the meteorological parameters

The concentration of particles in urban regions exhibit seasonal variability during the day due to the differences in meteorological parameters and emission sources (Sengupta et al., 2022). The particle concentration become higher during winter when the temperature was minimum and relative humidity was maximum (Fig. 4.27). The seasonal mean temperature during winter was 19°C during which the total particle number concentration was the highest. The lowest concentration of particles occurs in the monsoon season due to wet removal of particles by precipitation. Solar radiation and relative humidity are other important factors that aid particle formation and secondary pollutant formation. During the afternoon hours in almost all the seasons, the solar radiation increases, and the relative humidity decreases (Fig. 4.27). During spring, summer and autumn in the afternoon hours, the increase in solar radiation increases the secondary ozone formation and decreases the particle number concentration due to dispersion. The average solar radiation during the peak sunshine hours was around 870 Wm^{-2} during summer (Fig. 4.27) and lowest in winter (535 Wm^{-2}) (Fig. 4.27). Relative humidity was <50% during summer and in winter it was highest 95%. During spring, monsoon and autumn, the temperature and relative humidity were higher, and found in the range of 25° C to 32° C, and 54 to 71%, respectively. In general, the particle concentration peaks when the daily mean temperature was minimum and slumps when the daily mean temperature was high. This was due to the influence of the atmospheric boundary layer that varies with surface temperature; hence, the dispersion also varied accordingly (Bhandari et al., 2020; Gani et al., 2021). In winter, the particle concentration usually peaks due to temperature inversion; in summer, it was lower due to the strong air exchange. During nighttime, the surface temperature was lower, and the atmospheric BLH is also low, leading to a higher accumulation of particles. The meteorology plays a significant role in determining the nanoparticle concentration in the atmosphere. The planetary boundary layer height (PBLH) and ventilation coefficient directly influenced pollution concentration at ground level (Kompalli et al., 2018; Sorribas et al., 2015). During the winter, when the PBLH was observed lower than 1000 m (the lowest of all seasons) (Fig. 5c) and wind speed (Fig.

4.27f) was ~1 ± 0.5 m/s, resulting in lower ventilation coefficient (600 m^2s^{-1}, Table 4.8) (Fig. 4.27d), the highest mean average concentration of nanoparticles was observed (4.11 x 10^4 cm^3). During summer and spring, the wind speed and PBLH were high, and the resultant ventilation coefficient also reached the maximum (3500 m^2s^{-1}).

Table 4.8: Statistical summary of the meteorological parameters

Season	Parameter	Minimum	Maximum	Mean ± 1σ (standard deviation)	Median
Winter	T (ºC)	10.7	33.7	19.0 ± 4.5	18.4
	RH (%)	25.0	88.0	72.8 ± 17.5	80.6
	WS (ms^{-1})	0.1	9.0	1.0 ± 0.5	1.0
	SR (Wm^{-2})	4.3	278.4	40.5 ± 55.3	8.0
Spring	T (ºC)	16.9	42.7	26.6 ± 5.5	25.8
	RH (%)	13.8	87.9	54.5 ± 20	54.1
	WS (ms^{-1})	0.1	10.0	1.1 ± 0.9	1.0
	SR (Wm^{-2})	4.3	383.6	62.8 ± 83.6	7.8
Summer	T (ºC)	18.5	44.3	32.5 ± 5.2	32.0
	RH (%)	11.2	87.8	44.1 ± 18.1	42.1
	WS (ms^{-1})	0.2	11.7	1.4 ± 1.3	1.0
	SR (Wm^{-2})	3.4	468.1	91.4 ± 114.2	19.7
Monsoon	Ozone (µg/m^3)	0.5	184.7	37.4 ± 30.4	24.8
	T (ºC)	27.4	44.8	33.0 ± 3.4	31.9
	RH (%)	24.9	87.8	71 ± 16.4	74.4
	WS (ms^{-1})	0.2	11.0	1 ± 0.8	0.9
	SR (Wm^{-2})	5.5	393.2	73.1 ± 96.9	18.0
Autumn	T (ºC)	15.6	40.3	25.9 ± 5.7	25.5
	RH (%)	23.1	87.9	63.5 ± 17.9	67.9
	WS (ms^{-1})	0.2	6.6	0.9 ± 0.4	0.9
	SR (Wm^{-2})	4.4	311.5	49.8 ± 68.1	7.4

T - Temperature, RH - relative humidity, WS - wind speed and SR - solar radiation.

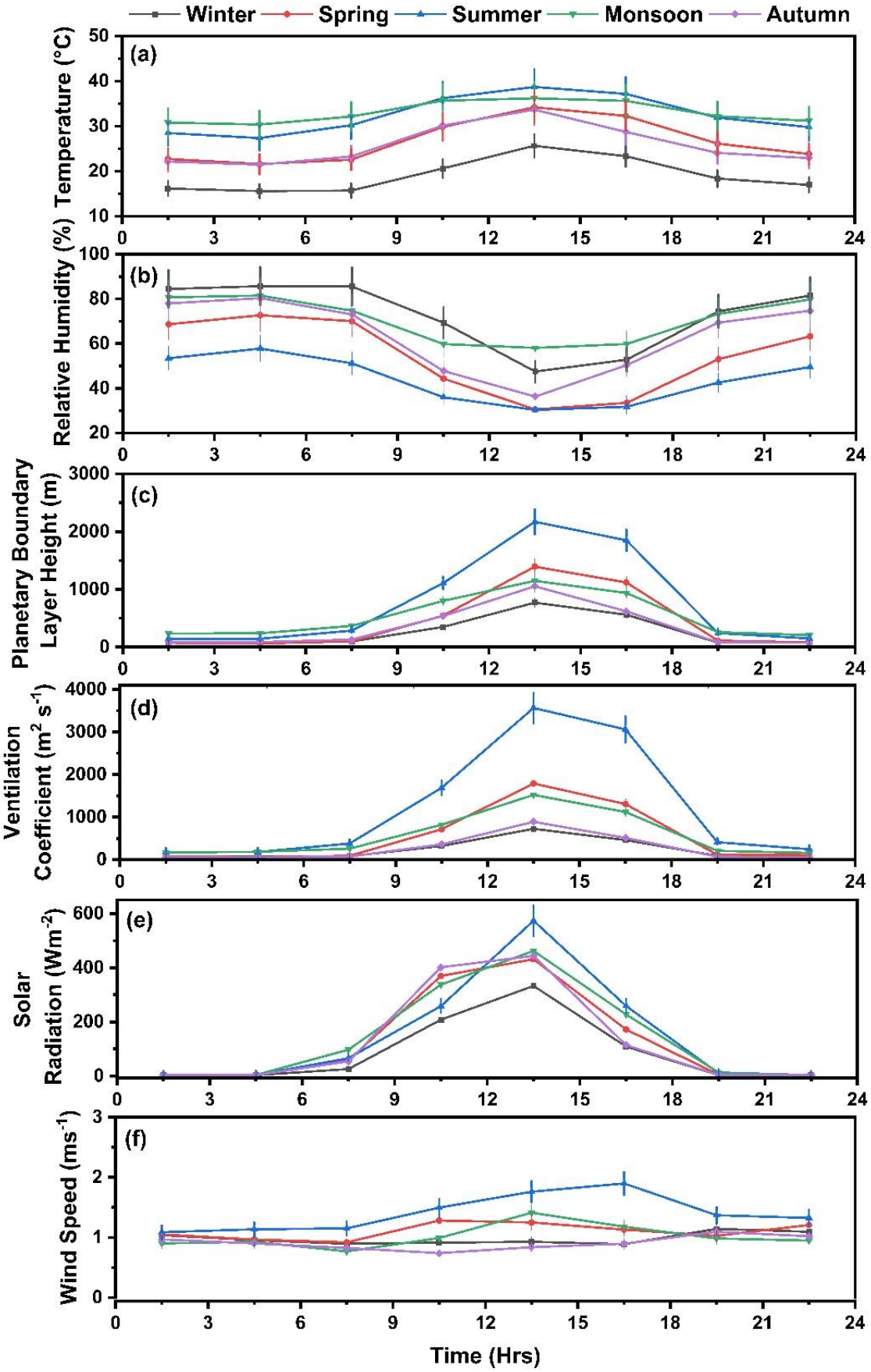
Winter
Spring
Summer
Monsoon
Autumn
(a)
Temperature (°C)
(b)
Relative Humidity (%)
(c)
Planetary Boundary Layer Height (m)
(d)
Ventilation Coefficient (m2 s-1)
(e)
Solar Radiation (Wm-2)
(f)
Wind Speed (ms-1)
Time (Hrs)

Figure 4.27: Diurnal variation of (a) ambient temperature, (b) relative humidity, (c) planetary boundary layer height, (d) ventilation coefficient, (e) solar radiation, and (f) wind speed during winter, spring, summer, monsoon and autumn seasons in Delhi

4.5.2 Influence of relative humidity and temperature on particle size distribution:

The analysis revealed that temperature and relative humidity influenced the size distribution of particles largely through the processes of condensation and coagulation (Figs. 4.28, 4.29). The concentration of particles in the lower size range, especially the nucleation mode, was significantly higher during low RH (<30%) (Fig. 4.28a) and high temperature (T>30ºC) (Fig. 4.29c) conditions that prevail during spring in the study area which favors the particles to undergo the natural gas-to-particle conversion mechanism. The mid-temperature range (20ºC- 30°C) and the mid-RH (30% - 60%) acted as a transition period during which the lower size particles undergo physical transformation in the atmosphere and their size distribution gradually changes increasing from smaller to the higher size. In the above RH and temperature regimes, the particle concentration ranged between 1.5 and 3.0×10^4 cm^{-3} in all the three modes (N_{nuc}, N_{satk}, and N_{latk}) irrespective of the season. In the lower temperature regime (<20°C) and higher RH (>60%) scenario, the concentrations of particles were higher in the accumulation mode size range (Fig. 4.28c, 4.29a). During the winter period, when the relative humidity was higher than 60% and the temperature was lower than 20ºC, the concentration of accumulation mode particles was also found higher due to the rapid condensation and coagulation of the engine exhausts (Dinoi et al., 2023). The natural gas to-particle formation process that occured during the warmer period led to a substantial increase in nucleation size particles. During this period, relative humidity remained low compared to the winter one.

Under higher RH, condensation process begins which increases the number concentrations in the accumulation mode, and this phenomenon is evident in the winter and autumn seasons, followed by the spring season. The analysis clearly indicates that apart from the intensity of emission sources over the study region, the particle number concentration and size distribution exhibit significant variations based on the prevalent meteorology, especially relative humidity and temperature.

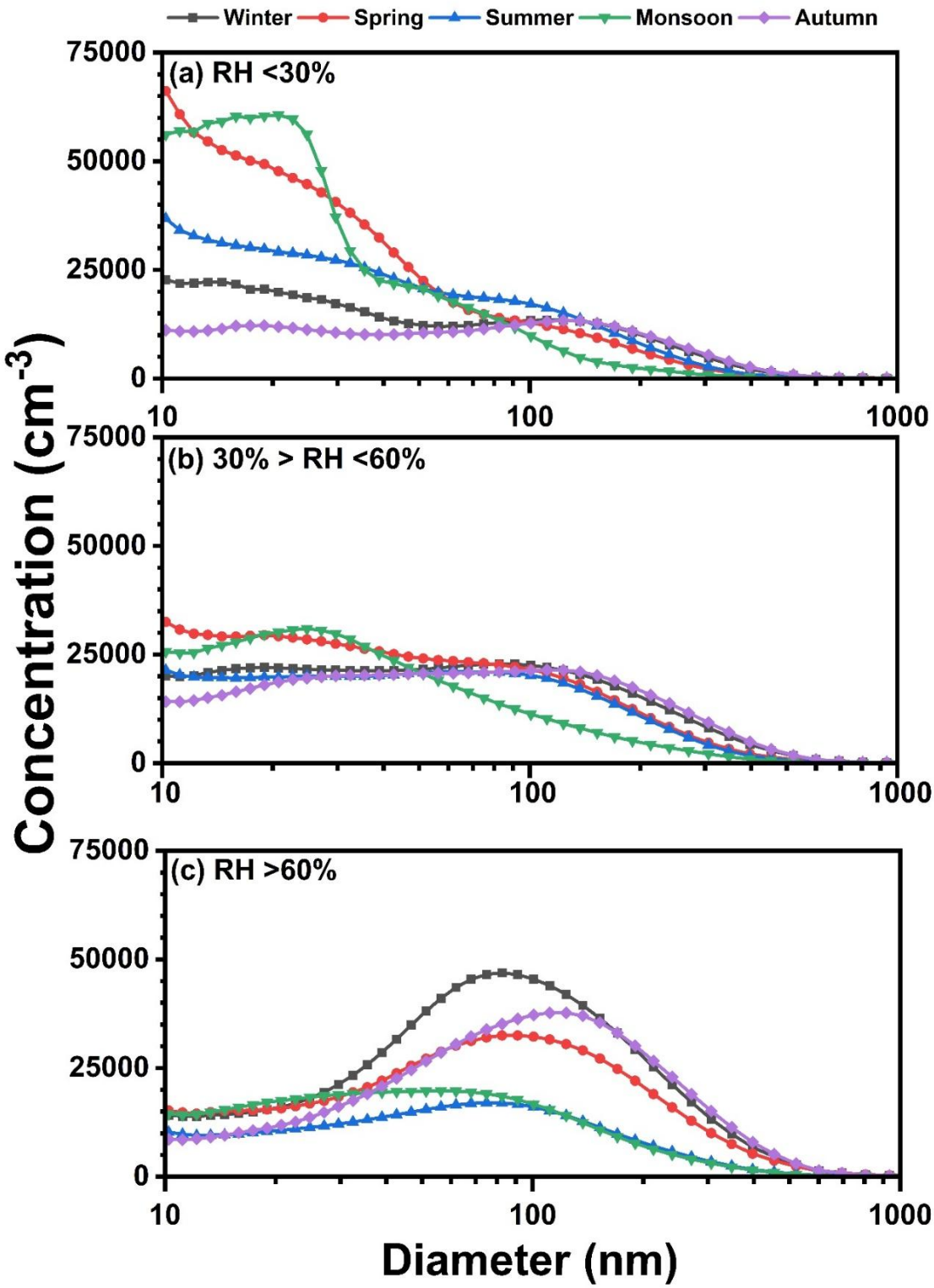

Figure 4.28: Particle number size distribution characterized for different conditions of relative humidity (RH) as (a) RH<30%, (b) 30%>RH<60%, and (c) RH>60% over Delhi in different seasons of the study period

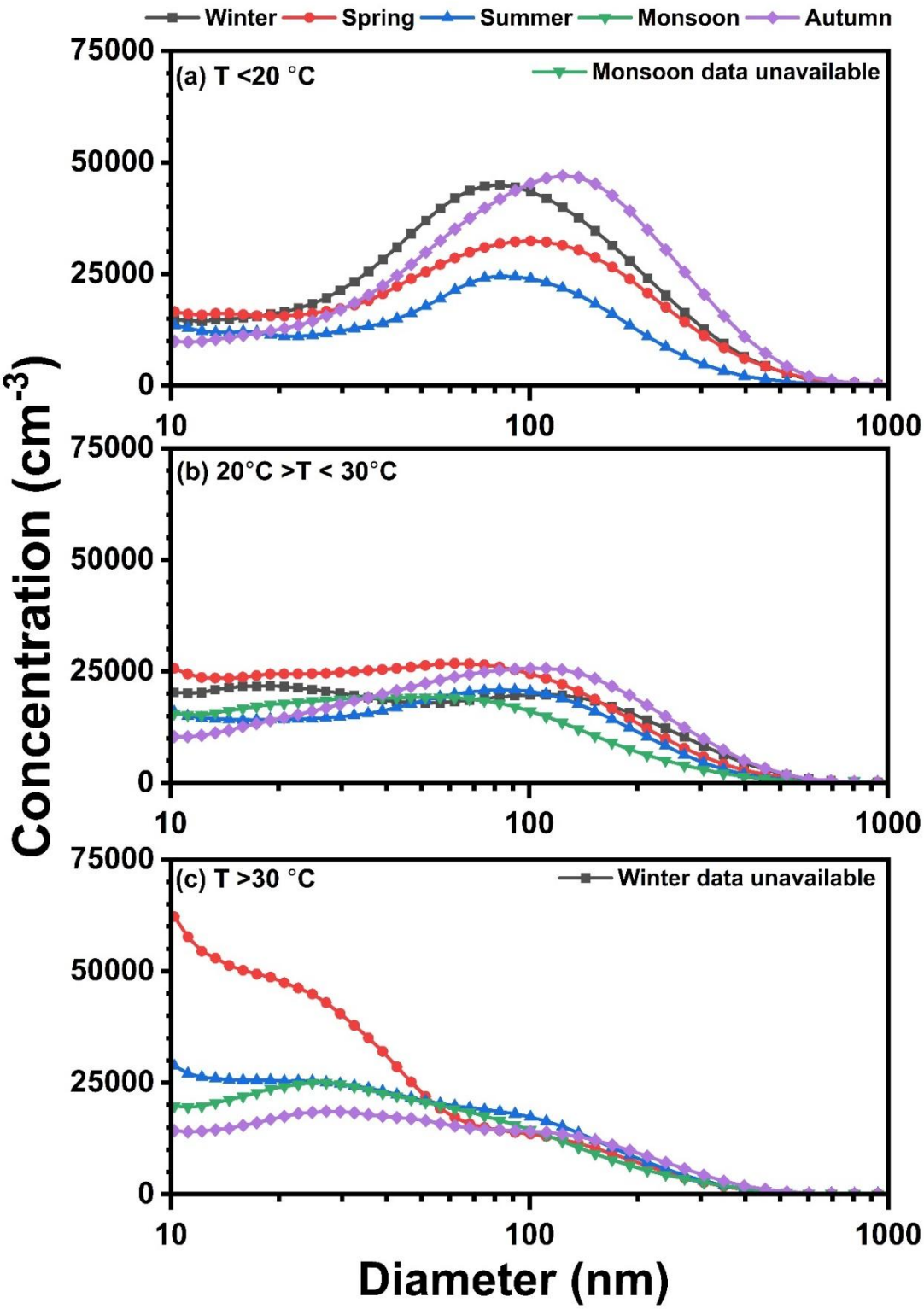

Figure 4.29: Particle number size distribution classified as a function of temperature (T, °C) over Delhi as (a) T<20°C, (b) 20°c>T<30°C, and (c) T>30°C in different seasons of the study period

4.5.3 Role of wind speed and direction on PNC

Wind and traffic induced turbulence determined the nanoparticle concentration in the study region (Mehel and Murzyn, 2015), in the same way as the direction of wind flow. The road where the monitoring location was located, is an urban street canyon, thus, wind recirculation is common. In summer, when wind speed was higher than 2 ms^{-1} (Fig. 4.30) during the mid-day time, N_{nuc} and N_{acc} particle concentrations were 2.0 x 10^4 and 0.75 x 10^4 cm^{-3} respectively, being the lowest concentration measured among all seasons. This revealed that higher wind speeds increase the dispersion rate of particles. The dispersion rate may vary based on the particle size and the wind intensity.

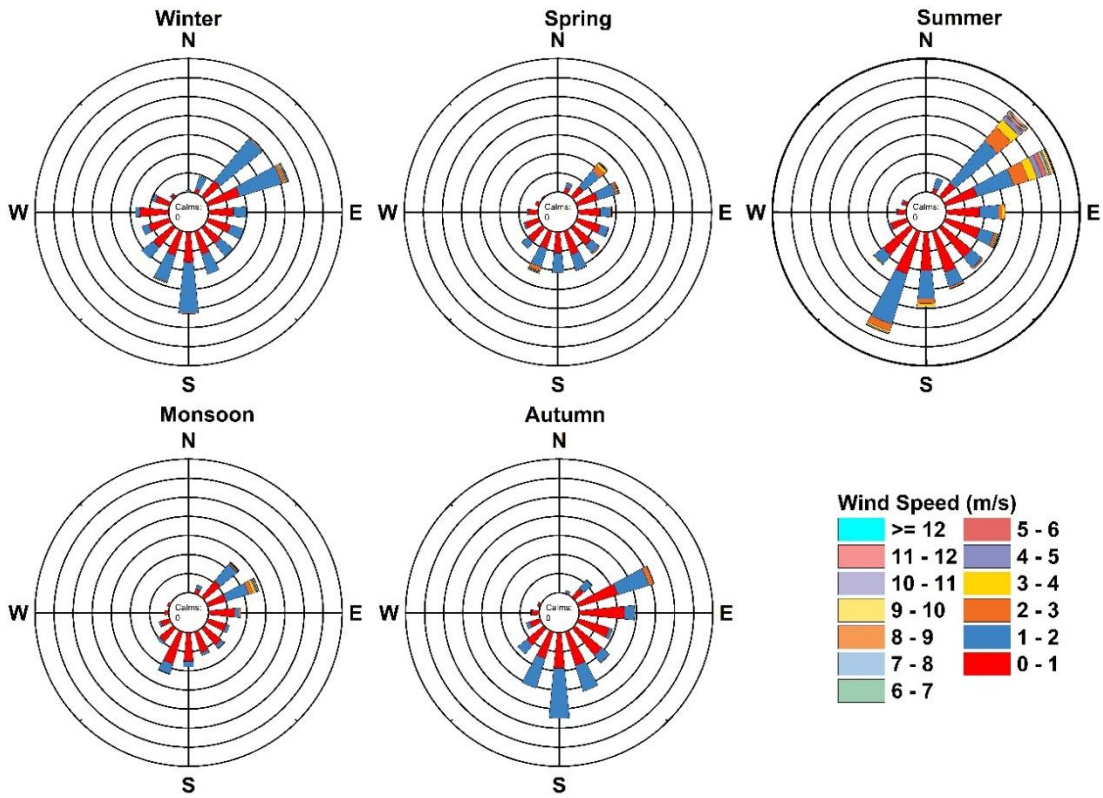

Figure 4.30: Wind rose diagram for the study area during the different seasons (winter, spring, summer, monsoon, and autumn)

The wind rose diagram showed that most of the wind flow in the monitoring site is from South-West towards North-East direction (Fig. 4.30). The monitoring location is covered with the arterial road on the south, and the monitoring station was

located north of the arterial road. The monitoring location was located on the leeward side of the arterial road which caused the dominance of windflow in the same direction throughout the year due to the country's driving pattern. The left-hand driving pattern of vehicles in W-E direction caused a traffic induced wind turbulence of S-W to N-E direction (Fig. 4.30) which is clearly visible throughout the study period.

4.5.4 Role of precipitation on PNC and PNSD

Apart from relative humidity, temperature, and wind parameters, precipitation plays a major role in determining the concentration of nanoparticles and their size distribution in the atmosphere. Thus, here, the particle size distribution was analysed before and after the precipitation to know its impact on number and size.

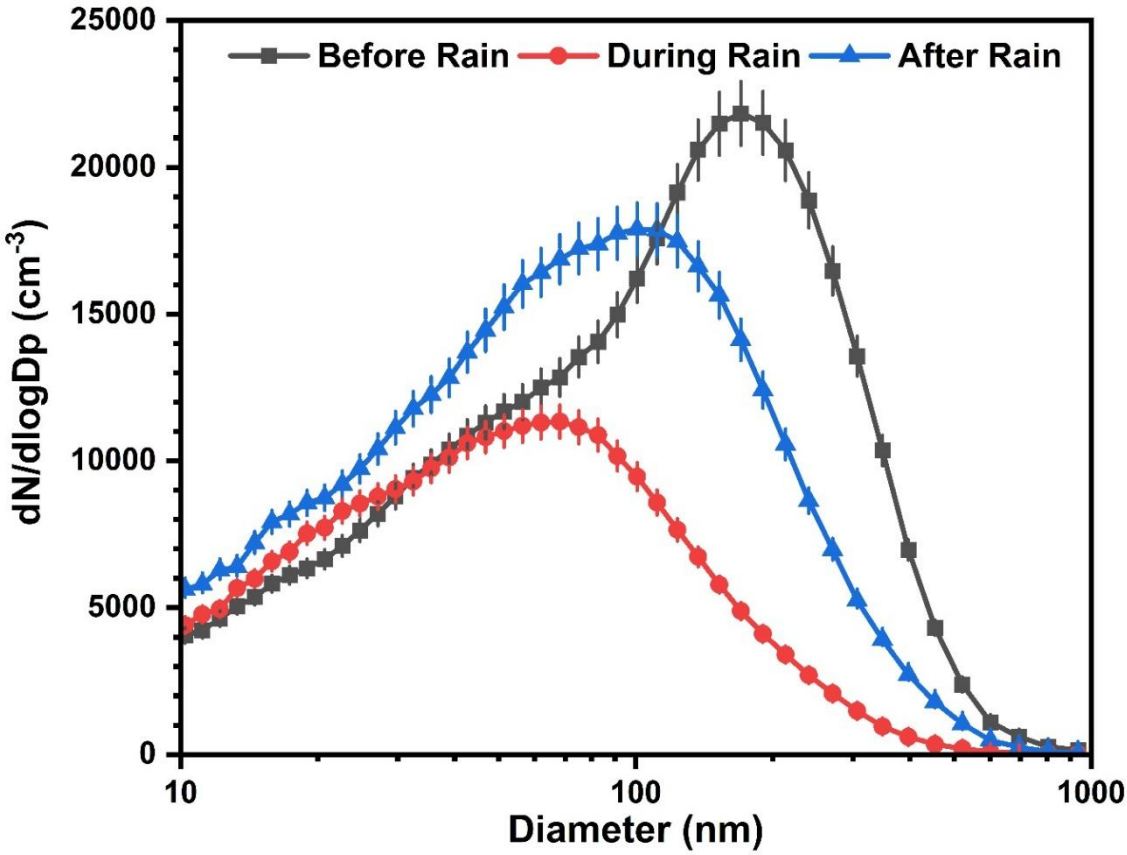

Figure 4.31: Particle number size distribution from 10 to 1000 nm during different phases of precipitation: before (17 October 2021), during (18 October 2021), and after

precipitation (19 October 2021) in the monitoring station in Delhi (vertical bars represent ± standard deviation from the mean)

Time-resolved particle concentration with respect to the nanoparticle size revealed that precipitation-induced wet scavenging was directly associated with particle removal, and that during the precipitation period the particle concentration was reduced to half of pre-precipitation one (2.2 x 10^4 to 1.1 x 10^4 cm^{-3}) (Fig. 4.31). The precipitation removed larger particles, especially N_{acc} (100 to 1000 nm), from the atmosphere (Andronache, 2004). Thus, the particle number size distribution during the post-precipitation showed a lower concentration in this range of particle sizes. During a normal day, when there was no precipitation, the hourly average concentration of the particles ranged from 5 to 7 x 10^4 cm^{-3} during the early morning hours (1 to 5 AM), especially in larger particle sizes (N_{acc}) (Fig. 4.32 a). This high concentration was the result of the coagulation processes among atmospheric particles (Fig. 4.32a). On the study day (18 October 2021) a precipitation of 1 to 3 mm occurred during the early morning hours when the concentration was observed maximum in the monitoring station. This resulted in a reduction of particle concentration, especially in the highest-size (N_{acc}), reaching ~ 3 x 10^4 cm^{-3} (Fig. 4.32 b). The precipitation process reduced the total concentration of the nanoparticles in the atmosphere (Fig. 4.33).

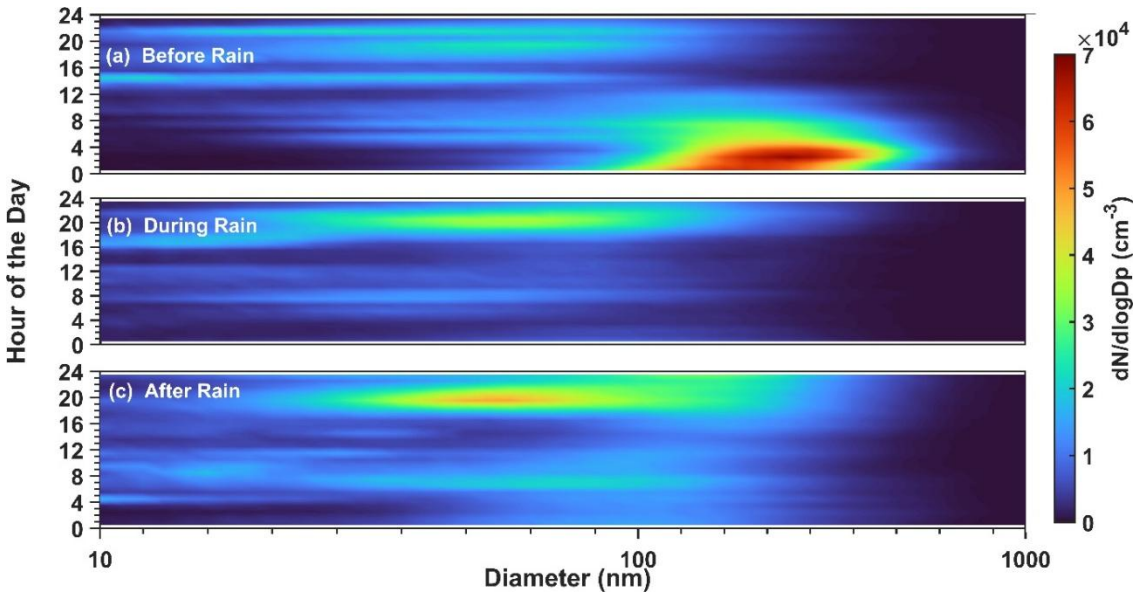

Figure 4.32: Time-resolved particle number size distribution from 10 to 1000 nm on consecutive days: day before (a) (17 October 2021), (b) day with (18 October 2021), and (c) day after (19 October 2021) precipitation in the monitoring station in Delhi

The concentration of N_{nuc} particles was found higher than larger-sized particles due to its greater diffusivity (Fig. 4.33a). The N_{atk} particles suffered greater diffusion during less-intensity rainfall, decreasing its concentration when the intensity of rainfall increased (Fig. 4.33b). In general, the particles in N_{atk} and N_{acc} were more influenced by the precipitation processes (Fig. 4.33b, c). Post-precipitation analysis showed a higher growth rate of particles, even though the concentration was less. In this regard, the particle growth was induced by the moisture content, which causes rapid condensation of smaller particles (Zhao et al., 2021).

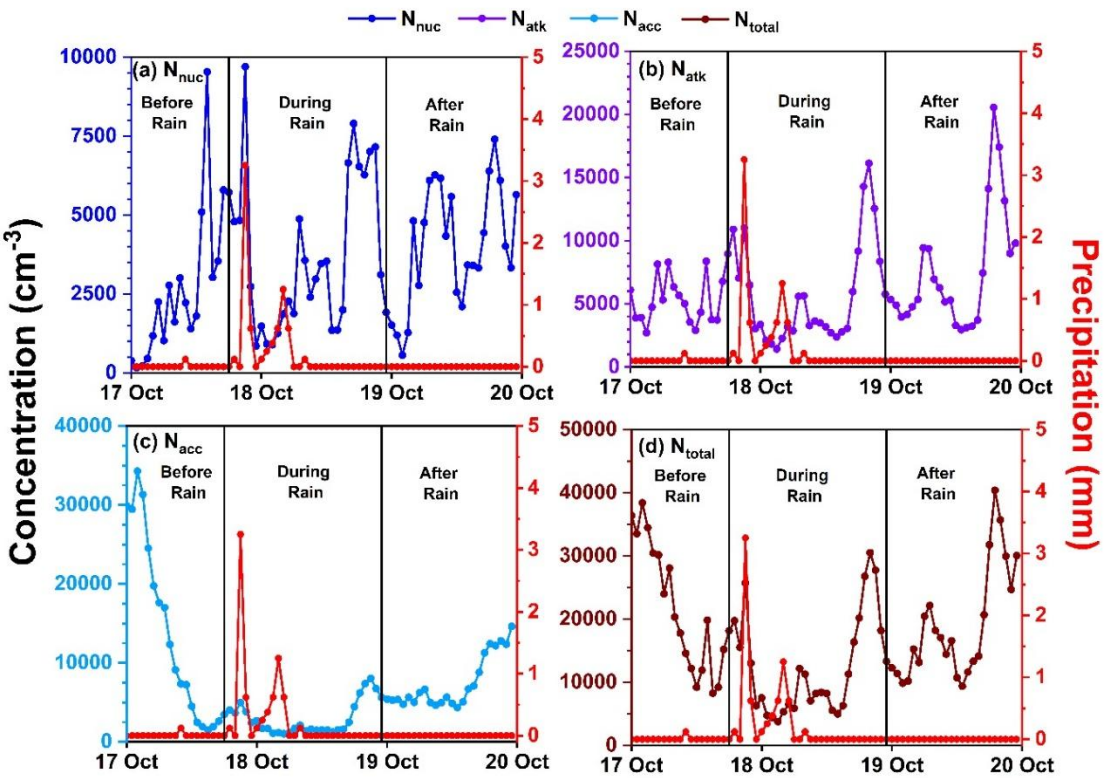

Figure 4.33: Temporal variation of particle number concentration before, during and after precipitation period for (a) N_{nuc} - 10 to 30 nm, (b) N_{atk} - 30 to 100 nm, (c) N_{acc} - 100 to 1000 nm and (d) N_{total} - 10 to 1000 nm from 17th October to 20th October 2021, in the monitoring station in Delhi

4.6 Health impacts assessment

Epidemiological studies have examined the relationship between exposure to air pollution and various human health issues (Sharma et al., 2023). Air pollution was the fourth leading risk factor for early death worldwide in 2019, according to the *State of Global Air* (Health Effects Institute, 2020). The particulate matter $PM_{2.5}$ was ranked as the fifth mortality risk factor in 2015, and around 4.2 million premature deaths were recorded in 2016 in low and middle-income countries globally (Manojkumar and Srimuruganandam, 2021a). Various control measures have been taken in the last few decades, such as emission norms, Bharat stage regulation (BS VI), odd-even vehicle policy schemes (Mishra et al., 2019; Tiwari et al., 2018), Graded Response Action Plan (GRAP) (Singh and Kulshrestha, 2020), and National Clean Air Action Plan (NCAP) (Sulania and Singh, 2019), have worked positively towards a decline in the concentration of particulate matter in India. However, on the other hand, UFP concentrations are increasing gradually (Sebastian, et al., 2021; Sharma et al., 2023) and emphasizing the need for further studies on UFPs. UFP also majorly affects morbidity, leading to premature death (Donaldson et al., 1998). The particles deposited in the respiratory system can interact with cells and bio-molecules. Therefore, evaluating the deposition rate of these particles in the respiratory system is crucial. The deposition rate of particles in different regions of the human respiratory system can be determined with size-segregated measurements of particles using a Multiple-Path Particle Dosimetry (MPPD) Model (Fig 4.34). This model is being widely used successfully for stimulating the deposition of size-segregated particles in the respiratory system. The unavailability of size-segregated data measurements is a significant limitation in this domain globally; however, recent advancements in instrumentation have enabled the measurement and analysis of size-segregated data. When the concentration of smaller-size particles is higher in the atmosphere, the deposition was found to be in the order of alveolar > bronchiolar > trachea bronchiolar > head regions (Ma et al., 2022). Few studies have analyzed the distribution of nanoparticles, their behavior, dynamics, and deposition potential in urban regions in different microenvironments. Estimation of particles during different vehicle fleet

hours along with the deposition potential for the commuters in the road microenvironment remains one of the potential and important areas to be explored.

4.6.1 Inhalable nanoparticle concentration

The Inhalable particle number (IPN) concentration is a mathematical estimation of an individual's exposure to a concentration of particles during various physical activities that have different inhalation volumes (Prabhu et al., 2019; Qiu et al., 2019). This method is considered as one of the easiest and reliable methods for analyzing the concentration of inhalable particle concentration for different rates of inhalation. The method uses the number concentration of the particles rather than the mass concentration, and as a result, captures better the health effects as it accounts for the number of particles that penetrate deeper into the alveoli and bronchioles (Kim et al., 2017; Koehler and Peters, 2015). The equation used for this calculation is given in equation below.

$$IPN(min^{-1}) = PNC(cm^{-3})\ x\ IR(cm^{3}min^{-1}) \quad -(15)$$

In equation, IPN represents the inhalable particle number, PNC represents the particle number concentration of nanoparticles, and IR represents the inhalation rate. Different IR rates are based on US EPA exposure guideline handbook, and IR rate varies based on different physical activities - light activity like walking results in less IR, and heavy activities such as running and weight lifting result in a higher IR. The deposition of air pollutants in the lungs during heavy exercise is 4.5 times higher than in the normal sitting or resting position (Ma et al., 2022). The advantage of this method is that it is the simplest mathematical method for calculating the inhalable particle number, and only the concentration of the particles is sufficient for calculation. The limitation of this method is that it provides only the concentration of the inhalable particle number with no significant insights into the actual concentration of the particles deposited in the respiratory system.

4.6.2. Particle dosimetry model

The deposition of ultrafine particles and other size range nanoparticles in the human respiratory tract (HRT) can be evaluated using an MPPD model version 3.04.

The Hammer Institute of Health Science, USA designed and developed this model. The dosimetry model is a well-validated software developed by Applied Research Associates, which is considered one of the most accurate models for dosimetry analysis and works based on computational fluid dynamics. More details about the model can be found at https://www.ara.com/mppd/. Further, this model is well-validated, tested, and widely used for research and education to estimate particle deposition in the human respiratory tract (Khan et al., 2022; Manojkumar and Srimuruganandam, 2021b, 2022b). It is considered as one of the best available models for analyzing deposition in the respiratory tract. The advantage of the model is that it can be used for a wide size range of particles starting from 0.001 µm (1 nm) to up to 100 µm ($1x10^5$ nm). The model can be used for different species, such as rats, rabbits, pigs, and humans. The major input parameters of the model are breathing frequency (BF), tidal volume (TV), upper respiratory tract volume (URT), and other parameters such as density, size distribution, and exposure conditions.

In the MPPD model, the exposure assessment can be customized for different exposure conditions under different assumptions, such as particles entering the respiratory tract via the nose through upright body orientation and dispersion. The particles are also assumed to be in multi-particle distribution mode. According to the model recommendation, the other model assumptions and constants are used from similar global studies. After incorporating the necessary assumptions, the model is used for simulation, and the results obtained on the concentration of nanoparticles deposited in different regions of the respiratory tract, such as the pulmonary, tracheobronchial, and alveolar regions, are analyzed. The simulations are done for different seasons, and peak and non-peak hours when conditions are quite different. The advantage of this model is that it can predict particle deposition in different regions of the respiratory tract, such as the alveoli, bronchus, and bronchiole. The model uses both theoretical and numerical fittings, an added advantage. The limitation of the model is that it requires size-segregated measurement data for running simulations, and another limitation is that predicted values of regional deposition might differ from actual deposition inside the respiratory tract. The variation occurs due to water vapor,

which condenses on the inhaled particles and influences the growth of particles in the biological tract of the human being inside the lungs under humid conditions.

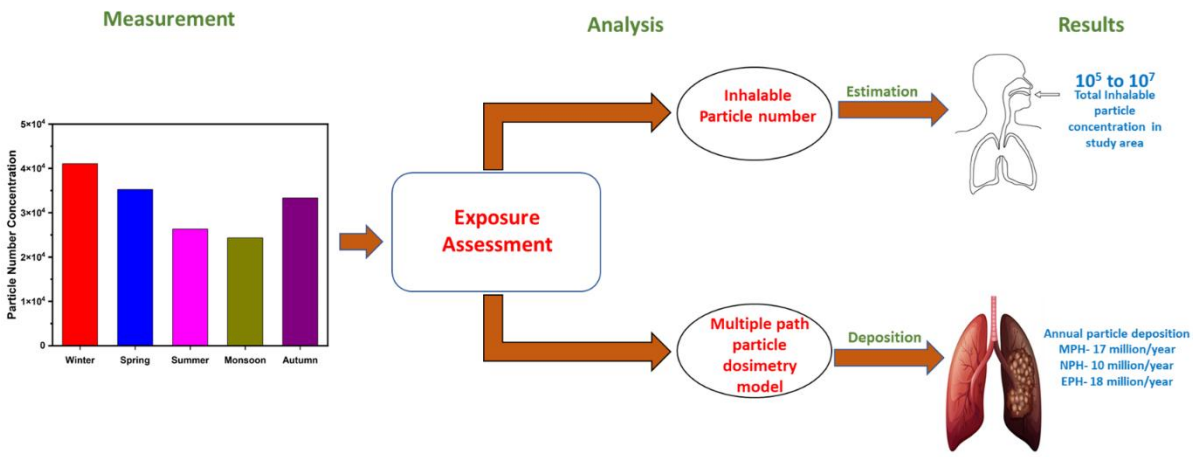

Figure 4.34: Pictorial representation of the health impact analysis methodology

4.6.3 Estimation of inhalable particle number concentration

The inhalable particle number (IPN) of different size fractions (UFP and total) calculated using equation (15) are plotted in Fig. 4.35. The total inhalable particle numbers determine the maximum possible exposure to different sizes of nanoparticles in the urban roadside environment, especially for motorists, drivers, police personnel, street vendors, and other people residing/working in the vicinity of the road. The exposure concentration of IPN in the study area varies from 1 million (10^6) to 10 million (10^7) particles per hour. The concentration varies based on the concentration of nanoparticles and inhalation rate (Fig. 4.35). In the spring season, the UFP shows a maximum inhalation of around 10^6 particles/hour under the severe inhalation category, which consumes about 100 cm^{-3}/min air volume, followed by winter (Fig. 4.35). The exposure rate is high in spring for all kinds of exposure activities followed by winter (Fig. 4.35). The inhalable particle concentration is directly proportional to the inhalation rate and the mean concentration of particles during a particular season. In semi-urban cities such as Dehradun in India, the inhalable particle concentration was around 200 million from the fireworks during the festival (Deepavali) (Prabhu et al., 2019). The increase in inhalable particle numbers during different seasons increases the vulnerability of humans. Ultrafine and nanoparticle exposure is higher in patients

with asthmatic disorders than in normal people. The prolonged exposure of these particles causes more deposition of particles in the pulmonary and alveolar regions. Exposure to particles at higher concentrations can easily reach the lungs. From there, the inhaled particles can penetrate to other organs through lung vasculature or mobile cells (Schraufnagel, 2020).

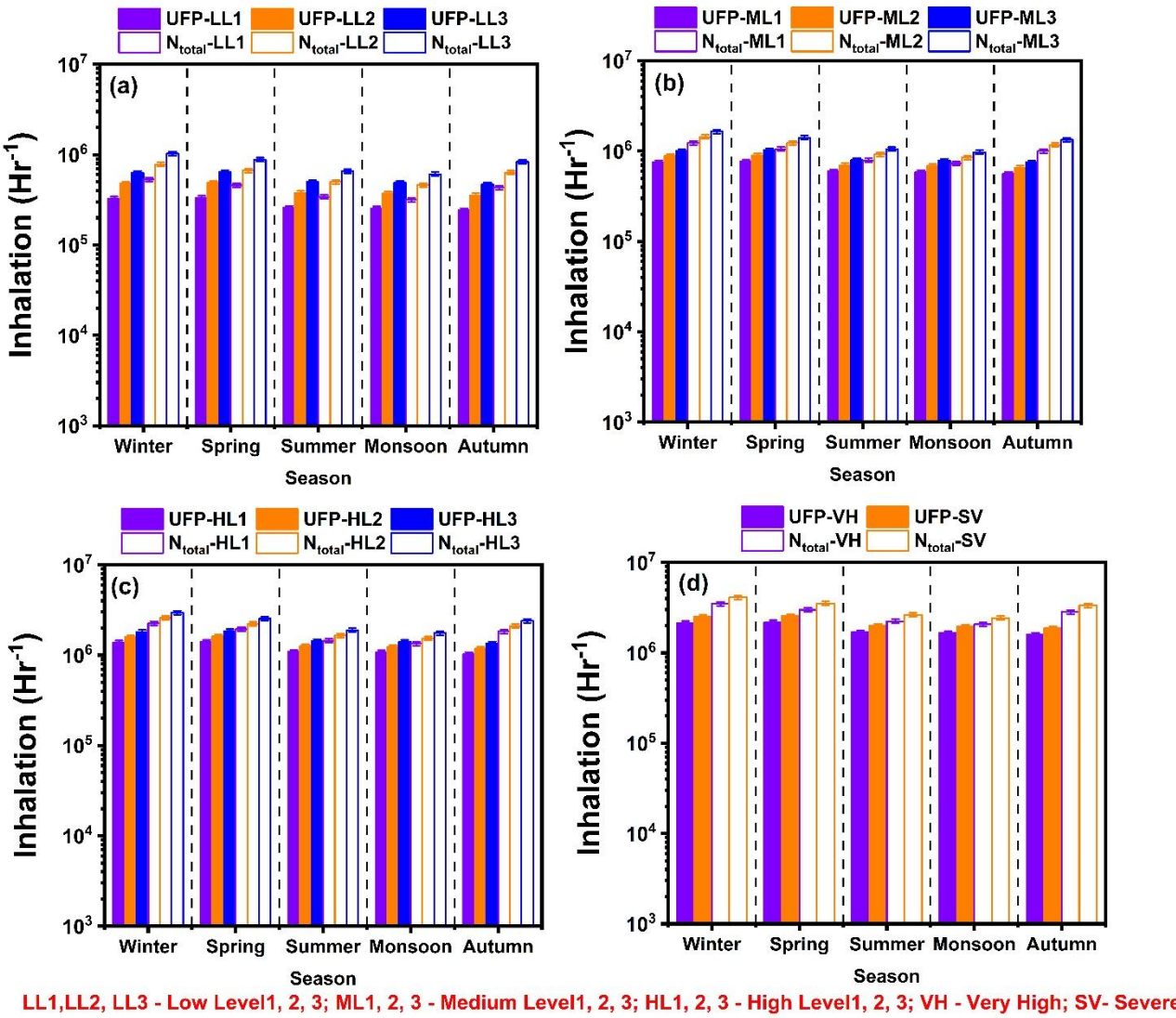

Figure 4.35: Inhalable particle number concentration for UFP (10 to 100 nm) and total particle number concentration ranging from 10 to 1000 nm (Total PNC) during different seasons for different inhalation volumes, a) light physical activity, b) medium physical activity, c) heavy physical activity, and d) very heavy and severe physical activity.

During higher IPN concentrations, populations at risk, such as the elderly and children, activity on the roadside can be restricted. The role of particulate matter is well known for the mortality and exacerbations in persons with chronic obstructive pulmonary disease (COPD), and exposure to number concentration of particles having lower mass and higher surface area is associated with stroke, ischemic heart disease, myocardial infarction, thrombotic stroke, and hypertension (Schraufnagel, 2020). The correlation between total mortality and cardiovascular mortality is high when the particle size decreases, showing that exposure to UFP/N_{acc} and overall total concentration are highly associated with various health impacts (Schraufnagel, 2020). The results from the study corroborate the above findings and emphasizes that these quantitative results will be crucial to devise measures to help improve public health.

4.6.4 Quantification of nanoparticle deposition in human lungs during peak non peak hours

The seasonal mean concentration of total PNC in the size range of 10 nm to 1000 nm during different seasons and different hours of the day is utilized to predict the deposition rates in different lung regions using the MPPD model (Fig. 4.36). The particle concentrations are classified into MPH, EPH, and NPH based on the vehicular fleet in the study region. The deposition of these particles in different regions and overall lung deposition is simulated using model parameters such as Functional Residual Capacity (FRC) = 3300 ml, Upper Respiratory Tract (URT) volume = 50ml, and the density of particle = 1.63 g/cm^{-3} (Gani et al., 2020), constant exposure condition, with upright body orientation and nasal breathing scenario. The constant values in the model are kept constant for all the seasons, and the concentration of nanoparticles at different hours of the day have been used to analyze the deposition as per the methodology adopted in previous studies (Manoj Kumar et al., 2019; Manoj Kumar and Srimuruganandam, 2022a). Constant values of FRC (3300 ml) and URT (50 ml) are utilized following the model recommendation and the various studies performed on the human respiratory system. Based on the variation in the concentration of particles, the exposure and deposition vary season to season (Fig. 4.36). The output of the model represents the deposition of particles in human lungs

similar to that of computerized tomography (CT) scan results of lung deposition (Khan et al., 2022).

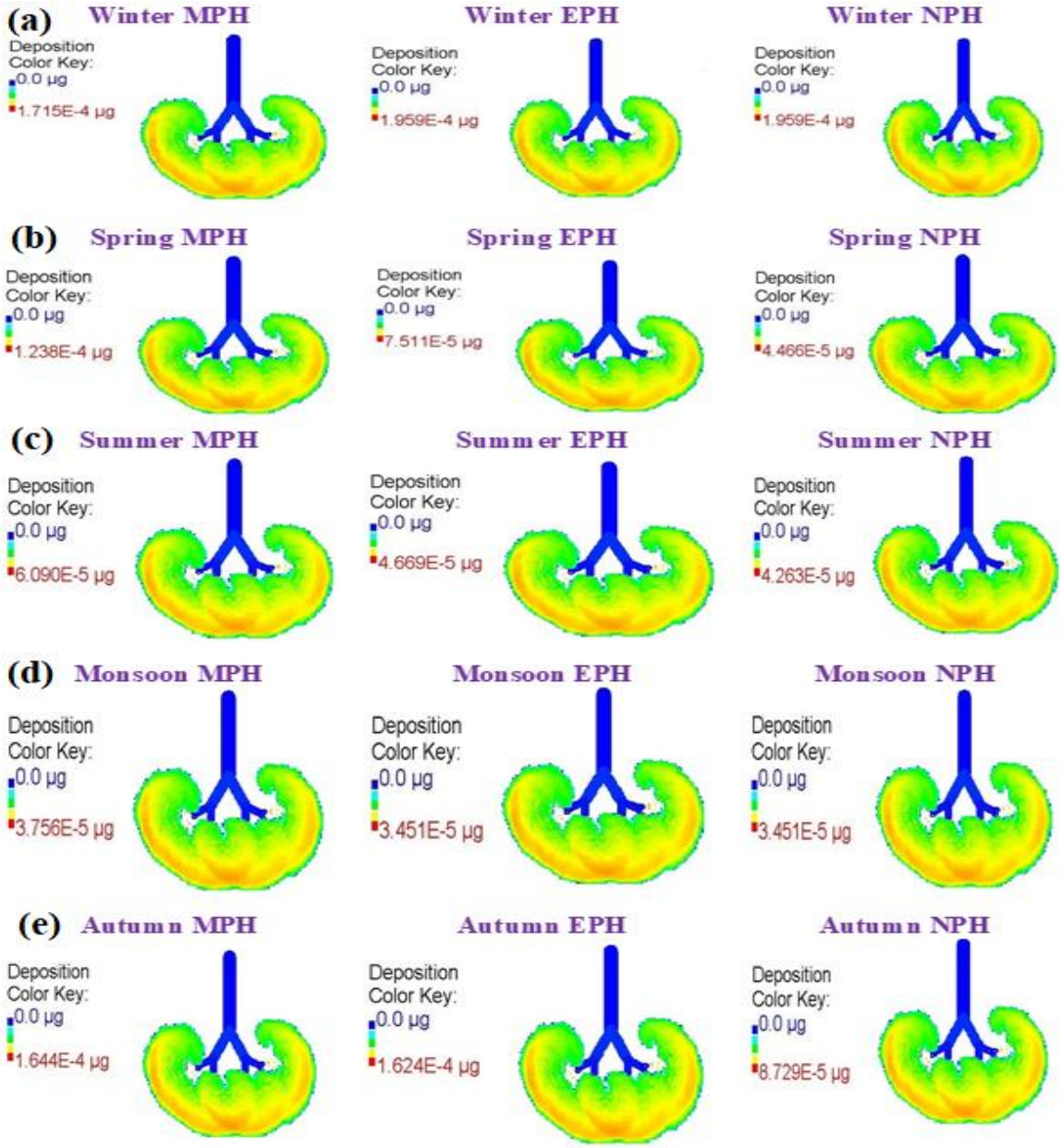

Figure 4.36: Deposition visualization using the mass rate of nanoparticles over Delhi in (a) winter, (b) spring, (c) summer, (d) monsoon, and (e) autumn, respectively. MPH represents morning peak hours, EPH represents evening peak hours, and NPH represents non-peak hours. The deposition rate is plotted as µg/hr and the color scheme represents the deposition density of the particles in human lungs

The deposition fraction of particles in the alveolar region ranges from 1.5 to 2.0 μg/min (Fig. 4.36). The order of deposition is alveolar > bronchiole > bronchus at a constant breathing rate of 12 LPM, and the variation in deposition geometry is depicted in Fig. 4.36. This breathing rate is chosen because the breathing rate of an adult is prescribed to be 12 LPM as per the USEPA Handbook, 2011. The breathing rate is kept constant as 12 LPM for all the different age groups to assess the deposition of nanoparticles in the human respiratory system at the same rate. Differences in deposition in different regions occur due to differences in deposition mechanism, particle concentration, and airway geometry (Izhar et al., 2016). The major mechanisms that affect particle deposition in the airways are diffusion, impaction, and sedimentation. The order of deposition ranges from the tracheobronchial (TB) region to the alveolar region based on the size of the particle inhaled. In the TB region, the higher deposition occurs due to the inertial impaction of the particles, and in the bronchiole and alveoli regions, it occurs due to sedimentation (Oliveira et al., 2019). Earlier studies found higher deposition of μm range particles in the head and TB regions with a flow rate ranging from 15 to 30 LPM (Islam et al., 2017).

In the present study, we observe that particles with higher diameters get deposited in the TB region, whereas particles with smaller diameters get deposited in the alveolar region. Higher deposition of particles in the bronchiole region will lead to pharyngitis and rhinitis disease in adults (Islam et al., 2017). The deposition fraction varies during various activities, which alters the breathing frequency. The variation in the deposition of particles in the lungs will subsequently lead to the development of carcinogenic cells based on the rate of deposition of the particles at different regions of the lungs (Gao et al., 2015; Wiebert et al., 2006). For example, adenocarcinoma develops in the outer regions of the lungs, and squamous cell carcinoma in the center region of the lungs (Manojkumar et al., 2019).

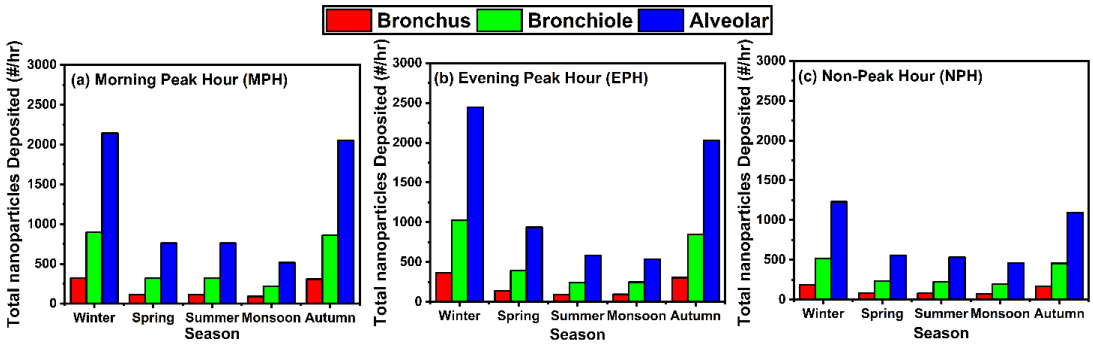

Figure 4.37: Total number of nanoparticles (per h) that get deposited in different parts of the human respiratory system during winter, spring, summer, monsoon, and autumn, respectively, during (a) MPH (morning peak hours), (b) EPH (evening peak hours) and (c) NPH (non-peak hours)

The deposition of nanoparticles in the alveolar region at a constant breathing rate of 12 LPM is highest during EPH of winter season (2445 particles/h and ~6 million particles/season) (Fig. 4.37b). The simulated model values show that the deposition of nanoparticles in different regions during EPH in the winter and autumn seasons is around 5 to 6 million particles, and for the rest of the seasons, it is 4-times lower and is about 1.5 to 2 million particles per season. The MPH deposition ranges from 1 to 6 million in different seasons. During the NPH, nanoparticle deposition in the human respiratory tract ranges from 1 to 3 million. The annual nanoparticle deposition is about 18 million during EPH, 17 million in MPH, and 10 million in NPH, respectively. The IPN predicted by the model based on the particle concentration lies in the range of 0.5 to 1 billion particles for a similar respiratory rate. The simulated model values show that the actual deposition occurring in the human respiratory system is less when compared to the estimated inhalable particle number concentration. The difference occurs due to various other factors that influence the deposition in the lungs. In the study region, the annual average nanoparticle deposition is ~500 µg/year in the roadside environment; in comparison, the concentration decreased over a location that was away from the roadside environment and was about 330 µg/year (Ma et al., 2022). Thus, on an annual scale the exposure concentration in the roadside environment is 30% higher than the environments/regions/locations that are away from roads in urban regions. This increase is attributed to vehicular exhaust over the study region, an urban

locale, which increases the concentration of particles on the roadside compared to an environment away from the roadside. The deposition of particles at a higher rate in the roadside environment poses a major health threat to the people who are working/living in the vicinity of the road (He and Qiu, 2022; Wang et al., 2021). Further, the deposition of nanoparticles is found to be higher in lower respiratory tract infections. These findings from the present study, provide various metrics and indicators for health risk assessment due to urban aerosols/urban pollution. The results also suggest that the inhalation of nanoparticles is more prevalent in the regions where the sources are located, thus, prevention of activities near the sources and source regions of nanoparticles will significantly help to reduce exposure to nanoparticles and associated health impacts.

4.6.5 Quantification of nanoparticle deposition in the human respiratory system

The deposition concentrations estimated by the MPPD model are during winter (1.31 x 10^{-3} µg/hr) with deposition rates of 0.29 µg/hr, followed by spring (1.13 x 10^{-3} µg/hr, 0.25 µg/hr), summer (8.8 x 10^{-4} µg/hr, 0.01 µg/hr), monsoon (1.1 x 10^{-3} µg/hr, 0.02 µg/hr) and autumn (7.88 x 10^{-4} µg/hr, 0.01 µg/hr), respectively (Fig. 4.38). The deposition concentration estimates are based on the concentration of particles and exposure time. An adult who works around 8 hours a day near roadside conditions experiences a deposition concentration of around 338 µg/year of nanoparticles. Similarly, the adult resident who resides/spends 24 hours a day near the road experiences a deposition of nanoparticles >1000 µg/year. The exposure concentration of particles is 25 times higher than the national annual standards for $PM_{2.5}$ (40µg/year) and 16 times higher than the PM_{10} (60µg/year). When compared to the WHO 2021 standard, the exposure concentration is ~200 times higher than the $PM_{2.5}$ (5µg/year) and 67 times higher than the PM_{10} (15µg/year) standards, emphasizing the vulnerability of citizens working or living in the vicinity of the road in the study region. It may be noted that the estimated particle deposition only corresponds to nanoparticles and not fine and coarse particles. The exposure estimation shows that the deposition of nanoparticles is found in the head airway tract for children below three years, however, for adults, the deposition is found only in the inner regions of the lungs. The variation in the deposition arises due to the differences in the development of

respiratory tract among infants, children and adults. The study region is surrounded by a mixture of educational and residential areas where the population (infants, children and adults) vulnerable to these exposures vary and leads to various health hazards (Balakrishnan et al., 2019; Pandey et al., 2021; Yadav et al., 2022).

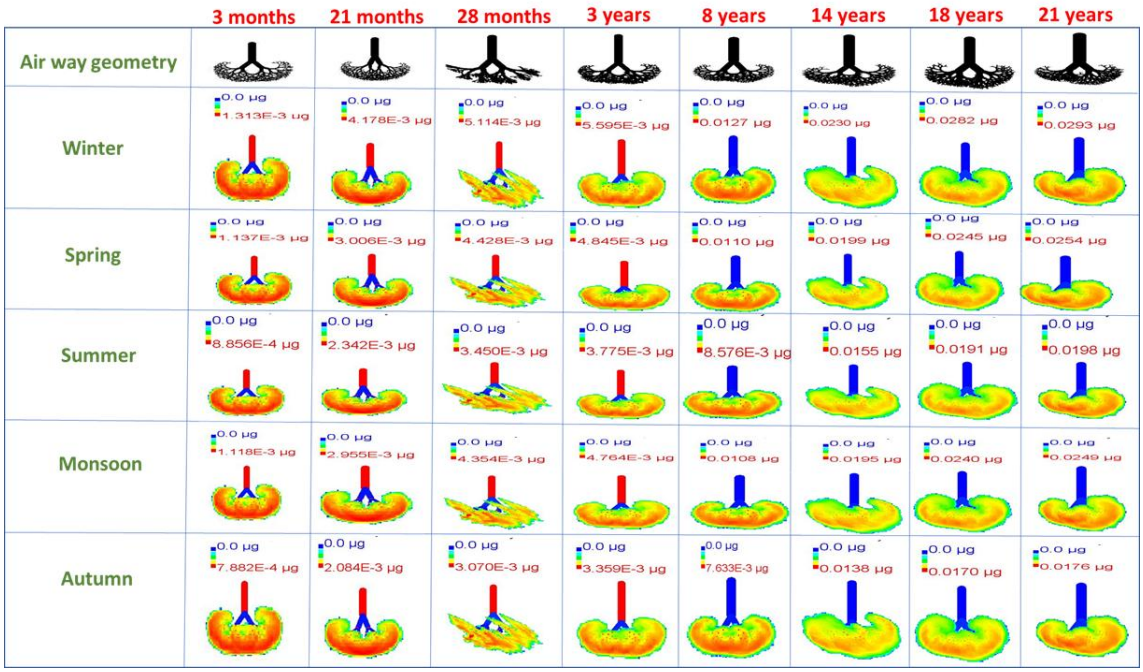

Figure 4.38: Estimated deposition of nanoparticles during different seasons (winter, spring, summer, monsoon, autumn) in the study region of Delhi for age groups from 3 months to 21 years using MPPD model

4.6.6 Quantification of total mass deposited during different seasons

The estimated mass of nanoparticles deposited in the respiratory system in a day in the road environment varies between 0.02 and 0.40 µg (Fig.4.39). In almost all seasons, the bronchiole deposition is less than 0.05 µg/day for different age groups. The alveolar deposition for infants and kids ranges from 0.05 µg/day to 0.10 µg/day, but for the age groups from 8 years to 21 years, the alveolar deposition is higher, and it varies from 0.30 µg/day to 0.40 µg/day (Fig.4.39). The estimated alveolar deposition for the 8 to 21 years age group is 0.32-0.40 µg/day in winter, 0.25-0.32 µg/day in spring, 0.20-0.27 µg/day in summer, 0.25-0.33 µg/day in monsoon and 0.20-0.25 µg/day in autumn. In winter, the deposition concentration is 2 times higher than in autumn for adults. The average nanoparticle deposition in the alveolar region of a

particular individual, irrespective of the age groups residing near the road in different seasons is 26.6 µg/day in winter, 14.6 µg/day in spring, 22 µg/day in summer, 23.1 µg/day in monsoon and 17.1 µg/day in autumn. The seasonal order of deposition is winter > monsoon> summer > autumn > spring.

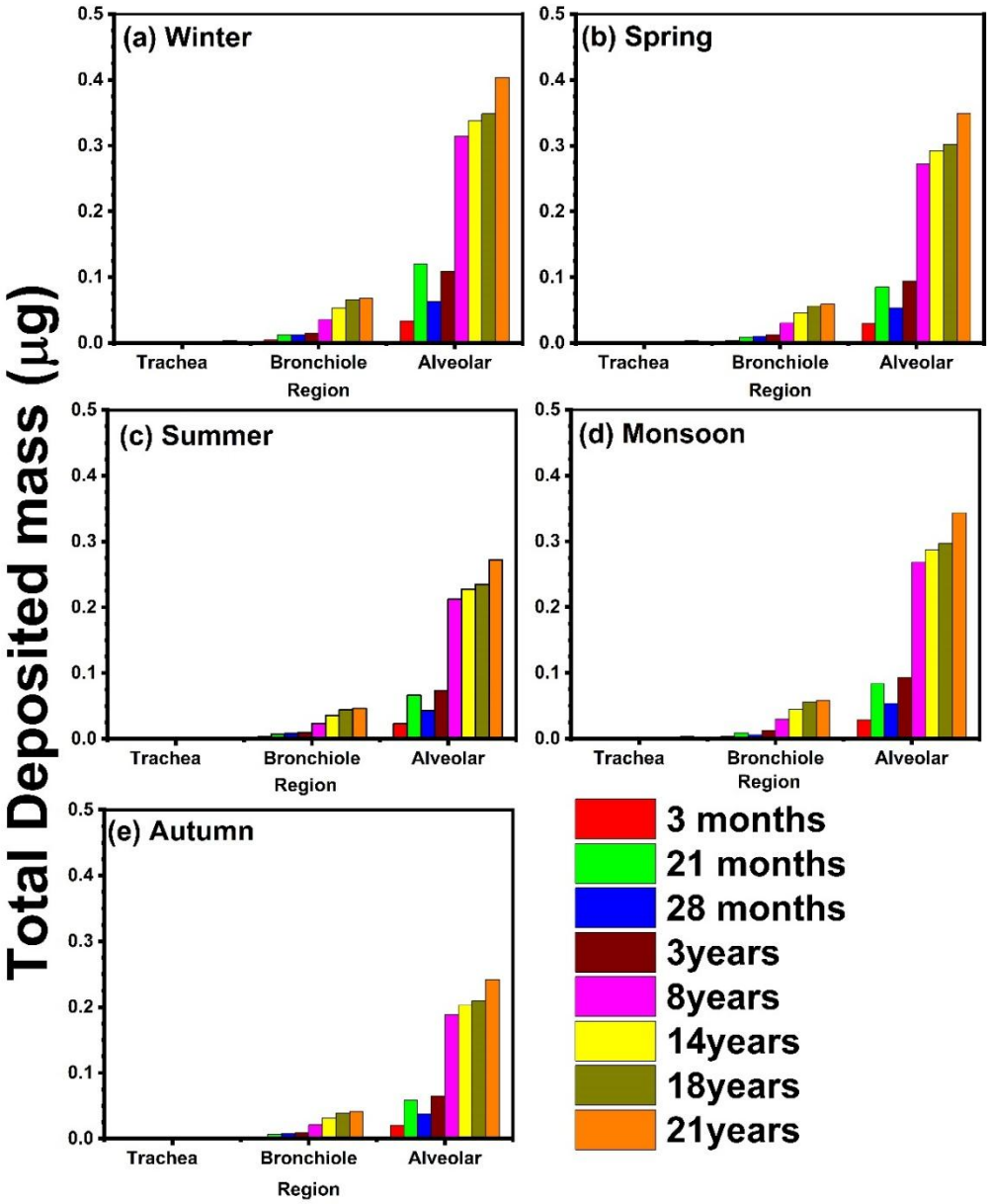

Figure 4.39: Estimated total deposited mass in different regions of respiratory system (trachea, bronchiole, and alveolar) during (a) winter, (b) spring, (c) summer, (d)

monsoon and (e) autumn in the study region of Delhi for different age groups ranging from from 3 months to 21 years using MPPD model

The seasons with more number of days in them account for more exposure periods and vice versa. It is estimated that in a year atleast about 100 µg of nanoparticles are deposited in the alveolar regions alone in adults in the study region. The age wise order of deposition of nanoparticles is adult (18 years and above) > adolescent (14 years) > child (3 to 8 years) > toddler > (21, 28 months) > infant (3 months). Thus, it is clear that, in urban areas where most residents are located near the road the vulnerability to nanoparticles is higher compared to other environmental regimes (rural, semi-ruban) irrespective of the exposure time or specified age group.

4.6.7 Quantification of total particle numbers deposited in different seasons

The daily deposition of nanoparticles in the alveolar regions ranges between 5 and 8 x 10^5 for adults in different seasons (Fig.4.40). The deposition of nanoparticles is estimated to be less in infants (3 months), gradually increases in children, and becomes higher in adults. Less than 2% of particles are deposited in the trachea region and 6-8% in the bronchiole region, whereas the remaining 90% get deposited in the alveolar regions. Due to its physical properties, most particles get deposited in the alveolar regions. Due to lesser mass, the nanoparticles penetrate the head and TB regions, so more deposition is found in the alveolar regions (Viitanen et al., 2017). The estimated total nanoparticle deposition in different regions of the human respiratory tract varies based on respiratory parameters such as tidal volume, functional breathing capacity, and breathing frequency. The age group of 21 years and above experiences more nanoparticle deposition than other age groups (Fig. 4.40). Nanoparticle deposition in the human respiratory tract can cause various health issues such as asthma, leukemia, prostate, and olfactory disorders (Manigrasso and Avino, 2012), thus, necessary mitigation measures need to be taken to reduce nanoparticle exposure, especially in urban regions.

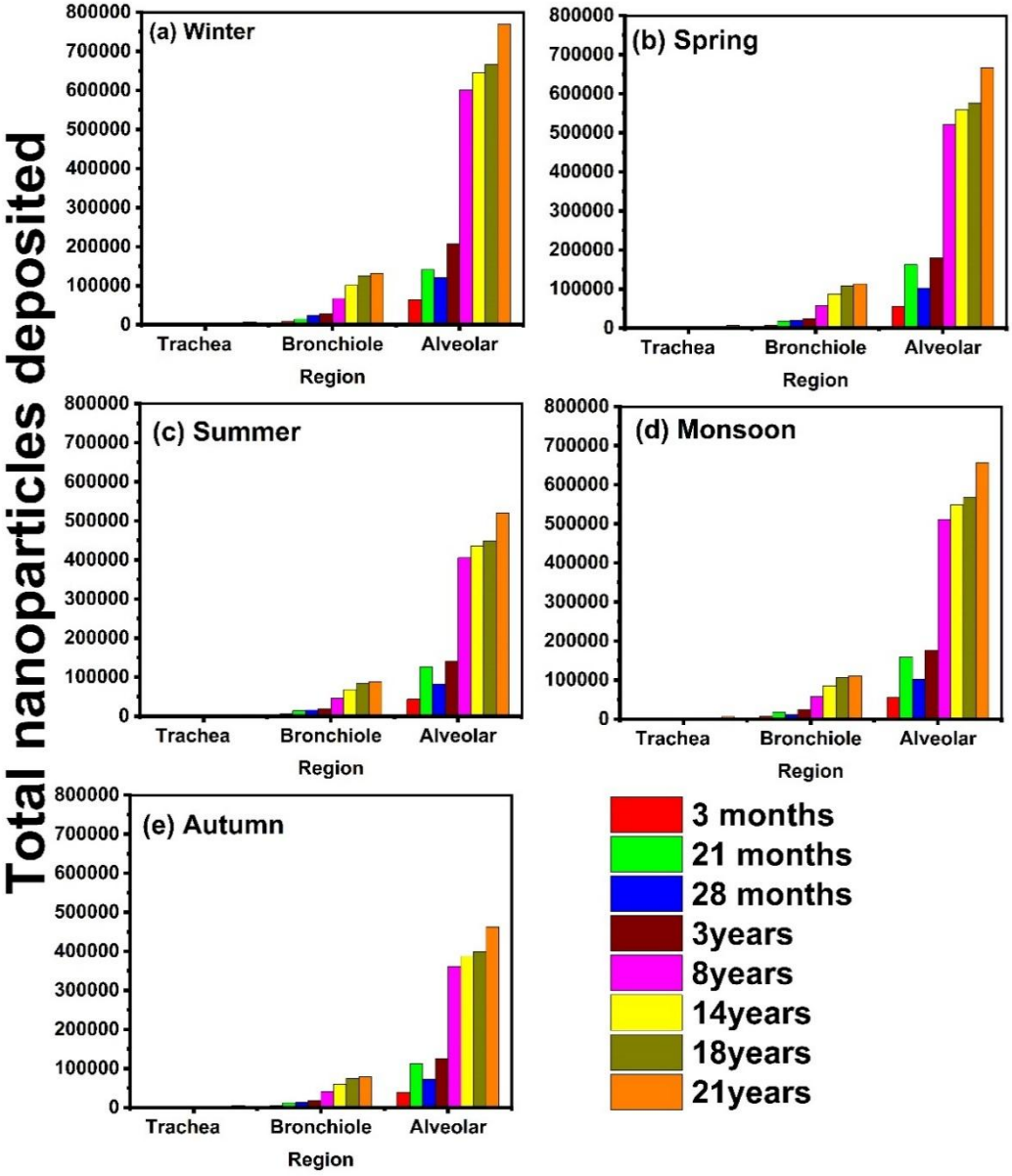

Figure 4.40: Total nanoparticle deposition estimated using MPPD model for different age groups in different regions of respiratory system, namely, trachea, bronchiole, and alveolar in (a) winter, (b) spring, (c) summer, (d) monsoon and (e) autumn) over Delhi

4.6.8 Deposition fraction of particles in different regions in the human respiratory tract

Deposition fraction indicates the fraction of nanoparticles inhaled which then get deposited in the respiratory system. The factors that influence the deposition include the mechanism and the airway structure which are based on the mass median diameter of the aerodynamic particles. The analysis shows that the deposition fraction in trachea region is minimal (<0.01). In the bronchiole region the deposition fraction is almost the same (~0.03) in all the seasons, suggesting that the deposition in the bronchiole region is less influenced by the seasonal variation in concentration and meteorology. The deposition fraction in the alveolar regions varies based on age and seasonal concentration.

The deposition fraction varies between 0.02 and 0.04 in the alveolar regions for different seasons. In winter, the fraction exceeds 0.04 for infants, suggesting that infants are more vulnerable during winter. The deposition in the alveolar region is 4-5 times greater than the deposition in the bronchiole region (Fig. 4.41). The difference in deposition in alveolar regions for adults is around 30 to 40% higher compared to infants and children. A previous $PM_{2.5}$ concentration-based deposition study also reported that the total deposition of particulate matter is seen more in children compared to other age groups (Manojkumar and Srimuruganandam, 2022) consistent with the present study. Several other studies showed that the particles with higher diameter deposit in the head region, and those with lower diameter deposit in the alveolar regions, which are corroborated by the present study.

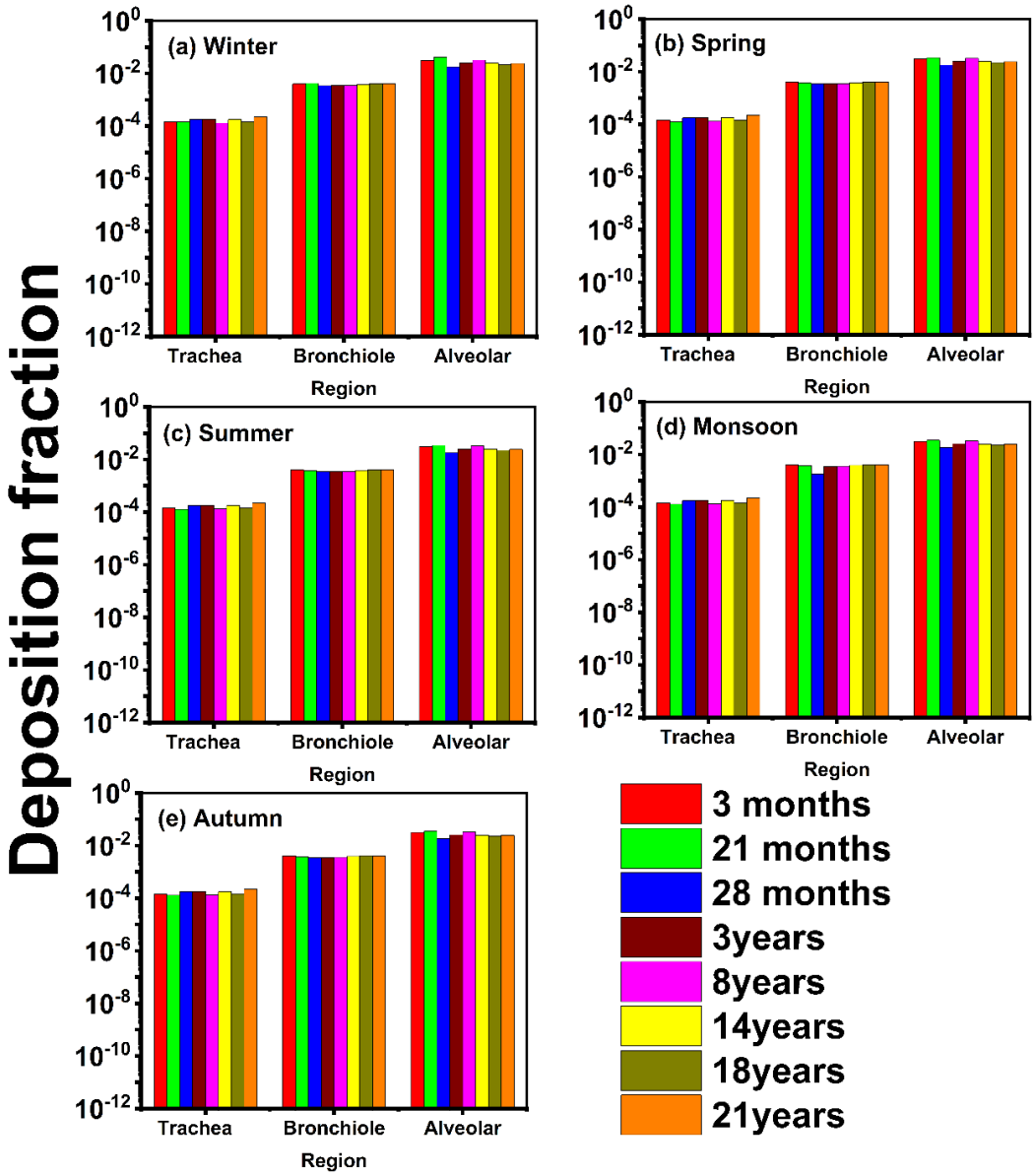

Figure 4.41: Deposition fraction of nanoparticles estimated using MPPD model for different age groups in the trachea, bronchiole, and alveolar regions of respiratory system during (a) winter, (b) spring, (c) summer, (d) monsoon and (e) autumn in the urban roadside study region of Delhi

4.7 Nanoparticle concentration analysis during episodic event

4.7.1. Firework episodic event

Diwali is one of the major festivals celebrated annually in India. The festival is celebrated in almost all parts of the country. It is celebrated by the bursting of crackers and lighting lamps (Ganguly, 2015; Garg and Gupta, 2018; Yadav et al., 2022a; Yadav et al., 2019). The crackers used for firework contains a large number of chemicals such as aluminum, sulfur, potassium nitrate, barium nitrate, charcoal, manganese, strontium nitrate, potassium and iron dust powder as a composition material for the manufacturing of firecrackers (Nishanth et al., 2012; Perrino et al., 2011; Sateesh et al., 2018). The lighting of fireworks emits different types of emissions into the atmosphere. It releases particulate matter, gaseous pollutants and toxic metals of significant quality. These particles stay in the atmosphere for a few days causing the formation of toxic smog. The pollutants are hazardous in nature and cause serious health effects as well (Kanawade et al., 2014). The study location is the national capital of India, New Delhi and is already facing severe pollution events throughout the year and majority of the time, the air quality remains in the poor category (Agarwal et al., 2020; Mishra et al., 2016; Mohan and Mishra, 2022). The air quality standards exceed national ambient air quality standards (Garg and Gupta, 2018; Goyal et al., 2021; Kanawade et al., 2020). The event Diwali falls under the post-monsoon season (beginning of the winter season) from October to November every year (Garg and Gupta, 2018; Ghei and Sane, 2018). During winter, air quality becomes poor due to the prevailing meteorological conditions such as relative humidity, boundary layer height and ventilation (Gani et al., 2020, 2021; Ramachandran and Rupakheti, 2022). Further increased emissions on Diwali also add more pollutants to the atmosphere. Recent studies found that air quality worsens during Diwali (Chatterjee et al., 2013; Kanawade et al., 2020; Parkhi et al., 2016; Yadav et al., 2022a; Yadav et al., 2019). People also call Delhi a Gas chamber during the pollution event. Apart from Diwali, Delhi is facing emission issues from sources such as vehicles, construction sites, road dust emission, industry sector, waste burning and also due to long-range transportation of pollutants of different geographical origins (Gani et al., 2019, 2020; Kumar et al., 2015; Mishra et al., 2016). Several studies in Delhi analyzed the impacts of crackers

on the local air quality and only very few studies reported an analysis of particles in number concentration (Garg and Gupta, 2018; Parkhi et al., 2016; Sateesh et al., 2018; Yadav et al., 2022b). This study analyzed the concentration and temporal variation of nano-size particles ranging from 10 to 1090 nm. The wide-range nanoparticles are classified into four different sub-categories such as Nucleation (10 to 30 nm), small Aitken (30 to 50 nm), large Aitken (50 to 100nm) and Accumulation mode (100 to 1000nm). The study focuses on the size distribution of different size range particles during the event of Diwali and the period adjacent to it. The study helps in understanding the pattern of emission of nanoparticles during the firework event. Because of the restriction on firecrackers use in the city, a reduction is found in the concentration of the particles. Although the use of fire crackers is restricted in the city but few fire work events still occurred on Diwali evening as a part of the tradition.

4.7.2 Temporal variation of Particle number concentration during episode

The hourly average concentration of the total particle number concentration (PNC) of the nanoparticles was found high during Diwali, especially during the evening hours when the fireworks event occurs regularly. The remaining days in the pre- and post-Diwali days represent the emission from the transportation sector that shows two peaks in a day during morning and evening peak hours. The concentration of the Diwali day reaches a maximum of about 9 x 10^4 cm^{-3} (Fig. 4.42) whereas the maximum concentration during the pre and post-Diwali was found in the range of 6 to 7 x 10^4 cm^{-3} (Fig. 4.42). During Diwali, the concentration of PNC was increased about 30% comparing pre-Diwali period and 19 % comparing post-Diwali period. The change in the percentage of concentration during the pre and post-Diwali periods was due to the existence of particles from the Diwali emissions especially in the post-Diwali period. The geometric mean diameter of the particle also showed an increase in their mean diameter during the Diwali period and the maximum concentration of the GMD was obtained during the post-Diwali phase compared to other phases due to the coagulation of the particles after the Diwali day. The different size particles such as N_{nuc} and N_{satk} were seen in less concentration during the Diwali period since they were not directly associated with Diwali emissions, N_{latk} (50 to 100 nm) was slightly associated with Diwali emissions and N_{acc} was observed in higher concentration showed a majority of

the particle was found above 100 nm from the Diwali emissions. The statistical analysis of different size particles during different monitoring periods with their minimum and maximum concentration was shown in Table.4.9.

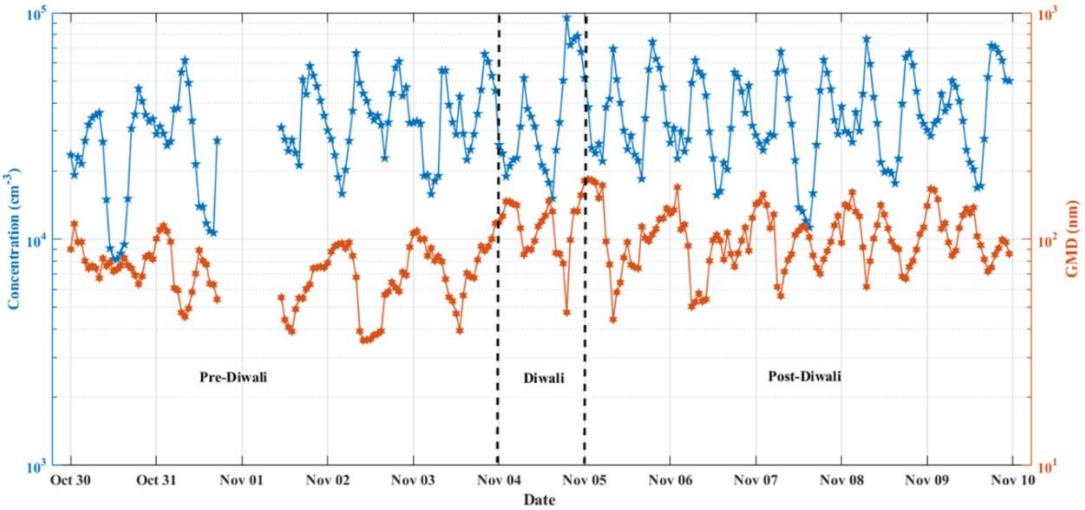

Figure 4.42: Daily variation of hourly averaged particle number concentration and GMD from 30th October to 10th November 2022

4.7.3 Size resolved particle distribution

The size distribution of the different size-resolved particles is plotted for three periods, namely the pre, post and Diwali periods, for distinguishing the different peaks occurring at different periods. The size distribution of the particles shows a clear single peak of higher concentration during the Diwali day in the size range of particles around 150 nm in the accumulation mode of the particles. The pre and post-Diwali concentrations show a gradual rise in the concentration from smaller to larger size, attaining a peak in the accumulation mode, whereas on Diwali, the N_{nuc} concentration decreases to a certain extent and then it starts to increase gradually from N_{satk} to N_{acc} (Fig. 4.43). This shows the presence of less particles during the period compared to another period. The concentration of the particle pattern was totally different from N_{nuc} to N_{latk} and $N_{acc.}$ During the pre-Diwali period, the lower size particle till N_{latk} mode concentration was found to be high, followed by the post-Diwali period and then by the Diwali period (Fig. 4.43). In N_{acc} the pattern was totally opposite i.e., higher concentration on Diwali period followed by a post-Diwali period and then by Diwali period. This indicates a clear representation of the particles and their sources. The

smaller size particle till 100 nm is directly associated with vehicular emissions found in the Pre and Post-Diwali period. During Diwali period, particles above 100 nm are found in higher concentrations and are associated with Diwali emissions.

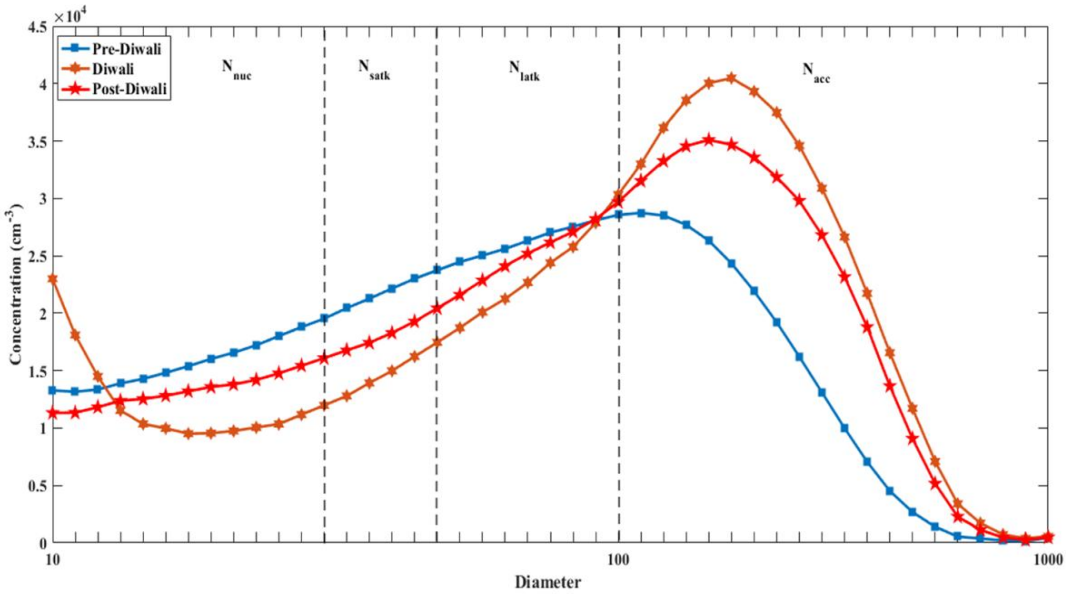

Figure 4.43: Particle number size distribution of N_{nuc}, N_{satk}, N_{latk} and N_{acc} during 30th October to 10th November 2022

4.7.4 Particle composition in total number concentration

The composition of different size particles throughout the monitoring period was done to analyze the role of different size particles in the total number concentration. This shows the percentage contribution of different size particles. The contribution of smaller size particles in total concentration was found to be high during the pre-Diwali period. The accumulation mode alone contributed to a higher extent of around 57% (Fig. 4.44) of the total particles on the Diwali day, followed by 48% to 55% in the post-Diwali period. The contribution of the fire emissions during the Diwali and post-Diwali was seen clearly in the figure 4.44. The total PNC concentration is based on the contribution from different size fractions emitted from different sources such as engine exhaust, biomass burning, and fire emissions in the urban regions. The hourly contribution of the different sizes to the total PNC is also analysed to clearly understand the emissions. The hourly emission contribution of the different size particles to the total PNC shows on Diwali day. The contribution of the accumulation

mode dominates 60 to 70% of the PNC during the Diwali evening and the next morning (Fig. 4.45b).

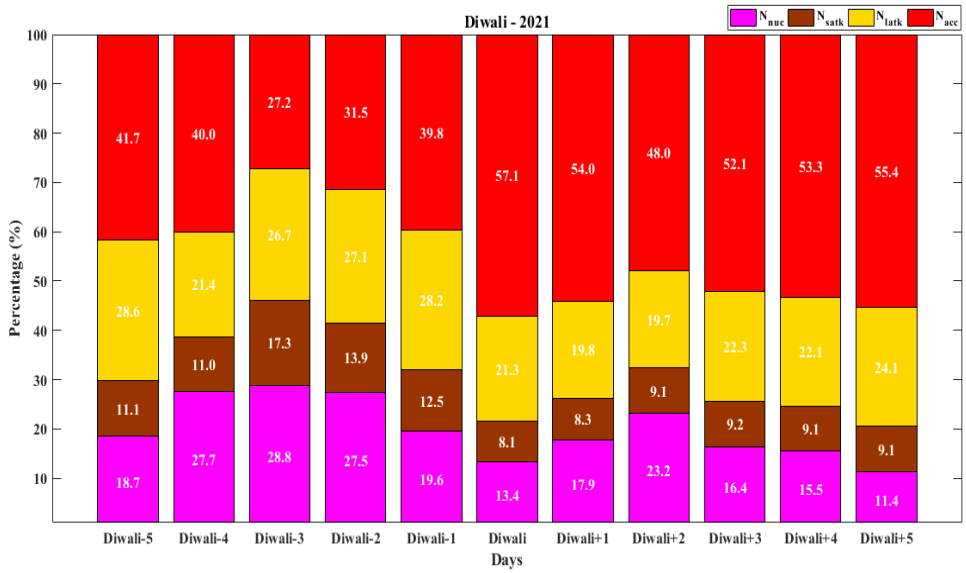

Figure 4.44: Percentage contribution of N_{nuc}, N_{satk}, N_{latk} and N_{acc} in Total PNC (30th October to 10th November 2022)

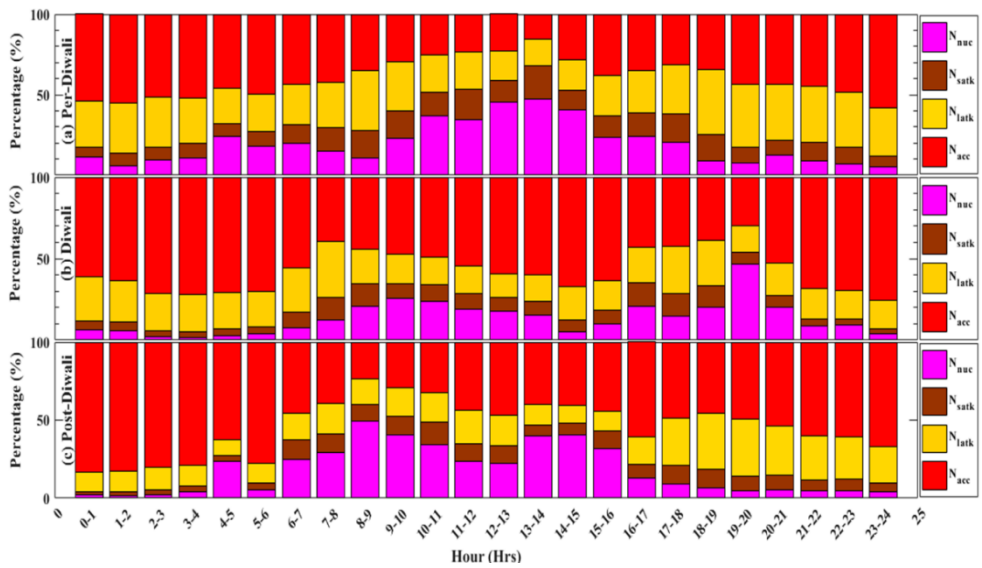

Figure 4.45: Hourly classified percentage contribution of N_{nuc}, N_{satk}, N_{latk} and N_{acc} in Total PNC during (a) pre-Diwali, (b) Diwali (c) post-Diwali from 3rd November to 5th November 2022

The Pre Diwali period showed an increase in the concentration of the Nucleation mode particles during the afternoon hour due to the effect of sun rays which causes nucleation burst events (Kompalli et al., 2018). Since the monitoring period falls under winter seasons, the higher concentration of solar radiation and ventilation was seen during the afternoon in Delhi (Fig. 4.45a). This can be clearly visualized during the Post Diwali day when the solar radiation starts to increase around 06:00 hrs, the concentration of the nucleation mode particles also seen increased (Fig. 4.45c). Whereas during the off-sunshine hours the nucleation mode particles again start to decrease and the concentration of PNC was dominated by the accumulation mode particles due to coagulation.

4.7.5. Heat map analysis during episodes

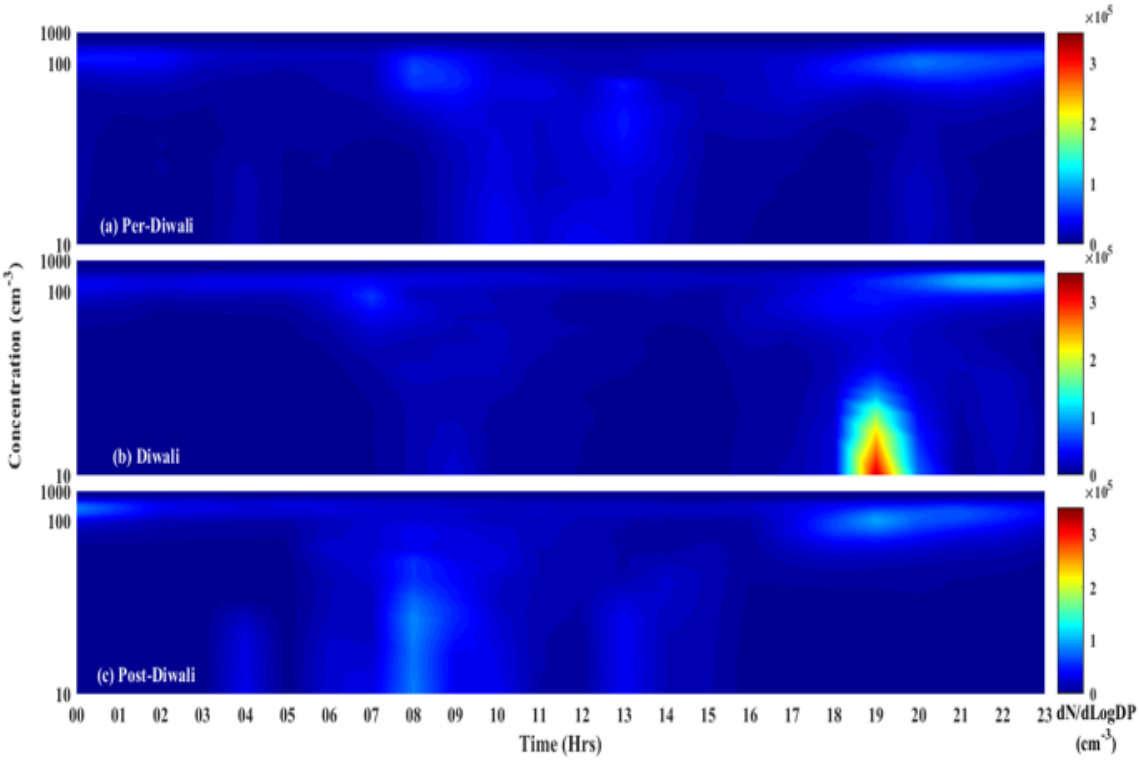

Figure 4.46: Heat map analysis of size-resolved particle distribution and GMD during (a) pre-Diwali, (b) Diwali and (c) post-Diwali from 3rd November to 5th November 2022

The heat map analysis is used to evaluate different size particles with respect to time. During Pre-Diwali period, in early morning and late evening, a thin hazy layer of

particles around 100 nm was found (Fig. 4.46a) in the concentration range of 1 x 10^5 cm^{-3} due to the accumulation of particles under low boundary layer conditions and less dispersion of particles. During the Diwali period in the evening around 18 to 20 Hrs. There is a clear visibility of particle emissions from fireworks in the range of 3 to 2 x 10^5 cm^{-3} (Fig. 4.46b) and the hazy layer of particles in pre-Diwali is seen in a similar pattern in the late evening and early morning on Diwali day with higher concentration due to the pollution load increased by Diwali. During the post-Diwali phase, during the morning (8 Hrs.), another emission source of around 1 x 10^5 cm^{-3} was due to the vehicular emissions, which added more particles apart from preexisting Diwali emission particles. In the Pre Diwali period, the vehicular emission contribution during the morning and evening peak hours is also clearly visible.

4.7.6 Correlation analysis of different size particles

The correlation analysis of particles with gaseous pollutants shows that the N_{acc} and N_{latk} show moderate to good correlation with particles associated with Diwali emissions and the correlation values are found to be higher during the post-Diwali phase. Certain pollutant, such as O_3 showed very less correlation (r^2 =0.1 to 0.2) (Fig. 4.47c) throughout the Diwali phases since O_3 was not directly associated with Diwali emissions.

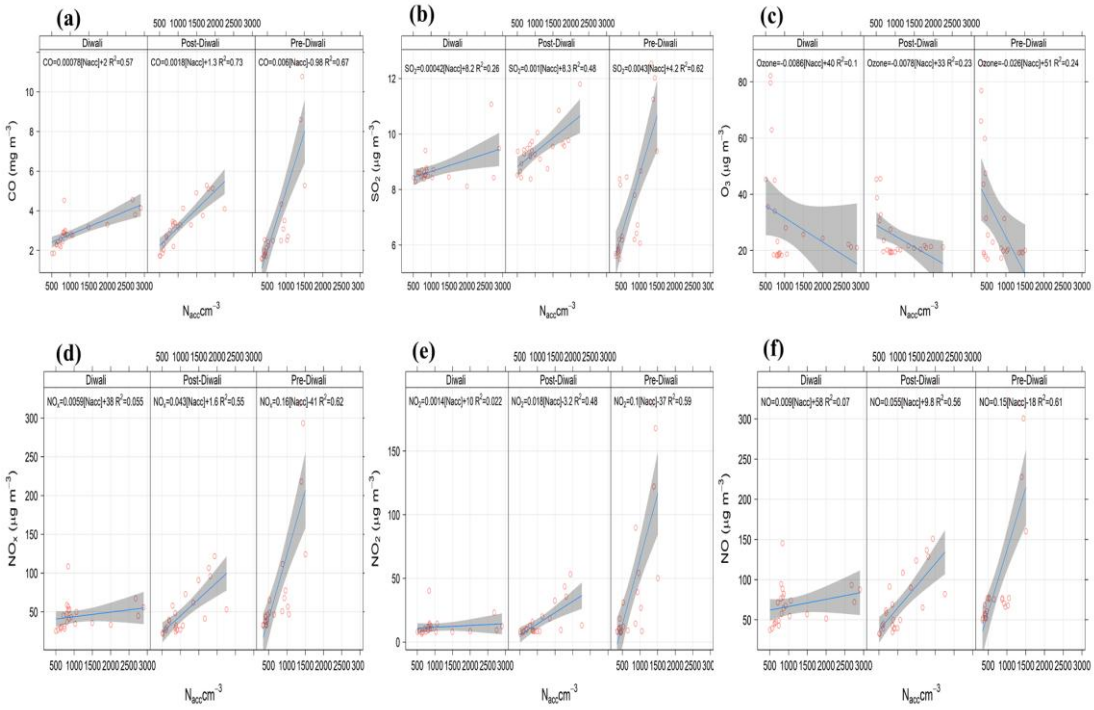

Figure 4.47: Correlation analysis of N_{acc} with(a) CO (b)SO_2 (c)O_3 (d)NO_x (e)NO_2 (f)NO during pre, post and Diwali period from 30th October to 10th November 2022

The Nitrogen components such as NOx, NO_2, NO showed the highest correlation values. The r^2 values ranged from 0.4 to 0.6 (Fig. 4.47 d-f) for the N_{acc} mode particles and for particles in N_{latk} mode the correlation values was found to be high in the post Diwali phase (r^2 =0.7) compared to the pre-Diwali (r^2 =0.2 to 0.3) and Diwali phase (r^2 =0.01 to 0.02) (Fig. 4.48 d-f). The r^2 of CO ranges from 0.6 to 0.7 (Fig. 4.47a) for the N_{acc} and for N_{latk} mode (r^2 =0.2 to 0.4) (Fig. 4.48a). The carbon emissions were high before Diwali and on Diwali, the concentration was found less and then during the post-Diwali phase, the values started to resume back to its original concentration. The correlation values were insignificant for the smaller sizes, such as N_{nuc} and N_{satk} mode particles.

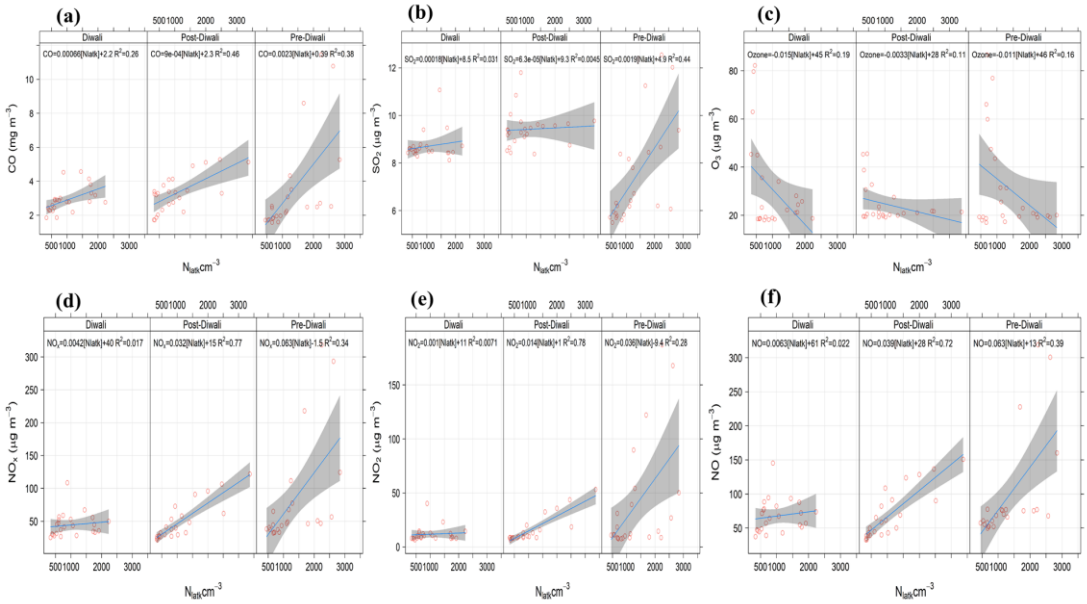

Figure 4.48: Correlation analysis of Nl_{atk} with(a) CO (b)SO_2 (c)O_3 (d)NO_x (e)NO_2 (f)NO during pre, post and Diwali period from 30th October to 10th November 2022

4.7.7 Summary

The particle number concentration of the nano particles ranging from 10 to 1090 nm was measured from 30th October to 10th November 2022. This period covers the major festival of the country like Diwali, which is usually celebrated through bursting of firecrackers. The Diwali day received the maximum particle number concentration of about 9 x 10^4 cm^{-3}. In the previous period and after the Diwali period, concentrations ranged from 6 to 7 x 10^4 cm^{-3}. On Diwali day, a 30 % increase in the concentration of the particles was observed compared to the normal day emissions. The increase in emissions was due to the fireworks events that occurred. In the post-Diwali period, the concentration was increased by 19 % compared to the pre-Diwali period due to the addition of Diwali emissions along with normal emissions. The particles in size range > 100 nm i.e., N_{acc} mode particles were seen in higher concentration. The size distribution of the particles showed a peak concentration of particles around 150 nm on Diwali day. Before the Diwali event, the smaller size particles in the range of $Nl_{atk,}$ i.e., 50 to 100 nm size particles were seen in peak concentration.

Table 4.9: statistical summary of different size pollutants during the different phases of the episodic event

S.no	Parameter	Value	Pre Diwali	Diwali	Post Diwali
1.	N_{nuc} (cm-^{3})	Minimum	87.3	27.4	38.8
		Maximum	2062.5	3428.2	2646.1
		Mean ± SD	606.2 ± 462.2	473.1 ±689	514 ± 495.8
2.	N_{satk} (cm-^{3})	Minimum	149.6	136.1	106
		Maximum	2455.9	1429.1	2336.3
		Mean ± SD	878.8 ± 539.3	599.2 ±396	732.5 ±551
3.	N_{latk} (cm-^{3})	Minimum	284.0	339.2	318.2
		Maximum	2842.7	2233.7	3483.2
		Mean ± SD	1113.1 ± 674.4	1003 ± 572	1074 ±781
4.	N_{acc} (cm-^{3})	Minimum	158.7	506.1	317.8
		Maximum	1505.7	2902.1	2258.1
		Mean ± SD	598.4 ± 278	1111 ±714	961.4 ± 337
5.	N_{total} (cm-^{3})	Minimum	8156	15120	11263
		Maximum	66314	95073	76588
		Mean ± SD	32550 ± 13957	38289± 23038	37203±15796
6.	GMD (nm)	Minimum	35	47	44
		Maximum	117	156	183
		Mean ± SD	73±20	119± 27	104±31
7.	NO_2 (µg/m^{3})	Minimum	6.80	6.6	6
		Maximum	187.2	40.2	68.8
		Mean ± SD	24.9 ±31.7	11.7 ±7	13.1 ±11.4
8.	NO (µg/m^{3})	Minimum	24.6	37.3	30.8
		Maximum	319	145.4	200.4
		Mean ± SD	76.7 ± 45.5	67.6 ±24.2	77.2 ±39.1
9.	NO_X (µg/m^{3})	Minimum	18.5	25.3	21.5
		Maximum	318.5	108.5	160.7
		Mean ± SD	59.7 ± 47.4	44.4 ±17.9	50.61 ±28.3
10.	SO_2 (µg/m^{3})	Minimum	5.1	8.1	8
		Maximum	12.5	11	11.8
		Mean ± SD	6.2 ± 1.2	8.6 ±0.5	8.7 ±0.5
11.	CO (mg/m^{3})	Minimum	0.3	1.8	0.9
		Maximum	11.4	4.5	5.6
		Mean ± SD	2.3 ± 1.81	2.8 ± 0.7	2.7 ±0.9
12.	Ozone (µg/m^{3})	Minimum	17	18	18.5
		Maximum	111.3	82	101.4
		Mean ± SD	37.1 ± 25.1	30.6 ±19.1	32.9 ±22

These size ranges are directly associated with exhaust emissions in urban regions. N_{acc} mode particles were observed in higher concentrations during Diwali days and the concentration was about 57% of the total concentrations, whereas before Diwali, the contribution was around 31 to 40 %. During the evening hours, when the firework events occured the percentage contribution of N_{acc} mode particles to the total

concentration reached around 60 to 70 %. During the pre-Diwali period, N_{nuc} particles in the mid-day received a higher concentration of about 25 to 28% due to the burst of particles. The heat map analysis showed clear evidence of a hazy thin layer of particle emissions during the morning and evening peak hours resulting from vehicular emissions. During Diwali day, especially during 18 to 20 Hrs. The particles' concentration was around 2 to 3 x 10^5 cm^{-3}. The correlation of gaseous pollutants shows a good correlation with N_{acc} and Nl_{atk} mode particles and for other smaller sizes, the correlation was not found. NOx, NO_2, NO showed a good correlation with N_{acc} (r^2 =0.4 to 0.6). The highest correlation of NOx, NO_2, NO that found throughout the monitoring period was (r^2 = 0.7) with N_{latk} mode particles during the post-Diwali phase. The correlation of N_{acc} mode with CO was observed to be high during the pre-Diwali period (r^2 =0.6 to 0.7) and less during the Diwali period. The study revealed the role of Diwali festival emissions on Particle number concentration of nano pollutants in the atmosphere. However, the usage of firecrackers in the National capital Delhi is reducing year to year due to the air pollution events occurring after Diwali.

CHAPTER – 5

CONCLUSIONS

5.1 Introduction

Deteriorating air quality in Delhi, India, has created global interest in understanding its issues due to its complex mixture of sources. The study analyzed the variation of different size nano pollutants in the region ranging from 10 to 1090 nm for a year period from December 2020 to November 2021. The study period includes two major classifications one is based on the changes in emission sources intensity and another one is based on the seasonal variation. The first part was conducted in the roadside environment near a busy road in Delhi from 1st April 2021 to 30th June 2021 (classified as Period I), and from 3rd October 2021 to 30th November 2021 (referred to as Period II) based on emission sources variation. The seasonal variation (winter, spring, summer, monsoon, and autumn) was analysed in megacity city Delhi for the first time. The nano-sized pollutants exhibit significant diurnal and seasonal variations due to differences in environmental conditions, emission sources, regional meteorology, and atmospheric dynamics. So, in this study, deposition of nanoparticles (size ranging from 10 to 1000 nm) in the human respiratory system using a Multiple Path particle Dosimetry (MPPD) over the urban megalopolis Delhi is estimated. The size distribution of particles in an urban roadside environment in the above size range is examined with respect to vehicular flow density, such as during the peak (morning, and evening) and non-peak hours. The major conclusions of the study are as follows.

5.2 Summary of nanoparticles concentration and meteorological role during different emission scenarios

The study found that the concentration of the particles in urban roadside microenvironments varies with increased or reduced anthropogenic activities, especially vehicular-based emissions. During Period I (during restriction (DR) phase), due to the various restriction for vehicular movement and other anthropogenic sources, less concentration was recorded in the study area (1.7 x 10^3). During the same DR phase, the recorded vehicle fleet was 49% less than the normal period. Similarly, after Diwali (AD) phase, which occurs immediately after Diwali, a maximum concentration

of particles (1.3x 10^4 cm^{-3}) was recorded. This was due to the contribution of both vehicular emissions and Diwali firecrackers emissions. The PNC concentration in AD phase increased by 35% compared to the previous phase. The particle number concentration found in the range of 10^3 cm^{-3} to 10^5 cm^{-3} during Periods I and II, except for the AD phase in Period II, in which PNC ranged from 10^4 cm-3 to 10^5 cm^{-3}. Apart from PNC, the geometric mean diameter (GMD) and size distribution of the particles also vary, which help to identify the source contributors. When emissions are complex, the GMD of the particles varies from 20 nm to 200 nm (Period II), but when emission sources are restricted, the range also narrows to 15 to 80 nm (Period I). Periods I and II received average precipitation of about 116 mm and 80 mm, respectively, resulting in the wet removal of particles in large quantities. In the entire study period, Period I experienced around 31 % less concentration of particles (~2.4 x 10^4 cm^{-3}) due to lockdown restrictions and, on the other hand, particle concentration was increased by 35% compared to normal conditions due to the sudden rise in firework emissions in Period II. In addition, the size distribution of particles also changed between two periods. The contribution of different size bins to the total concentration varies according to the sources. During the DR phase, when there was a restriction, the contribution of N_{nuc} and N_{satk} was less to N_{total} since they were directly associated with the vehicle-related exhaust in urban environment. N_{nuc} contribution is high in BR and DR phases, which are marked by average emissions. Events like Diwali and pollution events add more particles into the atmosphere along with the pre-existing regular emissions over an urban region, so the contribution of N_{acc} in N_{total} was high during the AD and DR II phases. Local and regional meteorology also played a significant role in deciding the PNC in the roadside environment. When the relative humidity was high, the coagulation of the particles occurs to a greater extent, and hence, the concentration becomes high (Period II). The diurnal behaviour showed high concentrations of the pollutants during the peak hours (morning and evening) because of vehicular emissions during normal conditions (without restriction). Wind speed and direction were the other factors influencing the concentration of these particles. Dispersion of particles occurred based on wind speed and direction: higher wind speeds resulted in higher dispersion, and vice versa.

The study presents detailed characteristics of PNC in the urban city of Delhi during various emission scenarios. The study confirms the role of traffic emissions in metropolitan cities in determining the particle load. The PNC estimates will be useful to determine the deposition of particles in the human respiratory system based on the various inhalation rates and associated physical activities. The particles in the nano-size range after deposition can potentially transport to other parts of the human body, creating more chronic and acute illnesses in the human body. The quantitative outcomes of the present study can thus be used to estimate human health impacts, develop policies/standards, and initiate mitigation measures for pollution events with implications to climate change and help move towards sustainability measures.

5.3 Summary of nanoparticles concentration and during different seasons

The nano-sized pollutants exhibit significant diurnal and seasonal variations due to differences in environmental conditions, emission sources, regional meteorology, and atmospheric dynamics. The concentration of particles was classified into four different sizes as N_{nuc} (10 to 30 nm, nucleation particles), N_{satk} (30 to 50 nm, small Aitken particles), N_{latk} (50 to 100 nm, large Aitken particles), and N_{acc} (100 to 1000 nm, accumulation mode particles), and the total particle number concentration (PNC) as N_{total} (or total PNC). PNC ranged between 10^4 cm^{-3} and 10^6 cm^{-3} over Delhi during the year, and the highest concentration is found during winter. On a seasonal scale, the concentration in winter was ~ 2 times higher than in monsoon, 1.6 times higher than in summer, and about 1.3 times higher than in autumn and spring. The diurnal variation analysis showed distinct characteristics of seasonal, primary, and secondary emissions throughout the day. The direct primary emissions from engine exhaust exhibit a prominent double hump structure during morning and evening peak hours in winter and autumn. The double hump structure was same for PNC and other gaseous pollutants related to vehicular emissions during these seasons. Appropriate correlation was found between carbon monoxide (CO) and N_{acc} (100 to 1000 nm) in all seasons (R^2~0.5), suggesting that emissions from fossil fuel combustion was the predominant source for gases and particles in the near-road curbside environment. Ozone concentration increaseed multi-fold during the peak sunshine hours due to photochemical reactions with nitrogen oxides (NOx) and volatile organic compounds

(VOCs) under the influence of sunlight and heat in all the seasons except in monsoon. The study also revealed that apart from differences in primary direct emissions, the particles undergo secondary transformation (through coagulation and condensation) due to the prevalent meteorological conditions that differ in different seasons.

The concentrations in different size ranged (N_{nuc}, N_{satk}, N_{latk} and N_{acc}) and their respective contributions to total PNC exhibit significant seasonal variations. During winter, larger size particles (large Aitken and accumulation) contributed more to the total due to coagulation, with accumulation mode alone contributing >40% to the total PNC. In winter, the concentration of accumulation mode particles (>500 nm) is higher in the evening hours due to the coagulation of smaller particles. N_{nuc}, N_{satk}, and N_{latk} (<100 nm) were higher in spring and summer during mid-day due to nucleation and/or ultrafine particle (UFP) burst events. The concentrations in the nucleation mode (smaller size) and accumulation (larger size) exhibited higher deviations in their respective contributions to the total, with N_{nuc} contributing 20% to 36% and N_{acc} accounting for 23% to 45% in all the seasons. In contrast, the concentrations in the medium size exhibit lesser variability as the contribution of N_{satk} varied to N_{total} from 12% to 17%, and N_{latk} varied from 22% to 26%, respectively during the year. The particle number concentrations and their contributions were influenced by differences in different emission sources and due to variations in other meteorological parameters such as wind speed, relative humidity, temperature, solar radiation and boundary layer height during day and night. The percentage contributions by different size particles to N_{total} during daytime and nighttime varied and the results clearly indicate the distinct role of diurnal variation in emission sources. The percentage contributions of nucleation mode followed by accumulation contribute >60% to N_{total} during daytime with their sum contribution being the highest in spring season (67%). During the warm periods of spring, summer and monsoon, N_{nuc} contributes ~45% to N_{total} during daytime due to the prevalent meteorology conditions which enabled freshly emitted exhaust emissions to remain in the atmosphere longer. Whereas in autumn and winter N_{nuc} contributed <30% to N_{total} in daytime. In stark contrast, the concentration of large particles, Nacc and Nlatk, dominated N_{total} during nighttime, and in particular in winter and autumn N_{acc} and N_{latk} contributed 77% to N_{total} owing to coagulation of emitted

particles as the prevalent atmospheric conditions (higher RH, lower temperature and BLH) favoured coagulation, with N_{acc} alone contributing ~50% in both the seasons. The contribution of N_{satk} and N_{latk} was less to N_{total} during daytime and nighttime and they do not exhibit significant seasonal variabilities – N_{satk} contributes 14-17% (daytime) and 10-16% (nighttime, whereas N_{latk} contributes 18-25% (daytime) and 23-29% (nighttime), respectively. The size distribution of particles in an urban roadside environment in the above size range is examined with respect to vehicular flow density, such as during the peak (morning, and evening) and non-peak hours. The UFP contributed 60 (autumn) to 80% (monsoon) to the total particle concentration in the study region. The concentration of UFP and N_{acc} during non-peak hours was less than that of peak hours, confirming the dominant influence of emissions from vehicular exhaust in the study region. The size distribution analysis of UFP in different seasons clearly identified the role of various emission sources such as direct emissions (winter, and autumn) and particle formation process (spring, and summer).

This study provides insights into the behavior, dynamics, contribution, and characteristics of air pollutants in the nano-size range in the atmosphere. The study concludes that the dynamics and profiling of nanoparticles on the environment and human health are not only related to the concentration of direct primary emissions but also depend on the gaseous precursors, meteorological conditions, and atmospheric dynamics of/and over a particular region. The results provide quantitative insights into the number concentrations of particles (air pollutants) in different size ranges from nucleation to accumulation and their behavior in a roadside urban environment of a highly polluted urban city on seasonal scales, which will be useful in devising control strategies aimed to improve air quality, public health, environment, and climate. Concentrations of particles from nucleation to accumulation modes are significantly higher in Delhi in winter than other seasons. Air quality across north India is found to worsen during winter due to increases in aerosols, and rising relative humidity (Paulot et al., 2022). Further, due to rapid industrialization and growth in population improving air quality is seen to be a big challenge for India (Xie et al., 2024). The winter $PM_{2.5}$ concentrations decreased in 2022 by 20%, out of which one-half of the reduction was attributed to favorable meteorological conditions in the last 5 years, which are unlikely

to persist in a warming world (Xie et al., 2024). An estimated 1.7 million premature mortalities in 2019 in India were attributed to severe surface-level air pollution according to a Global Burden of Disease study. Further, an estimated 15% of deaths in South Asia were linked to health effects of air pollution exposure (World Air Quality Report, 2020). These quantitative results on seasonal variations of air pollutants together with the knowledge on seasonal variations in meteorological parameters and atmospheric dynamics (e.g., lower BLH in winter favors trapping the pollutants near surface as opposed to summer) form a basis which can be effectively utilized while devising mitigation measures to enhance the positive effect of improving the air quality and public health.

5.4 Role of regional precursors and meteorology in determining the nanoparticles concentration in the study area

The nanoparticles concentration was not only associated with the intensity of the sources but also with local factors such as gaseous emissions in the region and meteorological conditions. Vehicular emissions contributed to nanoparticle concentration and other co-pollutants, such as NO, NO_2, NO_x, SO_2, CO, BC, and O_3. The evolution of the gaseous pollutant's concentration had similar trends to particles because they have the same origin (traffic emissions). The BC used as a tracer for transport emissions showed higher concentrations during nighttime. The concentration of gaseous pollutants also increased to around 3 to 5% during winter. Winter season in the study period experienced a shallow boundary layer < 1000 m, which promoted the pollution accumulation at the ground level, while during summer, the boundary layer reached up to 2400 m, which helped greater dispersion. Based on the wind speed and boundary layer height, the ventilation coefficient of the region also changed seasonally. Precipitation was another important factor for determining a region's total particle number concentration because it helped in wet scavenging of the pollutants, especially in the N_{acc} mode particles. The N_{nuc} underwent more diffusion during the precipitation due to their smaller size thus an increase in particles was observed. Precipitation from 1 to 3 mm can reduce the total particle concentration from 2.2×10^4 to 1.1×10^4 cm^{-3}. The precipitation process not only influenced the concentration but also played a role in the size distribution of the particles. The meteorology parameters, such as wind,

helped in particle dispersion, and relative humidity triggered their secondary transformation. Air recirculation in the street canyon due to vehicular flow turbulence was observed in the study region.

The study investigated the role of emission sources in determining the concentration of nanoparticles in the urban roadside environment establishing relationships with seasonal factors, meteorology (wind parameters, precipitation and relative humidity), and gaseous pollutants, which helps to understand the dynamics of these particles in the atmosphere. The outcomes of the study can be used to estimate the health hazards these pollutants pose in the urban environment, especially those residing/ working near the road microenvironment.

5.5 Exposure estimation of nanoparticles in the study area

An analysis of quantification of particles related to health effects is also performed. The inhalable particle number (IPN) concentration over the study region varied from 10 million to 1 billion during different seasons for different breathing rates. The estimated IPN at a constant breathing rate of 12 liters per minute (LPM) showed that the concentration varies from about half a billion to 1 billion throughout the year. The nanoparticle deposition in the human respiratory tract estimated using. The deposition in the evening peak hours (EPH) during the winter season was >5 million particles. The annual average deposition of particles in the roadside environment (present study, 500 µg/year) was about 30% higher (330 µg/year) than a non-roadside ambient environment that is away from the roadside. The deposition of nanoparticles ranges between 0.29 and 1.31×10^{-3} µg/hr in winter, followed by spring ($0.25\text{-}1.13\times 10^{-3}$ µg/hr), summer (0.01 × 10-3 - 1.13× 10-4 µg/hr), monsoon ($0.02\text{-}1.1\times 10^{-3}$ µg/hr) and autumn ($0.01\text{-}7.88 \times 10^{-4}$ µg/hr). The analysis reveals that an adult working 8 hours a day near the road environment in the study region experienced a nanoparticle deposition of 338 µg/year. Further, on a 24-h scale (day) the residents residing near the roadside experienced a 3-times higher deposition (>1000 µg/year of nanoparticles) in the study region clearly indicating a linearity between the deposition of nanoparticles and the hours of exposure. The daily deposited mass concentration ranged between 0.02 and 0.04 µg in the trachea region, followed by bronchiole < 0.05 µg; in alveolar

regions, the amount of particle mass deposited varied between 0.05 and 0.10 μg/day. The rate of deposition in the alveolar region was higher for the age group of 8 to 21 years due to the increased breathing frequency. In terms of deposition rate in different regions of the human respiratory tract, 90% of particles get deposited in the alveolar regions, 6-8% in the bronchiole region, and 2% in the trachea region, highlighting that the deposition of nanoparticles was dominant in the alveolar regions. The deposition fraction of particles ranged between 0.02 to 0.04 in the alveolar region which was 4-5 times higher than in the bronchiole region. Compared to children and infants, adults experienced 30 to 40% higher nanoparticle deposition in the respiratory system. It may be noted that the model estimates of nanoparticle deposition may vary in real time on a day to day basis as the deposition depends on lung parameters and humidity. The new quantitative insights gained on the seasonal variation in the deposition of nanoparticles in humans residing near roadside conditions are crucial to estimate the human health risk potential, especially in winter when the nanoparticles and their deposition rates are significantly higher. These findings, with implications to improved air quality and public health are vital for formulating mitigation measures on a seasonal scale for exposure reduction to different age groups, hitherto unavailable, can lead to a better and sustainable future. The deposition of particles in different regions of the human respiratory system depends on the sizes of particles inhaled. The UFP deposition is found to be higher in the lower respiratory regions. The results on inhalable particle number concentration during different activities provide insights into the health effects on vulnerable populations in road environments during different seasons. These quantitative results obtained on a seasonal basis over an urban area in a megacity are crucial and valuable inputs to analyze the deposition of pollutants for an individual working/living in the vicinity of the road, and further to develop strategies for air quality, policy formulation (such as restrictions), and measures for combating air quality and climate change.

5.6 Importance of the study

In the urban regions majority of the nanoparticles emissions come from the transportation sectors. The major transportation sector is road transport. The roadside microenvironment is the regions where the transportation emissions are found in higher concentration compared to the ambient environment. This study measured the concentration in the roadside microenvironment for year includes all the seasons and emission conditions is one of the first study of its kind in the study region. The study region is one of the highly urbanised city in the south Asia. The outcomes of the study help to represent further such cities similar to the study area. The results provide a detailed study during peak hours, different emission scenarios, day time and night time concentrations, role of gaseous precursors and role of meteorological parameters in determining the nanoparticles concentration. The study also examines the exposure of the nanoparticle's particles and their deposition. This study is one of the comprehensive study about the different aspects and features of the nanoparticles in the urban roadside microenvironments.

- The outcomes will enhance the knowledge about the nanoparticles in the urban atmosphere which is one of the major areas to focus for attaining clean air goals
- The study outcome prove the role of engine exhaust emission in the urban regions
- The study provides information about the different size engine exhaust emission which can be further used for the reduction of the emissions at the source.
- The results of the study help to estimate the health impacts of the residents living near the vicinity of the road as well as the people working in the vicinity of the road such as police personals, street vendors, delivery partners, drivers.
- The secondary transformation of the particle can also be studied using the primary emissions.
- The insights of the study help in policy formulation for the number concentration as suggested by the WHO for detecting and reducing the nanoparticles emissions.

- The results of the study help the policy makers to develop the mitigation measures for source specific pollution which provides more efficiency of the control measures.

These are some of the major outcomes of the study which emphasise the importance of the study.

5.7 Scope of further study

The study on the atmospheric nanoparticles is one of the grey areas where majority of the information's are found missing due to limited studies paves way for more further studies in this direction.

- The fuel-based nanoparticles emission in the real-world driving conditions can be studied for different vehicles to estimate the nanoparticles concentration
- Different vehicles (Two wheelers, four-wheelers and heavy vehicles) based studies can be performed in future to know the emissions scenario.
- More further studies can be conducted during different hours of the day such as day and night time, peak and non-peak hours and weekdays and weekends.
- The other microenvironments in urban regions such as tunnels, airport zones, industrial areas are the major other environments which needs to be explored.
- The Indoor environments is another major area where the concentration of nanoparticles play a crucial role in human health.
- The source apportionment of atmospheric nanoparticles is another grey area which needs to be explored for identifying the different complex sources and their composition in the atmospheric nanoparticle concentration.
- Apart from model studies clinical epidemiological studies should be conducted to assess the exact particle deposition occurred in the respiratory system.

5.8 Summary

The discussions in this chapter concludes the different results obtained from the study which is designed based on the objectives. The sections also cover the importance of the study and also the future scopes of the study which can be conducted in the further studies.

REFERENCES

Aggarwal, S., Jain, R., and Marshall, J. D. (2012). Real-time prediction of size-resolved ultrafine particulate matter on freeways. Environ. Sci. Tech. 46, 2234–2241. https://doi.org/10.1021/es203290p.

Agudelo-Castañeda, D. M., Teixeira, E. C., Rolim, S. B. A., Pereira, F. N., and Wiegand, F. (2013). Measurement of particle number and related pollutant concentrations in an urban area in South Brazil. Atmos. Environ, 70, 254–262. https://doi.org/10.1016/j.atmosenv.2013.01.029.

Agudelo-Castañeda, D. M., Teixeira, E. C., Schneider, I. L., Pereira, F. N., Oliveira, M. L. S., Taffarel, S. R., Sehn, J. L., Ramos, C. G., and Silva, L. F. O. (2016). Potential utilization for the evaluation of particulate and gaseous pollutants at an urban site near a major highway. Sci. of Tot. Environ. 543, 161–170. https://doi.org/10.1016/j.scitotenv.2015.11.030.

Akteruzzaman, M., Rahman, M. A., Rabbi, F. M., Asharof, S., Rofi, M. M., Hasan, M. K., Muktadir Islam, M. A., Khan, M. A. R., Rahman, M. M., and Rahaman, M. H. (2023). The impacts of cooking and indoor air quality assessment in the southwestern region of Bangladesh. Heliyon, 9. e12852. https://doi.org/10.1016/j.heliyon.2023.e12852.

Al–Dabbous, A. N., Kumar, P., and Khan, A. R. (2017). Prediction of airborne nanoparticles at roadside location using a feed–forward artificial neural network. Atmos. Poll. Res., 8, 446–454. https://doi.org/10.1016/j.apr.2016.11.004.

Almeida, D. S. de, Martins, J. A., Vidotto, L. H. B., and Martins, L. D. (2015). Study of Potential Health Damage Caused by Ultrafine Particles in Megacities Using a Pulmonary Deposition Model. J. Geosci. and Environ. Prot. 03, 67–71. https://doi.org/10.4236/gep.2015.36011.

Argyropoulos, G., Samara, C., Voutsa, D., Kouras, A., Manoli, E., Voliotis, A., Tsakis, A., Chasapidis, L., Konstandopoulos, A., and Eleftheriadis, K. (2016). Concentration levels and source apportionment of ultrafine particles in road microenvironments. Atmos Environ. 129, 68–78. https://doi.org/10.1016/j.atmosenv.2016.01.009.

Arub, Z., Singh, G., Habib, G., and Raman, R.S (2021). Highly significant impact of mineral dust on aerosol hygroscopicity at New Delhi. Atmos. Environ. 254, 118375. https://doi.org/10.1016/j.atmosenv.2021.118375.

Asgharian, B., Hofmann, W., and Bergmann, R. (2001). Particle deposition in a multiple-path model of the human lung. Aero. Sci. Tech. 34, 332–339. https://doi.org/10.1080/02786820119122.

Asgharian, B., Price, O., Creel, A., Chesnutt, J., Schroeter, J., Fallica, J., Erives, G., Rasheed, N., and Chemerynski, S. (2022). Simulation modeling of air and droplet temperatures in the human respiratory tract for inhaled tobacco products. J. Aero. Sci. 166, 106050. https://doi.org/10.1016/j.jaerosci.2022.106050.

Audignon-Durand, S., Ramalho, O., Mandin, C., Roudil, A., Le Bihan, O., Delva, F., and Lacourt, A. (2023). Indoor exposure to ultrafine particles related to domestic activities: A systematic review and meta-analysis. Sci. Tot. Environ. 904, 166947. https://doi.org/10.1016/j.scitotenv.2023.166947.

Babu, S. S., Kompalli, S. K., and Moorthy, K. K. (2016). Aerosol number size distributions over a coastal semi urban location: Seasonal changes and ultrafine particle bursts. Sci. Tot. Environ. 563–564, 351–365. https://doi.org/10.1016/j.scitotenv.2016.03.246.

Badami, M. M., Tohidi, R., and Sioutas, C. (2024). Los Angeles Basin's air quality transformation: A long-term investigation on the impacts of PM regulations on the trends of ultrafine particles and co-pollutants. J. Aero. Sci. 176, 106316. https://doi.org/10.1016/j.jaerosci.2023.106316.

Baldauf, R. W., Heist, D., Isakov, V., Perry, S., Hagler, G. S. W., Kimbrough, S., Shores, R., Black, K., and Brixey, L. (2013). Air quality variability near a highway in a complex urban environment. Atmos. Environ. 64, 169–178. https://doi.org/10.1016/j.atmosenv.2012.09.054.

Banerjee, T., and Christian, R. A. (2018). A review on nanoparticle dispersion from vehicular exhaust: Assessment of Indian urban environment. Atmos. Poll. Res. 9, 342–357. https://doi.org/10.1016/j.apr.2017.10.009.

Baxla, S. P., Roy, A. A., Gupta, T., Tripathi, S. N., and Bandyopadhyaya, R. (2009). Analysis of diurnal and seasonal variation of submicron outdoor aerosol mass and size distribution in a northern indian city and its correlation to black carbon. Aero. Air. Qual. Res. 9, 458–469. https://doi.org/10.4209/aaqr.2009.03.0017.

Belkacem, I., Helali, A., Khardi, S., Chrouda, A., and Slimi, K. (2022). Road traffic nanoparticle characteristics: Sustainable environment and mobility. Geosci. Front. 13, 101196. https://doi.org/10.1016/j.gsf.2021.101196.

Belkacem, I., Khardi, S., Helali, A., Slimi, K., and Serindat, S. (2020). The influence of urban road traffic on nanoparticles: Roadside measurements. Atmos. Environ. 242, 117786. https://doi.org/10.1016/j.atmosenv.2020.117786.

Benka-Coker, M. L., Peel, J. L., Volckens, J., Good, N., Bilsback, K. R., L'Orange, C., Quinn, C., Young, B. N., Rajkumar, S., Wilson, A., Tryner, J., Africano, S., Osorto, A. B., and Clark, M. L. (2020). Kitchen concentrations of fine particulate matter and particle number concentration in households using biomass cookstoves in rural Honduras. Environ. Poll. 258, 11367. https://doi.org/10.1016/j.envpol.2019.113697.

Bergmann, M. L., Andersen, Z. J., Amini, H., Ellermann, T., Hertel, O., Lim, Y. H., Loft, S., Mehta, A., Westendorp, R. G., and Cole-Hunter, T. (2021). Exposure to ultrafine particles while walking or bicycling during COVID-19 closures: A repeated measures study in Copenhagen, Denmark. Sci. Tot. Environ. 791. 148301. https://doi.org/10.1016/j.scitotenv.2021.148301.

Bergmann, M. L., Andersen, Z. J., Amini, H., Khan, J., Lim, Y. H., Loft, S., Mehta, A., Westendorp, R. G., and Cole-Hunter, T. (2022). Ultrafine particle exposure for bicycle commutes in rush and non-rush hour traffic: A repeated measures study in Copenhagen, Denmark. Environ. Poll. 294, 118631. https://doi.org/10.1016/j.envpol.2021.118631.

Bhandari, S., Gani, S., Patel, K., Wang, D. S., Soni, P., Arub, Z., Habib, G., Apte, J. S., and Hildebrandt Ruiz, L. (2020). Sources and atmospheric dynamics of organic aerosol in New Delhi, India: Insights from receptor modeling. Atmos. Chem. Phys. 20, 735–752. https://doi.org/10.5194/acp-20-735-2020.

Bhardawaj, A., Habib, G., Kumar, A., Singh, S., and Nema, A. K. (2017). A Review of Ultrafine Particle-Related Pollution during Vehicular Motion, Health Effects and Control. J. Environ Sci. Pub. Health. 01, 268–288. https://doi.org/10.26502/jesph.96120024.

Blanco-Alegre, C., Calvo, A. I., Alonso-Blanco, E., Castro, A., Oduber, F., and Fraile, R. (2022). Evolution of size-segregated aerosol concentration in NW Spain: A two-step classification to identify new particle formation events. J. Environ. Manag. 304, 114232. https://doi.org/10.1016/j.jenvman.2021.114232.

Borsós, T., Řimnáčová, D., Ždímal, V., Smolík, J., Wagner, Z., Weidinger, T., Burkart, J., Steiner, G., Reischl, G., Hitzenberger, R., Schwarz, J., and Salma, I. (2012). Comparison of particulate number concentrations in three Central European capital cities. Sci. Tot. Environ. 433, 418–426. https://doi.org/10.1016/j.scitotenv.2012.06.052.

Bouma, F., Janssen, N. A., Wesseling, J., van Ratingen, S., Strak, M., Kerckhoffs, J., Gehring, U., Hendricx, W., de Hoogh, K., Vermeulen, R., and Hoek, G. (2023). Long-term exposure to ultrafine particles and natural and cause-specific mortality. Environ. Intl. 175, 107960. https://doi.org/10.1016/j.envint.2023.107960.

Bousiotis, D., Pope, F. D., Beddows, D. C. S., Dall'Osto, M., Massling, A., Nøjgaard, J. K., Nordstrøm, C., Niemi, J. V., Portin, H., Petäjä, T., Perez, N., Alastuey, A., Querol, X., Kouvarakis, G., Mihalopoulos, N., Vratolis, S., Eleftheriadis, K., Wiedensohler, A., Weinhold, K., … Harrison, R. M. (2021). A phenomenology of new particle formation (NPF) at 13 European sites. Atmos. Chem. Phys. 21, 11905–11925. https://doi.org/10.5194/acp-21-11905-2021.

Brines, M., Dall'Osto, M., Beddows, D. C. S., Harrison, R. M., Gómez-Moreno, F., Núñez, L., Artíñano, B., Costabile, F., Gobbi, G. P., Salimi, F., Morawska, L., Sioutas, C., and Querol, X. (2015). Traffic and nucleation events as main sources of ultrafine particles in high-insolation developed world cities. Atmos. Chem. Phys. 15, 5929–5945. https://doi.org/10.5194/acp-15-5929-2015.

Buonanno, G., Stabile, L., and Morawska, L. (2014). Personal exposure to ultrafine particles: The influence of time-activity patterns. Sci. Tot. Environ. 468–469, 903–907. https://doi.org/10.1016/j.scitotenv.2013.09.016.

Carnerero, C., Pérez, N., Reche, C., Ealo, M., Titos, G., Lee, H. K., Eun, H. R., Park, Y. H., Dada, L., Paasonen, P., Kerminen, V. M., Mantilla, E., Escudero, M., Gómez-Moreno, F. J., Alonso-Blanco, E., Coz, E., Saiz-Lopez, A., Temime-Roussel, B., Marchand, N., … Querol, X. (2018). Vertical and horizontal distribution of regional new particle formation events in Madrid. Atmos. Chem. Phys. 18, 16601–16618. https://doi.org/10.5194/acp-18-16601-2018.

Carpentieri, M., and Kumar, P. (2011). Ground-fixed and on-board measurements of nanoparticles in the wake of a moving vehicle. Atmos. Environ. 45, 5837–5852. https://doi.org/10.1016/j.atmosenv.2011.06.079.

Carslaw, D. C., and Ropkins, K. (2012). Open air - An r package for air quality data analysis. Environ. Mode. and Soft. 27–28, 52–61. https://doi.org/10.1016/j.envsoft.2011.09.008.

Casquero-Vera, J. A., Lyamani, H., Titos, G., Moreira, G. de A., Benavent-Oltra, J. A., Conte, M., Contini, D., Järvi, L., Olmo-Reyes, F. J., and Alados-Arboledas, L. (2022). Aerosol number fluxes and concentrations over a southern European urban area. Atmos. Environ. 269, 118849. https://doi.org/10.1016/j.atmosenv.2021.118849.

Chen, C., Liu, S., Dong, W., Song, Y., Chu, M., Xu, J., Guo, X., Zhao, B., and Deng, F. (2021). Increasing cardiopulmonary effects of ultrafine particles at relatively low fine particle concentrations. Sci. Tot. Environ. 751, 141726. https://doi.org/10.1016/j.scitotenv.2020.141726.

Chen, C., Yao, M., Luo, X., Zhu, Y., Liu, Z., Zhuo, H., and Zhao, B. (2020). Outdoor-to-indoor transport of ultrafine particles: Measurement and model development of infiltration factor. Environ. Poll. 267, 115402. https://doi.org/10.1016/j.envpol.2020.115402.

Cheng, Y. H., Liu, Z. S., and Chen, C. C. (2010). On-road measurements of ultrafine particle concentration profiles and their size distributions inside the longest highway

tunnel in Southeast Asia. Atmos. Environ. 44, 763–772. https://doi.org/10.1016/j.atmosenv.2009.11.040.

Cheng, Y., Yan, L., Huang, Y., Wang, Q., Morawska, L., Zhaolin, G., Cao, J., Zhang, L., Li, B., and Wang, Y. (2019). Characterization of particle size distributions during winter haze episodes in urban air. Atmos. Res. 228, 55–67. https://doi.org/10.1016/j.atmosres.2019.04.033.

Chen, S. C., Tsai, C. J., Chou, C. C. K., Roam, G. D., Cheng, S. S., and Wang, Y. N. (2010). Ultrafine particles at three different sampling locations in Taiwan. Atmos. Environ. 44, 533–540. https://doi.org/10.1016/j.atmosenv.2009.10.044.

Chen, T. L., Hsiao, T. C., Chen, A. Y., Chang, K. E., Lin, T. C., Griffith, S. M., and Chou, C. C. K. (2024). A traffic-induced shift of ultrafine particle sources under COVID-19 soft lockdown in a subtropical urban area. Environ Intl, 187, 108658. https://doi.org/10.1016/j.envint.2024.108658.

Chen, Y., Fei, J., Sun, Z., Shen, G., Du, W., Zang, L., Yang, L., Wang, Y., Wu, R., Chen, A., and Zhao, M. (2020). Household air pollution from cooking and heating and its impacts on blood pressure in residents living in rural cave dwellings in Loess Plateau of China. Environ. Sci. Poll. Res. 27, 36677–36687. https://doi.org/10.1007/s11356-020-09677-1.

Chen, Y., Masiol, M., Squizzato, S., Chalupa, D. C., Zíková, N., Pokorná, P., Rich, D. Q., and Hopke, P. K. (2022). Long-term trends of ultrafine and fine particle number concentrations in New York State: Apportioning between emissions and dispersion. Environ. Poll. 310, 119797. https://doi.org/10.1016/j.envpol.2022.119797.

Cheung, H. C., Chou, C. C. K., Chen, M. J., Huang, W. R., Huang, S. H., Tsai, C. Y., and Lee, C. S. L. (2016). Seasonal variations of ultra-fine and submicron aerosols in Taipei, Taiwan: Implications for particle formation processes in a subtropical urban area. Atmos. Chem. Phys. 16, 1317–1330. https://doi.org/10.5194/acp-16-1317-2016.

Cheung, H. C., and Chou, C. K. (2013). Characterization of ultrafine particle number concentration and new particle formation in an urban environment of Taipei, Taiwan. Atmos. Chem. Phys. 13, 8935–8946. https://doi.org/10.5194/acp-13-8935-2013.

Cheung, H. C., Morawska, L., and Ristovski, Z. D. (2010). Observation of new particle formation in subtropical urban environment. Atmos. Chem. Phys. Discuss, 10, 22623–22652. https://doi.org/10.5194/acpd-10-22623-2010.

Chhabra, A., Turakhia, T., Sharma, S., Saha, S., Iyer, R., and Chauhan, P. (2020). Environmental impacts of fireworks on aerosol characteristics and radiative properties over a mega city, India. City Environ. Interact. 7, 100049. https://doi.org/10.1016/j.cacint.2020.100049.

Cong, X. C., Qu, J. H., and Yang, G. S. (2017). On-road measurements of pollutant concentration profiles inside Yangkou tunnel, Qingdao, China. Environ. Geochem. Health. 39, 1179–1190. https://doi.org/10.1007/s10653-016-9885-2.

Conte, M., Dinoi, A., Grasso, F. M., Merico, E., Guascito, M. R., and Contini, D. (2023). Concentration and size distribution of atmospheric particles in southern Italy during COVID-19 lockdown period. Atmos. Environ. 295, 119559. https://doi.org/10.1016/j.atmosenv.2022.119559.

Cusack, M., Pérez, N., Pey, J., Wiedensohler, A., Alastuey, A., and Querol, X. (2013). Variability of sub-micrometer particle number size distributions and concentrations in the Western Mediterranean regional background. Tellus, Series B: Chem. Phys. Met. 65, 19243. https://doi.org/10.3402/tellusb.v65i0.19243.

Dahari, N., Muda, K., Latif, M. T., Dominick, D., Hussein, N., and Khan, M. F. (2022). Seasonal variations of particle number concentration and its relationship with PM2.5 mass concentration in industrial-residential airshed. Environ. Geochem. Health. 44, 3377–3393. https://doi.org/10.1007/s10653-021-01099-3.

Dall'Osto, M., Querol, X., Alastuey, A., O'Dowd, C., Harrison, R. M., Wenger, J., and Gómez-Moreno, F. J. (2013). On the spatial distribution and evolution of ultrafine particles in Barcelona. Atmos. Chem. Phys. 13, 741–759. https://doi.org/10.5194/acp-13-741-2013.

Das, A., Baig, N. A., Yawar, M., Kumar, A., Habib, G., and Perumal, V. (2023). Size fraction of hazardous particulate matter governing the respiratory deposition and

inhalation risk in the highly polluted city Delhi. Environ. Sci. Poll. Res. 30, 11600–11616. https://doi.org/10.1007/s11356-022-22733-2.

Das, A., Kumar, A., Habib, G., and Vivekanandan, P. (2021). Insights on the biological role of ultrafine particles of size PM<0.25: A prospective study from New Delhi. Environ. Poll. 268, 115638. https://doi.org/10.1016/j.envpol.2020.115638.

Dasappa, S., and Camacho, J. (2021). Ultrafine Particulate Matter in Methane-Air Premixed Flames with Oxygen Enrichment. Front. Mech. Engi. 7, 739914 https://doi.org/10.3389/fmech.2021.739914.

Datta, A., Suresh, R., Gupta, A., Singh, D., and Kulshrestha, P. (2017). Indoor air quality of non-residential urban buildings in Delhi, India. Int. J. Sust. Buil. Environ. 6, 412–420. https://doi.org/10.1016/j.ijsbe.2017.07.005.

Davulienė, L., Khan, A., Šemčuk, S., Minderytė, A., Davtalab, M., Kandrotaitė, K., Dudoitis, V., Uogintė, I., Skapas, M., and Byčenkienė, S. (2022). Evaluation of Work-Related Personal Exposure to Aerosol Particles. Toxics. 10, 405. https://doi.org/10.3390/toxics10070405.

De Jesus, A. L., Rahman, M. M., Mazaheri, M., Thompson, H., Knibbs, L. D., Jeong, C., Evans, G., Nei, W., Ding, A., Qiao, L., Li, L., Portin, H., Niemi, J. V., Timonen, H., Luoma, K., Petäjä, T., Kulmala, M., Kowalski, M., Peters, A., … Morawska, L. (2019). Ultrafine particles and PM2.5 in the air of cities around the world: Are they representative of each other? Environ. Int. 129, 118–135. https://doi.org/10.1016/j.envint.2019.05.02.

Delapena, S., Piedrahita, R., Pillarisetti, A., Garland, C., Rossanese, M. E., Johnson, M., and Pennise, D. (2018). Using personal exposure measurements of particulate matter to estimate health impacts associated with cooking in peri-urban Accra, Ghana. Energy. Sust. Devel. 45, 190–197. https://doi.org/10.1016/j.esd.2018.05.013.

De Nazelle, A., Bode, O., and Orjuela, J. P. (2017). Comparison of air pollution exposures in active vs. passive travel modes in European cities: A quantitative review. Environ. Int. 99, 151–160. https://doi.org/10.1016/j.envint.2016.12.023.

Deng, C., Fu, Y., Dada, L., Yan, C., Cai, R., Yang, D., Zhou, Y., Yin, R., Lu, Y., Li, X., Qiao, X., Fan, X., Nie, W., Kontkanen, J., Kangasluoma, J., Chu, B., Ding, A., Kerminen, V. M., Paasonen, P., … Jiang, J. (2020). Seasonal characteristics of new particle formation and growth in urban Beijing. Environ. Sci. Tech. 54, 8547–8557. https://doi.org/10.1021/acs.est.0c00808.

Deng, C., Li, Y., Yan, C., Wu, J., Cai, R., Wang, D., Liu, Y., Kangasluoma, J., Kerminen, V. M., Kulmala, M., and Jiang, J. (2022). Measurement report: Size distributions of urban aerosols down to 1 nm from long-term measurements. Atmos. Chem. Phys. 22, 13569–13580. https://doi.org/10.5194/acp-22-13569-2022.

Deng, Q., Deng, L., Miao, Y., Guo, X., and Li, Y. (2019). Particle deposition in the human lung: Health implications of particulate matter from different sources. Environ. Res. 169, 237–245. https://doi.org/10.1016/j.envres.2018.11.014.

Dinoi, A., Gulli, D., Weinhold, K., Ammoscato, I., Calidonna, C. R., Wiedensohler, A., and Contini, D. (2023). Characterization of ultrafine particles and the occurrence of new particle formation events in an urban and coastal site of the Mediterranean area. Atmos. Chem. Phys. 23, 2167–2181. https://doi.org/10.5194/acp-23-2167-2023.

Dinoi, A., Weinhold, K., Wiedensohler, A., and Contini, D. (2021). Study of new particle formation events in southern Italy. Atmos. Environ. 244, 117920. https://doi.org/10.1016/j.atmosenv.2020.117920.

Donateo, A., Dinoi, A., and Pappaccogli, G. (2021). Impact on ultrafine particles concentration and turbulent fluxes of sars-cov-2 lockdown in a suburban area in italy. Atmos. 12, 12030407. https://doi.org/10.3390/atmos12030407.

Dröge, J., Klingelhöfer, D., Braun, M., and Groneberg, D. A. (2024). Influence of a large commercial airport on the ultrafine particle number concentration in a distant residential area under different wind conditions and the impact of the COVID-19 pandemic. Environ. Poll. 345, 123390. https://doi.org/10.1016/j.envpol.2024.123390.

Dumka, U. C., Kaskaoutis, D. G., Tiwari, S., Safai, P. D., Attri, S. D., Soni, V. K., Singh, N., and Mihalopoulos, N. (2018). Assessment of biomass burning and fossil

fuel contribution to black carbon concentrations in Delhi during winter. Atmos. Environ. 194, 93–109. https://doi.org/10.1016/j.atmosenv.2018.09.03.

Estévez-García, J. A., Schilmann, A., Riojas-Rodríguez, H., Berrueta, V., Blanco, S., Villaseñor-Lozano, C. G., Flores-Ramírez, R., Cortez-Lugo, M., and Pérez-Padilla, R. (2020). Women exposure to household air pollution after an improved cookstove program in rural San Luis Potosi, Mexico. Sci. Tot. Environ. 702,134456. https://doi.org/10.1016/j.scitotenv.2019.134456.

Ezz, W. N., Mazaheri, M., Robinson, P., Johnson, G. R., Clifford, S., He, C., Morawska, L., and Marks, G. B. (2015). Ultrafine particles from traffic emissions and children's health (UPTECH) in Brisbane, Queensland (Australia): Study design and implementation. Int. J. Environ. Res. Pub. Health. 12, 1687–1702. https://doi.org/10.3390/ijerph120201687.

Fangqun, Y. U. (2010). Diurnal and seasonal variations of ultrafine particle formation in anthropogenic SO_2 plumes. Environ. Sci. Tech. 44, 2011–2015. https://doi.org/10.1021/es903228a.

Farmer, D. K., Vance, M. E., Abbatt, J. P. D., Abeleira, A., Alves, M. R., Arata, C., Boedicker, E., Bourne, S., Cardoso-Saldaña, F., Corsi, R., Decarlo, P. F., Goldstein, A. H., Grassian, V. H., Hildebrandt Ruiz, L., Jimenez, J. L., Kahan, T. F., Katz, E. F., Mattila, J. M., Nazaroff, W. W., … Zhou, Y. (2019). Overview of HOMEChem: House Observations of Microbial and Environmental Chemistry. Environ. Sci.: Proc. Imp. 21, 1280–1300). https://doi.org/10.1039/c9em00228f.

Farrell, W., Weichenthal, S., Goldberg, M., Valois, M. F., Shekarrizfard, M., and Hatzopoulou, M. (2016). Near roadway air pollution across a spatially extensive road and cycling network. Environ. Poll. 212, 498–507. https://doi.org/10.1016/j.envpol.2016.02.041.

Fatima, S., Ahlawat, A., Mishra, S. K., Soni, V. K., and Guleria, R. (2022). Respiratory Deposition Dose of PM2.5 and PM10 Before, During and After COVID-19 Lockdown Phases in Megacity-Delhi, India. Mapan – J. Met. Soc. India. 37, 891–900. https://doi.org/10.1007/s12647-022-00548-3.

Fawzy, A., Woo, H., Raju, S., Belz, D. C., Putcha, N., Williams, M. S., McCormack, M. C., Kohler, K., and Hansel, N. N. (2024). Indoor particulate matter concentrations and air cleaner intervention association with biomarkers in former smokers with COPD. Environ. Res. 243, 117874. https://doi.org/10.1016/j.envres.2023.117874.

Fujitani, Y., Takahashi, K., Fushimi, A., Hasegawa, S., Kondo, Y., Tanabe, K., and Kobayashi, S. (2020). Particle number emission factors from diesel trucks at a traffic intersection: Long-term trend and relation to particle mass-based emission regulation. Atmos. Environ.: X, 5, 100055. https://doi.org/10.1016/j.aeaoa.2019.100055.

Fuller, C. H., Brugge, D., Williams, P. L., Mittleman, M. A., Durant, J. L., and Spengler, J. D. (2012). Estimation of ultrafine particle concentrations at near-highway residences using data from local and central monitors. Atmos. Environ. 57, 257–265. https://doi.org/10.1016/j.atmosenv.2012.04.004.

Fuller, R., Landrigan, P. J., Balakrishnan, K., Bathan, G., Bose-O'Reilly, S., Brauer, M., Caravanos, J., Chiles, T., Cohen, A., Corra, L., Cropper, M., Ferraro, G., Hanna, J., Hanrahan, D., Hu, H., Hunter, D., Janata, G., Kupka, R., Lanphear, B., … Yan, C. (2022). Pollution and health: a progress update. Lancet. Plan. Health. 6, e535–e547. https://doi.org/10.1016/S2542-5196(22)00090-0.

Gabdrashova, R., Nurzhan, S., Naseri, M., Bekezhankyzy, Z., Gimnkhan, A., Malekipirbazari, M., Tabesh, M., Khanbabaie, R., Crape, B., Buonanno, G., Hopke, P. K., Amouei Torkmahalleh, A., and Amouei Torkmahalleh, M. (2021). The impact on heart rate and blood pressure following exposure to ultrafine particles from cooking using an electric stove. Sci. Tot. Environ. 750, 141334. https://doi.org/10.1016/j.scitotenv.2020.141334.

Gani, S., Bhandari, S., Patel, K., Seraj, S., Soni, P., Arub, Z., Habib, G., Hildebrandt Ruiz, L., and Apte, J. S. (2020). Particle number concentrations and size distribution in a polluted megacity: The Delhi Aerosol Supersite study. Atmos. Chem. Phys. 20, 8533–8549. https://doi.org/10.5194/acp-20-8533-2020.

Gani, S., Chambliss, S. E., Messier, K. P., Lunden, M. M., and Apte, J. S. (2021). Spatiotemporal profiles of ultrafine particles differ from other traffic-related air

pollutants: Lessons from long-term measurements at fixed sites and mobile monitoring. Environmental Science: Atmos. 1, 558–568. https://doi.org/10.1039/d1ea00058f.

Garcia-Marlès, M., Lara, R., Reche, C., Pérez, N., Tobías, A., Savadkoohi, M., Beddows, D., Salma, I., Vörösmarty, M., Weidinger, T., Hueglin, C., Mihalopoulos, N., Grivas, G., Kalkavouras, P., Ondráček, J., Zíková, N., Niemi, J. V., Manninen, H. E., Green, D. C., … Querol, X. (2024). Inter-annual trends of ultrafine particles in urban Europe. Environ. Int. 185, 108510. https://doi.org/10.1016/j.envint.2024.108510.

Gerling, L., Löschau, G., Wiedensohler, A., and Weber, S. (2020). Statistical modelling of roadside and urban background ultrafine and accumulation mode particle number concentrations using generalized additive models. Sci. Tot. Environ. 703,134570. https://doi.org/10.1016/j.scitotenv.2019.134570.

Gerling, L., and Weber, S. (2022). Atmospheric transformation of urban particle number size distributions during the transport along street canyons as quantified by an aerosol sectional model. Atmos. Poll. Res. 13,101296. https://doi.org/10.1016/j.apr.2021.101296.

Ghei, D., and Sane, R. (2018). Estimates of air pollution in Delhi from the burning of firecrackers during the festival of Diwali. PLoS One. 13, e0205131. https://doi.org/10.1371/journal.pone.020037.

Giemsa, E., Soentgen, J., Kusch, T., Beck, C., Münkel, C., Cyrys, J., and Pitz, M. (2021). Influence of Local Sources and Meteorological Parameters on the Spatial and Temporal Distribution of Ultrafine Particles in Augsburg, Germany. Front. Environ. Sci. 8,609846. https://doi.org/10.3389/fenvs.2020.609846.

Goel, A., and Kumar, P. (2014). A review of fundamental drivers governing the emissions, dispersion and exposure to vehicle-emitted nanoparticles at signalised traffic intersections. Atmos. Environ. 97,316–331. https://doi.org/10.1016/j.atmosenv.2014.08.037.

Goel, A., and Kumar, P. (2015). Characterisation of nanoparticle emissions and exposure at traffic intersections through fast-response mobile and sequential measurements. Atmos Environ, 107, 374–390. https://doi.org/10.1016/j.atmosenv.2015.02.002.

Goel, A., and Kumar, P. (2016). Vertical and horizontal variability in airborne nanoparticles and their exposure around signalised traffic intersections. Environ. Poll. 214, 54–69. https://doi.org/10.1016/j.envpol.2016.03.033.

Gómez-Moreno, F. J., Pujadas, M., Plaza, J., Rodríguez-Maroto, J. J., Martínez-Lozano, P., and Artíñano, B. (2011). Influence of seasonal factors on the atmospheric particle number concentration and size distribution in Madrid. Atmos. Environ. 45, 3169–3180. https://doi.org/10.1016/j.atmosenv.2011.02.04.

Gordon, M., Staebler, R. M., Liggio, J., Li, S. M., Wentzell, J., Lu, G., Lee, P., and Brook, J. R. (2012). Measured and modeled variation in pollutant concentration near roadways. Atmos Environ. 57, 138–145. https://doi.org/10.1016/j.atmosenv.2012.04.022.

Gould, C. F., Schlesinger, S. B., Molina, E., Lorena Bejarano, M., Valarezo, A., and Jack, D. W. (2020). Long-standing LPG subsidies, cooking fuel stacking, and personal exposure to air pollution in rural and peri-urban Ecuador. J. Exp. Sci. Environ. Epid. 30, 707–720. https://doi.org/10.1038/s41370-020-0231-5.

Guo, L., Salimi, F., Wang, H., Hofmann, W., Johnson, G. R., Toelle, B. G., Marks, G. B., and Morawska, L. (2020). Experimentally determined deposition of ambient urban ultrafine particles in the respiratory tract of children. Environ Int. 145,106094. https://doi.org/10.1016/j.envint.2020.106094.

Hagler, G. S. W., Thoma, E. D., and Baldauf, R. W. (2010). High-resolution mobile monitoring of carbon monoxide and ultrafine particle concentrations in a near-road environment. J. Air. Wast. Manag. Asso. 60, 328–336. https://doi.org/10.3155/1047-3289.60.3.328.

Harrison, R. M., Beddows, D. C. S., Alam, M. S., Singh, A., Brean, J., Xu, R., Kotthaus, S., and Grimmond, S. (2019). Interpretation of particle number size

distributions measured across an urban area during the FASTER campaign. Atmos. Chem. Phys. 19, 39–55. https://doi.org/10.5194/acp-19-39-2019.

Harrison, R. M., Rob Mackenzie, A., Xu, H., Alam, M. S., Nikolova, I., Zhong, J., Singh, A., Zeraati-Rezaei, S., Stark, C., Beddows, D. C. S., Liang, Z., Xu, R., and Cai, X. (2018). Diesel exhaust nanoparticles and their behaviour in the atmosphere. Proceedings of the Roy. Soc. A: Math. Phys. Engi. Sci. 474,2220. https://doi.org/10.1098/rspa.2018.0492.

Herr, D., Jew, K., Wong, C., Kennell, A., Gelein, R., Chalupa, D., Raab, A., Oberdörster, G., Olschowka, J., O'Banion, M. K., and Elder, A. (2021). Effects of concentrated ambient ultrafine particulate matter on hallmarks of Alzheimer's disease in the 3xTgAD mouse model. Neu.Tox. 84, 172–183. https://doi.org/10.1016/j.neuro.2021.03.010.

Hillemann, L., Zschoppe, A., Caldow, R., Sem, G. J., and Wiedensohler, A. (2014). An ultrafine particle monitor for size-resolved number concentration measurements in atmospheric aerosols. J. Aero. Sci. 68, 14–24. https://doi.org/10.1016/j.jaerosci.2013.10.007.

Hopke, P. K., Feng, Y., and Dai, Q. (2022). Source apportionment of particle number concentrations: A global review. Sci. Tot. Environ. 819.153104. https://doi.org/10.1016/j.scitotenv.2022.153104.

Hoyos, C. D., Herrera-Mejía, L., Roldán-Henao, N., and Isaza, A. (2020). Effects of fireworks on particulate matter concentration in a narrow valley: the case of the Medellín metropolitan area. Environ. Mon. Asses. 192,6 https://doi.org/10.1007/s10661-019-7838-9.

Hudda, N., Eckel, S. P., Knibbs, L. D., Sioutas, C., Delfino, R. J., and Fruin, S. A. (2012). Linking in-vehicle ultrafine particle exposures to on-road concentrations. Atmos. Environ. 59, 578–586. https://doi.org/10.1016/j.atmosenv.2012.05.02.

Hussein, T., Al-Abdallat, A., Saleh, S. S. A., and Al-Kloub, M. (2022). Estimation of the Seasonal Inhaled Deposited Dose of Particulate Matter in the Respiratory System

of Urban Individuals Living in an Eastern Mediterranean City. Int. J. Environ. Res. Pub. Health. 19,4303. https://doi.org/10.3390/ijerph19074303.

Hussein, T., Dada, L., Hakala, S., Petäjä, T., and Kulmala, M. (2019). Urban aerosol particle size characterization in Eastern Mediterranean Conditions. Atmos. 10, 110710. https://doi.org/10.3390/atmos10110710.

Hu, W., Hu, M., Hu, W. W., Zheng, J., Chen, C., Wu, Y., and Guo, S. (2017). Seasonal variations in high time-resolved chemical compositions, sources, and evolution of atmospheric submicron aerosols in the megacity Beijing. Atmos. Chem. Phys. 17, 9979–10000. https://doi.org/10.5194/acp-17-9979-2017.

Hwan Kim, K., Woo, D., Lee, S. B., and Bae, G. N. (2015). On-road measurements of ultrafine particles and associated air pollutants in a densely populated area of Seoul, Korea. Aero. Air Qual. Res. 15, 142–153. https://doi.org/10.4209/aaqr.2014.01.0014.

Izhar, S., Rajput, P., and Gupta, T. (2018). Variation of particle number and mass concentration and associated mass deposition during Diwali festival. Urban Clim. 24, 1027–1036. https://doi.org/10.1016/j.uclim.2017.12.005.

Jayaratne, E. R., Ling, X., and Morawska, L. (2015). Comparison of charged nanoparticle concentrations near busy roads and overhead high-voltage power lines. Sci. Tot. Environ. 526, 14–18. https://doi.org/10.1016/j.scitotenv.2015.04.074.

Jbaily, A., Zhou, X., Liu, J., Lee, T. H., Kamareddine, L., Verguet, S., and Dominici, F. (2022). Air pollution exposure disparities across US population and income groups. Nat. 601, 228–233. https://doi.org/10.1038/s41586-021-04190-y.

Jeong, S. G., Wallace, L., and Rim, D. (2021). Contributions of Coagulation, Deposition, and Ventilation to the Removal of Airborne Nanoparticles in Indoor Environments. Environ. Sci. Tech. 55, 9730–9739. https://doi.org/10.1021/acs.est.0c08739.

Jeong, S. G., Wallace, L., and Rim, D. (2023). Size-resolved emission rates of episodic indoor sources and ultrafine particle dynamics. Environ. Poll. 338, 122680. https://doi.org/10.1016/j.envpol.2023.122680.

Jianhua, Y. U., Guinot, B., Tong, Y. U., Wang, X., and Wenqing, L. (2005). Seasonal Variations of Number Size Distributions and Mass Concentrations of Atmospheric Particles in Beijing. Adv. Atmos. Sci. 22,401,407. https://doi.org/10.1007/BF02918753.

Joerger, V. M., and Pryor, S. C. (2018). Ultrafine particle number concentrations and size distributions around an elevated highway viaduct. Atmos. Poll. Res. 9, 714–722. https://doi.org/10.1016/j.apr.2018.01.008.

Joodatnia, P., Kumar, P., and Robins, A. (2013). The behaviour of traffic produced nanoparticles in a car cabin and resulting exposure rates. Atmos. Environ. 65, 40–51. https://doi.org/10.1016/j.atmosenv.2012.10.025.

Jose, S., Mishra, A. K., Lodhi, N. K., Sharma, S. K., and Singh, S. (2021). Characteristics of Aerosol Size Distributions and New Particle Formation Events at Delhi: An Urban Location in the Indo-Gangetic Plains. Front. Ear. Sci. 9,750111. https://doi.org/10.3389/feart.2021.750111.

Joshi, M., Khan, A., Anand, S., and Sapra, B. K. (2016). Size evolution of ultrafine particles: Differential signatures of normal and episodic events. Environ. Poll. 208, 354–360. https://doi.org/10.1016/j.envpol.2015.10.00.

Junkermann, W., and Hacker, J. (2022). Unprecedented levels of ultrafine particles, major sources, and the hydrological cycle. Sci. Report. 12, 7410. https://doi.org/10.1038/s41598-022-11500-5.

Kalaiarasan, G., Kumar, P., Tomson, M., Zavala-Reyes, J. C., Porter, A. E., Young, G., Sephton, M. A., Abubakar-Waziri, H., Pain, C. C., Adcock, I. M., Mumby, S., Dilliway, C., Fang, F., Arcucci, R., and Chung, K. F. (2024). Particle Number Size Distribution in Three Different Microenvironments of London. Atmos. 15,15010045. https://doi.org/10.3390/atmos15010045.

Kanawade, V. P., Sebastian, M., Hooda, R. K., and Hyvärinen, A. P. (2022). Atmospheric new particle formation in India: Current understanding and knowledge gaps. Atmos. Environ. 270,118894. https://doi.org/10.1016/j.atmosenv.2021.118894.

Kanawade, V. P., Tripathi, S. N., Bhattu, D., and Shamjad, P. M. (2014). Sub-micron particle number size distributions characteristics at an urban location, Kanpur, in the Indo-Gangetic Plain. Atmos. Res. 147–148, 121–132. https://doi.org/10.1016/j.atmosres.2014.05.010.

Kang, K., Kim, T., and Kim, D. D. (2023). An Investigation of Concentration and Health Impacts of Aldehydes Associated with Cooking in 29 Residential Buildings. Ind. Air, 2463386. https://doi.org/10.1155/2023/2463386.

Kearney, J., Wallace, L., MacNeill, M., Xu, X., Vanryswyk, K., You, H., Kulka, R., and Wheeler, A. J. (2011). Residential indoor and outdoor ultrafine particles in Windsor, Ontario. Atmos. Environ. 45, 7583–7593. https://doi.org/10.1016/j.atmosenv.2010.11.002.

Kerminen, V. M., Chen, X., Vakkari, V., Petäjä, T., Kulmala, M., and Bianchi, F. (2018). Atmospheric new particle formation and growth: Review of field observations. Environ. Res. Let. 13, 103003. https://doi.org/10.1088/1748-9326/aadf3c.

Kesarkar, A. P., Dalvi, M., Kaginalkar, A., and Ojha, A. (2007). Coupling of the Weather Research and Forecasting Model with AERMOD for pollutant dispersion modeling. A case study for PM10 dispersion over Pune, India. Atmos. Environ. 41, 1976–1988. https://doi.org/10.1016/j.atmosenv.2006.10.042.

Khan, S., Gurjar, B. R., and Sahu, V. (2022). Deposition modeling of ambient particulate matter in the human respiratory tract. Atmos. Poll. Res. 13,101565. https://doi.org/10.1016/j.apr.2022.101565.

Klemm, O., Ahrens, A., Arnswald, M., Bethke, R., Berger, D. F., Blankenhaus, K., Blauth, L., Breuer, B., Buchholz, S., Burek, F., Ehrnsperger, L., Funken, S., Henninger, E., Hohl, J., Jöllenbeck, N., Kirgasser, P., Kuhls, M., Paas, B., Roters, L. A., … Schlüter, H. (2022). The Impact of Traffic and Meteorology on Urban Particle Mass and Particle Number Concentrations: Student-Led Studies Using Mobile Measurements before, during, and after the COVID-19 Pandemic Lockdowns. Atmos. 13, 62. https://doi.org/10.3390/atmos13010062.

Kontkanen, J., Deng, C., Fu, Y., Dada, L., Zhou, Y., Cai, J., Daellenbach, K. R., Hakala, S., Kokkonen, T. V., Lin, Z., Liu, Y., Wang, Y., Yan, C., Petäjä, T., Jiang, J., Kulmala, M., and Paasonen, P. (2020). Size-resolved particle number emissions in Beijing determined from measured particle size distributions. Atmos. Chem. Phys. 20, 11329–11348. https://doi.org/10.5194/acp-20-11329-2020.

Kota, M., Fankam, S. H., Cao, B. T., Desouza, S.-J., El-Gendy, P., Gurjar, A., Larrahondo, B. R., Hama, J. S., Kakosimos, S., Morawska, K., Muula, L., and Wu, A. S. (2022). Mitigating exposure to cooking emissions in kitchens of low-middle income homes: A guide for home occupants, owners, builders and local councils. to cooking emissions in kitchens of low-middle income homes: A guide for home occupants, owners, builders and local councils. Univ surr. https://doi.org/10.15126/900568.

Kulmala, M., Dada, L., Daellenbach, K. R., Yan, C., Stolzenburg, D., Kontkanen, J., Ezhova, E., Hakala, S., Tuovinen, S., Kokkonen, T. V., Kurppa, M., Cai, R., Zhou, Y., Yin, R., Baalbaki, R., Chan, T., Chu, B., Deng, C., Fu, Y., … Kerminen, V. M. (2021). Is reducing new particle formation a plausible solution to mitigate particulate air pollution in Beijing and other Chinese megacities? Fara. Disc. 226, 334–347. https://doi.org/10.1039/d0fd00078g.

Kulshreshtha, P., and Khare, M. (2010). A comparative study of indoor air pollution and its respiratory impacts in Delhi, India. WIT Tran. Eco. Environ. 136, 287–296. https://doi.org/10.2495/AIR100251.

Kulshreshtha, P., and Khare, M. (2011). Indoor exploratory analysis of gaseous pollutants and respirable particulate matter at residential homes of Delhi, India. Atmos. Poll. Res. 2, 337–350. https://doi.org/10.5094/APR.2011.038.

Kulshreshtha, P., Khare, M., and Seetharaman, P. (2008). Indoor air quality assessment in and around urban slums of Delhi city, India. Indo. Air, 18, 488–498. https://doi.org/10.1111/j.1600-0668.2008.00550.x.

Kulshrestha, A., Satsangi, P. G., Masih, J., and Taneja, A. (2009). Metal concentration of PM2.5 and PM10 particles and seasonal variations in urban and rural environment

of Agra, India. Sci. Tot. Environ. 407, 6196–6204. https://doi.org/10.1016/j.scitotenv.2009.08.050.

Kumar Kompalli, S., Suresh Babu, S., Krishna Moorthy, K., M Gogoi, M., S Nair, V., and Prakash Chaubey, J. (2014). The formation and growth of ultrafine particles in two contrasting environments: A case study. Ann. Geophys., 32, 817–830. https://doi.org/10.5194/angeo-32-817-2014.

Kumar, P., Fennell, P., and Britter, R. (2008a). Effect of wind direction and speed on the dispersion of nucleation and accumulation mode particles in an urban street canyon. Sci. Tot. Environ. 402, 82–94. https://doi.org/10.1016/j.scitotenv.2008.04.032.

Kumar, P., Fennell, P., and Britter, R. (2008b). Measurements of particles in the 5-1000 nm range close to road level in an urban street canyon. Sci. Tot. Environ. 390, 437–447. https://doi.org/10.1016/j.scitotenv.2007.10.013.

Kumar, P., and Gupta, N. C. (2013a). Assessment of Particle Number Concentration in Different Transportation Modes along a route in Delhi. Int. J. Curr. Engi. Tech. http://inpressco.com/category/ijcet.

Kumar, P., and Gupta, N. C. (2013b). Assessment of Particle Number Concentration in Different Transportation Modes along a route in Delhi. 3,1. http://inpressco.com/category/ijcet.

Kumar, P., Gurjar, B. R., Nagpure, A. S., and Harrison, R. M. (2011). Preliminary estimates of nanoparticle number emissions from road vehicles in megacity Delhi and associated health impacts. Environ. Sci. Tech. 45, 5514–5521. https://doi.org/10.1021/es2003183.

Kumar, P., Hama, S., Abbass, R. A., Nogueira, T., Brand, V. S., Wu, H. W., Abulude, F. O., Adelodun, A. A., Anand, P., Andrade, M. de F., Apondo, W., Asfaw, A., Aziz, K. H., Cao, S. J., El-Gendy, A., Indu, G., Kehbila, A. G., Ketzel, M., Khare, M., … Nagendra, S. M. S (2022). In-kitchen aerosol exposure in twelve cities across the globe. Environ. Int. 162,107155. https://doi.org/10.1016/j.envint.2022.107155.

Kumar, P., Kumar, A., and Lead, J. R. (2012). Nanoparticles in the Indian environment: Known, unknowns and awareness. Environ. Sci. Tech. 46, 7071–7072. https://doi.org/10.1021/es302308h.

Kumar, P., Morawska, L., Birmili, W., Paasonen, P., Hu, M., Kulmala, M., Harrison, R. M., Norford, L., and Britter, R. (2014). Ultrafine particles in cities. Environ. Int. 66, 1–10 https://doi.org/10.1016/j.envint.2014.01.013.

Kumar, P., Pirjola, L., Ketzel, M., and Harrison, R. M. (2013). Nanoparticle emissions from 11 non-vehicle exhaust sources - A review. Atmos. Environ. 67, 252–277. https://doi.org/10.1016/j.atmosenv.2012.11.011.

Kumar, P., Robins, A., Vardoulakis, S., and Britter, R. (2010). A review of the characteristics of nanoparticles in the urban atmosphere and the prospects for developing regulatory controls. Atmos. Environ. 44, 5035–5052. https://doi.org/10.1016/j.atmosenv.2010.08.016.

Yadav, S.K., Sharma, R., Kumar, S., Agarwal, A., Mohan, V., Kumar Mishra, R., and Shukla, A. (2022). Urban air pollution reduction: evidence from phase-wise analysis of COVID-19 pandemic lockdown. Arab J Geosci. 14, 1413 .https://doi.org/10.1007/s12517-021-07777-x/.

Kuula, J., Timonen, H., Niemi, J. V, Manninen, H. E., Rönkkö, T., Hussein, T., Fung, P. L., Tarkoma, S., Laakso, M., Saukko, E., Ovaska, A., Kulmala, M., Karppinen, A., Johansson, L., and Petäjä, T. (2022). Opinion: Insights into updating Ambient Air Quality Directive (2008/50EC). Atmos. Chem. Phys. 22, 4801–4808. https://doi.org/10.5194/acp-2021-854.

Kuye, A., and Kumar, P. (2023). A review of the physicochemical characteristics of ultrafine particle emissions from domestic solid fuel combustion during cooking and heating. Sci. Tot. Environ. 86, 163747. https://doi.org/10.1016/j.scitotenv.2023.163747.

Kwak, J., Lee, S., and Lee, S. (2014). On-road and laboratory investigations on non-exhaust ultrafine particles from the interaction between the tire and road pavement

under braking conditions. Atmos. Environ. 97, 195–205. https://doi.org/10.1016/j.atmosenv.2014.08.014.

Kwon, H. S., Ryu, M. H., and Carlsten, C. (2020). Ultrafine particles: unique physicochemical properties relevant to health and disease. Exp. Mol. Med. 52, 318–328. https://doi.org/10.1038/s12276-020-0405-1.

Lammers, A., Janssen, N. A. H., Boere, A. J. F., Berger, M., Longo, C., Vijverberg, S. J. H., Neerincx, A. H., Maitland - van der Zee, A. H., and Cassee, F. R. (2020). Effects of short-term exposures to ultrafine particles near an airport in healthy subjects. Environ. Int. 141, 105779. https://doi.org/10.1016/j.envint.2020.105779.

Lee, E. S., Xu, B., and Zhu, Y. (2012). Measurements of ultrafine particles carrying different number of charges in on- and near-freeway environments. Atmos. Environ. 60, 564–572. https://doi.org/10.1016/j.atmosenv.2012.06.085.

Lee, W. C., Wolfson, J. M., Catalano, P. J., Rudnick, S. N., and Koutrakis, P. (2014). Size-resolved deposition rates for ultrafine and submicrometer particles in a residential housing unit. Environ. Sci. Tech. 48, 10282–10290. https://doi.org/10.1021/es502278k.

Lenz, L., Bensch, G., Chartier, R., Kane, M., Ankel-Peters, J., and Jeuland, M. (2023). Releasing the killer from the kitchen? Ventilation and air pollution from biomass cooking. Dev. Engi. 8, 108. https://doi.org/10.1016/j.deveng.2023.100108.

Lepistö, T., Barreira, L. M. F., Helin, A., Niemi, J. V., Kuittinen, N., Lintusaari, H., Silvonen, V., Markkula, L., Manninen, H. E., Timonen, H., Jalava, P., Saarikoski, S., and Rönkkö, T. (2023). Snapshots of wintertime urban aerosol characteristics: Local sources emphasized in ultrafine particle number and lung deposited surface area. Environ. Res. 231, 116068. https://doi.org/10.1016/j.envres.2023.116068.

Li, J., Fan, G., Ou, Y., and Deng, Q. (2023). Characteristics and control strategies of indoor particles: An updated review. Ene. Buil. 294,113232. https://doi.org/10.1016/j.enbuild.2023.113232.

Li, L., Wang, Q., Zhang, Y., Liu, S., Zhang, T., Wang, S., Tian, J., Chen, Y., Hang Ho, S. S., Han, Y., and Cao, J. (2022). Impact of reduced anthropogenic emissions on

chemical characteristics of urban aerosol by individual particle analysis. Chemos. 303,135013. https://doi.org/10.1016/j.chemosphere.2022.135013.

Li, L., Wu, J., Hudda, N., Sioutas, C., Fruin, S. A., and Delfino, R. J. (2013). Modeling the concentrations of on-road air pollutants in Southern California. Environ. Sci. Tech. 47, 9291–9299. https://doi.org/10.1021/es401281r.

Lin, S., Ryan, I., Paul, S., Deng, X., Zhang, W., Luo, G., Dong, G. H., Nair, A., and Yu, F. (2022). Particle surface area, ultrafine particle number concentration, and cardiovascular hospitalizations. Environ. Poll. 310,119795. https://doi.org/10.1016/j.envpol.2022.119795.

Li, Q. Q., Guo, Y. T., Yang, J. Y., and Liang, C. S. (2023). Review on main sources and impacts of urban ultrafine particles: Traffic emissions, nucleation, and climate modulation. Atmos. Environ.:X.19,100221 https://doi.org/10.1016/j.aeaoa.2023.100221.

Liu, J., and Cui, S. (2014). Meteorological influences on seasonal variation of fine particulate matter in cities over southern Ontario, Canada. Adv. Met. 169476. https://doi.org/10.1155/2014/169476.

Liu, L., Zhang, J., Du, R., Teng, X., Hu, R., Yuan, Q., Tang, S., Ren, C., Huang, X., Xu, L., Zhang, Y., Zhang, X., Song, C., Liu, B., Lu, G., Shi, Z., and Li, W. (2021). Chemistry of Atmospheric Fine Particles During the COVID-19 Pandemic in a Megacity of Eastern China. Geophy. Res. Let. 48, e2020GL09161. https://doi.org/10.1029/2020GL09161.

Li, Z., Guo, J., Ding, A., Liao, H., Liu, J., Sun, Y., Wang, T., Xue, H., Zhang, H., and Zhu, B. (2017). Aerosol and boundary-layer interactions and impact on air quality. In Nat. Sci. Rev. 4,810–833. https://doi.org/10.1093/nsr/nwx117.

Lorelei de Jesus, A., Thompson, H., Knibbs, L. D., Kowalski, M., Cyrys, J., Niemi, J. V., Kousa, A., Timonen, H., Luoma, K., Petäjä, T., Beddows, D., Harrison, R. M., Hopke, P., and Morawska, L. (2020). Long-term trends in PM2.5 mass and particle number concentrations in urban air: The impacts of mitigation measures and extreme

events due to changing climates. Environ. Poll. 263,114500. https://doi.org/10.1016/j.envpol.2020.114500.

Lv, Y., Chen, X., Wei, S., Zhu, R., Wang, B., Chen, B., Kong, M., and Zhang, J. (Jensen). (2020). Sources, concentrations, and transport models of ultrafine particles near highways: a Literature Review. Buil. Environ. 186, 107325. https://doi.org/10.1016/j.buildenv.2020.107325.

Machaczka, O., Jirik, V., Brezinova, V., Vrtkova, A., Miturova, H., Riedlova, P., Dalecka, A., Hermanova, B., Slachtova, H., Siemiatkowski, G., Osrodka, L., and Sram, R. J. (2021). Evaluation of fine and ultrafine particles proportion in airborne dust in an industrial area. Int. J. Environ. Res. Pub. Health. 18, 8915. https://doi.org/10.3390/ijerph18178915.

Madureira, J., Slezakova, K., Costa, C., Pereira, M. C., and Teixeira, J. P. (2020). Assessment of indoor air exposure among newborns and their mothers: Levels and sources of PM10, PM2.5 and ultrafine particles at 65 home environments. Environ. Poll. 264, 114746. https://doi.org/10.1016/j.envpol.2020.114746.

Ma, L., Zhang, Y., Lin, Z., Zhou, Y., Yan, C., Zhang, Y., Zhou, W., Ma, W., Hua, C., Li, X., Deng, C., Qi, Y., Dada, L., Li, H., Bianchi, F., Petäjä, T., Kangasluoma, J., Jiang, J., Liu, S., … Liu, Y. (2022). Deposition potential of 0.003–10 μm ambient particles in the humidified human respiratory tract: Contribution of new particle formation events in Beijing. Ecotox. Environ. Safety. 243, 114023. https://doi.org/10.1016/j.ecoenv.2022.114023.

Ma, N., and Birmili, W. (2015). Estimating the contribution of photochemical particle formation to ultrafine particle number averages in an urban atmosphere. Sci. Tot Environ. 512–513, 154–166. https://doi.org/10.1016/j.scitotenv.2015.01.009.

Manigrasso, M., Costabile, F., Liberto, L. Di, Gobbi, G. P., Gualtieri, M., Zanini, G., and Avino, P. (2020). Size resolved aerosol respiratory doses in a Mediterranean urban area: From PM10 to ultrafine particles. Environ. Int. 141,105714. https://doi.org/10.1016/j.envint.2020.105714.

Manojkumar, N., Monishraj, M., and Srimuruganandam, B. (2021). Commuter exposure concentrations and inhalation doses in traffic and residential routes of Vellore city, India. Atmos. Poll. Res. 12, 219–230. https://doi.org/10.1016/j.apr.2020.09.002.

Manojkumar, N., and Srimuruganandam, B. (2021a). Health benefits of achieving fine particulate matter standards in India – A nationwide assessment. Sci. Tot. Environ, 763,142999. https://doi.org/10.1016/j.scitotenv.2020.142999.

Manojkumar, N., and Srimuruganandam, B. (2021b). Investigation of on-road fine particulate matter exposure concentration and its inhalation dosage levels in an urban area. Build. and Environ. 198,107914. https://doi.org/10.1016/j.buildenv.2021.107914.

Manojkumar, N., and Srimuruganandam, B. (2022a). Age-specific and seasonal deposition of outdoor and indoor particulate matter in human respiratory tract. Atmos. Poll. Res. 13, 101298. https://doi.org/10.1016/j.apr.2021.101298.

Manojkumar, N., and Srimuruganandam, B. (2022b). Size-segregated particulate matter characteristics in indoor and outdoor environments of urban traffic and residential sites. Urban Clim. 44,101232. https://doi.org/10.1016/j.uclim.2022.101232.

Manojkumar, N., Srimuruganandam, B., and Nagendra, S. M.S. (2019). Application of multiple-path particle dosimetry model for quantifying age specified deposition of particulate matter in human airway. Ecotoxi. Environ. Safety. 168, 241–248. https://doi.org/10.1016/j.ecoenv.2018.10.091.

Marval, J., and Tronville, P. (2022). Ultrafine particles: A review about their health effects, presence, generation, and measurement in indoor environments. Build. Environ. 216,108992. https://doi.org/10.1016/j.buildenv.2022.108992.

Masiol, M., Squizzato, S., Chalupa, D. C., Utell, M. J., Rich, D. Q., and Hopke, P. K. (2018). Long-term trends in submicron particle concentrations in a metropolitan area of the northeastern United States. Sci. Tot. Environ. 633, 59–70. https://doi.org/10.1016/j.scitotenv.2018.03.151.

Meier, R., Eeftens, M., Aguilera, I., Phuleria, H. C., Ineichen, A., Davey, M., Ragettli, M. S., Fierz, M., Schindler, C., Probst-Hensch, N., Tsai, M. Y., and Künzli, N. (2015). Ambient ultrafine particle levels at residential and reference sites in urban and rural Switzerland. Environ. Sci. Tech. 49, 2709–2715. https://doi.org/10.1021/es505246m.

Meskhidze, N., Jaimes-Correa, J. C., Petters, M. D., Royalty, T. M., Phillips, B. N., Zimmerman, A., and Reed, R. (2019). Possible Wintertime Sources of Fine Particles in an Urban Environment. Journal of Geophysical Research: Atmos. 124, 13055–13070. https://doi.org/10.1029/2019JD031367.

Michaelis, S., Loraine, T., and Howard, C. V. (2021). Ultrafine particle levels measured on board short-haul commercial passenger jet aircraft. Environ. Health. 20,89. https://doi.org/10.1186/s12940-021-00770-7.

Miller, F. J., Asgharian, B., Schroeter, J. D., and Price, O. (2016). Improvements and additions to the Multiple Path Particle Dosimetry model. J. Aero. Sci. 99, 14–26. https://doi.org/10.1016/j.jaerosci.2016.01.018.

Mishra, V. K., Aggarwal, M. L., Berghmans, P., Frijns, E., Int Panis, L., and Chacko, K. M. (2015). Dynamics of ultrafine particles inside a roadway tunnel. Environ. Mon. Asses. 187, 1–12. https://doi.org/10.1007/s10661-015-4948-x.

Mogno, C., Palmer, P. I., Knote, C., Yao, F., and Wallington, T. J. (2021). Seasonal distribution and drivers of surface fine particulate matter and organic aerosol over the Indo-Gangetic Plain. Atmos. Chem. Phys. 21, 10881–10909. https://doi.org/10.5194/acp-21-10881-202.

Mohan, V., Soni, V.K, and Kumar Mishra, R. (2024). Analysing the impact of day-night road traffic variation on ultrafine particle number size distribution and concentration at an urban site in the megacity Delhi. Atmos. Poll. Res. 15,102065. https://doi.org/10.1016/j.apr.2024.102065.

Mohan, V., Soni, V. K., and Mishra, R. K. (2024). Geographical variability of ultrafine particle concentrations in urban and background regions in India. Urban Clim. 56, 102066. https://doi.org/10.1016/j.uclim.2024.102066.

Mohtar, A. A. A., Latif, M. T., Baharudin, N. H., Ahamad, F., Chung, J. X., Othman, M., and Juneng, L. (2018). Variation of major air pollutants in different seasonal conditions in an urban environment in Malaysia. Geosci. Let. 5, 21. https://doi.org/10.1186/s40562-018-0122-y.

Morales Betancourt, R., Galvis, B., Balachandran, S., Ramos-Bonilla, J. P., Sarmiento, O. L., Gallo-Murcia, S. M., and Contreras, Y. (2017). Exposure to fine particulate, black carbon, and particle number concentration in transportation microenvironments. Atmos. Environ. 157, 135–145. https://doi.org/10.1016/j.atmosenv.2017.03.006.

Moreno-Ríos, A. L., Tejeda-Benítez, L. P., and Bustillo-Lecompte, C. F. (2022). Sources, characteristics, toxicity, and control of ultrafine particles: An overview. Geosci. Front. 13, 101147. https://doi.org/10.1016/j.gsf.2021.101147.

Moreno, T., Reche, C., Ahn, K. H., Eun, H. R., Kim, W. Y., Kim, H. S., Fernández-Iriarte, A., Amato, F., and Querol, X. (2020). Using miniaturised scanning mobility particle sizers to observe size distribution patterns of quasi-ultrafine aerosols inhaled during city commuting. Environ. Res. 191, 109978. https://doi.org/10.1016/j.envres.2020.109978.

Mosonik, B. C., Kibet, J. K., and Ngari, S. M. (2019). Simulating the Health Impact of Particulate Emissions from Transport Fuels Using Multipath Particle Deposition Model (MPPD). Op. J. Mod. Sim. 07, 115–124. https://doi.org/10.4236/ojmsi.2019.72006.

Munir, S., Chen, H., and Crowther, R. (2022). The effect of COVID-19 lockdown on atmospheric total particle numbers, nanoparticle numbers and mass concentrations in the UK. Atmos. Poll. Res. 13, 101548. https://doi.org/10.1016/j.apr.2022.101548.

Nabizadeh, R., Yousefi, M., and Azimi, F. (2018). Study of particle number size distributions at Azadi terminal in Tehran, comparing high-traffic and no traffic area. Met.:X. 5, 1549–1555. https://doi.org/10.1016/j.mex.2018.11.013.

Nazaroff, W. W. (2023). Ten questions concerning indoor ultrafine particles. Build. Environ. 243, 110641. https://doi.org/10.1016/j.buildenv.2023.110641.

Noble, S. R., and Hudson, J. G. (2019). Effects of Continental Clouds on Surface Aitken and Accumulation Modes. Journal of Geophysical Research: Atmospheres, 124(10), 5479–5502. https://doi.org/10.1029/2019JD030297.

Nøjgaard, J. K., Nguyen, Q. T., Glasius, M., and Sørensen, L. L. (2012). Nucleation and Aitken mode atmospheric particles in relation to O3 and NOX at semirural background in Denmark. Atmospheric Environment, 49, 275–283. https://doi.org/10.1016/j.atmosenv.2011.11.040.

Okam, A., Sanderson, P., Harrison, R. M., and Delgado-Saborit, J. M. (2024). Morphological and chemical characterisation of indoor quasi-ultrafine particles. Atmospheric Environment, 318. https://doi.org/10.1016/j.atmosenv.2023.120245.

Okuljar, M., Kuuluvainen, H., Kontkanen, J., Garmash, O., Olin, M., Niemi, J. V., Timonen, H., Kangasluoma, J., Tham, Y. J., Baalbaki, R., Sipilä, M., Salo, L., Lintusaari, H., Portin, H., Teinilä, K., Aurela, M., Dal Maso, M., Rönkkö, T., Petäjä, T., and Paasonen, P. (2021). Measurement report: The influence of traffic and new particle formation on the size distribution of 1-800nm particles in Helsinki-a street canyon and an urban background station comparison. Atmospheric Chemistry and Physics, 21(13), 9931–9953. https://doi.org/10.5194/acp-21-9931-2021.

Orikasa, N., Saito, A., Yamashita, K., Tajiri, T., Zaizen, Y., Kuo, T. H., Kuo, W. C., and Murakami, M. (2020). Seasonal Variations of Atmospheric Aerosol Particles Focused on Cloud Condensation Nuclei and Ice Nucleating Particles from Ground-Based Observations in Tsukuba, Japan. Scientific Online Letters on the Atmosphere, 16, 212–219. https://doi.org/10.2151/sola.2020-036.

Ou, J., Hu, Q., Liu, H., Xu, S., Wang, Z., Ji, X., Wang, X., Xie, Z., and Kang, H. (2021). Exploring the impact of new particle formation events on PM2.5 pollution during winter in the Yangtze River Delta, China. Journal of Environmental Sciences (China), 111, 75–83. https://doi.org/10.1016/j.jes.2021.01.005.

Padró-Martínez, L. T., Patton, A. P., Trull, J. B., Zamore, W., Brugge, D., and Durant, J. L. (2012). Mobile monitoring of particle number concentration and other traffic-related air pollutants in a near-highway neighborhood over the course of a year.

Atmospheric Environment, 61, 253–264. https://doi.org/10.1016/j.atmosenv.2012.06.088.

Patel, H., Talbot, N., Dirks, K., and Salmond, J. (2023). The impact of low emission zones on personal exposure to ultrafine particles in the commuter environment. Science of the Total Environment, 874. https://doi.org/10.1016/j.scitotenv.2023.162540.

Patel, K., Bhandari, S., Gani, S., Campmier, M. J., Kumar, P., Habib, G., Apte, J., and Hildebrandt Ruiz, L. (2021). Sources and Dynamics of Submicron Aerosol during the Autumn Onset of the Air Pollution Season in Delhi, India. ACS Earth and Space Chemistry, 5(1), 118–128. https://doi.org/10.1021/acsearthspacechem.0c00340.

Phairuang, W., Hata, M., and Furuuchi, M. (2021). A review of ambient nanoparticles (PM0.1) in South East Asian cities: biomass and fossil burning impacts. https://doi.org/10.20944/preprints202108.0575.v1.

Pipal, A. S., Rohra, H., Tiwari, R., and Taneja, A. (2021). Particle size distribution, morphometric study and mixing structure of accumulation and ultrafine aerosols emitted from indoor activities in different socioeconomic micro-environment. Atmospheric Pollution Research, 12(4), 101–111. https://doi.org/10.1016/j.apr.2021.02.015.

Pirhadi, M., Mousavi, A., Sowlat, M. H., Janssen, N. A. H., Cassee, F. R., and Sioutas, C. (2020). Relative contributions of a major international airport activities and other urban sources to the particle number concentrations (PNCs) at a nearby monitoring site. Environmental Pollution, 260. https://doi.org/10.1016/j.envpol.2020.114027.

Pöhlker, M. L., Zhang, M., Campos Braga, R., Krüger, O. O., Pöschl, U., and Ervens, B. (2021). Aitken mode particles as CCN in aerosol- And updraft-sensitive regimes of cloud droplet formation. Atmospheric Chemistry and Physics, 21(15), 11723–11740. https://doi.org/10.5194/acp-21-11723-2021.

Pokhrel, A. K., Bates, M. N., Acharya, J., Valentiner-Branth, P., Chandyo, R. K., Shrestha, P. S., Raut, A. K., and Smith, K. R. (2015). PM2.5 in household kitchens of

Bhaktapur, Nepal, using four different cooking fuels. Atmospheric Environment, 113, 159–168. https://doi.org/10.1016/j.atmosenv.2015.04.060.

Posselt, K. P., Neuberger, M. and Köhler, D. (2019). Fine and ultrafine particle exposure during commuting by subway in Vienna. Wiener Klinische Wochenschrift, 131(15–16), 374–380. https://doi.org/10.1007/s00508-019-1516-3.

Prabhu, V., Prakash, J., Soni, A., Madhwal, S., and Shridhar, V. (2019). Atmospheric aerosols and inhalable particle number count during Diwali in Dehradun. City and Environment Interactions, 2. https://doi.org/10.1016/j.cacint.2019.100006.

Pushpawela, B., Jayaratne, R., and Morawska, L. (2018). Differentiating between particle formation and growth events in an urban environment. Atmospheric Chemistry and Physics, 18(15), 11171–11183. https://doi.org/10.5194/acp-18-11171-2018.

Ragettli, M. S., Ducret-Stich, R. E., Foraster, M., Morelli, X., Aguilera, I., Basagaña, X., Corradi, E., Ineichen, A., Tsai, M. Y., Probst-Hensch, N., Rivera, M., Slama, R., Künzli, N., and Phuleria, H. C. (2014). Spatio-temporal variation of urban ultrafine particle number concentrations. Atmospheric Environment, 96, 275–283. https://doi.org/10.1016/j.atmosenv.2014.07.049.

Rajagopal, K., Mohan, V., and Mishra, R. K. (2024). Are Delhi residents exposed to lesser particle number concentration due to the firework ban in the city? Air Quality, Atmosphere and Health. https://doi.org/10.1007/s11869-024-01532-3.

Rajagopal, K., Ramachandran, S., and Mishra, R. K. (2023). Roadside measurements of nanoparticles and their dynamics in relation to traffic sources in Delhi: Impact of restrictions and pollution events. Urban Climate, 51. https://doi.org/10.1016/j.uclim.2023.101625.

Rajagopal, K., Ramachandran, S., and Mishra, R. K. (2024a). Seasonal variation of particle number concentration in a busy urban street with exposure assessment and deposition in human respiratory tract. Chemosphere, 366. https://doi.org/10.1016/j.chemosphere.2024.143470.

Rajagopal, K., Ramachandran, S., and Mishra, R. K. (2024b). Size resolved particle contribution to vehicle induced ultrafine particle number concentration in a

metropolitan curbside region. Atmospheric Environment, 337, 120773. https://doi.org/10.1016/j.atmosenv.2024.120773.

Reche, C., Moreno, T., Martins, V., Minguillón, M. C., Jones, T., de Miguel, E., Capdevila, M., Centelles, S., and Querol, X. (2017). Factors controlling particle number concentration and size at metro stations. Atmospheric Environment, 156, 169–181. https://doi.org/10.1016/j.atmosenv.2017.03.002.

Reggente, M., Peters, J., Theunis, J., Van Poppel, M., Rademaker, M., De Baets, B., and Kumar, P. (2015). A comparison of strategies for estimation of ultrafine particle number concentrations in urban air pollution monitoring networks. Environmental Pollution, 199, 209–218. https://doi.org/10.1016/j.envpol.2015.01.034.

Ren, J., Liu, J., Li, F., Cao, X., Ren, S., Xu, B., and Zhu, Y. (2016). A study of ambient fine particles at Tianjin International Airport, China. Science of the Total Environment, 556, 126–135. https://doi.org/10.1016/j.scitotenv.2016.02.186.

Rentschler, J., and Leonova, N. (2023). Global air pollution exposure and poverty. Nature Communications, 14(1). https://doi.org/10.1038/s41467-023-39797-4.

Resmi, C. T., Nishanth, T., Satheesh Kumar, M. K., Balachandramohan, M., and Valsaraj, K. T. (2019). Temporal changes in air quality during a festival season in Kannur, India. Atmosphere, 10(3). https://doi.org/10.3390/atmos10030137.

Ridolfo, S., Amato, F., and Querol, X. (2024). Particle number size distributions and concentrations in transportation environments: a review. In Environment International (Vol. 187). Elsevier Ltd. https://doi.org/10.1016/j.envint.2024.108696.

Riley, E. A., Gould, T., Hartin, K., Fruin, S. A., Simpson, C. D., Yost, M. G., and Larson, T. (2016). Ultrafine particle size as a tracer for aircraft turbine emissions. Atmospheric Environment, 139, 20–29. https://doi.org/10.1016/j.atmosenv.2016.05.016.

Rosati, B., Christiansen, S., Wollesen De Jonge, R., Roldin, P., Jensen, M. M., Wang, K., Moosakutty, S. P., Thomsen, D., Salomonsen, C., Hyttinen, N., Elm, J., Feilberg, A., Glasius, M., and Bilde, M. (2021). New Particle Formation and Growth from

Dimethyl Sulfide Oxidation by Hydroxyl Radicals. ACS Earth and Space Chemistry, 5(4), 801–811. https://doi.org/10.1021/acsearthspacechem.0c00333.

Rose, C., Collaud Coen, M., Andrews, E., Lin, Y., Bossert, I., Lund Myhre, C., Tuch, T., Wiedensohler, A., Fiebig, M., Aalto, P., Alastuey, A., Alonso-Blanco, E., Andrade, M., Artinano, B., Arsov, T., Baltensperger, U., Bastian, S., Bath, O., Beukes, J. P., … Laj, P. (2021). Seasonality of the particle number concentration and size distribution: A global analysis retrieved from the network of Global Atmosphere Watch (GAW) near-surface observatories. Atmospheric Chemistry and Physics, 21(22), 17185–17223. https://doi.org/10.5194/acp-21-17185-2021.

Sabaliauskas, K., Evans, G., and Jeong, C. H. (2012). Source identification of traffic-related ultrafine particles data mining contest. Procedia Computer Science, 13, 99–107. https://doi.org/10.1016/j.procs.2012.09.118.

Sabaliauskas, K., Jeong, C. H., Yao, X., Jun, Y. S., and Evans, G. (2013). Cluster analysis of roadside ultrafine particle size distributions. Atmospheric Environment, 70, 64–74. https://doi.org/10.1016/j.atmosenv.2012.12.025.

Sabaliauskas, K., Jeong, C. H., Yao, X., Jun, Y. S., Jadidian, P., and Evans, G. J. (2012). Five-year roadside measurements of ultrafine particles in a major Canadian city. Atmospheric Environment, 49, 245–256. https://doi.org/10.1016/j.atmosenv.2011.11.052.

Saha, P. K., Ashik-Un-Noor, S., Robinson, A. L., and Presto, A. A. (2024). In-vehicle ultrafine and fine particulate matter exposures during commuting in a South Asian megacity: Dhaka, Bangladesh. Atmospheric Environment, 321. https://doi.org/10.1016/j.atmosenv.2024.120340.

Saha, P. K., Hankey, S., Marshall, J. D., Robinson, A. L., and Presto, A. A. (2021). High-Spatial-Resolution Estimates of Ultrafine Particle Concentrations across the Continental United States. Environmental Science and Technology, 55(15), 10320–10331. https://doi.org/10.1021/acs.est.1c03237.

Saha, P. K., Robinson, E. S., Shah, R. U., Zimmerman, N., Apte, J. S., Robinson, A. L., and Presto, A. A. (2018). Reduced Ultrafine Particle Concentration in Urban Air:

Changes in Nucleation and Anthropogenic Emissions. Environmental Science and Technology, 52(12), 6798–6806. https://doi.org/10.1021/acs.est.8b00910.

Saha, P. K., Zimmerman, N., Malings, C., Hauryliuk, A., Li, Z., Snell, L., Subramanian, R., Lipsky, E., Apte, J. S., Robinson, A. L., and Presto, A. A. (2019). Quantifying high-resolution spatial variations and local source impacts of urban ultrafine particle concentrations. Science of the Total Environment, 655, 473–481. https://doi.org/10.1016/j.scitotenv.2018.11.197.

Salvi, S., and Apte, K. (2016). Household air pollution and its effects on health. In F1000Research (Vol. 5). F1000 Research Ltd. https://doi.org/10.12688/f1000research.7552.1.

Sarangi, B., Aggarwal, S. G., Kunwar, B., Kumar, S., Kaur, R., Sinha, D., Tiwari, S., and Kawamura, K. (2018). Nighttime particle growth observed during spring in New Delhi: Evidences for the aqueous phase oxidation of SO2. Atmospheric Environment, 188, 82–96. https://doi.org/10.1016/j.atmosenv.2018.06.018.

Sarangi, C., Tripathi, S. N., Qian, Y., Kumar, S., and Ruby Leung, L. (2018). Aerosol and Urban Land Use Effect on Rainfall Around Cities in Indo-Gangetic Basin From Observations and Cloud Resolving Model Simulations. Journal of Geophysical Research: Atmospheres, 123(7), 3645–3667. https://doi.org/10.1002/2017JD028004.

Sarica, T., Sartelet, K., Roustan, Y., Kim, Y., Lugon, L., Marques, B., D'Anna, B., Chaillou, C., and Larrieu, C. (2023). Sensitivity of pollutant concentrations in urban streets to asphalt and traffic-related emissions. Environmental Pollution, 332. https://doi.org/10.1016/j.envpol.2023.121955.

Sateesh, M., Soni, V. K., and Raju, P. V. S. (2018). Effect of Diwali Firecrackers on Air Quality and Aerosol Optical Properties over Mega City (Delhi) in India. Earth Systems and Environment, 2(2), 293–304. https://doi.org/10.1007/s41748-018-0054-x.

Saxena, P., Srivastava, A., Verma, S., Shweta, Singh, L., and Sonwani, S. (2020). Analysis of Atmospheric Pollutants During Fireworks Festival 'Diwali' at a

Residential Site Delhi in India. In Energy, Environment, and Sustainability (pp. 91–105). Springer Nature. https://doi.org/10.1007/978-981-15-0540-9_4.

Schraufnagel, D. E. (2020). The health effects of ultrafine particles. In Experimental and Molecular Medicine (Vol. 52, Issue 3, pp. 311–317). Springer Nature. https://doi.org/10.1038/s12276-020-0403-3.

Schwarz, M., Schneider, A., Cyrys, J., Bastian, S., Breitner, S., and Peters, A. (2023). Impact of ultrafine particles and total particle number concentration on five cause-specific hospital admission endpoints in three German cities. Environment International, 178. https://doi.org/10.1016/j.envint.2023.108032.

Sharma, M., Khare, M., and Mishra, R. K. (2024). Air quality changes in Delhi due to open waste burning: an accidental fire in Bhalswa landfill. International Journal of Environmental Science and Technology, 21(1), 655–664. https://doi.org/10.1007/s13762-023-04921-w.

Shen, J., Bigi, A., Marinoni, A., Lampilahti, J., Kontkanen, J., Ciarelli, G., Putaud, J. P., Nieminen, T., Kulmala, M., Lehtipaloa, K., and Bianchi, F. (2021). Emerging Investigator Series: COVID-19 lockdown effects on aerosol particle size distributions in northern Italy. Environmental Science: Atmospheres, 1(5), 214–227. https://doi.org/10.1039/d1ea00016k.

Shrestha, R. K., Gallagher, M. W., and Connolly, P. J. (2016). Diurnal and seasonal variations of meteorology and aerosol concentrations in the foothills of the nepal himalayas (Nagarkot: 1,900 m asl). Asia-Pacific Journal of Atmospheric Sciences, 52(1), 63–75. https://doi.org/10.1007/s13143-016-0002-3.

Simon, M. C., Hudda, N., Naumova, E. N., Levy, J. I., Brugge, D., and Durant, J. L. (2017). Comparisons of traffic-related ultrafine particle number concentrations measured in two urban areas by central, residential, and mobile monitoring. Atmospheric Environment, 169, 113–127. https://doi.org/10.1016/j.atmosenv.2017.09.003.

Singh, A. K., Hazarika, N., Kumar, U., and Srivastava, A. (2021). Assessment of size distribution of aerosols at kitchen environments in Delhi, India. Urban Climate, 37. https://doi.org/10.1016/j.uclim.2021.100819.

Singh, A., Pant, P., and Pope, F. D. (2019). Air quality during and after festivals: Aerosol concentrations, composition and health effects. In Atmospheric Research (Vol. 227, pp. 220–232). https://doi.org/10.1016/j.atmosres.2019.05.012.

Sly, P. D., and Schüepp, K. (2012). Nanoparticles and Children's Lungs: Is there a need for caution? In Paediatric Respiratory Reviews (Vol. 13, Issue 2, pp. 71–72). https://doi.org/10.1016/j.prrv.2011.07.005.

Song, S., Wu, Y., Xu, J., Ohara, T., Hasegawa, S., Li, J., Yang, L., and Hao, J. (2013). Black carbon at a roadside site in Beijing: Temporal variations and relationships with carbon monoxide and particle number size distribution. Atmospheric Environment, 77, 213–221. https://doi.org/10.1016/j.atmosenv.2013.04.055.

Squizzato, S., Masiol, M., Emami, F., Chalupa, D. C., Utell, M. J., Rich, D. Q., and Hopke, P. K. (2019). Long-Term changes of source apportioned particle number concentrations in a metropolitan area of the northeastern United States. Atmosphere, 10(1). https://doi.org/10.3390/atmos10010027.

Stabile, L., Cauda, E., Marini, S., and Buonanno, G. (2014). Metrological assessment of a portable analyzer for monitoring the particle size distribution of ultrafine particles. Annals of Occupational Hygiene, 58(7), 860–876. https://doi.org/10.1093/annhyg/meu025.

Stafoggia, M., Cattani, G., Forastiere, F., Di Menno di Bucchianico, A., Gaeta, A., and Ancona, C. (2016). Particle number concentrations near the Rome-Ciampino city airport. Atmospheric Environment, 147, 264–273. https://doi.org/10.1016/j.atmosenv.2016.09.062.

Steenland, K., Pillarisetti, A., Kirby, M., Peel, J., Clark, M., Checkley, W., Chang, H. H., and Clasen, T. (2018). Modeling the potential health benefits of lower household air pollution after a hypothetical liquified petroleum gas (LPG) cookstove intervention. Environment International, 111, 71–79. https://doi.org/10.1016/j.envint.2017.11.018.

Straaten, A., Meier, F., Scherer, D., and Weber, S. (2022). Significant reduction of ultrafine particle emission fluxes to the urban atmosphere during the COVID-19 lockdown. Science of the Total Environment, 838. https://doi.org/10.1016/j.scitotenv.2022.156516.

Sun, J., Birmili, W., Hermann, M., Tuch, T., Weinhold, K., Merkel, M., Rasch, F., Müller, T., Schladitz, A., Bastian, S., Löschau, G., Cyrys, J., Gu, J., Flentje, H., Briel, B., Asbach, C., Kaminski, H., Ries, L., Sohmer, R., … Wiedensohler, A. (2020). Decreasing trends of particle number and black carbon mass concentrations at 16 observational sites in Germany from 2009 to 2018. Atmospheric Chemistry and Physics, 20(11), 7049–7068. https://doi.org/10.5194/acp-20-7049-2020.

Sun, J., Birmili, W., Hermann, M., Tuch, T., Weinhold, K., Spindler, G., Schladitz, A., Bastian, S., Löschau, G., Cyrys, J., Gu, J., Flentje, H., Briel, B., Asbach, C., Kaminski, H., Ries, L., Sohmer, R., Gerwig, H., Wirtz, K., … Wiedensohler, A. (2019). Variability of black carbon mass concentrations, sub-micrometer particle number concentrations and size distributions: results of the German Ultrafine Aerosol Network ranging from city street to High Alpine locations. Atmospheric Environment, 202, 256–268. https://doi.org/10.1016/j.atmosenv.2018.12.029.

Sun, L., and Singer, B. C. (2023). Cooking methods and kitchen ventilation availability, usage, perceived performance and potential in Canadian homes. Journal of Exposure Science and Environmental Epidemiology, 33(3), 439–447. https://doi.org/10.1038/s41370-023-00543-z.

Takegawa, N., Murashima, Y., Fushimi, A., Misawa, K., Fujitani, Y., Saitoh, K., and Sakurai, H. (2021). Characteristics of sub-10 nm particle emissions from in-use commercial aircraft observed at Narita International Airport. Atmospheric Chemistry and Physics, 21(2), 1085–1104. https://doi.org/10.5194/acp-21-1085-2021.

Tanda, S., Ličbinský, R., Hegrová, J., and Goessler, W. (2019). Impact of New Year's Eve fireworks on the size resolved element distributions in airborne particles. Environment International, 128, 371–378. https://doi.org/10.1016/j.envint.2019.04.071.

Tang, R., and Pfrang, C. (2023). Indoor particulate matter (PM) from cooking in UK students' studio flats and associated intervention strategies: evaluation of cooking methods, PM concentrations and personal exposures using low-cost sensors. Environmental Science: Atmospheres, 3(3), 537–551. https://doi.org/10.1039/d2ea00171c.

Tawiah, T., Shupler, M., Gyaase, S., Anderson de Cuevas, R., Saah, J., Nix, E., Twumasi, M., Quansah, R., Puzzolo, E., Pope, D., and Asante, K. P. (2022). The Association between Household Air Pollution and Blood Pressure in Obuasi Municipality, Ghana. Atmosphere, 13(12). https://doi.org/10.3390/atmos13122033.

Tiwari, M., Sahu, S. K., Bhangare, R. C., Yousaf, A., and Pandit, G. G. (2014). Particle size distributions of ultrafine combustion aerosols generated from household fuels. Atmospheric Pollution Research, 5(1), 145–150. https://doi.org/10.5094/APR.2014.018.

Tiwari, S., Thomas, A., Rao, P., Chate, D. M., Soni, V. K., Singh, S., Ghude, S. D., Singh, D., and Hopke, P. K. (2018). Pollution concentrations in Delhi India during winter 2015–16: A case study of an odd-even vehicle strategy. Atmospheric Pollution Research, 9(6), 1137–1145. https://doi.org/10.1016/j.apr.2018.04.008.

Tremper, A. H., Jephcote, C., Gulliver, J., Hibbs, L., Green, D. C., Font, A., Priestman, M., Hansell, A. L., and Fuller, G. W. (2022). Sources of particle number concentration and noise near London Gatwick Airport. Environment International, 161. https://doi.org/10.1016/j.envint.2022.107092.

Vaghmaria, N., Mevada, N., and Maliakal, J. (2018). Impact of Diwali festival on aerosol optical properties over an Urban city, Ahmedabad (India). Aerosol and Air Quality Research, 18(2), 522–532. https://doi.org/10.4209/aaqr.2017.04.0124.

Velasco, E., and Tan, S. H. (2016). Particles exposure while sitting at bus stops of hot and humid Singapore. Atmospheric Environment, 142, 251–263. https://doi.org/10.1016/j.atmosenv.2016.07.054.

Vicente, E. D., Calvo, A. I., Sainnokhoi, T. A., Kováts, N., de la Campa, A. S., de la Rosa, J., Oduber, F., Nunes, T., Fraile, R., Tomé, M., and Alves, C. A. (2024). Indoor

PM from residential coal combustion: Levels, chemical composition, and toxicity. Science of the Total Environment, 918. https://doi.org/10.1016/j.scitotenv.2024.170598.

Vu, T. V., Delgado-Saborit, J. M., and Harrison, R. M. (2015). Review: Particle number size distributions from seven major sources and implications for source apportionment studies. In Atmospheric Environment (Vol. 122, pp. 114–132). Elsevier Ltd. https://doi.org/10.1016/j.atmosenv.2015.09.027.

Vu, T. V., Ondracek, J., Zdímal, V., Schwarz, J., Delgado-Saborit, J. M., and Harrison, R. M. (2017). Physical properties and lung deposition of particles emitted from five major indoor sources. Air Quality, Atmosphere and Health, 10(1), 1–14. https://doi.org/10.1007/s11869-016-0424-1.

Wang, X. R., and Oliver Gao, H. (2011). Exposure to fine particle mass and number concentrations in urban transportation environments of New York City. Transportation Research Part D: Transport and Environment, 16(5), 384–391. https://doi.org/10.1016/j.trd.2011.03.001.

Wang, Y., Hopke, P. K., Chalupa, D. C., and Utell, M. J. (2011). Long-term study of urban ultrafine particles and other pollutants. Atmospheric Environment, 45(40), 7672–7680. https://doi.org/10.1016/j.atmosenv.2010.08.022.

Wang, Y., Zhu, Y., Salinas, R., Ramirez, D., Karnae, S., and John, K. (2008). Roadside measurements of ultrafine particles at a busy urban intersection. Journal of the Air and Waste Management Association, 58(11), 1449–1457. https://doi.org/10.3155/1047-3289.58.11.1449.

Watson, Z., Tiszenkel, L., Pour Biazar, A., Knupp, K., and Lee, S. H. (2023). Effects of boundary layer dynamics and meteorology on ultrafine particle formation and growth. Atmospheric Environment, 309. https://doi.org/10.1016/j.atmosenv.2023.119952.

Weber, S., Kordowski, K., and Kuttler, W. (2013). Variability of particle number concentration and particle size dynamics in an urban street canyon under different

meteorological conditions. Science of the Total Environment, 449, 102–114. https://doi.org/10.1016/j.scitotenv.2013.01.044.

Weichenthal, S., Farrell, W., Goldberg, M., Joseph, L., and Hatzopoulou, M. (2014). Characterizing the impact of traffic and the built environment on near-road ultrafine particle and black carbon concentrations. Environmental Research, 132, 305–310. https://doi.org/10.1016/j.envres.2014.04.007.

Weichenthal, S., Van Ryswyk, K., Goldstein, A., Shekarrizfard, M., and Hatzopoulou, M. (2016). Characterizing the spatial distribution of ambient ultrafine particles in Toronto, Canada: A land use regression model. Environmental Pollution, 208, 241–248. https://doi.org/10.1016/j.envpol.2015.04.011.

Wu, C. A., Chen, Y. T., Young, L. H., Chang, P. K., Chou, L. T., Chen, A. Y., and Hsiao, T. C. (2023). Ultrafine particles in urban settings: A combined study of volatility and effective density revealed by VT-DMA-APM. Atmospheric Environment, 312. https://doi.org/10.1016/j.atmosenv.2023.120054.

Wu, H., Li, Z., Hai, S., Gao, Y., Jiang, J., Zhao, B., Cribb, M., Zhang, D., Pu, D., Liu, M., Wang, C., Lan, J., and Wang, Y. (2024). Vertical transport of ultrafine particles and turbulence evolution impact on new particle formation at the surface Canton Tower. Atmospheric Research, 302. https://doi.org/10.1016/j.atmosres.2024.107290.

Wu, H., Li, Z., Li, H., Luo, K., Wang, Y., Yan, P., Hu, F., Zhang, F., Sun, Y., Shang, D., Liang, C., Zhang, D., Wei, J., Wu, T., Jin, X., Fan, X., Cribb, M., Fischer, M. L., Kulmala, M., and Petäjä, T. (2021). The impact of the atmospheric turbulence-development tendency on new particle formation: A common finding on three continents. National Science Review, 8(3). https://doi.org/10.1093/nsr/nwaa157.

Xiang, J., Hao, J., Austin, E., Shirai, J., and Seto, E. (2021). Characterization of cooking-related ultrafine particles in a US residence and impacts of various intervention strategies. Science of the Total Environment, 798. https://doi.org/10.1016/j.scitotenv.2021.149236.

Xie, J., Qiao, D., Han, R., Deng, T., and Wang, J. (2021). New Definition of Ultrafine Particles in Mine Paste and Its Relationship with Rheological Properties. Advances in Civil Engineering, 2021. https://doi.org/10.1155/2021/5560899.

Yadav, S. K., Kompalli, S. K., Gurjar, B. R., and Mishra, R. K. (2021). Aerosol number concentrations and new particle formation events over a polluted megacity during the COVID-19 lockdown. Atmospheric Environment, 259. https://doi.org/10.1016/j.atmosenv.2021.118526.

Yadav, S. K., Kumar, M., Sharma, Y., Shukla, P., Singh, R. S., and Banerjee, T. (2019). Temporal evolution of submicron particles during extreme fireworks. Environmental Monitoring and Assessment, 191(9). https://doi.org/10.1007/s10661-019-7735-2.

Yadav, S. K., Mishra, R. K., and Gurjar, B. R. (2019). Ultrafine Particles in Concern of Vehicular Exhaust—An Overview. In Energy, Environment, and Sustainability (pp. 7–38). Springer Nature. https://doi.org/10.1007/978-981-13-3299-9_2.

Yadav, S. K., Mishra, R. K., and Gurjar, B. R. (2022a). Assessment of the effect of the judicial prohibition on firecracker celebration at the Diwali festival on air quality in Delhi, India. Environmental Science and Pollution Research, 29(57), 86247–86259. https://doi.org/10.1007/s11356-021-17695-w.

Yadav, S. K., Mishra, R. K., and Gurjar, B. R. (2022b). Fireworks induced quasi-ultrafine particle number concentration and size-resolved elemental distribution in megacity Delhi. Arabian Journal of Geosciences, 15(1). https://doi.org/10.1007/s12517-021-09385-1.

Yadav, S. K., Mishra, R. K., and Gurjar, B. R. (2022c). Ultrafine particle number concentration and its size distribution during Diwali festival in megacity Delhi, India: Are 'green crackers' safe? Journal of Environmental Management, 317. https://doi.org/10.1016/j.jenvman.2022.115459.

Yang, Z., He, Z., Zhang, K., Zeng, L., and de Nazelle, A. (2021). Investigation into Beijing commuters' exposure to ultrafine particles in four transportation modes: bus, car, bicycle and subway. Atmospheric Environment, 266. https://doi.org/10.1016/j.atmosenv.2021.118734.

Yao, Y., Chen, X., Chen, W., Gao, K., Zhang, H., Zhang, L., Han, Y., Xue, T., Wang, Q., Wang, T., Xu, Y., Wang, J., Qiu, X., Que, C., Zheng, M., and Zhu, T. (2022). Transcriptional pathways of elevated fasting blood glucose associated with short-term exposure to ultrafine particles: A panel study in Beijing, China. Journal of Hazardous Materials, 430. https://doi.org/10.1016/j.jhazmat.2022.128486.

Yerramsetti, V. S., Sharma, A. R., Gauravarapu Navlur, N., Rapolu, V., Dhulipala, N. S. K. C., and Sinha, P. R. (2013). The impact assessment of Diwali fireworks emissions on the air quality of a tropical urban site, Hyderabad, India, during three consecutive years. Environmental Monitoring and Assessment, 185(9), 7309–7325. https://doi.org/10.1007/s10661-013-3102-x.

Yin, G., Liu, C., Hao, L., Chen, Y., Wang, W., Huo, J., Zhao, Q., Zhang, Y., Duan, Y., Fu, Q., Chen, R., and Kan, H. (2019). Associations between size-fractionated particle number concentrations and COPD mortality in Shanghai, China. Atmospheric Environment, 214. https://doi.org/10.1016/j.atmosenv.2019.116875.

Yu, F., Luo, G., Arjunan Nair, A., Schwab, J. J., Sherman, J. P., and Zhang, Y. (2020). Wintertime new particle formation and its contribution to cloud condensation nuclei in the Northeastern United States. Atmospheric Chemistry and Physics, 20(4), 2591–2601. https://doi.org/10.5194/acp-20-2591-2020.

Zhang, J., Chen, Z., Shan, D., Wu, Y., Zhao, Y., Li, C., Shu, Y., Linghu, X., and Wang, B. (2024). Adverse effects of exposure to fine particles and ultrafine particles in the environment on different organs of organisms. In Journal of Environmental Sciences (China) (Vol. 135, pp. 449–473). Chinese Academy of Sciences. https://doi.org/10.1016/j.jes.2022.08.013.

Zhang, M., Wang, X., Chen, J., Cheng, T., Wang, T., Yang, X., Gong, Y., Geng, F., and Chen, C. (2010). Physical characterization of aerosol particles during the Chinese New Year's firework events. Atmospheric Environment, 44(39), 5191–5198. https://doi.org/10.1016/j.atmosenv.2010.08.048.

Zhang, T., Zhu, Z., Gong, W., Xiang, H., and Fang, R. (2016). Characteristics of fine particles in an urban atmosphere—relationships with meteorological parameters and

trace gases. International Journal of Environmental Research and Public Health, 13(8). https://doi.org/10.3390/ijerph13080807.

Zhang, X., Zhang, Y., Sun, J., Zheng, X., Li, G., and Deng, Z. (2017). Characterization of particle number size distribution and new particle formation in an urban environment in Lanzhou, China. Journal of Aerosol Science, 103, 53–66. https://doi.org/10.1016/j.jaerosci.2016.10.010.

Zhang, Z., Lv, X., Wei, Z., Guan, J., Zhang, Y., Chen, S., and He, H. (2022). Effects of cooking and window opening behaviors on indoor ultrafine particle concentrations in urban residences: A field study in Yangtze River Delta region of China. Building and Environment, 207. https://doi.org/10.1016/j.buildenv.2021.108488.

Zhang, Z., Zhu, W., Hu, M., Liu, K., Wang, H., Tang, R., Shen, R., Yu, Y., Tan, R., Song, K., Li, Y., Zhang, W., Zhang, Z., Xu, H., Shuai, S., Li, S., Chen, Y., Li, J., Wang, Y., and Guo, S. (2021). Formation and evolution of secondary organic aerosols derived from urban-lifestyle sources: Vehicle exhaust and cooking emissions. Atmospheric Chemistry and Physics, 21(19), 15221–15237. https://doi.org/10.5194/acp-21-15221-2021.

Zhao, J., Birmili, W., Wehner, B., Daniels, A., Weinhold, K., Wang, L., Merkel, M., Kecorius, S., Tuch, T., Franck, U., Hussein, T., and Wiedensohler, A. (2020). Particle mass concentrations and number size distributions in 40 homes in germany: Indoor-to-outdoor relationships, diurnal and seasonal variation. Aerosol and Air Quality Research, 20(3), 576–589. https://doi.org/10.4209/aaqr.2019.09.0444.

Zheng, T., Peng, Z. R., He, H. Di, Zhang, S., and Wu, Y. (2022). Horizontal profiles of size-segregated particle number concentration and black carbon beside a major roadway. Atmospheric Environment: X, 16. https://doi.org/10.1016/j.aeaoa.2022.100187.

Zheng, T., Wang, H. W., Li, X. B., Peng, Z. R., and He, H. Di. (2021). Impacts of traffic on roadside particle variations in varied temporal scales. Atmospheric Environment, 253. https://doi.org/10.1016/j.atmosenv.2021.118354.

Zhou, Y., Dada, L., Liu, Y., Fu, Y., Kangasluoma, J., Chan, T., Yan, C., Chu, B., Daellenbach, K. R., Bianchi, F., Kokkonen, T. V., Liu, Y., Kujansuu, J., Kerminen, V. M., Petäjä, T., Wang, L., Jiang, J., and Kulmala, M. (2020). Variation of size-segregated particle number concentrations in wintertime Beijing. Atmospheric Chemistry and Physics, 20(2), 1201–1216. https://doi.org/10.5194/acp-20-1201-2020.

Zhu, Y., Hinds, W. C., Kim, S., and Sioutas, C. (2002). Concentration and size distribution of ultrafine particles near a major highway. Journal of the Air and Waste Management Association, 52(9), 1032–1042. https://doi.org/10.1080/10473289.2002.10470842.

Zhu, Y., Hinds, W. C., Shen, S., and Sioutas, C. (2004). Seasonal trends of concentration and size distribution of ultrafine particles near major highways in Los Angeles. Aerosol Science and Technology, 38(SUPPL. 1), 5–13. https://doi.org/10.1080/02786820390229156.

Zhu, Y., Sulaymon, I. D., Xie, X., Mao, J., Guo, S., Hu, M., and Hu, J. (2022). Airborne particle number concentrations in China: A critical review. In Environmental Pollution (Vol. 307). Elsevier Ltd. https://doi.org/10.1016/j.envpol.2022.119470.

Zimmerman, A., Petters, M. D., and Meskhidze, N. (2020). Observations of new particle formation, modal growth rates, and direct emissions of sub-10 nm particles in an urban environment. Atmospheric Environment, 242. https://doi.org/10.1016/j.atmosenv.2020.117835.

Zou, C., Liao, X., Huang, H., Tang, Y., Li, Z., Li, J., Yu, C., and Zhu, F. (2024). Particle size, carbon composition and sources of indoor dust in Nanchang, China. Atmospheric Pollution Research, 15(4). https://doi.org/10.1016/j.apr.2024.102052.

ANNEXURES

Annexure Table.1 F-Test for variance obtained between different phases in two study periods.

Period- I			**Period-II**		
Phase	**BR**	**DR**	**Phase**	**BD**	**AD**
Mean	32121	24372	Mean	24192	42461
Variance	223711144	146426271	Variance	114995765	373545594
Observations	409	918	Observations	409	192
Df	408	917	Df	408	191
F	2		F	0	
P(F<=f) one-tail	0		P(F<=f) one-tail	0	
F Critical one-tail	1		F Critical one-tail	1	
Phase	*DR*	*AR*	*Phase*	*AD*	*DRII*
Mean	24372	25265	Mean	42461	39532
Variance	146426271	202240814	Variance	373545594	389046175
Observations	918	596	Observations	192	432
Df	917	595	Df	191	431
F	1		F	1	
P(F<=f) one-tail	0		P(F<=f) one-tail	0	
F Critical one-tail	1		F Critical one-tail	1	
Phase	*BR*	*AR*	*Phase*	*BD*	*DRII*
Mean	32121	25265	Mean	24192	39532
Variance	223711144	202240814	Variance	114995765	389046175
Observations	409	596	Observations	409	432
Df	408	595	Df	408	431
F	1		F	0	
P(F<=f) one-tail	0		P(F<=f) one-tail	0	
F Critical one-tail	1		F Critical one-tail	1	

Annexure Table. 2 95% confidence interval values in different size ranges and phases

Phase	N_{nuc}	N_{satk}	N_{latk}	N_{acc}	N_{total}
BR	3089	1987	1771	658	60451
DR	1970	1488	1736	1055	47580
AR	2286	1882	1579	471	49283
BD	1557	1759	2121	972	52114
AD	1708	2093	3356	1722	77391
DRII	1445	2344	3568	1625	78632

Annexure Table. 3 Levene test for variance and significance in different size ranges and phases.

Period – I			**Period-II**		
N_{nuc}	F value	Pr(>F)	N_{nuc}	F value	Pr(>F)
2	42.02361	1.37E-18	2	2.812837	0.060392
1920	NA	NA	1330	NA	NA
N_{satk}	F value	Pr(>F)	N_{satk}	F value	Pr(>F)
2	15.02892	3.34E-07	2	14.48712	5.97E-07
1920	NA	NA	1330	NA	NA
N_{latk}	F value	Pr(>F)	N_{latk}	F value	Pr(>F)
2	4.673534	0.009446	2	58.66576	3.83E-25
1920	NA	NA	1330	NA	NA
N_{acc}	F value	Pr(>F)	N_{acc}	F value	Pr(>F)
2	43.02785	5.25E-19	2	37.26233	1.80E-16
1920	NA	NA	1330	NA	NA
N_{total}	F value	Pr(>F)	N_{total}	F value	Pr(>F)
2	8.631657	0.000185	2	35.33078	1.12E-15
1920	NA	NA	1330	NA	NA
AT	F value	Pr(>F)	AT	F value	Pr(>F)
2	55.5216	3.62E-24	2	3.688203	0.025275
1920	NA	NA	1321	NA	NA
RH	F value	Pr(>F)	RH	F value	Pr(>F)
2	21.97782	3.65E-10	2	2.019814	0.13309
1920	NA	NA	1321	NA	NA
SR	F value	Pr(>F)	SR	F value	Pr(>F)
2	6.292932	0.001888	2	8.762333	0.000166
1920	NA	NA	1321	NA	NA

LIST OF PUBLICATION AND THEIR PROOFS

Urban Climate 51 (2023) 101625

Contents lists available at ScienceDirect

Urban Climate

journal homepage: www.elsevier.com/locate/uclim

Roadside measurements of nanoparticles and their dynamics in relation to traffic sources in Delhi: Impact of restrictions and pollution events

Kanagaraj Rajagopal [a], S. Ramachandran [b], Rajeev Kumar Mishra [a,*]

[a] Department of Environmental Engineering, Delhi Technological University, Delhi 110042, India
[b] Space and Atmospheric Sciences Division, Physical Research Laboratory, Ahmedabad 380009, India

ARTICLE INFO

Keywords:
Nano pollutants
Number concentration
Traffic emission
Ultra fine particles
Urban aerosols

ABSTRACT

Due to rapid urbanization, Delhi experiences frequent pollution events, and the particulate matter load exceeds the prescribed limit often. This study analyzes nanoparticles (10 to 1090 nm) during different emission scenarios, seasonal and meteorological conditions in two phases: April to June 2021 (Period I) and October to November 2021 (Period II). Period I experienced around 31% less concentration of particles ($\sim 2.4 \times 10^4$ cm^{-3}) due to lockdown restrictions and, on the other hand, particle concentration increased by 35% compared to normal conditions due to the sudden rise in firework emissions in Period II. Except for the post-Diwali phase (10^4 cm^{-3} to 10^5 cm^{-3}), the concentrations lie between 10^3 cm^{-3} and 10^5 cm^{-3}. The Aitken modes contribute 10 to 30% of total concentration in both periods. Particles in nucleation and accumulation modes contribute 30 to 40%, 20 to 30%, 15 to 25%, and 35 to 50% in Periods I and II, respectively. Number concentration-based studies are essential for estimating the potential impacts on human health due to air pollution. The study provides information regarding vehicle emission-based particle concentration under various emission scenarios in urban cities, which is crucial for estimation of emissions, health impact assessment, future policy formulation and strategy measures.

1. Introduction

In an urban environment, traffic-related air pollution occurs due to a mixture of both particulate matter and gases in a complex

Abbreviations: Acc, Accumulation mode; AD, After Diwali; AR, After Restriction; BD, Before Diwali; BR, Before Restriction; cm^{-3}, per Cubic Centimeter; CNG, Compressed Natural Gas; COVID-19, Coronavirus Disease - 2019; CPC, Condensed Particle Counter; DMA, Differential Mobility Analyzer; Dp, Diameter of the Particle; DR, During Restriction; DR-II, During Restriction II; DTU, Delhi Technological University; E, East; *E*-Rickshaws, Electric rickshaws; Eqn, Equation; GMD, Geometric Mean Diameter; HCV, Heavy Commercial Vehicle; hpa, hecto pascal pressure unit; Hrs, Hour; ISO, International Organization for Standardization; Latk, Large aitken mode; LCV, Light Commercial Vehicle; LDMA, Large Differential Mobility Analyzer; LPM, Liters Per Minute; m, Meter; MBq, Megabecquerel; m/s, Meter per Second; N, North; NA, Not Applicable; NCT, National Capital Territory; nm, nanometer; Nuc, Nucleation mode; PNC, Particle Number Concentration; RH, Relative Humidity; Satk, Small Aitken Mode; SD, Standard Deviation; S. No, Serial Number; SR, Solar Radiation; SVOC, Soluble Volatile Organic Compounds; AT/Temp, Ambient Temperature; Total, Total Particle Number Concentration; UFP, Ultrafine Particles; USA, United States of America; VOC, Volatile Organic Compounds; W/m^{-2}, Watt per square meter; WS, Wind Speed.

* Corresponding author.
E-mail address: rajeevkumarmishra@dtu.ac.in (R.K. Mishra).

https://doi.org/10.1016/j.uclim.2023.101625
Received 25 October 2022; Received in revised form 20 May 2023; Accepted 22 July 2023
Available online 1 August 2023

Atmospheric Environment 337 (2024) 120773

Contents lists available at ScienceDirect

Atmospheric Environment

journal homepage: www.elsevier.com/locate/atmosenv

Size resolved particle contribution to vehicle induced ultrafine particle number concentration in a metropolitan curbside region

Kanagaraj Rajagopal [a], S. Ramachandran [b], Rajeev Kumar Mishra [a,*]

[a] Department of Environmental Engineering, Delhi Technological University, Delhi, India
[b] Space and Atmospheric Sciences Division, Physical Research Laboratory, Ahmedabad, India

HIGHLIGHTS

- Seasonal nanoparticle number concentration (PNC) in Delhi varies from 10^4 to 10^6 cm^{-3}.
- Particles in nucleation mode contribute >30% to PNC in summer, spring and monsoon.
- Accumulation mode particles contribute >35% to PNC in winter and autumn.
- Higher relative humidity favors coagulation resulting in higher concentration of N_{acc}.
- Correlation between N_{acc} and Carbon Monoxide is higher due to transport emissions.

ARTICLE INFO

Keywords:
Particle number concentration
Seasonal variation
Transport emissions
Urban pollution and meteorology
Implications

ABSTRACT

The concentrations and behavior of nano particles (10–1000 nm) in Delhi, a densely populated megacity, in different seasons (winter, spring, summer, monsoon, and autumn) are examined, for the first time. The concentration of particles is classified into four different sizes as N_{trac} (10–30 nm, nucleation), N_{tatk} (30–50 nm, small Aitken), N_{latk} (50–100 nm, large Aitken), and N_{acc} (100–1000 nm, accumulation mode), and the total (10–1000 nm) particle number concentration (PNC) as N_{total}. PNC ranges between 10^4 cm^{-3} and 10^6 cm^{-3} over Delhi during the year, and the highest concentration occurs in winter. Winter concentration is 2, 1.6 and 1.3 times higher than monsoon, summer, autumn and spring concentrations, respectively. N_{trac}, N_{tatk}, N_{latk} and N_{acc} and their respective contributions to total PNC exhibit significant seasonal variations. During winter N_{latk} and N_{acc} contribute more to total due to coagulation, with N_{acc} alone contributing >40% to total PNC. N_{trac}, N_{tatk}, and N_{latk} are higher in spring and summer during mid-day due to nucleation and/or ultrafine particle burst events. The direct primary emissions from engine exhaust produce a prominent double hump structure during morning and evening peak hours in winter and autumn. PNC and their contributions exhibit day-night variations as they are influenced by variations in emission sources and meteorological parameters (wind speed, relative humidity, temperature, solar radiation and boundary layer height) between day and night. Carbon monoxide correlates positively with N_{acc} in all seasons ($R^2 \geq 0.5$) as fossil fuel emission is a predominant source for gases and particles in the study environment. These quantitative results on seasonal variations of nano particles and air pollutants together with the knowledge on seasonal variations in meteorological parameters and atmospheric dynamics provide a foundation which can positively contribute better to the urban planning and devising mitigation measures aimed at improving air quality and public health.

1. Introduction

The air quality of any region depends on the quantity and quality of different particles present in the atmosphere (Yadav et al., 2021; Zhao et al., 2020). These particles in the atmosphere can cause several health impacts, including cardiovascular and pulmonary diseases (Kanawade et al., 2020; Kaur et al., 2005; Sharma et al., 2024; Schraufnagel, 2020). The particles present in the air vary based on size, shape, and composition, and their potential to create health impact also depends on these characteristics (Gao et al., 2015; Gurjar et al., 2010; Kumar et al., 2011;

* Corresponding author.
E-mail address: rajeevkumarmishra@dtu.ac.in (R.K. Mishra).

https://doi.org/10.1016/j.atmosenv.2024.120773
Received 7 May 2024; Received in revised form 15 August 2024; Accepted 21 August 2024
Available online 23 August 2024

Chemosphere 366 (2024) 143470

Contents lists available at ScienceDirect

Chemosphere

journal homepage: www.elsevier.com/locate/chemosphere

Seasonal variation of particle number concentration in a busy urban street with exposure assessment and deposition in human respiratory tract

Kanagaraj Rajagopal [a], S. Ramachandran [b], Rajeev Kumar Mishra [a,*]

[a] Department of Environmental Engineering, Delhi Technological University, Delhi, 110042, India
[b] Space and Atmospheric Sciences Division, Physical Research Laboratory, Ahmedabad, 380009, India

HIGHLIGHTS

- Ultrafine particles (UFPs) contribute around 60–80 % to total particle number concentration (PNC) over Delhi.
- Inhalation particle number concentration varies between 0.5 and 1 billion over Delhi during the year.
- The particle deposition ranges from 0.43 to 0.26 μg/min over Delhi during the year.
- The concentration of particles in the urban roadside is nearly 30% higher than an environment away from the road.
- The results are crucial for initiating mitigation measures aimed to improve air quality and public health.

GRAPHICAL ABSTRACT

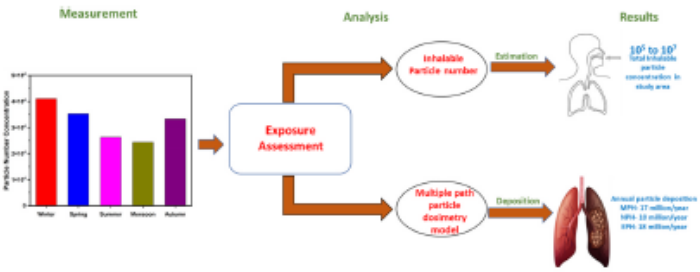

ARTICLE INFO

Handling Editor: Jian-Ying Hu

Keywords:
Air pollution exposure
Human health
Particle dosimetry model
Peak vs. non-peak hours
Ultrafine particles

ABSTRACT

Ultrafine particles (UFP) associated with air quality and health impacts are a major concern in growing urban regions. Concentrations of UFP (particles of size between 10 and 100 nm) and accumulation mode (N_{acc}) (particles of size >100 and up to 1000 nm), are analyzed over a highly polluted megacity, Delhi, in conjunction with vehicular flow density, during peak (morning, and evening) and non-peak hours. UFP contributes ≥60% to total particle concentration during autumn and monsoon. UFP concentrations are about 50,000 particles per cm^3 in winter which reduces to about 25,000 particles during monsoon. N_{acc} are about 20,000 (winter) and 10,000 (monsoon) particles per cm^3. UFP concentration and N_{acc} during peak hours are at least twice higher than those obtained in non-peak hours, confirming the dominant influence of emissions from vehicular exhaust in the study region. Seasonal analysis of UFP size distribution reveals that direct emissions dominate the particle concentrations during winter and autumn, whereas new particle formation mechanism contributes the highest in spring and summer. Assessment of inhalable particle number concentration and particle deposition in the human respiratory tract using Multiple Path Particle Dosimetry (MPPD) model, performed for the first time, shows that the order in which these particles deposit in the human respiratory tract is alveoli > bronchiole > bronchus. The deposition ranges between 10 and 18 million nanoparticles during different hours of the day, whereas the estimated inhalable particle concentration (IPN) varies between 0.5 and 1 billion. Results on the IPN during activities classified from light (walking), medium, heavy, very heavy to severe (long-distance running) provide insights into health effects on vulnerable populations. These quantitative results obtained over a megacity on

* Corresponding author.
E-mail address: rajeevkumarmishra@dtu.ac.in (R.K. Mishra).

https://doi.org/10.1016/j.chemosphere.2024.143470
Received 12 April 2024; Received in revised form 28 August 2024; Accepted 3 October 2024
Available online 3 October 2024

ARTICLE IN PRESS

Atmospheric Pollution Research xxx (xxxx) xxx

Contents lists available at ScienceDirect

Atmospheric Pollution Research

journal homepage: www.elsevier.com/locate/apr

Influence of local meteorology and gaseous pollutant emissions on atmospheric nanoparticle concentrations in a pedestrian way in urban region

Kanagaraj Rajagopal [a], S. Ramachandran [b], Rajeev Kumar Mishra [a,*]

[a] Department of Environmental Engineering, Delhi Technological University, 110042, India
[b] Space and Atmospheric Sciences Division, Physical Research Laboratory, Ahmedabad, 380009, India

ARTICLE INFO

Keywords:
Air pollution
Engine exhausts
Gaseous emissions
Meteorology
Ultrafine particles
Urban climate

ABSTRACT

The roadside environment is one of the major sources of nanoparticle emission in the urban regions. The complex mixture of different pollutants makes it hard to understand the dynamics and behavior of nanoparticles. The study aims to analyze the dynamics of atmospheric nanoparticles ranging from 10 to 1000 nm along with local meteorological conditions and gaseous pollutants in a pedestrian way at a busy street in Delhi, a megalopolis in India, during all five major seasons of the study area. Nucleation mode particles were higher during the spring season, whereas the contribution of Aitken mode particles dominated the total particle number concentrations in the rest of the seasons. Due to the influence of vehicular sources, rush hour concentrations were higher than during non-rush hours. Thus, the diurnal pattern in particle concentration strongly coincided with emissions associated with the vehicular flow. During the winter season, the average total particle number concentration was observed to be maximum (4.1×10^4 cm^{-3}) with a higher surface area of particles of 3.5×10^{-3} mm^2 m^{-3}. Compared to the monsoon season, the concentration of NO_X was 5 times higher in winter. The boundary layer height in the study region ranged from 600 to 2400 m during different seasons, and the maximum ventilation coefficient was observed to be > 3000 m^{2}s^{-1} during summer. Precipitation reduced the concentration of particles by half, from 2.2 x 10^4 to 1.1 x 10^4 cm^{-3}, due to wet scavenging. The study revealed that the concentrations of particles depend not only on primary emissions but also are influenced by local meteorology and other co-emitted pollutants. Understanding the dynamics of atmospheric nanoparticles in urban roadside environments as outlined in this study is crucial to devise necessary mitigation measures for people residing near the road in order to reduce health impact and improve air quality.

1. Introduction

Rapid urbanization and economic growth lead to serious air pollution issues in the Indian subcontinent. The complex mixture of sources contributes to poor air quality in urban cities, with emissions from traffic-related sources dominant among them (Sharma et al., 2024). Exhaust and non-exhaust (break, tyre wear and dust resuspension) emissions are two major emissions classifications from the transportation sector. Traffic-related exhaust emissions originate from different categories of vehicles, such as two, three-wheelers, personal/commercial cars, buses, and heavy vehicles (trucks, lorries, and cranes) (Belkacem et al., 2020; Pandey et al., 2022; Rogula-Kozłowska, 2014; Wu et al., 2021). Engine exhaust emits a wide range of pollutants, such as particulates and gaseous pollutants, based on the type of ignition, fuel used etc. (Myung and Park, 2012; Rajagopal et al., 2023; Yu et al., 2022). Emission norms for vehicles in India are based on the Bharath Stage VI standard with an emission limit for particulate matter (PM) < 4.5 mg/km and nitrogen oxide (NO_X) < 60 mg for petrol and < 80 mg for diesel engines (Rao et al., 2021). Apart from these emissions, the engine exhaust also emits particles that range from a few nanometers to micrometers (Patton et al., 2017; Sabaliauskas et al., 2012; Zhu et al., 2021). The nanoparticle emissions from the engine exhaust are broadly classified as nucleation mode (N_{nuc}, 1–30 nm), Aitken mode (N_{atk}, 30–100 nm), and accumulation mode (N_{acc}, 100–1000 nm) (Kumar

Peer review under responsibility of Turkish National Committee for Air Pollution Research and Control.

* Corresponding author.
E-mail address: rajeevkumarmishra@dtu.ac.in (R.K. Mishra).

https://doi.org/10.1016/j.apr.2024.102358
Received 3 June 2024; Received in revised form 7 November 2024; Accepted 7 November 2024
Available online 8 November 2024

Please cite this article as: Kanagaraj Rajagopal et al., *Atmospheric Pollution Research*, https://doi.org/10.1016/j.apr.2024.102358

Air Quality, Atmosphere & Health (2024) 17:1617–1627
https://doi.org/10.1007/s11869-024-01532-3

Are Delhi residents exposed to lesser particle number concentration due to the firework ban in the city?

Kanagaraj Rajagopal[1] · Vignesh Mohan[1] · Rajeev Kumar Mishra[1]

Received: 18 August 2023 / Accepted: 5 February 2024 / Published online: 29 February 2024

Abstract
Diwali, the fireworks festival of India, adds more atmospheric particles within a short period of time and deteriorates the air quality. Short-term policies like banning crackers during fireworks festivals can help improve urban air quality. The present study analyzed particle number concentration, ranging from 10 to 1000 nm, in 2021 and 2022. A reduction in the concentration of particle number concentration (from 3.8×10^4 cm^{-3} to 3.1×10^4 cm^{-3}) was observed due to the ban on crackers in the urban city of Delhi. The concentration range changes from 10^5 cm^{-3} to 10^4 cm^{-3}. The contribution of different size ranges, Nucleation (10 to 30 nm), Aitken (30 to 100 nm), and Accumulation (100 to 1000 nm) are analyzed. During Diwali day, the Accumulation mode particles contribute to around 60% to 83% to the total particle number concentration. The exposure to total inhalable particle concentration on Diwali (During ban on firecrackers) was reduced by about 18%, i.e., 1.6 million particles per day. The study results show that emissions in urban regions can be reduced significantly by proper implementation of policy and participation from citizens. Reducing particle emissions paves the way for air quality improvement, health impact mitigation, and sustainability. Sustainability goals focus on clean air for all, and health improvement in polluted regions as interim goals, that can be achieved by implementing proper mitigation measures, which consequently help fight climate change.

Keywords Diwali emission · Delhi air quality · Firework emissions · Particle number concentration

Introduction

Diwali is one among the major festivals in India, and it is celebrated by bursting of crackers and lighting of lamps throughout the country every year (Ganguly 2015; Garg and Gupta 2018; Yadav et al. 2019, 2022a). The firecrackers used during the festival use different chemicals such as aluminum, sulfur, potassium nitrate, barium nitrate, charcoal, manganese, strontium nitrate, potassium, and iron dust powder as a composition material for the manufacturing of firecrackers (Nishanth et al. 2012; Perrino et al. 2011; Sateesh et al. 2018). The bursting of crackers emits different types of atmospheric pollutants, such as particulate matter, ultrafine particles, gaseous pollutants, and toxic metals of significant quantity (Chatterjee et al. 2013; Izhar et al. 2018; Vaghmaria et al. 2018; Yerramsetti et al. 2013). These particles stay in the atmosphere for a few days, causing the formation of toxic smog (Cetin 2015; Ertugrul et al. 2019; Ozenen Kavlak et al. 2021). The pollutants are hazardous and cause serious health effects (Kanawade et al. 2014).

Delhi is one of the highly urbanized cities which experiences frequent pollution events. Air quality in the city remains in the poor category for most of the year (Agarwal et al. 2020; Mishra et al. 2016; Mohan and Kumar 2022). The air quality consistently exceeds the national standards (Garg and Gupta 2018; Goyal et al. 2021; Kanawade et al. 2020). Diwali festival usually falls under October and November, the start of the winter season in Delhi (Garg and Gupta 2018; Ghei and Sane 2018). The winter period

Highlights
1. A firework ban can reduce up to 20% to 22% of Aitken and Accumulation mode particles on the Diwali festival.
2. Firework emissions contribute up to 83% of accumulation mode particles in total particle number concentration.
3. Crackers ban reduced inhalable particle concentration on Diwali day, leading to less exposure.
4. The percentage contribution of different size ranges to total particle number concentration is based on the sources present.

✉ Rajeev Kumar Mishra
rajeevkumarmishra@dtu.ac.in

[1] Department of Environmental Engineering, Delhi Technological University, 110042 Delhi, India

Curriculum Vitae/Brief Profile

Kanagaraj Rajagopal

Mobile: +91-9042579948

Mail: udumalaikanagu@gmail.com

To work with an organization which gives me ample opportunity to learn and grow along with the organization and to prove myself worthy of shouldering the responsibilities assigned to me

EDUCATIONAL DETAILS

Education	Institute	Percentage Obtained	Year of completion
Ph.D. Environmental Engineering	Delhi Technological University	_	2024(expected)
M.Tech Green Energy Technology	Pondicherry University	8.2 (CGPA)	2018
B.E Environmental Engineering	Park College of Technology	6.9(CGPA)	2015
HSC	RKR Grks MHSS	78.41	2011
SSLC	RKR Grks MHSS	82.8	2009

WORK EXPERIENCE

YEAR	Role and Organization
May 2015 to June 2016	Jr. Environmental Engineer
2018 (Nov)- 2019(July)	Project Associate/JRF – IIT-Roorkee
2019 (Sep) – 2020 (Jan)	JRF – Delhi Technological University

AREA OF INTEREST

- Ultrafine particles.
- Urban aerosols.
- Gridded emission inventory.
- Air & Noise pollution monitoring.
- Environmental impact assessment.
- Carbon emissions, climate change.

Software Skill

- Arc GIS / QGIS
- Origin
- MATLAB

- R statistical tool
- AirQ+
- Multiple path particle dosimetry model.

PROJECTS / DISSERTATION

- B.E Dissertation - EIA on Residential Building Construction in Coimbatore city.
- Diwali Air and noise pollution study in Coimbatore with Tamilnadu Pollution Control Board (TNPCB) in 2013 &2014.
- Coimbatore city traffic noise pollution study in 2013&2014.
- M.Tech Dissertation - Photocatalytic degradation of Textile dyes using solar concentrating helical tubular reactor.
- Ph.D. Study of nano-size particle dynamics in urban road microenvironment in Delhi.

RESEARCH PROJECTS

- 1. Megacity Delhi atmospheric emission quantification, assessment and impacts (DelhiFlux) URL (https://www.urbanair-india.org/delhiflux) funded by Ministry of Earth Sciences.
- 2. The air pollution study during the Odd-Even Scheme in Delhi was funded by DTU.
- 3. Proxy Relationship of Ultrafine Particles Number Concentration, New Particle Formation and Its Growth Rate in Transport Microenvironment in Delhi funded by CPCB.

SEMINAR / TRAINING/WORKSHOP

- Participated in one day workshop at Park College of Technology, "Carbon sequestration and Climate Change"
- Participated in a two-day seminar on "Emerging trends in the environment" at Kochi conducted by Kerala Environmental Congress.
- Participated in the Smart City conference Organized by Park College of Technology in the year 2015.
- Participated in the MODEL presentation on "GREEN BUILDING DESIGN" at TNAU and bagged 2nd prize (2013).
- Participated in IDEAL IDEA contest conducted by TNAU and WON IInd prize (2014).
- Attended In-plant training in ABC Techno Labs pvt ltd, Coimbatore
- Participated in the MODEL presentation contest conducted by TRP Engineering College, Trichy.
- Participated in the International Workshop on Energy Materials and Devices (IWEMD 2018) organized by Pondicherry University.
- Participated in an International Workshop on Sustainable Building Materials and Construction Conducted by Pondicherry University.
- Participated in Biogas plant Installation and operation workshop at CGET.
- Participated in TNAU Eco-fest 2017 and won First Price in Paper presentation also, the team bagged the Overall Champion trophy for Pondicherry University.

INTERNATIONAL CONFERENCE

1.Kanagaraj Rajagopal, Kanak Sharma, Mayank Goyal, T. Vijayakumar, Rajeev Kumar Mishra (2023). Prediction of fuel usage policy implementation with household air pollution and contributions towards sustainability in Indian subcontinent**.** SERB Sponsored International Conference on "Technological Advancements in Materials and Manufacturing for Industrial Environment from 5th to 6th may at KPRIET.

2. Kanagaraj Rajagopal, S. Ramachandran, Rajeev Kumar Mishra (2022). Measurements of Size Resolved Nanoparticle Concentration and its Distribution in Polluted Urban Environment during Induced Firework Event.7th Indian International Conference on Air Quality Management (IICAQM 2022), organized in association with IIT Madras, IIT Kharagpur, IIT Guwahati, University of California (USA), University of Bath (UK), Asian Institute of Technology (Thailand), Mahidol University (Thailand) and Australian National University (Australia) from 27 November to 1st December 2022 at IIT Madras, India.

3. Kanagaraj Rajagopal, S. Ramachandran, Rajeev Kumar Mishra (2023). Traffic-Induced ultrafine particle concentration in megacity Delhi. 8th Indian International Conference on Air Quality Management (IICAQM 2023) jointly organized by IIT Madras, IISc Bangalore, IIT Guwahati, Australian National University (Australia), Mahidol University (Thailand), University of Bath (UK), Asian Institute of Technology (Thailand), University of California, Riverside (USA), IIT Bombay and IIT Kanpur from 4th to 8th December 2022 at IISc Bangalore, India.

4. Shailendra Kumar Yadav, Monika Sharma, **Kanagaraj Rajagopal**, Vignesh Mohan, Veerendra Sahu, Rajeev Kumar Mishra, Bhola Ram Gurjar (2023). Investigating the effects of Delhi's odd-even vehicle registration policy on particle number concentration**.** International conference on waste recycling and environmental technology (WRET-20254) from 8th to 9th February at BBAU.

MEMBERSHIP

1. Life member of the Air Quality Management Association.
2. Member of Green Energy Forum.
3. Member of the Society for Indoor Environment.
4. Member of the European Geoscience Union.
5. Member of Environmental Engineers Association.
6. Member of The Aerosol Society.

BOOK CHAPTERS PUBLISHED

- Shailendra Kumar Yadav, **Rajagopal, K.**, Priya, A.K., Sharma, G.D., 2020. Smart Waste Management and Energy Extraction from Waste in Indian Smart Cities – A Review, in: Contaminants and Clean Technologies. CRC Press, pp. 321–330. https://doi.org/10.1201/9780429275852-19.
- Shailendra Kumar Yadav, **Rajagopal, K.**, 2019. Hydroponic Treatment System Plant for Canteen Wastewater Treatment in Park College of Technology, in: Zero Waste. CRC Press, pp. 187–202. https://doi.org/10.1201/9780429059247-12.

- Kumar, P, **Rajagopal, K**., 2019. Plastic for Sustainability- Fundamentals of Plastic Waste Management. DBH publishers and distributors, volume-12, pages 142-144 https://doi.org/10.13140/RG.2.2.32476.21128.

RESEARCH PAPER PUBLISHED

- 1**. Rajagopal, K.,** Ramachandran, S., and Mishra, R.K **(2024).** Influence of local meteorology and gaseous emission on atmospheric nanoparticle concentrations in the pedestrian way in the urban region. *Atmospheric pollution research***.** 102358. https://doi.org/10.1016/j.apr.2024.102358.
- 2. Rajagopal, K., Ramachandran, S., & Mishra, R.K (2024). Seasonal variation of particle number concentration measurements in an urban busy street exposure assessment and deposition in human respiratory tract. Chemosphere, 366,143470 https://doi.org/10.1016/j.chemosphere.2024.143470.
- 3. **Rajagopal, K**., Ramachandran, S., & Mishra, R.K. (2024). Size resolved particle contribution to vehicle induced ultrafine particle number concentration in a metropolitan curbside region. Atmopsheric Environment, 337, 120773. https://doi.org/10.1016/j.atmosenv.2024.120773.
- 4. **Rajagopal, K.,** Mohan, V. & Mishra, R.K. (2024). Are Delhi residents exposed to lesser particle number concentration due to the firework ban in the city? Air Quality, Atmosphere & Health, 1-11 https://doi.org/10.1007/s11869-024-01532-3.
- 5. **Rajagopal, K**., Ramachandran, S., & Mishra, R.K. (2023). Roadside measurements of nanoparticles and their dynamics in relation to traffic sources in Delhi: Impact of restrictions and pollution events. Urban Climate, 51, 101625. https://doi.org/10.1016/j.uclim.2023.101625.

TECHNICAL MAGAZINES PUBLISHED

- Operation and Maintenance of STP- an Engineering view (Water Today magazine).
- Operation and Maintenance of Sewage Treatment Plant Non-Engineering View (Water Today magazine).
- Waste Water Generation Estimation and Sustainable Sanitation Development (Water Today magazine).

EDITORIAL IN NEWSPAPER

Telegraph UK: Nanoparticle emissions from Delhi's transport sector could trigger significant health risks: Study – Business Telegraph
Gulf News: Nanoparticle emissions from vehicles in Delhi may raise health risks: Study | India – Gulf News
PTI: Delhi transport sector could trigger significant health risk.
PTI Bhasha: दिल्ली मेंसड़कों पर वाहनों सेननौकण का उत्सर्जनर्ज स्वास्थ्य जोखिमपदौ कर सकता है: अध्ययन
IANS: Nanoparticle emissions from vehicles in Delhi may raise health risks: Study
Money control: Delhi sees rise in nanoparticle emissions, researchers warn of serious health risks
Indian Express: 'Nanoparticles from vehicle fumes can cause acute illness': Study looks at 2021 Delhi data over two periods
Times of India (Delhi): 'After lockdown, 35% rise in nanoparticle emissions' | Delhi News –
Times of India Times of India (Nagpur): Nanoparticles pose a mega risk to Delhi | Nagpur News - Times of India

Mid-day: Nanoparticle emissions from vehicles in Delhi may raise health risks: Study
Economic Times: Nanoparticle emissions from Delhi's transport sector could trigger significant health risks: Study - The Economic Times
ET Auto: Nanoparticle emissions from Delhi's transport sector could trigger significant health risks: Study, ET Auto
Hindustan: दिल्ली की हवा मेंननौकण का खतरनाक स्तर, वज्ञैानि कों नेकि या आगाह, कि न्हेंज्यादा जोखि म?
News9: Delhi witnesses rise in nanoparticle emissions from transport sector that may lead to serious health risks: Study
The Print (Hindi): दिल्ली मेंसड़कों पर वाहनों सेननौकण का उत्सर्जनर्ज स्वास्थ्य जोखिमपदै कर सकता है: अध्ययन – ThePrint Hindi
NewsClick (Hindi): दिल्ली मेंसड़कों पर वाहनों सेननौकण का उत्सर्जनर्ज स्वास्थ्य जोखिमपदै कर सकता है: अध्ययन | न्यज़ू क्लि क
Business Standard: Nanoparticle emissions from vehicles in Delhi pose health risks: Study
Dainik Bhaskar: Nanoparticle emissions from vehicles in Delhi may raise health risks: Study – Bhaskar Live
Navbharat Times: Delhi Air Pollution, दिल्ली की हवा मेंतरै रहा सांस का 'दश्मन', जानेंक्यों डरा रही येनई स्टडी
The Patriot: Study Reveals Potential Health Risks Due to Nanoparticle Emissions from Delhi's Transportation Sector - The Patriot
Climate Samurai: Delhi Grapples with Soaring Levels of Hazardous Nanoparticles in Urban Air: study – Climate Samurai
Hindi Nav Samachar: दिल्ली की शहरी हवा में ननौकणों के बढ़तेस्तर की चेतावनी – नवसचंर समाचार .कॉम
Latestly: देश की खबरें| दिल्ली मेंसड़कों पर वाहनों सेननौकण का उत्सर्जनर्ज स्वास्थ्य जोखि मपदै कर सकता है: अध्ययन | LatestLY हिन्दी
Dynamite News: दिल्ली मेंसड़कों पर वाहनों सेननौकण का उत्सर्जनर्ज स्वास्थ्य जोखि म पदै कर सकता है: अध्ययन - डाइनामाइट न्यज़ू
Siasat Daily: Nanoparticle emissions from vehicles in Delhi may raise health risks: Study
Lokmat Times: Nanoparticle emissions from vehicles in Delhi may raise health risks: Study
Janta Se Rishta: दिल्ली मेंवाहनों सेनि कलनेवाले ननौकणों सेस्वास्थ्य जोखि म बढ़ सकता है: अध्ययन | Nanoparticle emissions from vehicles in Delhi may raise health risks
IBC24: दिल्ली मेंसड़कों पर वाहनों सेननै ोकण का उत्सर्जनर्ज स्वास्थ्य जोखि म पदैकर सकता है: अध्ययन |
ETV Bharat: Nanoparticle emissions from Delhi's transport sector could trigger significant health risks: Study
Newsdrum: Nanoparticle emissions from Delhi's transport sector could trigger significant health risks: Study

DECLARATION

I hereby declare that all the information furnished by me is true to the best of my knowledge and belief.

[Kanagaraj R]

Impact of the Research in online and print media (National and International)

हिन्दु

वाहनों के प्रदूषित कणों से स्वास्थ्य पर पड़ रहा असर

नई दिल्ली, एजेंसी। दिल्ली में सड़क किनारे वातावरण में नैनोकण का खतरनाक स्तर पाया गया है, जिसका सीधा संबंध वाहनों से निकलने वाले धुएं से है। इससे स्वास्थ्य संबंधी चिंताएं बढ़ रही हैं। यह जानकारी एक अध्ययन के दौरान सामने आई। अध्ययन में बताया गया कि मनुष्य के बाल से 600 गुना बारीक होने के कारण ये कण फेफड़ों, रक्त में प्रवेश कर सकते हैं।

पत्रिका 'अर्बन क्लाइमेट' में प्रकाशित इस अध्ययन को उत्तर-पश्चिमी दिल्ली में बवाना रोड पर किया गया था, जो दिल्ली को रोहतक से जोड़ता है। दिल्ली प्रौद्योगिकी विश्वविद्यालय में पर्यावरण अभियांत्रिकी विभाग के सहायक प्रोफेसर राजीव कुमार मिश्रा ने कहा कि अध्ययन में पाया गया है कि जब हवा की गति तेज होती है तो ये कण सड़क के नजदीकी क्षेत्रों में फैल जाते हैं। इससे जोखिम बढ़ जाता है।

[redacted]

'After lockdown, 35% rise in nanoparticle emissions'

Kushagra.Dixit@timesgroup.com

New Delhi: Scientists have found that after the Covid lockdown eased in Delhi, the emission of nanoparticles, which are super-fine pollutants, increased by 35% on the city's roadside.

Nanoparticles are fine pollutants which are about 1/1000th of particulate matter. They cannot be filtered out by N-95 masks.

Scientists in the department of environmental engineering at Delhi Technological University (DTU) and the space and atmospheric sciences division of the Physical Research Laboratory in Ahmedabad did a study on the roadside nanoparticles in Delhi and their impact on health and air quality.

The study, called "Roadside Measurements of Nanoparticles and their Dynamics in Relation to Traffic Sources in Delhi: Impact of Restrictions and Pollution Events", found that after the lockdown, the nanoparticles had increased.

The researchers led by Dr Rajeev Kumar Mishra, faculty in the department of environmental engineering in DTU, professor S Ramachandran of the Physical Research Laboratory, and Kanagaraj Rajagopal, a research scholar in the advance air and acoustics research laboratory in DTU, identified the concentration of the nanoparticles present on the roadside.

The study includes a series of events in 2021, such as the lockdown, pollution events, Diwali and the time period before and after these events. It aims to identify the reduction of nano pollutants based on the emission sources.

In Delhi, 10,000 to 10,00,000 nanoparticles are found in a cubic centimetre of air. During the lockdown period, when vehicles on the road were reduced to around 50%, the nanoparticle concentration was reduced by 31 %. At the same time, events such as Diwali increased nanoparticle concentration up to 35 %, compared to usual emissions," Mishra said, adding that the nanoparticles in the range of 10 to 100-nm size were directly from vehicle engine exhaust that were released on the roadside.

The study said that when windspeed is high, the nano pollutants got dispersed to surrounding regions, increasing exposure among residents living near the road.

"For a city like Delhi, residential zones adjacent to the road will automatically mean higher exposure for residents. The nanoparticles are more vulnerable in terms of human health because they are much smaller than PM2.5 or PM10," the study pointed out.

These nanoparticles are 600 times smaller than the thickness of human hair and can penetrate deep into the lungs and blood stream.

"These nanoparticles have the potential to penetrate our bloodstream and can be deposited in different parts of the human body, including the brain.... People working or living near the road, such as police personnel, street vendors, drivers, motorcyclists, delivery personnel and the urban poor living near the road are more exposed to them," Mishra said.

The study also suggests that policy formulation towards the concentration of the particles was required for reducing their emission from engine sources to mitigate the impact these particles have on the atmosphere and human health.

10th
ary
tia
le, but
ay. We
e still
ill re-
oment
Rohit,
; Neil.

सड़कों के आसपास रहने वालों को नैनोपार्टिकल उत्सर्जन से खतरा

शिप्रा सुमन • वाल्ली दिल्ली

राजधानी में बढ़ते वायु प्रदूषण पर दिल्ली प्रौद्योगिकी विश्वविद्यालय ने सड़क किनारे के वातावरण पर शोध किया है। इसमें पता चला है कि सड़क किनारे के क्षेत्रों में रहने वाले लोगों को नैनोपार्टिकल उत्सर्जन से जोखिम बढ़ सकता है। डीटीयू के पर्यावरण इंजीनियरिंग विभाग के डा. राजीव कुमार मिश्रा के नेतृत्व में शोधकर्ताओं की एक टीम ने इस अध्ययन को पूरा किया। इसमें अहमदाबाद के भौतिक अनुसंधान प्रयोगशाला के प्रो. एस रामचंद्रन और दिल्ली प्रौद्योगिकी विश्वविद्यालय के एडवांस एयर एंड एकोस्टिक्स रिसर्च लेबोरेटरी के रिसर्च स्कालर कनगराज राजगोपाल शामिल रहे।

जीटी करनाल रोड पर मुकरबा चौक के पास उड़ती धूल • हरीश कुमार

यह अध्ययन सड़क किनारे के वातावरण में मौजूद नैनो कणों की सांद्रता को पहचान करने के उद्देश्य से किया गया है। इस शोध को डीटीयू के 'अर्बन क्लाइमेट जर्नल' में विस्तार से दिया गया है।

डा. राजीव कुमार मिश्रा ने बताया कि शोध में वर्ष 2021 में हुए लाकडाउन के दौरान और उसके बाद दिवाली के दौरान, उसके बाद की स्थिति को मुख्य रूप से अध्ययन किया गया है। इसका उद्देश्य उत्सर्जन स्रोतों के आधार पर नैनो प्रदूषकों की कमी की पहचान करना था। इसमें सड़क के किनारे के वातावरण, पैदल चलने वाले राहगीरों के मार्ग में मौजूद नैनो कणों को 10 से 1000 एनएम आकार तक मापा गया। दिल्ली में हवा के 10,000 से 10,00,000 घन सेंटीमीटर नैनोपार्टिकल पाए जाते हैं। इसमें ज्ञात हुआ कि लाक डाउन अवधि के दौरान जब वाहनों का चलना लगभग 50 प्रतिशत तक कम कर दिया गया था, तो नैनोपार्टिकल की एकाग्रता भी 31 प्रतिशत से कम हो गई थी। जबकि इसी बीच दिवाली के दौरान सामान्य उत्सर्जन की तुलना में नैनोपार्टिकल एकाग्रता को 35 प्रतिशत तक बढ़ा दिया।

स्वास्थ्य के लिए अधिक खतरनाक हैं नैनो पार्टिकल्स : शोध में यह पाया गया कि सीधे वाहन इंजन से निकलने वाले 10 से 100 नैनो मीटर आकार के नैनोपार्टिकल सड़क के किनारे के क्षेत्रों में अधिक पाए गए। जब हवा की गति अधिक होती है, तो सड़क के किनारे नैनो प्रदूषक सड़क के आसपास के क्षेत्रों में फैल जाते हैं, जिससे सड़क के पास रहने वाले निवासियों के लिए जोखिम बढ़ सकता है। नैनोपार्टिकल स्वास्थ्य के लिहाज से अधिक असुरक्षित हैं, क्योंकि यह पीएम 2.5 या पीएम 10 की तुलना मानव बाल के आकार से 600 गुना छोटे हैं, इसलिए फेफड़ों में प्रवेश कर सकते हैं। नैनो कणों में हमारे रक्तप्रवाह में प्रवेश करने की क्षमता है। यह मस्तिष्क के हिस्सों में जमा हो सकते हैं।

worldautoforum.com/nanoparticle-emissions-from-delhis-transport-sector-could-trigger-significant-health-risks-study/

World Auto Forum — Connect, Grow, Share, Win! — 14 Glorious Years

Search..

WAF AUTO NEWS

HOME | MEMBERS ZONE | WAF PROGRAMS | NEWS | WAF TV | THINK TANK | CXO CAFÉ | WAF ROCKSTARS | ANNUAL PARTNERS | WAF VENTURES

Contact us

...nanoparticle emissions from Delhi's transport sector could

RECENT POSTS

- Overwhelming Response to 7th WAFit! – AI at Automotive | Triggered Industry Leaders | Stellar Media Coverage
- MG Motor retail sales up 31% in Sep at 5,003 units
- Govt aims to complete about 85% of road projects on time this fiscal: Anurag Jain
- Hindustan Zinc signs deal to deploy GreenLine's LNG-powered trucks
- Epsilon inks pact to acquire Johnson Matthey's LFP cathode tech centre in Germany

RECENT COMMENTS

- Obraz Galeria Sztuki on Elon Musk and others urge AI pause, citing 'risks to society'

CATEGORIES

- Auto Expo
- Auto Expo
- AutoNews
- MasterClass
- NewsWires

timesofindia.indiatimes.com/city/delhi/after-lockdown-35-rise-in-nanoparticle-emissions/articleshow/104150869.cms?from=mdr

LIVE VIDEO | Medithon Session 4 | Heart care

NEWS / CITY NEWS / DELHI NEWS / 'After Lockdown, 35% Rise In Nanoparticle Emissions'

TRENDING | Chennai Airport | Bangalore School Timings | Varanasi Car Accident | Bihar Caste Census | Sanjay Singh

'After lockdown, 35% rise in nanoparticle emissions'

Kushagra Dixit / TNN / Updated: Oct 4, 2023, 11:43 IST

195 PTS | SHARE | AA | FOLLOW US

You're Reading

'After lockdown, 35% rise in nanoparticle emissions'

Tech on the rise in India! Here's how the MIT xPRO program can help...

A study conducted in Delhi found that the emission of nanoparticles, which are fine pollutants, increased by 35% on the city's roadside after the Covid lockdown eased. These nanoparticles, which are 1/1000th the size of particulate matter, c ... Read More

ADVERTISEMENT

Trending Stories

In City | Entire Website

दिप्रिंट

राजनीति | देश | डिफेंस | एजुकेशन | हेल्थ | अर्थजगत | विदेश | मत-विमत | समाज-संस्कृति

होम » देश » दिल्ली में सड़कों पर वाहनों से नैनोकण का उत्सर्जन स्वास्थ्य जोखिम पैदा कर सकता है : अध्ययन

देश

दिल्ली में सड़कों पर वाहनों से नैनोकण का उत्सर्जन स्वास्थ्य जोखिम पैदा कर सकता है : अध्ययन

भाषा 3 October, 2023 04:25 pm IST

Like 0

लोकप्रिय

- 'मारने की साजिश', इमरान खान की पत्नी बुशरा बीबी ने IHC में लगाई गुहार, बोलीं- उन्हें जहर दिया जा सकता है
  दिप्रिंट टीम · 3 October, 2023
- आधे घंटे में दो बार आया दिल्ली-NCR में भूकंप, कुछ सेकेंड तक कांपती रही धरती
  दिप्रिंट टीम · 3 October, 2023

Sections

Tuesday, Oct 03, 2023
EPAPER | TODAY'S PAPER

ENGLISH | தமிழ் | বাংলা | മലയാളം | ગુજરાતી | हिंदी | मराठी | BUSINESS | बिज़नेस

Newsletters

The Indian EXPRESS
JOURNALISM OF COURAGE

Home Delhi India Explained Opinion Entertainment Sports Politics Lifestyle Tech Education Investigations Research Videos Audio SUBSCRIBE Sign In

TRENDING Mini Crosswords Join WhatsApp Channel Latest News Top News Asian Games Premium Stories UPSC Special Health Specials

News / Cities / Delhi / 'Nanoparticles from vehicle fumes can cause acute illness': Study looks at 2021 Delhi data over two periods

'Nanoparticles from vehicle fumes can cause acute illness': Study looks at 2021 Delhi data over two periods

The study analysed nanoparticles (10 to 1090 nanometers in diameter) in the city in 2021, over two periods — from April to June, and October to November. These "very small particles" may come from natural sources or from human activities.

By: Express News Service
New Delhi | October 4, 2023 03:53 IST

Follow Us

NewsGuard

LIVE BLOG

Mumbai News Live Updates: 31 deaths at Nanded hospital expose state's flawed medicine procurement; CM denies shortage of
2 hours ago

Delhi News Live Updates: NewsClick founder Prabir Purkayastha arrested

siasat.com/nanoparticle-emissions-from-vehicles-in-delhi-may-raise-health-risks-study-2712826/

سیاست
The Siasat Daily

Home Telangana Hyderabad India Middle East Entertainment Business Photos Videos

Siasat.com / News / Delhi / Nanoparticle emissions from vehicles in Delhi may raise health risks: Study

Nanoparticle emissions from vehicles in Delhi may raise health risks: Study

Due to rapid urbanisation, Delhi experiences frequent pollution events, and the particulate matter load exceeds the prescribed limit often.

IANS Indo-Asian News Service | Posted by Mansoor Hameed | Published: 4th October 2023 8:24 pm IST

TRENDING NEWS

To perform at a birthday in Delhi, Salman Khan charged Rs...

List of 5 upcoming movies of Salman Khan

List of most educated countries in the world: Know where India stands

sakshipost.com/news/nanoparticle-emissions-vehicles-delhi-may-raise-health-risks-study-235047

SAKSHI POST

Live TV EPaper Telugu Education Y.S.R Careers

Search..

Today's News AP Telangana National World Entertainment Sports Lifestyle Photos Others

Home » Lifestyle

Nanoparticle emissions from vehicles in Delhi may raise health risks: Study

Oct 04, 2023, 18:35 IST

Latest

'Border 2' casting is not finalised, clears Nidhi Dutta
October 05, 2023

republicworld.com/india-news/general-news/nanoparticle-emissions-from-delhis-transport-sector-could-trigger-significant-health-risks-study-articleshow.html

View in Hindi: R. भारत
View in Bangla: R. বাংলা
View in Kannada: R. ಕನ್ನಡ

R. REPUBLICWORLD.COM

LIVE TV

The Debate | India News | Politics News | Business News | Web Stories | Sports News | World News | Education News | Entert

English News / India News / General News / Nanoparticle emissions from Delhi's transport sector could trigger significant health risks: Study

Last Updated: 3rd October, 2023 22:14 IST

Nanoparticle Emissions From Delhi's Transport Sector Could Trigger Significant Health Risks: Study

The study looked at different sizes of nanopollutants, ranging from 10 to 1000 nm, as well as how many vehicles were on the road and the weather conditions.

General News | Written By Press Trust Of India

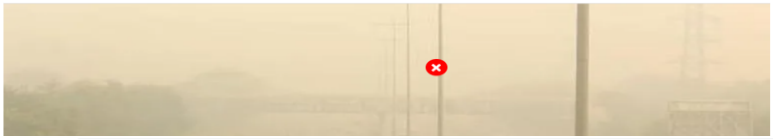

PRESS TRUST OF INDIA

Search... | Subscriber Login

MAIN PAGE | NATIONAL | FOREIGN | GAME | MEANING | APPOINTMENT | FEATURE | FROM BOOKS | PRESS RELEASE | FACT CHECK | PTI ENGLISH

National

Nanoparticle emissions from vehicles on Delhi roads may pose health risks: Study

Updated: Oct 3 2023 4:26PM

New Delhi, October 3 (Language) Dangerous levels of nanoparticles have been found in the air of Delhi, especially in the roadside environment, which is directly related to the smoke emitted from vehicles and is raising health concerns. This information was obtained from a study.

Nanoparticles are extremely small particles, whose diameter often ranges from 10 to 1000 nanometers (nm).

Please log in to get detailed story.

IMPORTANT NEWS

- Modi to inaugurate and lay foundation stone of projects worth Rs 12,600 crore in Madhya Pradesh today
- BJP's "anti-OBC DNA" exposed on caste census: Surjewala
- BJP leaders protest near AAP office, demand Kejriwal's resignation
- ED raids premises of AAP MP Sanjay Singh in case related to Delhi Excise Policy
- Handcuffs are not far away: BJP tells Kejriwal after ED raids at Sanjay Singh's residence
- Three people dead, 23 army personnel missing after flash floods in Sikkim
- Privilege Committee will hold its first meeting on Danish Ali-Bidhuri dispute case on October 10.

PRESS TRUST OF INDIA

PRESSBEE برس بي
Trusted Sources مصادر موثوقة

Home | News | Middle East | Contact US

Nanoparticle emissions from vehicles in Delhi may raise health risks: Study

News room odisha - News

Latest News

- â□□Battle of the Kensâ□□: Dem senator mocks vote to remove McCarthy, â□□outtake from â□□The Hunger Gamesâ□□â□□
- Catherine Kennedy Anderson – Celebrity Wife, Marketing and Communication Director | Wiki, Age, Height, Net Worth, Relationship, Ethnicity, Career
- Football rumours: Kaoru Mitoma has heart set on re-signing with Brighton
- 14 CapRadio board members resign, citing lack of support from Sac State

October 3, 2023

patriot

Reports | Cinema | Culture & Books | Delhi | Profile | Sports | Lifestyle | Health and Wellness | Preview | Photo Feature | Buzz | Community

Epaper | Videos | About us

HOME / DELHI NCR / STUDY REVEALS POTENTIAL HEALTH RISKS DUE TO NANOPARTICLE EMISSIONS FROM DELHI'S TRANSPORTATION SECTOR

Delhi NCR | Environment

Study Reveals Potential Health Risks Due to Nanoparticle Emissions from Delhi's Transportation Sector

October 3, 2023 PATRIOT BUREAU

Nanoparticles in the size range of 10 to 1000 nm, directly linked to vehicular engine exhaust, were found to be more prevalent in roadside areas. During periods of high wind speed, these particles dispersed into the surrounding regions near the road, potentially increasing exposure to nearby residents

Latest Popular Trending

Delhi NCR Environment
Study Reveals Potential Health Risks Due to Nanoparticle Emissions from Delhi's Transportation Sector

Delhi NCR Preview
Echoes and Constellation: KNMA kickstarts the Cultural Season

Delhi NCR
6.2 magnitude quake in Nepal, strong tremors in Delhi-NCR

onlymyhealth.com/nanoparticle-emissions-from-vehicles-could-lead-to-health-problems-study-in-hindi-1696502997

Onlymyhealth | Hindi | SHORTS | Search | Check BMI

MENU | Dabur Vedic Tea | IVF Special | Health and diseases | Diet and fitness | grooming tips | parenting | pregnancy | web stories | children's names

Health - Health News - Latest

Study: Health problems increase due to exposure to nano particles emitted from vehicles.

According to a recent study, nano particles found in Delhi's vehicles can harm health. Let us know about it.

Written by: Kunal Mishra Updated at: Oct 05, 2023 16:28 IST

SHARE

MORE FOR YOU

Eye Care Tips: How to choose eye glasses to keep eyes healthy while driving? Learn

newsdrum.in/national/nanoparticle-emissions-from-delhis-transport-sector-could-trigger-significant-health-risks-study-1435200

NEWS DRUM

NATIONAL | INTERNATIONAL | ANALYSIS | OPINION | BUSINESS | PERSONAL FINANCE | SPORTS | TECHNOLOGY | LIFESTYLE | ENTERTAINMENT

#National

Nanoparticle emissions from Delhi's transport sector could trigger significant health risks: Study

NewsDrum Desk
03 Oct 2023

Follow Us

Subscribe to our Newsletter!

Be the first to get exclusive offers and the latest news

Your Name

Email address

I'm not a robot

Subscribe Now

Latest Stories

Mumbai suburban train services partially hit due to non-completion of rail...

NEWS CLICK | राजनीति | अर्थव्यवस्था | विज्ञान | संस्कृति | भारत | अंतरराष्ट्रीय | हमारे लेख | हमारे वीडियो | English

आप एक स्वतंत्र और सवाल पूछने वाले मीडिया के हक़दार हैं। हमें आप जैसे पाठक चाहिए। स्वतंत्र और बेबाक मीडिया का समर्थन करें। सदस्यता लें और समर्थन करें।

दिल्ली में सड़कों पर वाहनों से नैनोकण का उत्सर्जन स्वास्थ्य जोखिम पैदा कर सकता है : अध्ययन

भाषा | 03 Oct 2023 पर्यावरण

ये कण पीएम 2.5 (हवा में मौजूद 2.5 माइक्रो मीटर से कम व्यास के कण) या पीएम 10 की तुलना में बहुत छोटे आकार के होने के कारण मानव स्वास्थ्य के लिए अधिक खतरनाक हैं।

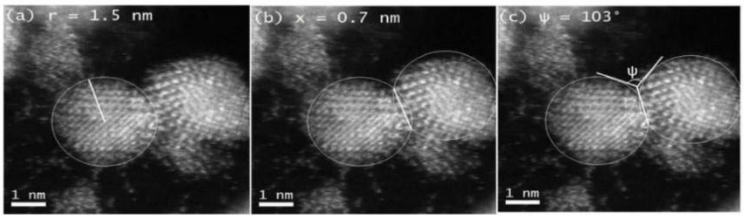

Photo Courtesy : ResearchGate

RELATED STORIES

- दिल्ली सरकार ने सर्दियों में प्रदूषण रोकने के लिए पटाखों की बिक्री, इस्तेमा...
- दुनिया के सबसे प्रदूषित शहर दिल्ली में लोगों की जीवन प्रत्याशा 11.9 सा...
- यमुना का जलस्तर धीरे-धीरे घट रहा, भारी बारिश नहीं हुई तो हालात जल्द...
- दिल्ली : यमुना नदी का पानी आईटीओ, राजघाट में घुसा
- दिल्ली में वायु गुणवत्ता 'ख़राब' श्रेणी में पहुंची
- दिल्ली की वायु गुणवत्ता 'ख़राब' श्रेणी में पहुंची

news9live.com/health/delhi-witnesses-rise-in-nanoparticle-emissions-from-transport-sector-that-may-lead-to-serious-health-risks-study-2308001

ENG | news9 | HOME | LATEST | WEB STORIES | INDIA | LIFE Goals | SPORTS | ENTERTAINMENT | CRIME | KNOWLEDGE | HEALTH | VIDEOS | PHOTOS | MORE

Join News9 On WhatsApp | Earthquake | World Cup 2023 | Business News | Karnataka News | Bengaluru News | BULLISH ON INDIA

Home » Health » Delhi Witnesses Rise In Nanoparticle Emissions From Transport Sector...

Delhi witnesses rise in nanoparticle emissions from transport sector that may lead to serious health risks: Study

Nanoparticles are very dangerous since they may enter the lungs, circulation, and even the brain deeply and are considerably smaller than PM 2.5 or PM 10 (600 times smaller than human hair).

Written By: Sneha Kumari
Updated On: 04 Oct 2023 11:39:AM

Latest News

This 250-metre-long tunnel at Mahakal Temple will ensure darshan for 8 lakh devotees | Watch

District Magistrate Kumar Purushottam said that the tunnel will open behind the temple's sanctum sanctorum. There has been a significant ...
6 minutes ago

Trevor Noah wraps India tour with Taj Mahal

मुद्दे October 3, 2023

दिल्ली की शहरी हवा में नैनोकणों के बढ़ते स्तर की चेतावनी

नवसंचार समाचार .कॉम

Search here

- Create an Account
- Your Profile
- लेख भेजना Submit Article
- Email
- मानद संबद्ध संपादक मंडल

संपर्क सिर्फ ई- पत्र से या मोबाइल पर , पत्राचार नहीं—शैलेश कुमार, संपादक

****
****

****

ललित जैन

Shailesh
October 12, 2012

बद्रि चटर्जी :: दिल्ली की शहरी हवा में नैनोकणों के बढ़ते स्तर की चेतावनी दी गई है, जिससे लोगों, खासकर सड़कों के पास रहने वाले लोगों के स्वास्थ्य को गंभीर खतरा हो सकता है। जैसे-जैसे सर्दी और उसके साथ हवा की गुणवत्ता में गिरावट का मौसम आता है, अध्ययन से पता चलता है कि नागरिक, विशेषकर सड़कों के पास रहने वाले लोग, विशेष रूप से जोखिम में हैं।

केवल 10 से 1000 नैनोमीटर व्यास वाले ये नैनोकण अदृश्य हैं लेकिन अत्यधिक खतरनाक हैं। मानव बाल से 600 गुना छोटे होने के कारण, वे फेफड़ों, रक्तप्रवाह और यहां तक कि मस्तिष्क में भी गहराई तक प्रवेश करते हैं।

एशियन गेम्स 2023

NBT नवभारत टाइम्स Hindi

IND | अपना बाजार | LOGIN

NBT+ चुनाव राज्य मनोरंजन लाइफस्टाइल धर्म दुनिया खेल बिजनेस टेक COP-28

दिल्ली ईपेपर राजनीति अन्य खबरें

ट्रेंडिंग #ब्रेकिंग न्यूज #संजय सिंह के घर रेड #दिल्ली मौसम अपडेट #एशियन गेम्स

Hindi News / Metro / Delhi / Other News / Delhi Air Pollution Study Show Nanoparticle Emissions From Vehicles Pose Health Risks:

दिल्ली की हवा में तैर रहा सांस का 'दुश्मन', जानें क्यों डरा रही ये नई स्टडी

Edited By अनिल कुमार | भाषा | Updated: 3 Oct 2023, 6:19 pm

Subscribe YouTube 8M

दिल्ली में सर्दियों को बढ़ते ही प्रदूषण का लेवल बढ़ जाता है। इसमें दिल्ली के आसपार हरियाणा और पंजाब में पराली का जलना प्रमुख कारण होता। इस बीच प्रदूषण को लेकर एक स्टडी सामने आई हैं। यह...

Match 9, ICC Men's T20 World Cup Su...
4 OCT MDV 9/1 2.5 ov KUW
Play In Progress

आज का तापमान
31°C दिल्ली H 33 / L 24 Clear

Markets News Tech/Startups Portfolio Commodities Mutual Funds Personal Finance Forum Videos Invest Now Subscription

Business Markets Stocks Economy Companies Trends IPO Opinion EV Special

Delhi sees rise in nanoparticle emissions, researchers warn of serious health risks

Nanoparticles are highly hazardous because they are much smaller than PM 2.5 or PM 10 — 600 times smaller than human hair — and can penetrate deep into the lungs, bloodstream, and even the brain

MONEYCONTROL NEWS | OCTOBER 03, 2023 / 08:09 PM IST

mid-day.com/lifestyle/health-and-fitness/article/nanoparticle-emissions-from-vehicles-in-delhi-may-raise-health-risks-study-23312642

Search Here | 05 October, 2023 (Thursday) | Web Stories | Shots | Today's E-Paper

Mid-day Gujarati Inquilab

mid-day SUBSCRIBE

Mumbai News Entertainment Sports Lifestyle Photos Podcast Timepass Sunday Mid-Day Mumbai Guide Videos Brand Media Mid-Day Gold Multispeciality Hospital Survey

Ganpati Contest NEW | Text Shots | City News | News for You | Web Stories | Crime News | Bollywood News | Monsoon Special | Horoscope

Breaking News | ...iness in Chembur high-rise! | Fuel station planned near WEH: Mumbai's Aarey forest will shrink some more | Maharashtra: Metal wire walls make Matheran trails s

Home > Lifestyle News > Health And Fitness News > Article > Nanoparticle emissions from vehicles in Delhi may raise health risks Study

Nanoparticle emissions from vehicles in Delhi may raise health risks: Study

Updated on: 05 October,2023 12:37 PM IST | New Delhi
IANS |

Share: FOLLOW ON Google News Text AA AA

Due to rapid urbanisation, Delhi experiences frequent pollution events, and the particulate matter load exceeds the prescribed limit often

Share

More Stories

Mumbai LIVE: 4 held over cannabis

medlarge.com/news/top-news/nanoparticle-emissions-from-transport-major-health-risk-in-delhi-study

HOME | SHORT NEWS | COVID-19 UPDATES | HOSPITALS | IN CONVERSATION | RESEARCH | ABOUT | PRIVACY POLICY | मेडलार्ज – हिन्दी

Nanoparticle emissions from transport major health risk in Delhi: Study

(2 votes, average: 5.00 out of 5)

October 3, 2023 Medlarge Top News, Latest

Trending

Mandaviya refutes allegations of reducing NEET PG Cut Off for daughter

lokmattimes.com/international/nanoparticle-emissions-from-vehicles-in-delhi-may-raise-health-risks-study-1/

Download App | Epaper | LOKMAT TIMES | Marathi | Hindi | FOLLOW US : | Google News | City

City | Latest News | Cricket | National | International | Maharashtra | Chhatrapati Sambhajinagar | Nagpur | Entertainment | More

Nanoparticle emissions from vehicles in Delhi may raise health risks: Study

By IANS | Published: October 4, 2023 06:30 PM

New Delhi, Oct 4 Vehicular emissions that release toxic nanoparticles in Delhi may be hazardous to health, according ...

हिन्दुस्तान | FREE e-paper | select City | sign in | Write here

home | NCR | Cricket | live score | Country | Entertainment | education | Photo | Video | Foreign | Business | career | Religion

trending news

Temperature falling rapidly in Delhi, sky will be clear today

Good news for thousands of Home Guard soldiers, services extended for 6 more months

Terrorists wanted to terrorize Delhi on Diwali, planned bomb blasts at 6 places

Took away laptop and mobile, police also brought Abhisar to the police station; Raid on NewsClick

Immediate action will be taken on women's complaint, All Women PCR will be run in Delhi

hindi news ▸ NCR ▸ Dangerous level of nanoparticles in Delhi's air, scientists ...

Dangerous level of nanoparticles in Delhi's air, scientists warn, who is at greater risk?

There are often discussions about pollution in Delhi. Now dangerous levels of nanoparticles have been found in the air of Delhi, especially in the roadside environment. Scientists have warned about this.

Krishna Singh • Bhasha, New Delhi

must read

If you are going to invest money in Suzlon Energy shares then definitely read this news.

Students offered namaz in school program, Hindu organizations created ruckus; Gujarat government ordered investigation

Eclipse October 2023: Temples will be closed before this eclipse, know when is Sutak period starting?

Formula milk can increase the risk of obesity in children, study revealed

How will this new change in GST law affect businessmen? Know the advantages and disadvantages of DRC-01C

Wednesday, October 04, 2023 latest news

लेटेस्टली

QUICKLY # SOCIALLY COUNTRY FOREIGN TAKE AUTO GAME ENTERTAINMENT LIFESTYLE VIRAL

PHOTO GALLERY VIDEO ELECTION

Home / Agency News

Country news Nanoparticle emissions from vehicles on Delhi roads may pose health risks: Study

Get Latest Hindi News, Breaking News on India at LatestLY Hindi. Dangerous levels of nanoparticles have been found in Delhi's air, especially in the roadside environment, which is directly linked to vehicle exhaust and is raising health concerns. This information was obtained from a study.

Agency News Bhasha | Oct 03, 2023 04:16 PM IST A- A+

New Delhi, October 3 Dangerous levels of nanoparticles have been found in Delhi's air, especially in the roadside environment, which is directly linked to vehicle exhaust and is raising healt

Google News Telegram Bot

LATEST NEWS TRENDING NEWS

Ram Charan spotted barefoot at Mumbai airport, RRR actor's simplicity won the hearts of fans (Watch Video)

ICC ODI World Cup 2023: Before the ODI World Cup, Michael Vaughan predicted the teams to reach the semi-finals, Australia did not get a place.

Maharashtra: Political turmoil intensifies in Maharashtra, Ajit Pawar angry! Shinde-Fadnavis met Amit Shah

Fake Universities List: Beware! Delhi has the highest number of fake universities, UGC released a new list

Mark Zuckerberg Injured: Meta CEO

LATEST LY

jantaserishta.com/science/nanoparticle-emissions-from-vehicles-in-delhi-may-raise-health-risks-study-2878868

दिल्ली-एनसीआर भारत राज्य छत्तीसगढ़ PHOTO STORIES विश्व मनोरंजन वीडियो खेल धर्म-अध्यात्म विज्ञान CG-DPR EPAPER व्यापार जरा हटके प्रौढो

लाइफ स्टाइल सम्पादकीय लेख

विज्ञान

दिल्ली में वाहनों से निकलने वाले नैनोकणों से स्वास्थ्य जोखिम बढ़ सकता है: अध्ययन

₹165.45

Neha Yadav 4 Oct 2023 8:51 PM

जनता से रिश्ता 11 अक्टूबर से रद्द रहेगी दुर्ग-गो पैसेंजर, कई ट्रेनें भी प्रभावित

jansatta.com/national/nano-particle-emission-from-vehicles-in-delhi-is-a-health-threat/3029276/

Thursday, October 5, 2023 English | தமிழ் | বাংলা | മലയാളം | ગુજરાતી | हिंदी | मराठी | Business | बिज़नेस | Insurance हमें फॉलो करें

जनसत्ता Sign

राष्ट्रीय मनोरंजन खेल फोटो विजुअल स्टोरीज वीडियो ऑटो राशिफल आस्था मुद्दा समझें टेक्नोलॉजी राज्य ट्रेंडिंग विचार अंतरराष्ट्रीय ऑडियो

Jansatta Special Elections Health & Fitness Hindi Kahaniya

जरूर पढ़िए संजय सिंह तक कैसे पहुंची दिल्ली शराब घोटाले की आंच, दिनेश अरोड़ा से क्या है केजरीवाल का कनेक्शन? शर्मा

Hindi News / National / Nano Particle Emission From Vehicles In Delhi Is A Health Threat

दिल्ली में वाहनों से नैनो-कण का उत्सर्जन स्वास्थ्य के लिए खतरा

अध्ययन के अनुसार, 10 से 1000 एनएम आकार के नैनोकण का सबसे अधिक असर सड़क किनारे के स्थानों पर पाया गया।

Written by एजेंसी | Edited by Bishwa Nath Jha

नई दिल्ली | October 4, 2023 12:02 IST

हमें फॉलो करें

अपडेट

Japan Earthquake: जापान में 6.6 तीव्रता के भूकंप के झटके, सुनामी का अलर्ट जारी

ग्रहों के राजकुमार बुध करेंगे तुला राशि में प्रवेश, इन 3 राशि वालों के शुरू होंगे अच्छे दिन, हर कार्य में मिलेगी सफलता

Vidyut Jamwal Wedding: विद्युत जामवाल के घर जल्द बजेगी शहनाई, लंदन में होगी शादी की रस्में! जानिए कौन है होने वाली दुल्हनिया?

Amazon Great Indian Festival: फ्लिप डिजाइन वाले


in.investing.com/news/nanoparticle-emissions-from-vehicles-in-delhi-may-raise-health-risks-study-3836110
Investing.com
Sign In
Sign Up
MARKETS
TOOLS
NEWS & ANALYSIS
News : Latest News Most Popular News Forex News Commodities News Stock Market News Economic Indicators
Notifications
Saved Items
My Portfolio
Public Channels
Crude Oil WTI
HDFC Bank
Reliance Industries
Steel Authority
SBI
Tata Consultancy
Suzlon Energy
Larsen & Toubro
Nanoparticle emissions from vehicles in Delhi may raise health risks: Study
IANS • General News • 2023-10-04 13:16
PORTFOLIO
Indices Commodities Shares
Majors Futures
Nifty 50 19,653.05 +107.30 +0.55%
BSE Sensex 65,938.16 +306.59 +0.47%
Nifty Bank 44,358.70 +145.35 +0.33%
Nasdaq 100 14,723.22 -53.03 -0.36%
S&P 500 4,258.19 -5.56 -0.13%
Major World Indices
Name Chg% Adv. / Dec
Nifty 50 +0.52%
BSE Sensex +0.48%
Nifty Bank +0.31%
Nasdaq 100 -0.36%
S&P 500 -0.13%


india.postsen.com/local/1141361.html
HOME BREAKING NEWS SPORTS BUSINESS LOCAL TECHNOLOGY WORLD COVID-19 HEALTH
TRENDS LIFESTYLE MOVIES MUSIC TV BOOKS ART CELEBRITIES
Nanoparticle emissions from vehicles on Delhi roads may pose health risks: Study
LOCAL Wallace Local a day ago REPORT
(b) x = 0.7 nm
(c) ψ =
1 nm
1 nm
Nanoparticle emissions from vehicles on Delhi roads may pose health risks: Study
The story of a police officer who lives with a bullet fired by Veerappan's accomplices
2 months ago
Big news for railway passengers in Haryana! Rohtak-Maham-Hansi railway project work completed, trains will run on the track from this day
LOCAL
a day ago
Pink cold has entered Haryana, see how the weather will be in the coming days.
LOCAL
a day ago


IBC24
सवाल आपका है
शहर प्रदेश विधानसभा चुनाव 2023 देश दुनिया खेल वीडियो बिज़नेस एंटरटेनमेंट
HOT NOW
#SarkarOnIBC24 #ibc24mindsummit #IBC24JanSamvad #JanKarwan #23MePradesh24MeDesh
Home » Country » Nanoparticles emissions from vehicles on roads in Delhi could pose health risks: Study
दिल्ली में सड़कों पर वाहनों से नैनोकण का उत्सर्जन स्वास्थ्य जोखिम पैदा कर सकता है : अध्ययन
दिल्ली में सड़कों पर वाहनों से नैनोकण का उत्सर्जन स्वास्थ्य जोखिम पैदा कर सकता है : अध्ययन
:Bhasha October 3, 2023 / 04:10 PM IST
IBC24
BREAKING
बड़ी खबर

ianslive.in/nanoparticle-emissions-from-vehicles-in-delhi-may-raise-health-risks-study--20231004181506

OCTOBER 5, 2023 | FOLLOW US:

IANS live

Home | National | Sports | International | Business | Entertainment | Science & Technology

Nanoparticle emissions from vehicles in Delhi may raise health risks: Study

BY IANS

jooble

LATEST NEWS

Amitabh praises 'Aai' technology: 'Nothing can repla...

King to drop his new album 'New Life': 'Sometimes being...

msn.com/hi-in/news/other/द-ल्ल-क-हव-में-नेन-कण-क-खतरन-क-स्तर-वेज्ञ-न-क-ं-ने-क-य-आग-ह-क-न्हें-ज्य-द-ज-ख-म/ar-AA1hCDDd

Start | वेब पर खोज करें | साइन इन करें

find out | Personalize

Hindustan + Follow

Dangerous level of nanoparticles in Delhi's air, scientists warn, who is at greater risk?

Story by Language• 1day 1 day

delhi pollution

PMP® Online Course - Training Partner By PMI - Learn From Home - Online Class

Simplilearn

Visit Hindustan

England vs New Zealand Live Score: World Cup 2023 starts fro...

PM Modi Rajasthan MP Visit Live: PM Modi reaches Jodhpur in...

After Bihar, in another state OBC is more than others, this much...

gyanhigyan.com/national/society/nanoparticle-emissions-from-vehicles-in-delhi-may-raise/cid12377366.htm

HOME / NATIONAL / SOCIETY

Nanoparticle emissions from vehicles in Delhi may raise health risks: Study

New Delhi, Oct 4 (IANS) Vehicular emissions that release toxic nanoparticles in Delhi may be hazardous to health, according to a study.

By GyanhiGyan Desk | Oct 4, 2023, 18:30 IST

LATEST NEWS

THU,5 OCT 2023
Finding More Than Romance: 4 Tips for Making Travel Friends on Dating Apps

THU,5 OCT 2023
Gurminder Singh new Advocate General of Punjab

THU,5 OCT 2023
Delhi Excise Policy case: SC clarifies question was not to implicate AAP

THU,5 OCT 2023
'Border 2' casting is not finalised, clears Nidhi Dutta

POLITICS

SAT,24 SEP 2022
Why Manipur HC declared Lorho S Pfoze's MP candidature null and void

SAT,24 SEP 2022
INDIAN DIPLOMAT: Peace in the subcontinent will be possible only when...

gulfnews.com/world/asia/india/nanoparticle-emissions-from-vehicles-in-delhi-may-raise-health-risks-study-1.1696428798372

MENU | GULF NEWS | INDIA | Dhuhr 12:10PM | Subscribe now

Nanoparticle emissions from vehicles in Delhi may raise health risks: Study

Due to rapid urbanisation, Delhi experiences frequent pollution events

Published: October 04, 2023 18:02
IANS

Follow us +

TRENDING

Kuwait Ministry of Interior fires over 800 expats

Dos and don'ts for visitors at Al Rawda Al Sherifa

Riyadh Season to kick off Ronaldo museum

Philippines: Hackers reveal hospital bills, health data

Fear of switching off:

glamsham.com entertainment magazine

HOME | OTT | TV | BOLLYWOOD | REGIONAL | INTERNATIONAL | MUSIC | WORLD

Home › World › Health & Lifestyle

Study: Nanoparticle emissions from vehicles in Delhi may raise health risks

Vehicular emissions that release toxic nanoparticles in Delhi may be hazardous to health, according to a study.

By **Agency News Desk** 4 October 2023

follow us on Google NEWS

ENTERTAINMENT TODAY

- Ram Charan is 'glad to meet nation's pride' MS Dhoni
- Mrigdeep Singh Lamba shares old BTS pic of Fukraas with SRK
- Shruti Haasan's 'The Eye' selected for Greek International Film Festival
- 'Mansion 24' trailer blends jump scares with nerve-wracking tension
- 'Malhari' hitmakers Prashant Ingole, Vishal Dadlani reunite for sports anthem 'India India'

etvbharat.com/english/science-and-technology/nanoparticle-emissions-from-delhis-transport-sector-could-trigger-significant-health-risks/na20231003151528999999962

Assamese | Bengali | English | Gujarati | Hindi | Kannada | Malayalam | Marathi | Oriya | Punjabi | Tamil | Telugu | Urdu

HEADLINES | STATE | BHARAT | INTERNATIONAL | SITARA | GALLERY | VIDEO | CRIME | CHAMPION | BUSINESS | SCIENCE & TECH | SUKHIBHAVA | OPINION

ETV BHARAT
ETV Bharat
National

HOME / SCIENCE AND TECHNOLOGY / NANOPARTICLE EMISSIONS FROM DELHIS TRANSPORT SECTOR COULD TRIGGER SIGNIFICANT HEALTH RISKS

Nanoparticle emissions from Delhi's transport sector could trigger significant health risks: Study

PTI

Published: Oct 3, 2023, 3:15 PM

Follow Us

Nanoparticle emissions from Delhi's transport sector could trigger significant health risks: Study

Apple releases new iOS 17 update to fix iPhone 15 overheating issue

X stops showing headlines with articles, allows only image & domain name

AI-powered Google Pixel 8 phones bring new camera tools, 7 yrs of key updates

BENCHMARKS LIVE Nifty 19,402.00 ↓ -126.75 | FEATURED FUNDS Canara Robeco Small C... | 3Y RETURN ↑ 36.5 % INVEST NOW | Search Stock Quotes, News, Mutual Funds and more

Subscribe Sign In

THE ECONOMIC TIMES | News

English Edition | Today's Paper

Home ETPrime Markets News Industry Rise Politics Wealth Mutual Funds Tech Careers Opinion NRI Panache ET NOW Spotlight

India Decoded Web Stories Morning Brief Podcast Newsblogs Economy Industry Politics Company Defence More

Business News › News › India › Nanoparticle emissions from Delhi's transport sector could trigger significant health risks: Study

Nanoparticle emissions from Delhi's transport sector could trigger significant health risks: Study

PTI • Last Updated: Oct 03, 2023, 04:30 PM IST

SHARE FONT SIZE SAVE PRINT COMMENT

Synopsis

A study conducted in Delhi, India, has found high levels of nanoparticles in the air, particularly in roadside areas, due to vehicle engine exhaust. Nanoparticles, which are extremely small and invisible to the naked eye, pose greater health risks compared to larger particles like PM 2.5 or PM 10. The study focused on Bawana Road in Delhi, a location with heavy vehicular traffic. It revealed that nanoparticle concentrations vary with human activities and weather conditions.

ET Healthworld.com

From The Economic Times

Login

News Exclusives Leaders Speak Events Awards Webinars More

Pharma • Policy • Medical Devices • Diagnostics • Industry • Hospitals

nel
the latest
health
Follow

RE-Pharma Summit
The 4th edition of the REPharma Summit, themed "Reinvent, Restructure, and...

Download App
Save your favourite articles with seamless reading experience.

ETHealth Newsletters
Explore and Subscribe to our Daily Newsletters

Industry • 3 Min Read

Nanoparticle emissions from Delhi's transport sector could trigger significant health risks: Study

A study conducted in Delhi, India, has found high levels of nanoparticles in the air, particularly in roadside areas, due to vehicle engine exhaust. Nanoparticles, which are extremely small and invisible to the naked eye, pose greater health risks compared to larger particles like PM 2.5 or PM 10. The study focused on Bawana Road in Delhi, a location with heavy vehicular traffic. It revealed that nanoparticle concentrations vary with human activities and weather conditions.

easternmirrornagaland.com/nanoparticle-emissions-from-vehicles-in-delhi-may-raise-health-risks-study/

THURSDAY, OCTOBER 05, 2023

EASTERN MIRROR

JOURNALISM FOR JUSTICE

Eastern Mirror

HOME NEWS ARTS AND ENTERTAINMENT LIFESTYLE SCIENCE AND TECH SPORTS OPINION FEATURE PHOTO GALLERY E-PAPER

Home > Health > Nanoparticle Emissions From Vehicles in Delhi May Raise Health Risks — Study

HEALTH

Nanoparticle Emissions From Vehicles in Delhi May Raise Health Risks — Study

By IANS
Updated: Oct 04, 2023 10:01 pm

डाइनामाइट न्यूज़

Englis

उत्तर प्रदेश | राष्ट्रीय | राजनीति | विशेष खबरें | क्राइम | एक मुलाक़ात

दिल्ली में सड़कों पर वाहनों से नैनोकण का उत्सर्जन स्वास्थ्य जोखिम पैदा कर सकता है : अध्ययन

डीएन ब्यूरो

मंगलवार, 3 अक्टूबर 2023, दोपहर 4:27 बजे

दिल्ली की हवा में, विशेष रूप से सड़कों के किनारे के वातावरण में नैनोकण का खतरनाक स्तर पाया गया है, जिसका सीधा संबंध वाहनों से निकलने वाले धुएं से है और इससे स्वास्थ्य संबंधी चिंताएं बढ़ रही हैं। एक अध्ययन से यह जानकारी मिली। पढ़िये डाइनामाइट न्यूज़ की पूरी रिपोर्ट

Important Links

- News
- Events
- One Week One Lab (OWOL)
- Tenders
- Recruitment
- Technology Profile
- Right to Information Cell
- Customer Feedback
- Indian Highway Capacity Manual
- CSIR-CRRI welcomes CSR Funds from Industries for R&D in Road Sector
- Photo Galleries
- CSIR Vision 2030
- CSIR India R&D Projects
- CSIR Scientific ethics in CRRI
- List of Promo Films for Events at IISF 2020
- Booking of Test Services

Notifications and Announcements

News and Announcements

How these forensics on wheels help Delhi cops put cons behind bars

NEW DELHI: The mobile forensics vans introduced to save time while lifting and analysing evidence from crime scenes have till August visited over 25,000 spots since their induction in February. This has proved a boon for police in their investigation. Forensic experts are able to perform on-the-spot forensic tests in the vans before sending them for further analyses to the Forensic Science Laboratory. The spots visited this year till August related to house theft (10,492), burglary (4,164),...

After lockdown, 35% rise in nanoparticle emissions

NEW DELHI: Scientists have found that after the Covid lockdown eased in Delhi, the emission of nanoparticles, which are super-fine pollutants, increased by 35% on the city's roadside. Nanoparticles are fine pollutants which are about 1/1000th of particulate matter. They cannot be filtered out by N-95 masks. Scientists in the department of environmental engineering at Delhi Technological University (DTU) and the space and atmospheric sciences division of the Physical Research Laboratory in...

Over 80% of women complain buses don't stop for them at halts, says survey

NEW DELHI: About 80.2% of women bus users surveyed during a study reported instances of the public transporters not halting for them at designated stops, a report by Greenpeace India released Tuesday said. While 29% of the respondents faced such instances 'frequently', 50.2% said they experienced this 'occasionally' and 20.8% said they hadn't witnessed such episodes. Besides, 54.2% respondents said they were targeted with comments and faced discrimination from drivers, conductors and male...

CLIMATE SAMURAI

HOME | SOLAR | WIND | ELECTRIC VEHICLES | CLIMATE | INDUSTRY SPEAKS | DIRECT | LET'S BREATHE | MARKET | INNOVATION | VIDEOS | HYDRO & BIOFUELS | MORE | CONTACT

Delhi Grapples with Soaring Levels of Hazardous Nanoparticles in Urban

Recent Posts

- Renaissance Solar and Electronic Materials (RSOLEC) Embarks on $300 Million Investment to Revolutionize Solar Industry
- Delhi Grapples with Soaring Levels of Hazardous Nanoparticles in Urban Air: study
- NTPC School of Business and CPI India Join Forces for Clean Energy Transition"
- USD 80 Million Federal Grant Awarded to Partnership Led by Roeslein Alternative Energy for Climate-Smart Agriculture Project

Wednesday, October 4, 2023 info@businesstelegraph.co.uk Home

BUSINESS TELEGRAPH

finance global economy tech cryptocurrency autos retail science startups more

Business Telegraph > autos > Nanoparticle emissions from Delhi's transport sector could trigger significant health risks: Study – ETV Bharat

AUTOS

Nanoparticle emissions from Delhi's transport sector could trigger significant health risks: Study – ETV Bharat

October 3, 2023

posted on Oct. 03, 2023 at 10:45 am

Search and hit enter...

Latest News

TikTok Halts E-Commerce Service In Indonesia Following Ban

New Zealand's Reserve Bank Maintains Official Cash Rate At 5.5%, Impacting

---

Business Standard

Wednesday, October 04, 2023 | 11:55 AM IST EN | Hindi

Home Latest E-Paper Market Opinion Asian Games Sports Elections More Subscribe

Home / India News / Nanoparticle emissions from vehicles in Delhi pose health risks: Study

Nanoparticle emissions from vehicles in Delhi pose health risks: Study

The monitoring location is surrounded by educational institutions, households, and commercial areas where the dominant source of pollution is vehicular, the researchers said

Latest News View More >

In this section All

Govt owned refiners increase Russian oil imports despite G7 price cap

'Coming soon': Ashwini Vaishnaw shares pics of Vande Bharat sleeper trains

Govt office wall in HP's Dharamsala defaced with pro-Khalistan graffiti

Most Popular

---

bhaskarlive.in/nanoparticle-emissions-from-vehicles-in-delhi-may-raise-health-risks-study/

BHASKAR LIVE

ENGLISH NEWS

HOME NATIONAL INTERNATIONAL ENTERTAINMENT SPORTS TECHNOLOGY LIFESTYLE SOCIAL EDUCATION

Nanoparticle emissions from vehicles in Delhi may raise health risks: Study

October 4, 2023 IANS New Lifestyle 0

LIVE CRICKET SCORE

RECENT LIVE UPCOMING

10th Match, ICC Cricket World Cup Warm-up Matches 2023

AUS vs PAK

351/7(50.0) 337/10(47.4)

Australia win by 14 runs

DETAILS

9th Match, ICC Cricket World Cup Warm-up Matches 2023

IND vs NED

0/0(0) 0/0(0)

Match abandoned without a ball bowled

DETAILS

8th Match, ICC Cricket World Cup Warm-up Matches 2023

CRICTIMES EMBED

theasianindependent.co.uk/nanoparticle-emissions-from-vehicles-in-delhi-may-raise-health-risks-study/

Sign in / Join HOME UK INDIA WORLD ARTICLES Videos BUSINESS TECH HEALTH SPORTS E-PAPER

THE ASIAN INDEPENDENT UNITED KINGDOM

HOME UK INDIA WORLD ARTICLES VIDEOS BUSINESS TECH HEALTH SPORTS E-PAPER

Home › HEALTH › Nanoparticle emissions from vehicles in Delhi may raise health risks: Study

HEALTH HOME INDIA TECH

Nanoparticle emissions from vehicles in Delhi may raise health risks: Study

By **A Supran** - October 5, 2023

amritvichar.com/article/408182/nanoparticle-emissions-from-vehicles-on-delhi-roads-may-pose-health#gsc.tab=0

ENHANCED BY Google

अमृत विचार एक सम्पूर्ण अखबार

UTTAR PRADESH UTTARAKHAND CHHATTISGARH COUNTRY FOREIGN BUSINESS GAME ENTERTAINMENT RELIGION CULTURE HOROSCOPE EPAPE

BREAKING na's advice to the players Kharge spoke about floods in Sikkim and Himachal Pradesh, said- Government should make a fresh strategy for

healthy body

Nanoparticle emissions from vehicles on Delhi roads may pose health risks: Study

By Ashpreet On 04 Oct 2023 14:58:09

breaking news

Jaipur: More than 50 lakh voters will vote in 19 assembly constituencies, voters in the age group of 18-19 years increased.
05 Oct 2023 11:28:14

UNICEF executive director met CM Yogi
05 Oct 2023 11:16:24

Hindus have the mentality of being a minority, they lack brotherhood, why did the French journalist say this?
05 Oct 2023 11:15:09

2 TIMES

Fineprint Of Pollution: Why Roadsides Tell A Toxic Tale

Maximum Nanoparticle Buildup In Winter, Puts Your Lungs At Risk

Kushagra.Dixit
@timesofindia.com

New Delhi: Delhi Technological University (DTU) conducted research examining nanoparticle deposits in lungs across different age groups in Delhi.

Nanoparticles are airborne pollutants that mostly get deposited in the alveoli of the lungs. Research indicated 30% higher concentrations near roads compared to other areas. Post-Covid, the levels increased by 35% as traffic volume rose. The research spanned a year, covering all major seasonal variations in the region.

The study was led by associate professor Rajeev Kumar Mishra and research scholar Karnagaraj Rajagopal of DTU's Advance Air and Acoustics Research Laboratory alongside S. Ramachandran, senior professor at Physical Research Laboratory, Ahmedabad.

They focused on northern Delhi's atmospheric nanoparticle levels. "Air quality is a major concern. Pollutants in air are directly associated with human health, especially in urban regions that are more vulnerable to different types of atmospheric pollutants. In this study, for the first time, the concentration of atmospheric nanoparticles in an urban roadside environment was analysed, and the deposition of these in the human respiratory tract was quantified using a multiple-path particle dosimetry model. The measured seasonal mean nanoparticle concentration ranges from 24,085 to 41,000 particles per cubic cm," Mishra said.

The findings appeared in various international journals. The research highlighted how seasonal factors, including boundary layer height, wind speed, and precipitation, affect concentrations. Higher relative humidity was found to promote nanoparticle growth. Nanoparticles were most concentrated near emission sources, becoming more toxic through atmospheric chemical and physical changes.

"The nanoparticles emitted from vehicles are found in different sizes based on the vehicle's combustion. Petrol and CNG vehicles emit smaller nanoparticles than diesel vehicles. The type of fuel and the emission technology play a role in emissions," said Mishra. Health models revealed these particles bypass respiratory defences, reaching the alveoli. "The alveoli region of the lungs showed deposition, approximately 0.05 µg per day for an individual living near the road. The deposition varies for an individual working 8 hours near the road and residents residing 24 hours near the road. The deposition for individuals working near the road for 8 hours was found to be 5 times more than the annual PM2.5 concentration standards," the study said. Findings showed 90% of nanoparticles were in the alveoli. The research indicated infants face greater risks due to their developing respiratory systems.

Results suggested current anti-pollution standards need strengthening. "WHO also emphasises that nanoparticles present in the atmospheric air also need to be checked frequently since these have more potential impacts than particulate matter. So, the study results suggest that policymakers should include particle number concentration in the upcoming Bharat Stage VI (BSVI) standards to reduce nanoparticle emissions," the report stated.

TINY PARTICLES, HUGE HEALTH IMPACT

Nanoparticle buildup peaks in winter and is lowest in spring
Winter > Monsoon > Summer > Autumn > Spring

EXPOSURE LEVELS NEAR ROADS

People working near roads inhale about 338 µg/year of nanoparticles

Residents living near roads face three times higher exposure at 1,016 µg/year

Health Risks of Nanoparticle Deposition
Asthma | Chronic obstructive pulmonary disease (COPD) | Potential carcinogenic effects